



Escola d'Enginyeria

Departament d'Enginyeria Química

Hydrogen Production from Wastewater in Single Chamber Microbial Electrolysis Cells: Studies towards its Scaling-up

Programa de Doctorat en Ciència i Tecnologia Ambientals

Institut de Ciència i Tecnologia Ambientals

Memòria per a obtenir el Grau de Doctor
per la Universitat Autònoma de Barcelona
sota la direcció del Dr Albert Guisasola i Canudas
i del Dr Juan Antonio Baeza Labat

Núria Montpart i Planell

Juny 2014

Als meus pares Martí i Montserrat,
a la meva germana Mireia i a en Jonas

Acknowledgements

This research was partially funded by Carburos Metálicos-Air Products Group and the Spanish Government, under the project BIOSOS (CDTI, program Ingenio 2010).

The author thanks Universitat Autònoma de Barcelona for the PIF PhD grant that allowed to conduct her research and to participate in academic tasks.

Microbial electrolysis cells (MEC) are microbially catalyzed systems that offer the possibility to valorize wastewater by producing hydrogen, which is a valuable energy carrier and a widely used reactant in the chemical industry. Some energy input is required to drive the process, therefore real implementation of this technology will only be possible if a positive energy balance between the energy obtained as hydrogen and the energy supplied is achieved. A single chamber membrane-less configuration of MEC reduces energy requirements and design and operation complexity, being a priori a more convenient configuration for scale-up. The main drawback of a single chamber configuration is hydrogen availability for other microorganisms, which decreases hydrogen production and purity.

Different approaches were taken in this thesis to increase the performance of single chamber membrane-less MEC, having the aim to increase the chances for this system to be scaled up.

A proper exoelectrogenic biofilm development on the anode was key to ensure better system efficiencies. Coulombic efficiency was used to evaluate the inoculation of the anode in microbial fuel cell configuration, studying the effects of design parameters such as the area of cathode or the external resistance. It was observed that an optimal area of cathode might exist and that working at the optimal external resistance was of importance. The cathodic biofilm was also investigated, observing an oxygen barrier effect that maintained the anode in anaerobic conditions. The use of high external resistances during the inoculation process was observed to enhance the electroactivity of the exoelectrogenic biofilm, and it was also investigated as a selection procedure to allow the growth of biomass that efficiently deals with the energy input in MEC. In view of a real use of MEC treating wastewater, a consortium between fermentative bacteria that could degrade complex substrates to simpler compounds and exoelectrogenic bacteria was developed and used to bioaugment the anodic biofilm.

In order to improve hydrogen production and purity, a strategy to avoid methanogenesis in single chamber MEC by reducing the hydrogen retention time was tested in the long term for both readily biodegradable synthetic wastewater and complex synthetic wastewater. The strategy, consisting in hydrogen stripping by sparging nitrogen, was

effective but presented limitations depending on the complex substrate consumed, showing the need to combine it with other strategies.

Also, a fuel cell was tested as a low cost monitoring tool for biohydrogen producing systems at lab scale. The signal obtained correlated well with hydrogen supplied and was as efficient as other reference analytical methodologies such as gas chromatography. The use of this device could allow the implementation of control and optimization strategies in the process.

Finally, the opportunities for crude glycerol to produce hydrogen in MEC were explored, seeing that it was constraint in single chamber but it was possible in double chamber configuration. Methanol, often contained in crude glycerol, was also used effectively in MEC. Electrofermentation of synthetic glycerol was also studied as a possible technology to give an added value to biodiesel industry wastewater by enhancing the production of 1,3-propanediol.

With the work developed in this thesis it was concluded that scaling up single chamber MEC for hydrogen production has opportunities if a series of strategies are addressed: (i) the development of efficient anodic biofilms, highly electroactive and with capacity to treat a wide range of compounds, (ii) the use of wastewater with low methanogenesis potential and (iii) operation at low hydrogen retention time and low hydraulic retention time.

This thesis was the first one completed in the research line of Bioelectrochemical Systems in GENOCOV group (Research Group on Biological Treatment of Liquid and Gas Effluents) at Universitat Autònoma de Barcelona.

Les cel·les microbianes d'electròlisi (MEC) són sistemes biocatalitzats que ofereixen la possibilitat de valoritzar aigües residuals produint hidrogen, el qual és un bon vector energètic i un reactiu àmpliament utilitzat a la indústria química. L'aportació d'energia és necessària per a dur a terme el procés, i per tant la implementació d'aquesta tecnologia només serà possible si s'assoleix un balanç energètic positiu entre l'energia subministrada i l'energia obtinguda en forma d'hidrogen. La configuració de MEC en una sola cambra i sense membrana redueix els requeriments energètics del procés a més a més de simplificar-ne el disseny i la complexitat en l'operació, sent a priori una configuració més adient de cara a l'escalat del sistema. El principal inconvenient d'aquesta configuració és la disponibilitat de l'hidrogen per altres microorganismes, que en redueix la producció i la puresa.

En aquesta tesi, es varen considerar diferents mesures per a millorar el rendiment de MEC en una sola cambra i sense membrana, amb l'objectiu d'augmentar les oportunitats d'escalat d'aquest sistema.

El desenvolupament d'un biofilm exoelectrogen adequat va ser clau per a millorar l'eficiència del sistema. L'eficiència coulòmbica es va utilitzar com a paràmetre per a avaluar la inoculació de l'ànode en configuració de cel·la microbiana de combustible, estudiant els efectes de paràmetres de disseny tals com l'àrea de càtode o la resistència externa. Es va observar que una àrea de càtode òptima podria existir i que treballar a la resistència externa òptima era important. El biofilm catòdic també es va investigar, observant-ne un efecte barrera per a l'oxigen que permetia mantenir l'ànode en condicions anaeròbies. Es va observar que l'ús d'elevades resistències externes durant el procés d'inoculació afavoria electroactivitat del biofilm exoelectrogen, i es va investigar com a possible procediment de selecció que permetés créixer biomassa que fes servir de manera eficient l'aportació d'energia en MEC. En vista a l'ús de les MEC per a tractar aigües residuals reals, es va bioaugmentar el biofilm anòdic amb un consorci microbià constituït per bacteris fermentadors amb capacitat de degradar substrats complexos a compostos simples i per bacteris exoelectrògens.

Per tal d'augmentar la producció i la puresa de l'hidrogen produït, es va estudiar a llarg termini una estratègia per a reduir el temps de retenció d'hidrogen al sistema i així evitar la metanogènesi en MEC d'una sola cambra. L'estratègia, que consistia en

arrossegar l'hidrogen del sistema per bombolleig de nitrogen, va ser efectiva tot i que va presentar limitacions depenent del substrat consumit, indicant la necessitat de combinar aquesta estratègia amb d'altres.

A més a més, es va estudiar l'ús d'una pila de combustible com a una eina econòmica de monitorització de producció biològica d'hidrogen a escala de laboratori. La senyal obtinguda correlacionava correctament amb l'hidrogen subministrat, sent tan eficient com d'altres metodologies d'anàlisi de referència com la cromatografia de gasos. L'ús d'aquest instrument podria arribar a permetre la implementació d'estratègies de control i optimització en el procés.

Finalment, es va investigar l'oportunitat de produir hidrogen del glicerol residual provinent de la indústria del biodiesel en MEC, que es veié limitada en MEC d'una sola cambra però que va ser possible en configuració de doble càmara. El metanol, sovint contingut en el glicerol residual, també es va usar de manera efectiva com a substrat en MEC. L'electrofermentació de glicerol sintètic també es va estudiar com a possible tecnologia per a valoritzar les aigües residuals de la indústria del biodiesel afavorint la producció de 1,3-propanodiol.

Segons el treball desenvolupat en aquesta tesi es va concloure que l'escalat d'una MEC d'una sola cambra per a la producció d'hidrogen té opcions d'implementació si: (i) es desenvolupa un biofilm anòdic adequat, molt electroactiu i amb capacitat de tractar un rang ampli de substrats, (ii) s'usen aigües residuals amb baixa tendència a la proliferació de poblacions metanogèniques i (iii) s'opera a baix temps de retenció de l'hidrogen i baix temps de retenció hidràulic.

Aquesta tesi va ser la primera tesi finalitzada de la línia de recerca en Sistemes Bioelectroquímics del grup GENOCOV (Grup de Tractament Biològic d'Efluents Líquids i Gasosos) a la Universitat Autònoma de Barcelona.

Las celdas microbianas de electrólisis (MEC) son sistemas biocatalizados que ofrecen la posibilidad de valorizar aguas reales produciendo hidrógeno, el cual es un buen vector energético y un reactivo ampliamente usado en la industria química. El aporte de energía es necesario para llevar a cabo el proceso, y como consecuencia la implementación de esta tecnología sólo será posible si se consigue un balance positivo entre la energía subministrada y la energía obtenida como hidrógeno. La configuración de MEC en una sola cámara sin membrana reduce los requerimientos energéticos del proceso además de simplificar su diseño y operación, siendo a priori una configuración más adecuada para el escalado del sistema. El principal inconveniente de esta configuración es la disponibilidad de hidrógeno por otros microorganismos, que acaban reduciendo su producción y pureza.

En esta tesis, se tomaron distintas estrategias para mejorar el rendimiento de MEC en una sola cámara y sin membrana, con el objetivo de aumentar las posibilidades de escalado de este sistema.

El desarrollo de un biofilm exoelectrógeno adecuado fue clave para mejorar la eficiencia del sistema. La eficiencia coulombica se utilizó como parámetro para evaluar la inoculación del ánodo en configuración de celda microbiana de combustible, estudiando los efectos de parámetros de diseño tales como el área de cátodo o la resistencia externa. Se observó que un área óptima podría existir y que trabajar a la resistencia externa óptima era de importancia. El biofilm catódico también se investigó, observando un efecto de barrera para el oxígeno que permitía mantener el ánodo en condiciones anaerobias. Se observó que el uso de resistencias externas elevadas durante el proceso de inoculación favorecía la electroactividad del biofilm exoelectrógeno, y se investigó como posible procedimiento de selección que permitiera crecer biomasa que utilizase de manera eficiente el aporte de energía en MEC. En vista al uso de las MEC para tratar aguas residuales reales, se bioaumentó el biofilm anódico con un consorcio microbiano constituido por bacterias fermentadoras con capacidad de degradar sustratos complejos a compuestos más simples y por bacterias exoelectrógenas.

Con el objetivo de aumentar la producción y pureza de hidrógeno producido, se estudió a largo plazo una estrategia para reducir el tiempo de retención del hidrógeno en el sistema y así evitar la metanogénesis en MEC de una sola cámara. La estrategia, que

consistía en eliminar el hidrógeno del sistema por burbujeo de nitrógeno, fue efectiva aunque presentó limitaciones dependiendo del sustrato consumido, indicando la necesidad de combinarla con otras acciones.

Además, se estudió el uso de una pila de combustible como herramienta de bajo coste para monitorizar la producción de biohidrógeno a escala laboratorio. La señal obtenida correlacionaba correctamente con el hidrógeno subministrado, siendo tan eficiente como otras metodologías de análisis como la cromatografía de gases. El uso de este instrumento podría llegar a permitir la implementación de estrategias de control y optimización en el proceso.

Finalmente, se investigó la oportunidad de producir hidrógeno a partir de glicerol residual proveniente de la industria del biodiesel en MEC, que se vio limitada en MEC de una sola cámara pero fue posible en configuración de doble cámara. El metanol, a menudo presente en el glicerol residual, también se usó efectivamente como sustrato en MEC. La electrofermentación de glicerol sintético también se estudió como posible tecnología para valorizar aguas residuales de la industria del biodiesel favoreciendo la producción de 1,3-propanodiol.

Con el trabajo desarrollado en esta tesis se puede concluir que el escalado de una MEC de una sola cámara para la producción de hidrógeno tiene opciones para su implementación si: (i) se desarrolla un biofilm anódico adecuado, muy electroactivo y con capacidad de tratar un amplio rango de sustratos, (ii) se usan aguas residuales con baja tendencia a la proliferación de poblaciones metanogénicas y (iii) se trabaja a bajo tiempo de retención de hidrógeno y bajo tiempo de residencia hidráulico.

Esta tesis fue la primera tesis finalizada de la línea de investigación en Sistemas Bioelectroquímicos en el grupo GENOCOV (Grupo de Tratamiento Biológico de Efluentes Líquidos y gaseosos) en la Universitat Autònoma de Barcelona.

Les piles à électrolyse microbiennes (MEC en anglais pour « Microbial electrolysis cells ») sont des systèmes catalysés par des microorganismes qui permettent de valoriser les eaux usées en produisant de l'hydrogène, lequel est un vecteur énergétique à haute valeur ainsi qu'un réactif couramment utilisé dans l'industrie chimique. Un apport énergétique est cependant nécessaire pour que le procédé fonctionne. Par conséquent, l'implémentation industrielle de cette technologie n'est réalisable que si l'énergie obtenue sous forme d'hydrogène est supérieure aux apports énergétiques extérieurs. La configuration des MEC sous forme de chambre unique sans membrane réduit la demande en énergie et la complexité du système et de son opération. Cette configuration est donc, a priori, plus adaptée pour une application industrielle. Le principal inconvénient d'une configuration en chambre unique est la disponibilité de l'hydrogène comme substrat pour d'autres organismes, ce qui réduit la production d'hydrogène et sa pureté.

Différentes approches ont été étudiées dans cette thèse pour augmenter la performance des MEC à chambre unique sans membrane, le but étant d'augmenter les chances de passage à échelle industrielle de ce système.

Le développement d'un biofilm électrogénique approprié sur l'anode est un élément clé pour assurer une meilleure efficacité du système. L'efficacité coulombique a été utilisée pour évaluer l'inoculation de l'anode en configuration de pile à combustible microbienne, en étudiant l'influence de paramètres de dimensionnement tels que la surface de la cathode ou la résistance externe. Les résultats ont montré qu'une surface optimale pour la cathode pourrait exister, et que travailler à la résistance extérieure optimale permettait de fortement augmenter l'efficacité du système. Le biofilm sur la cathode a également été étudié, montrant qu'il agit comme une barrière pour l'oxygène, maintenant ainsi l'anode en conditions anaérobies. L'utilisation de résistances externes élevées durant le procédé d'inoculation a permis d'augmenter l'électroactivité du biofilm électrogénique, et cette stratégie a été proposée comme procédure de sélection pour la croissance de microorganismes ayant la capacité d'utiliser efficacement les apports énergétiques dans les MEC. Dans l'objectif d'utiliser les MEC pour le traitement d'eaux usées réelles, un consortium composé de bactéries fermentaires pouvant dégrader des substrats complexes en composés plus simples et de bactéries électrogéniques a été développé et utilisé pour bioaugmenter le biofilm de l'anode.

Afin d'améliorer la production d'hydrogène et sa pureté, une stratégie visant à réduire le temps de séjour de l'hydrogène pour éviter la méthanogenèse dans les MEC à chambre unique a été testée sur le long terme pour le traitement d'eaux usées synthétiques facilement biodégradables et d'eaux usées synthétiques complexes. Cette stratégie, qui consiste à extraire l'hydrogène par barbotage d'azote gazeux (stripage), s'est montrée efficace mais s'avère avoir des limitations suivant le substrat complexe consommé, montrant la nécessité de la combiner avec d'autres stratégies.

Une pile à combustible a également été testée comme appareil d'analyse bon marché pour le suivi de la bioproduction d'hydrogène à l'échelle du laboratoire. Le signal obtenu corrélait bien avec la quantité d'hydrogène fournie et cette méthode s'est avérée aussi efficace que d'autres méthodes analytiques de référence telles que la chromatographie gazeuse. L'utilisation de ce dispositif pourrait permettre l'implémentation de stratégies de contrôle et d'optimisation du procédé.

Finalement, la possibilité de produire de l'hydrogène à partir de glycérol brut dans des MEC à chambre unique a été explorée, montrant qu'elle est limitée par le métabolisme des bactéries homoacétogènes. L'électro-fermentation de glycérol synthétique a également été étudiée comme une technologie possible pour donner une valeur ajoutée aux eaux usées de l'industrie du biodiesel en produisant du 1,3-propanediol.

Le travail développé dans cette thèse a permis de conclure que le passage à échelle industrielle des MEC à chambre unique pour la production d'hydrogène semble faisable si une série de stratégies sont appliquées : (i) le développement d'un biofilm efficace sur l'anode, fortement électroactif et avec la capacité de traiter une large gamme de composés, (ii) l'utilisation d'eaux usées avec un faible potentiel de méthanogénèse, et (iii) l'exploitation du système à un faible temps de séjour de l'hydrogène et un faible temps de séjour hydraulique.

Cette thèse est la première terminée de l'axe de recherche en Systèmes Bioélectrochimiques dans le groupe GENOCOV (Groupe de Traitement d'Effluents Liquides et Gazeux) à l'Universitat Autònoma de Barcelona.

Table of contents

Part I: General Introduction	1
Chapter 1. General introduction	2
1.1. Current energy context.....	2
1.2. Hydrogen as a renewable energy source.....	3
1.3. Bioelectrochemical systems.....	5
1.3.1. Anode respiring bacteria.....	6
1.3.2. Exploiting anode respiring bacteria in bioelectrochemical systems.....	7
1.4. Hydrogen production in single chamber microbial electrolysis cells.....	10
1.5. Research motivations and thesis overview	15
1.5.1. Research motivations.....	15
1.5.2. Thesis overview	15
Chapter 2. Objectives	17
References	18
Part II: Materials and Methods	22
Chapter 1. Reactor designs and inoculation protocol.....	23
1.1. Reactor designs	23
1.2. Inoculation protocol	29
Chapter 2. Media and analytical techniques.....	31
2.1. Synthetic media description.....	31
2.2. Analytical methods	33
Chapter 3. System thermodynamics and parameters to report system efficiency.....	37
3.1. Thermodynamics and the electromotive force.....	37
3.2. Reporting system performance and efficiency	38
Chapter 4. Electrochemical techniques	41
4.1. Polarization and power curve	41
4.2. Cyclic voltammetry.....	42
References	45
Part III: Results and Discussion.....	48
Chapter 1. Improving the inoculation process in MFC: what limits coulombic efficiency in microbial fuel cells?	49

1.1.	Introduction.....	50
1.2.	Materials and methods	53
1.3.	Results and discussion	55
1.3.1.	The role of the area of cathode and the external resistance.....	55
1.3.1.1.	Finding the optimal cathodic area.....	55
1.3.2.	Cathodic biofilm effects	59
1.3.3.	External resistance effects during inoculation in MFC	68
1.4.	Conclusions.....	75
Chapter 2.	Biomass selection and bioaugmentation in MXC	77
2.1.	Introduction.....	78
2.2.	Materials and methods	80
2.3.	Results and discussion	82
2.3.1.	Evaluation of ARB selection inoculating at different R_{ext}	82
2.3.2.	Bioaugmentation of bioelectrochemical systems with microbial consortia	89
2.4.	Conclusions.....	100
Chapter 3.	Methanogenic population control.....	101
3.1.	Introduction.....	102
3.2.	Materials and methods	105
3.3.	Results and discussion	107
3.3.1.	Methanogenic population control in readily biodegradable synthetic wastewater	107
3.3.2.	Methanogenic population control with complex synthetic wastewater..	114
3.3.3.	Practical implications	125
3.4.	Conclusions.....	127
Chapter 4.	On-line monitoring of hydrogen production	129
4.1.	Introduction.....	130
4.2.	Materials and methods	131
4.3.	Results and discussion	133
4.3.1.	Instrument characterization and calibration	133
4.3.2.	Implementation in MEC: online monitoring of hydrogen production ...	138
4.3.3.	Practical implications	140
4.4.	Conclusions.....	142

Chapter 5. Case study: treatment of biodiesel industry wastewater with bioelectrochemical systems	143
5.1. Introduction.....	144
5.2. Materials and methods	146
5.2.1. Hydrogen production in single chamber MEC with biodiesel industry wastewater	146
5.2.2. Glycerol electrofermentation.....	146
5.3. Results and discussion	149
5.3.1. Hydrogen production in single chamber MEC with biodiesel industry wastewater	149
5.3.2. Other possibilities in BES for glycerol: Redirection of glycerol fermentation pathways in a microbially catalysed electrochemical cell	156
5.4. Conclusions.....	164
References	165
Part IV: General Conclusions and Future Perspectives	174
Part V: Appendix.....	178
Appendix A: Code of the mathematical model for MEC.....	179
Appendix B: Glossary and abbreviations	183
Glossary.....	183
List of acronyms and abbreviations.....	186
Appendix C: Curriculum Vitae	188

Part I: General Introduction

Chapter 1. General introduction

1.1. Current energy context

The modern society has reached extreme advances in the last two centuries. From the steam engine to technologies like computing or telecommunications, most technologies developed rely on the use of fossil fuels as driving energy. An oil dependent society is the result of all these advances, which is not the most desirable situation taking into account the non renewable nature of these fuels. The progressive shortage of fossil fuel resources is generating social and economical problems and the potential of exhaust gases in greenhouse effect contributes to global warming and climate change. Institutions worldwide are aware of the consequences of an oil dependent economy and are putting efforts on trying to change current habits, enhancing the development of alternative renewable energy sources. To prevent or slow down climate change, a decrease or stabilization of greenhouse gases is required. To achieve this, the Kyoto protocol was introduced in 1998¹. According to this protocol the European Union decided in 2008 to reduce de greenhouse gasses emissions by 20% in 2020 compared to 1990 levels. To achieve this reduction, in 2020, 20% of the produced energy should be from renewable resources and 10% of the fuels used in the EU should be biobased². Data from Eurostat quantifies in 14% the share of renewables in the gross final energy consumption in the European Union in 2012³. In a larger scale, the International Energy Agency estimated in 5% of the total primary energy supply of the OECD the share of biofuels and biobased energy, being 8.6% the global contribution of renewable⁴.

Renewable energies developed so far are in different levels of maturity. By far wind and sun are the most studied energy resources. Although well developed and available in large quantities, they are fluctuating sources with low flexibility and storage complexity. Other renewable energies such as biodiesel rely on the use of biomass. Nevertheless the use of land to produce biofuels has as main drawback the possible competition with crops aimed at nutrition purposes, which can lead to an increase in first necessity products price. Biowastes are alternative sources for biofuels, having the advantages of not competing with the food chain and that the valorization of the residues is accomplished. Here, the concept of biorefinery is introduced denoting the exploitation of wastes for conversion to fuels, power, heat and value-added chemicals.

To date, the only technology that has proven to be capable of valorizing waste streams on a commercial scale is anaerobic digestion⁵, producing methane that can be mainly used as a fuel. One emerging technology to address both waste reduction and valorization are bioelectrochemical systems, which offer the possibility to obtain electrical power, in systems known as microbial fuel cells (MFC), and the possibility to obtain a wide range of value-added compounds such as hydrogen in systems known as microbial electrolysis cells (MEC). The possible flowsheet of a bioelectrochemical-based wastewater biorefinery is presented in Figure 1.1. Besides from wastewater purification a whole range of chemicals could be recovered in an energetically self sustained process. In terms of wastewater treatment, bioelectrochemical systems could treat both municipal and industrial wastewater and they could have possibilities as a decentralized treatment. Another advantage when compared to the conventional treatment is the low sludge production.

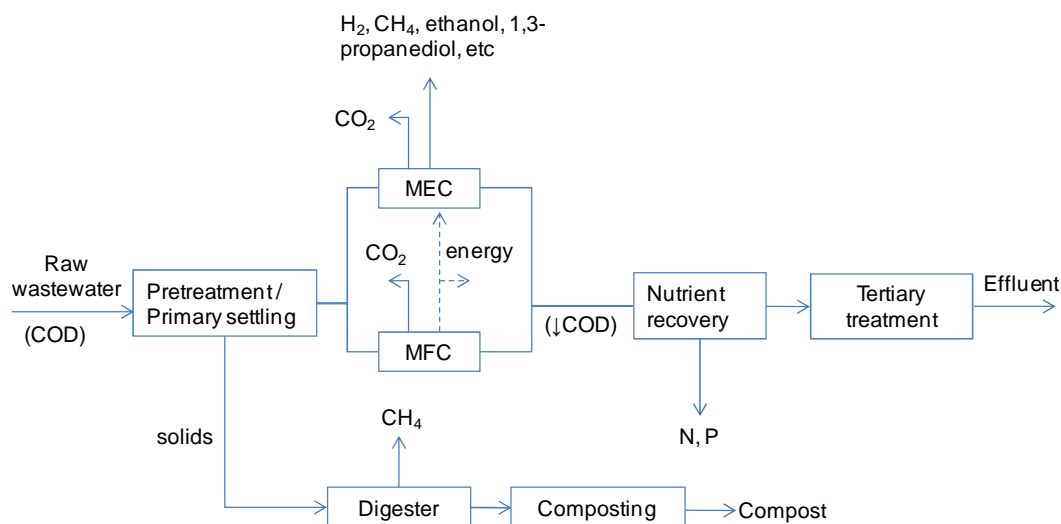


Figure 1.1. Possible flowsheet of a future bioelectrochemical-based wastewater biorefinery (Adapted from Rabaey and Rozendal, 2010⁶)

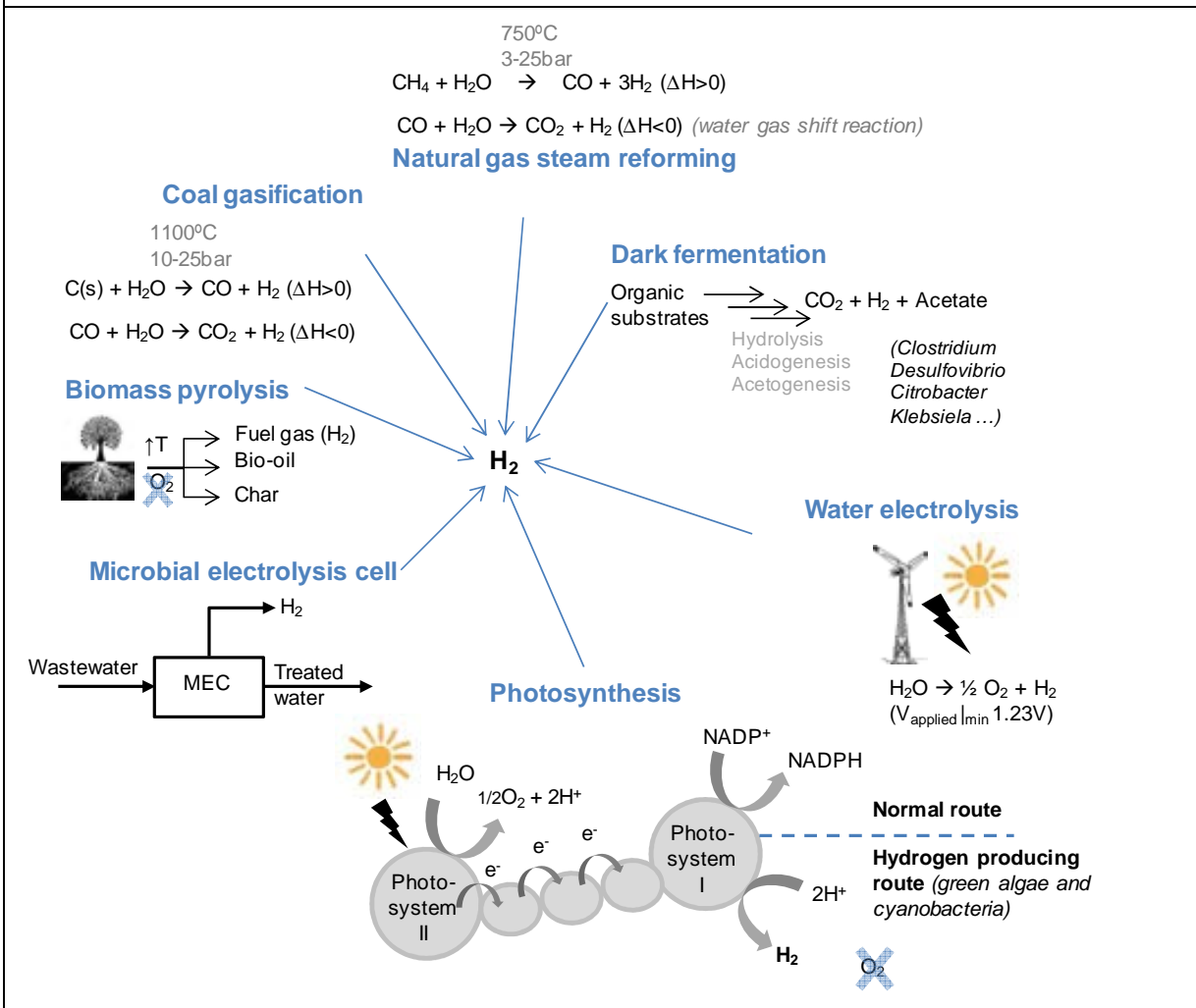
1.2. Hydrogen as a renewable energy source

The historical development of energy carriers moves towards more hydrogen rich fuels (C, coal \rightarrow $-\text{CH}_2-$, oil \rightarrow CH_4 , natural gas \rightarrow H_2 , hydrogen), which together with the necessity to avoid carbon dioxide emissions converts hydrogen to the energy carrier of the future. Besides from being a valuable energy carrier, hydrogen is an important feedstock to the chemical industry. Due to the many uses of hydrogen, the hydrogen industry is large and mature. For example, about 10^8 m^3 (at 1 atm) of hydrogen are sold in the United States each year⁷.

Although hydrogen is often presented as a clean energy vector not directly contributing to the greenhouse effect, it is currently mainly produced by natural gas steam reforming and therefore it cannot be considered either renewable or carbon-neutral fuel. Apart from the natural gas steam reforming processes, electrolysis of water is the most widely used method for hydrogen production. Water electrolysis to hydrogen and oxygen can be achieved by supplying an energy input to the system (minimum of 1.23 V) and it is considered a promising technology when using a renewable energy source like solar and wind power⁸. Biologically produced hydrogen, though, offers the possibility to upgrade wastewater or biowastes generating hydrogen that is renewable with no net contribution to the greenhouse effect. When compared to methane, hydrogen is more interesting given that it has higher combustion energy (-143 kJ g^{-1} for hydrogen vs. -50 kJ g^{-1} for methane) and given that water is its only combustion product.

Hydrogen can be produced biologically by photosynthesis, dark fermentation and bioelectrochemistry. Despite the great possibilities, bio-hydrogen production is not yet practical because of limitations inherent to each technology. Photosynthetic hydrogen presents technical challenges due to oxygen sensitivity and fermentative hydrogen production offers low conversion from the organic substrate to hydrogen^{7,9}. Regarding bioelectrochemistry, hydrogen can be produced in microbial electrolysis cells, a technology that emerged in the last decade^{10,11} with high potential for hydrogen production but, still, with many hurdles to overcome.

Regardless of the source, whether hydrogen becomes the fuel of the future or not is not only a matter of developing production technologies but also distribution, storage and safety⁸. However, the research community is continuously making progresses. To give some examples, hydrogen powered buses run in cities like Madrid, Reykjavik, London, etc, hydrogen refueling stations can be found along some California's highways and in India fuel cells are used as backup power for telecommunication facilities¹². Public investment and policy makers play and are expected to play a key role in the transition, increasing energy security by contributing to energy diversification. Regarding hydrogen as a chemical, there will remain a demand for hydrogen whether or not a hydrogen economy will develop.

Box 1. | Overview of hydrogen producing technologies^{7,9,13-16}**1.3. Bioelectrochemical systems**

Bioelectrochemical systems comprise emerging technologies that combine the metabolism of microorganisms with electrochemistry. As an electrochemical cell the system is comprised by two electrodes: an anode, where an oxidation reaction takes place (loss of electrons), and a cathode, where a reduction reaction occurs (gain of electrons). The electrical connection of both electrodes allows the flow of electrons from the anode to the cathode. The electrodes are surrounded by an electrolyte, a conductive aqueous solution where charged species diffuse. An ionic exchange membrane can physically separate both electrodes in an anodic and a cathodic half-cell or chamber, containing the anolyte and the catholyte respectively.

In bioelectrochemical systems oxidation and reduction reactions can be microbially catalyzed. The metabolism of these microorganisms is linked to the electrodes and, therefore,

they are generally called electroactive microorganisms. Microorganisms whose metabolism is related to anodic processes are the ones with the most studied and best understood metabolic mechanisms. The so called anode respiring bacteria (ARB) oxidize the organic matter available and use an insoluble anode as the terminal electron acceptor in anaerobic conditions, i.e. in absence of other possible electron acceptors like oxygen, nitrate and sulphate. ARB are also known as exoelectrogenic bacteria, given the fact that they extracellularly transfer the electron to the anode.

1.3.1. Anode respiring bacteria

The observation of microorganisms with the ability to transport electrons extracellularly was first reported by Potter in 1912¹⁷ but it was not until the end of the century that their metabolism was better described and that research in their technical exploitation was initiated^{18–21}. Phyla of microorganisms that have been reported to have exoelectrogenic abilities comprise *alpha*-, *beta*-, *gamma*- and *delta*-proteobacteria, firmicutes, acidobacteria and yeasts²². Substrate-utilization capabilities of most of these microorganisms are limited to simple fermentation products, such as acetate and hydrogen. However some members can utilize a wider range of substrates, such as propionate, butyrate, lactate and glucose^{23–25}. Examples of those able to completely oxidize substrates coupling this oxidation to reduction of electrodes include *Geobacter sulfureducens*, *Geobacter metallireducens*, *Geobacter electrodophilus*, *Shewanella oneidensis*, *Pseudomonas aeruginosa*, *Desulfuromonas acetoxidans*, *Rhodospirillum rubrum* and *Geothrix fermentans*²⁶.

Different mechanisms have been proposed for ARB to transfer electrons extracellularly (Figure 1.2). Direct electron transfer to the electrode requires physical contact between the microbial cell and the anode. This can be achieved by the outer membrane proteins (c-type cytochromes), responsible of the electron transport chain, or by contact through long and conductive appendages called nanowires. Electron transfer between the cell and the anode can be also mediated through the interaction of mediators, or electron shuttles, that are sequentially reduced and oxidized. Electron shuttles can be produced by the same bacteria or can be artificially added²⁷. Mechanisms are not exclusive for different species and in bioelectrochemical systems vary depending on the operational mode^{28,29}.

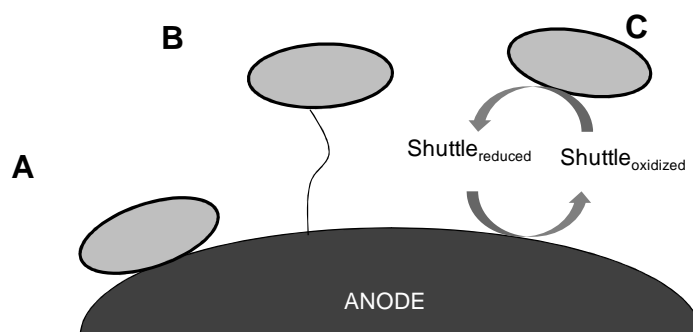


Figure 1.2. Extracellular electron transfer mechanisms for anode respiring bacteria (A) Direct transfer by direct contact or through a conductive biofilm matrix (B) Direct transfer by nanowires (C) Indirect transfer by means of electron shuttles.

1.3.2. Exploiting anode respiring bacteria in bioelectrochemical systems

The oxidation of organic matter by ARB on the anode is coupled to a reduction reaction on the cathode. Depending on the reduction reaction, the thermodynamics of the overall process is favored (negative Gibbs free energy) or it requires some energy input to drive it. The flow of electrons is favored towards more positive potentials. In MFC the reduction potential of the process occurring in the anode is lower than that occurring on the cathode and therefore the electrical connection of the anode with a cathode produces an electron flow that can be used elsewhere as electricity. On the contrary, the reduction potential of the reaction occurring on the cathode is lower than that of the anode in MEC and an energy input is required to drive the process and to obtain the product of interest (Figure 1.3). With these fundamentals numerous processes can be achieved in bioelectrochemical systems.

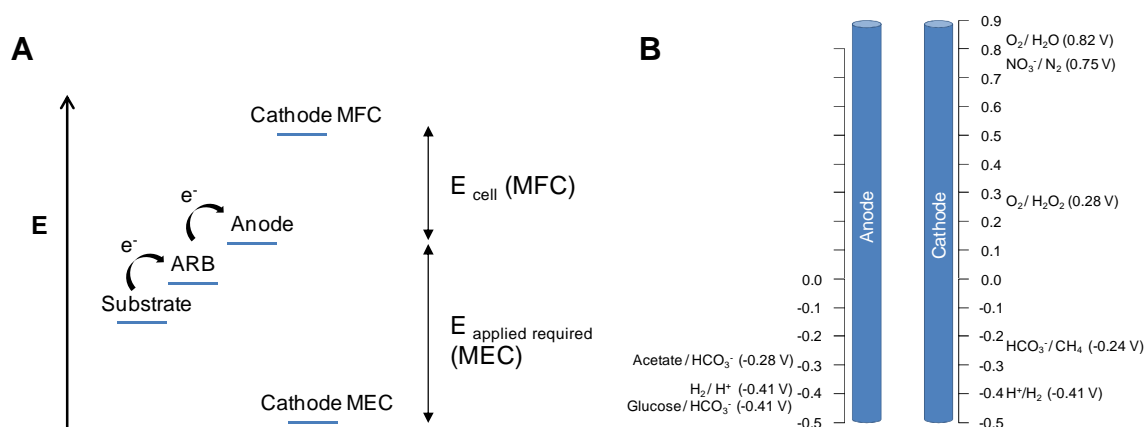
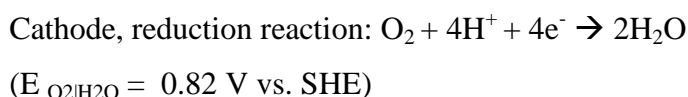
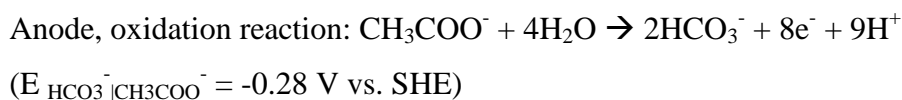


Figure 1.3. (A) Electron flow according to electrodes potential, E (B) Scale of theoretical potentials associated to redox processes at pH 7 and 298 K (shown against the standard hydrogen electrode).

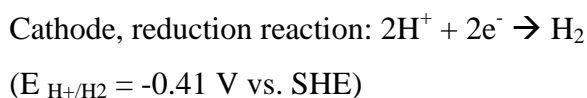
The thermodynamics of the overall reaction can be evaluated in terms of Gibbs free energy, ΔG_r (J), but it can also be evaluated in terms of overall cell electromotive force, E_{emf} (V), defined as the potential difference between the cathode and the anode, which is positive for a thermodynamically favorable reaction.

In MFC (Figure 1.4A), a carbon source is oxidized under anaerobic conditions by ARB, using the anode as final electron acceptor. Electrons flow along the electrical circuit to the cathode. Protons produced during the substrate oxidation diffuse to the cathode and they are consumed in the oxygen reduction reaction. Different conditions are therefore met in both electrodes, requiring an anaerobic environment in the anode surroundings and aerobic conditions around the cathode. When acetate is the electron donor the reactions occurring in each electrode can be expressed as:



With an overall cell electromotive force of $E_{\text{emf}} = E_{\text{cathode}} - E_{\text{anode}} = 1.1 \text{ V}$

In MEC (Figure 1.4B) using acetate as electron donor, the oxidation reaction is identical to the one described for MFC. Unlike MFC, anaerobic conditions are also met in the cathode surroundings in MEC, and the cathodic reaction occurring is the reduction of protons to hydrogen:



With an overall cell electromotive force of $E_{\text{emf}} = E_{\text{cathode}} - E_{\text{anode}} = -0.13 \text{ V}$

Therefore, in MFC about 1.1 V can be theoretically produced from acetate, whereas in MEC for hydrogen production a minimum energy input of about 0.13 V is required to drive the process (at 298 K and pH 7).

Besides electrons, during the biodegradation of organic matter protons are also produced. The transport of electrons from the anode to the cathode needs to be compensated to meet the

electroneutrality condition, i.e. that the solution is electrically neutral. The fact that not only protons and hydroxyls but other charged species can be responsible of maintaining the electroneutrality leads to pH gradients in the system, experiencing a pH drop in the anodic environment (due to protons formation) and a pH increase in the cathodic environment (due to protons consumption / hydroxyls formation). Such pH gradients are more significant when an ionic exchange membrane (anion exchange membrane or cation exchange membrane) is present in the system. In contrast, when the system lacks a membrane, pH gradients affect in a rather local scale. The reduction potential of both the oxidation and the reduction reactions will vary according to pH, leading to changes in the attainable or required thermodynamic values^{30,31}.

In practice, the voltage that can be obtained or that is required in bioelectrochemical systems differs from the thermodynamically possible values because of a whole variety of voltage losses occurring in the system, which decrease the attainable voltage in MFC and increase the voltage requirements in MEC.

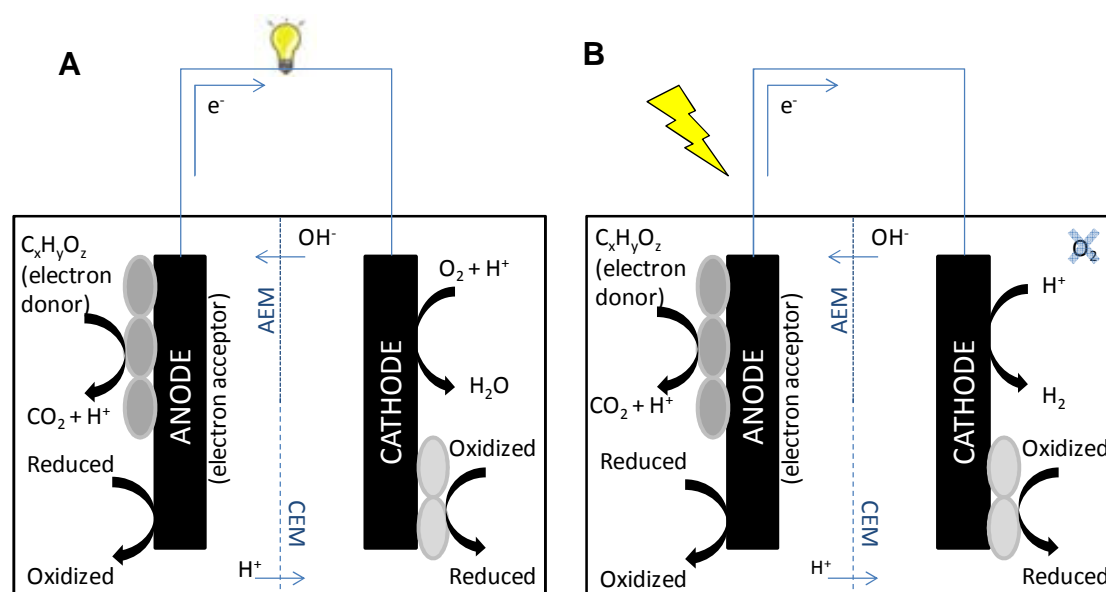


Figure 1.4. Schematics of (A) a microbial fuel cell and (B) a microbial electrolysis cell. Oxidation and reduction processes can occur electrochemically or can be microbially catalyzed. Both processes can be physically separated by an ionic exchange membrane, selectively allowing cations flow (CEM) or anions flow (AEM).

Voltage losses in bioelectrochemical systems can be divided into electrode overpotentials and ohmic losses of the system. Electrode overpotentials are the result of activation losses (related to the activation energy needed for the reactions to occur in each electrode), bacterial metabolic losses (the higher the energy gain for bacteria the higher the voltage loss in the

system) and concentration losses, related to mass transport limitations. Regarding ohmic losses, they include voltage losses related to the resistance to the flow of electrons in electrodes and connections and the resistance to the flow of ions in the electrolytes and the membrane (if present). Current dependent voltage losses are generally referred to as internal resistance (R_{int}).

Overpotentials can be decreased increasing the electrode surface area, improving the electrode catalysis, increasing the operating temperature or through the establishment of an enriched biofilm on the electrode. Ohmic losses are generally minimized by reducing the electrode spacing, using membranes with low resistivity and increasing the solution conductivity³².

The use of ionic exchange membranes in bioelectrochemical systems physically separates the anode and cathode, and therefore it separates oxidation and reduction products. However a configuration with membrane increases voltage losses. In fact, Rozendal estimated between 0.26 and 0.38 V the voltage loss associated with an ionic exchange membrane³¹. The removal of the membrane not only can simplify the construction, operation and maintenance of bioelectrochemical systems, but it also decreases the internal resistance and reduces the gradients of pH, theoretically increasing the output of the system. Throughout this document a membrane-less configuration will be referred to as single chamber system. Any other possible single chamber configuration will be clearly stated.

1.4. Hydrogen production in single chamber microbial electrolysis cells

As introduced before, the production of hydrogen in the cathode is possible under complete anaerobic conditions and supplying an energy input. Although hydrogen production in MEC has the potential to be an interesting technology, this technology still faces some hurdles that prevent the scale-up and the real implementation of the system. The need of high applied voltages and the proliferation of other microbial populations are to date the main weaknesses of this technology³³.

Hydrogen production in MEC from wastewater will only be justified if a positive energy balance exists, i.e. if the energy that can be obtained from hydrogen exceeds the energy supplied to drive the process. As mentioned before, voltage losses increase to a large extent the requirements in applied voltage. Indeed, the voltage applied in MEC to drive hydrogen

production is not reported to be lower than 0.4 V, despite the thermodynamically required voltage of 0.13 V, and most works use between 0.6-1 V of applied voltage.

Hydrogen can potentially be produced in single chamber MEC, being the main advantage of this configuration the decrease in internal resistance and thus the decrease in voltage requirements. The effects of pH gradients are also reduced. The fact that both electrolytes are not physically separated, though, contributes to the growth of microorganisms that do not only compete with ARB for the substrate, but also for hydrogen (Figure 1.5). Methanogenic *archaea* are able to grow in the system consuming acetate (acetoclastic methanogens) and hydrogen (hydrogenotrophic methanogens). As a result of their growth and activity, hydrogen production decreases and the gas obtained is less rich in hydrogen. This represents a loss in terms of energy obtained from MEC, since hydrogen possesses higher combustion energy than methane. It also introduces extra costs when the goal is using hydrogen as a feedstock, since a previous separation process would be necessary. Other hydrogen scavengers like homoacetogenic and hydrogen oxidizing ARB can develop in the system as well, leading to a hydrogen recycling scenario, or what is the same, an electron recycling scenario³⁴ (Figure 1.6). In such situation no net hydrogen production is observed, since hydrogen produced on the cathode can be used by hydrogen oxidizing ARB as the electron donor and it is also consumed by homoacetogenic bacteria to produce acetate. The addition of chemical inhibitors of hydrogen scavengers is not an economically feasible option in view of the scale-up of the process.

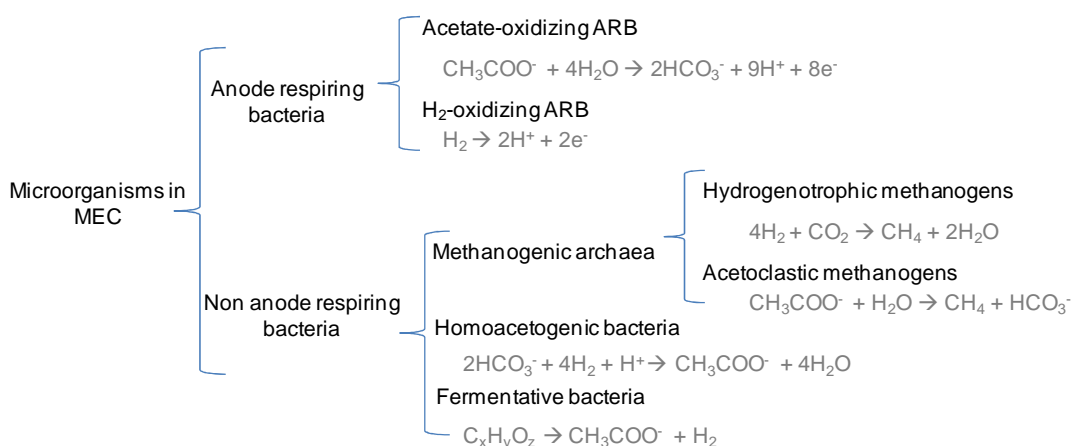


Figure 1.5. Microbial distribution in a single chamber MEC

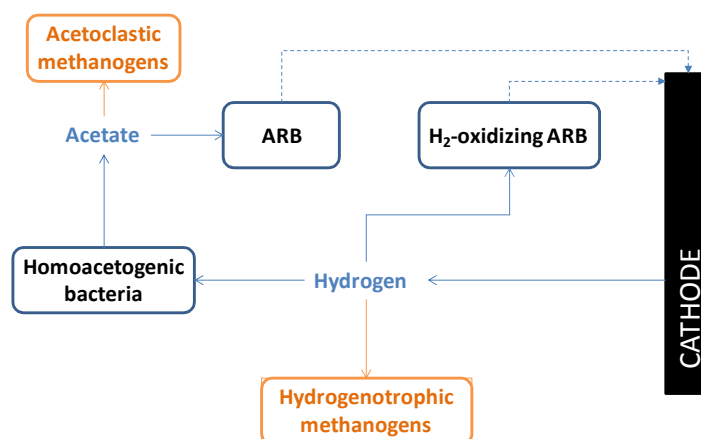


Figure 1.6. Hydrogen and acetate flows leading to the hydrogen recycling scenario in single chamber MEC. Discontinuous line represents the flow of electrons.

Another aspect that limits the implementation of MEC for hydrogen production is the use of electrodes catalyzed by noble metals like platinum, which are highly expensive. Alternatives to platinum such as nickel, alloys like molybdenum disulfide and low cost materials like stainless steel wool have been suggested^{35–37}.

Hitherto the highest hydrogen production in single chamber MEC has been reported by Call and Logan³⁸ ($3.12 \text{ m}^3 \text{ m}^{-3} \text{ d}^{-1}$, $\text{m}^3 \text{ H}_2 \cdot \text{m}^{-3} \text{ reactor} \cdot \text{d}^{-1}$) using a platinum based cathode at 0.8 V of applied voltage. The first trials on single chamber MEC scale-up, either using synthetic or real wastewater, could not avoid methanogenic *archaea* proliferation^{39,40}. In contrast, the maximum hydrogen production in double chamber configuration has been reported by Jeremiasse et al.³⁶ ($50 \text{ m}^3 \text{ m}^{-3} \text{ d}^{-1}$) using a nickel foam cathode at 1 V of applied voltage. First trials on double chamber MEC scale-up have shown high purity hydrogen production, with production of $1\text{--}2.6 \text{ m}^3 \text{ m}^{-3} \text{ d}^{-1}$ from synthetic wastewater (controlled applied voltage, 0.51–0.91 V)⁴¹ and $0.015 \text{ m}^3 \text{ m}^{-3} \text{ d}^{-1}$ from domestic wastewater (1.1 V applied voltage)⁴².

Figure 1.7 summarizes the achievements and relevant applications developed in the field of bioelectrochemical systems since the observation of electroactive microorganisms by Potter. As it can be observed, this is a very recent expanding research field with large possibilities.

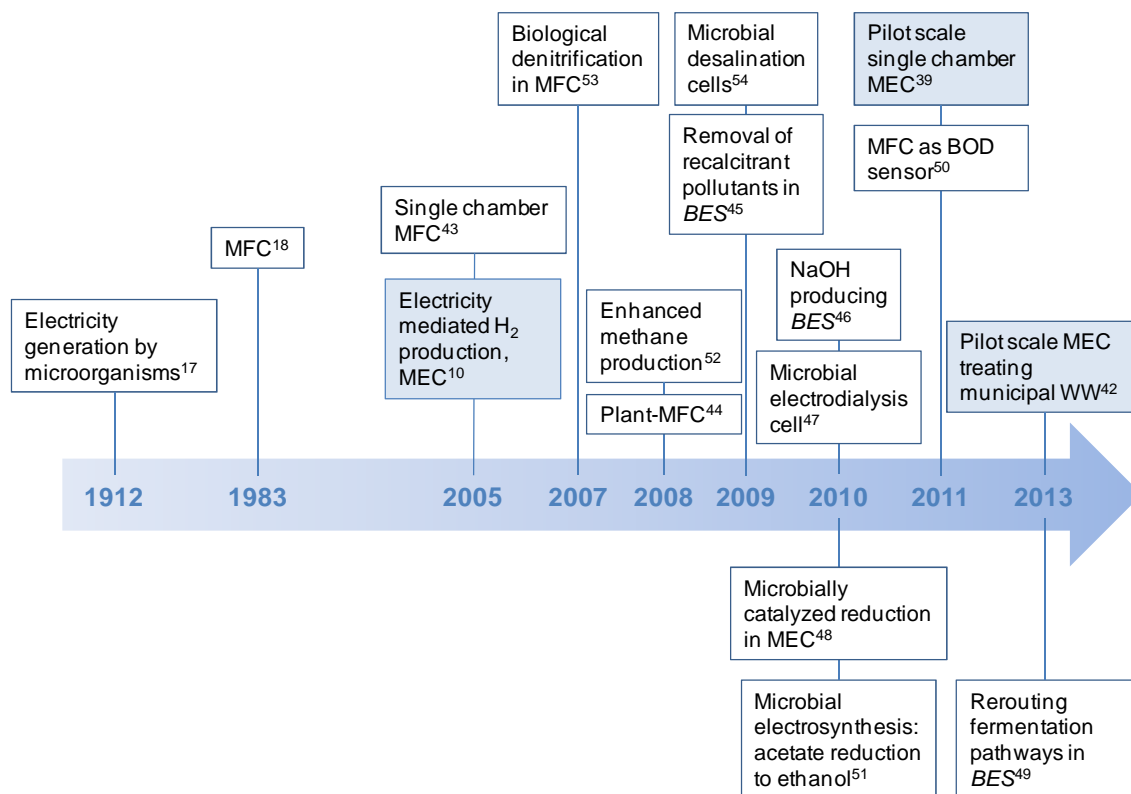


Figure 1.7. Major achievements of bioelectrochemical systems (BES). WW: wastewater. BOD: biological oxygen demand. ^{10,17,18,39,42–54}

This introduction is intended at giving a brief view on bioelectrochemical systems and hydrogen production in MEC. First aid reference literature for a deeper insight into the topic is following recommended for new readers:

For a detailed vision on fundamentals, methodology and applications

- Rabaey, K.; Angenent, L.; Schröder, U.; Keller, J. *Bioelectrochemical Systems: From Extracellular Electron Transfer to Biotechnological Application*; IWA Publishing: London, U.K.; New York, U.S.A., 2009.
- Logan, B. E. *Microbial fuel cells*; Wiley-Interscience: Hoboken, N.J., 2008; p. 200.
- Logan, B. E.; Hamelers, B.; Rozendal, R.; Schröder, U.; Keller, J.; Freguia, S.; Aelterman, P.; Verstraete, W.; Rabaey, K. *Microbial fuel cells: Methodology and technology*. Environ. Sci. Technol. 2006, 40, 5181–5192.

For a first introduction to biological hydrogen production and MEC

- Lee, H.-S.; Vermaas, W. F. J.; Rittmann, B. E. *Biological hydrogen production: prospects and challenges*. Trends Biotechnol. 2010, 28, 262–271.

- Call, D.; Logan, B. E. *Hydrogen production in a single chamber microbial electrolysis cell lacking a membrane*. Environ. Sci. Technol. 2008, 42, 3401–3406.
- Cheng, S.; Logan, B. E. *Sustainable and efficient biohydrogen production via electrohydrogenesis* SCIENCE. 2007, 104, 18871–18873.

For a deep insight on electrochemically active microorganisms

- Lovley, D. R. *Bug juice: harvesting electricity with microorganisms*. Nat. Rev. Microbiol. 2006, 4, 497–508.
- Babauta, J.; Renslow, R.; Lewandowski, Z.; Beyenal, H. *Electrochemically active biofilms: facts and fiction. A review*. Biofouling 2012, 28, 789–812.

For an overview of prospects and challenges

- Clauwaert, P.; Aelterman, P.; Pham, T. H.; De Schamphelaire, L.; Carballa, M.; Rabaey, K.; Verstraete, W. *Minimizing losses in bio-electrochemical systems: the road to applications*. Appl. Microbiol. Biotechnol. 2008, 79, 901–913.
- Zhang, Y.; Angelidaki, I. *Microbial electrolysis cells turning to be versatile technology: Recent advances and future challenges*. Water Res. 2014, 56C, 11–25.

1.5. Research motivations and thesis overview

This thesis is framed in one of the research lines of the GENOCOV group (Research Group on Biological Treatment of Liquid and Gas Effluents) in the Department of Chemical Engineering at the Universitat Autònoma de Barcelona. This group was born in the 1990s with the aim to conduct research on improving the current biological wastewater treatment systems. With the intention to benefit from the chemical and energy content of wastewater, rather than just treating it, a research line on bioelectrochemical systems for hydrogen production from wastewater was created in 2009. This thesis was started on 2010 with the initial goal of testing the feasibility to scale up a single chamber MEC for hydrogen production.

1.5.1. Research motivations

MEC real implementation will only be possible if a positive energy balance between the energy obtained and the energy supplied is achieved. Therefore one of the main hurdles that MEC for hydrogen production needs to overcome is the requirement of high applied voltage that results from voltage losses in the system. A single chamber membrane-less configuration of MEC reduces to large extent the voltage losses and has as advantage the simple construction and operation. A priori, it is therefore a more convenient configuration for scale-up. The main drawback of a single chamber configuration is hydrogen availability for other microorganisms, which decreases hydrogen production and purity. In this thesis, the opportunities for a single chamber membrane-less MEC and the challenges that this system faces motivated the development of bioanodes that could lower the system energy requirements and the development of strategies to decrease hydrogen losses. The fact that the system is aimed at treating wastewater motivated the use of complex carbon sources with different biodegradability. The background and knowledge on process control of the research group also motivated the use of practices that could further be used for process optimization and control, e.g. using an inert gas to decrease hydrogen retention time or monitoring hydrogen production coupling the system to a fuel cell.

1.5.2. Thesis overview

This document is divided into five parts. The first part (*General introduction*), in which this section is included, is the introduction to the topic and the statement of the objectives of this

thesis. The second part (*Materials and methods*) comprises the lab setups description and all common procedures used in this work. The third part (*Results and discussion*) presents in five separate chapters the works developed to fulfill the thesis objectives. A brief introduction to the work and specific methodology have been included. The first chapter of the third part discusses the works aimed at improving the anode inoculation in MFC; the second chapter aims at determining procedures for bioaugmentation of the system with biomass with low energy requirements and biomass able to grow on complex substrates; the third chapter focuses on the minimization of methanogenic populations by reducing hydrogen retention time; the fourth chapter presents a low cost technique to monitor hydrogen production and finally in chapter five the use of a real wastewater is evaluated in bioelectrochemical systems. The fourth part of this thesis (*Conclusions*) summarizes the conclusions drawn from all the work presented. A glossary and list of abbreviations have been included in the fifth part (*Appendix*).

The format and length of this document have the aim of giving the keys to understand the described and discussed experiments performed throughout the research period in order to get a worthy document with “musts” and “must nots” for the following researchers in the group.

Chapter 2. Objectives

This work investigates in those aspects that still prevent the scale-up or that will ease the scale-up of single chamber microbial electrolysis cell for hydrogen production from wastewater. With this aim the following objectives have been set:

- Development of strategies to enhance the growth and activity of electroactive microorganisms on the anode during inoculation.
- Decrease of voltage requirements in MEC by improving inoculation and selection techniques.
- Minimization of methanogenic activity without addition of chemical inhibitors.
- Determination of the opportunities of substrates with different biodegradability to be treated in single chamber MEC for hydrogen production.
- Implementation of low cost techniques for MEC monitoring that enable future process control strategies.

References for Part I: General Introduction

- (1) United Nations Framework Convention on Climate Change. *Kyoto-Protocol*; 1998.
- (2) EU. *European Commission's Second Strategic Energy Review*; 2008.
- (3) <http://epp.eurostat.ec.europa.eu/portal/page/portal/energy>.
- (4) International Energy Agency. *2013 Key World Energy Statistics*; 2013.
- (5) Rozendal, R. A.; Hamelers, H. V. M.; Rabaey, K.; Keller, J.; Buisman, C. J. N. Towards practical implementation of bioelectrochemical wastewater treatment. *Trends Biotechnol.* 2008, 26, 450–459.
- (6) Rabaey, K.; Rozendal, R. A. Microbial electrosynthesis - revisiting the electrical route for microbial production. *Nat. Rev. Microbiol.* 2010, 8, 706–716.
- (7) Lee, H.-S.; Vermaas, W. F. J.; Rittmann, B. E. Biological hydrogen production: prospects and challenges. *Trends Biotechnol.* 2010, 28, 262–271.
- (8) Züttel, A.; Borgschulte, A.; Schlapbach, L. *Hydrogen as a future energy carrier*; Wiley-VCH Verlag: Weinheim, 2008.
- (9) Drapcho, C. M.; Nghim, N. P.; Walker, T. *Biofuels Engineering Process Technology*; McGraw-Hill: New York etc., 2008.
- (10) Liu, H.; Grot, S.; Logan, B. E. Electrochemically assisted microbial production of hydrogen from acetate. *Environ. Sci. Technol.* 2005, 39, 4317–4320.
- (11) Rozendal, R. A.; Buisman, C. J. N. Process for producing hydrogen. Patent WO2005005981, 2005.
- (12) Partnership for Advancing the Transition to Hydrogen (PATH). *Annual Report on World Progress in Hydrogen*; 2011.
- (13) Weissermel, K.; Arpe, H.-J. *Industrial organic chemistry*; Wiley-VCH: Weinheim, 2003.
- (14) Bartacek, J.; Zabranska, J.; Lens, P. N. L. Developments and constraints in fermentative hydrogen production. *Biofuels, Bioprod. Biorefining* 2007, 1, 201–214.
- (15) Riis, T.; Hagen, E.; Vie, J. S. V.; Ulleberg, O.; Sandrock, G. *Hydrogen Production and Storage: R&D Priorities and Gaps*; 2006.
- (16) Bridgwater, A. V. Review of fast pyrolysis of biomass and product upgrading. *Biomass and Bioenergy* 2012, 38, 68–94.

-
- (17) Potter, M. C. Electrical effects accompanying the decomposition of organic compounds. *Proc R Soc London* 1912, 84, 266–276.
- (18) Stirling, J. L.; Bennetto, H. P.; Delaney, G. M.; Mason, J. R.; Roller, S. D.; Tanaka, K.; Thurston, C. F. Microbial fuel cells. *Biochem. Soc. Trans.* 1983, 11, 451–453.
- (19) Bennetto, H. P. Electricity generation by microorganisms. *Biotechnol Edu* 1990, 1, 163–168.
- (20) Lovley, D. R.; Holmes, D. E.; Nevin, K. P. Dissimilatory Fe(III) and Mn(IV) reduction. *Adv. Microb. Physiol.* 2004, 49, 219–286.
- (21) Kim, B. H.; Kim, H. J.; Hyun, M. S.; Park, D. H. Direct electrode reaction of Fe(III)-reducing bacterium, *Shewanella putrefaciens*. *J. Microbiol. Biotechnol.* 1999, 9, 127–131.
- (22) Logan, B. E. Exoelectrogenic bacteria that power microbial fuel cells. *Nat. Rev. Microbiol.* 2009, 7, 375–381.
- (23) Lovley, D. R.; Giovannoni, S. J.; White, D. C.; Champine, J. E.; Phillips, E. J. P.; Gorby, Y. A.; Goodwin, S. *Geobacter metallireducens* gen. nov. sp. nov., a microorganism capable of coupling the complete oxidation of organic compounds to the reduction of iron and other metals. *Arch. Microbiol.* 1993, 159, 336–344.
- (24) Holmes, D. E.; Nevin, K. P.; Lovley, D. R. Comparison of 16S rRNA, *nifD*, *recA*, *gyrB*, *rpoB* and *fusA* genes within the family *Geobacteraceae* fam. nov. *Int. J. Syst. Evol. Microbiol.* 2004, 54, 1591–1599.
- (25) Debabov, V. G. Electricity from microorganisms. *Microbiology* 2008, 77, 123–131.
- (26) Hurst, C. J.; Crawford, R. L. *Manual of environmental microbiology*; 3rd ed.; ASM Press: Washington, 2007; pp. 1137–1146.
- (27) Lovley, D. R. Bug juice: harvesting electricity with microorganisms. *Nat. Rev. Microbiol.* 2006, 4, 497–508.
- (28) Borole, A. P.; Reguera, G.; Ringeisen, B.; Wang, Z.-W.; Feng, Y.; Kim, B. H. Electroactive biofilms: Current status and future research needs. *Energy Environ. Sci.* 2011, 4, 4813.
- (29) Busalmen, J. P.; Esteve-Núñez, A.; Feliu, J. M. Whole Cell Electrochemistry of Electricity-Producing Microorganisms Evidence an Adaptation for Optimal Exocellular Electron Transport. *Environ. Sci. Technol.* 2008, 42, 2445–2450.
- (30) Gil, G.-C.; Chang, I.-S.; Kim, B. H.; Kim, M.; Jang, J.-K.; Park, H. S.; Kim, H. J. Operational parameters affecting the performance of a mediator-less microbial fuel cell. *Biosens. Bioelectron.* 2003, 18, 327–334.

-
- (31) Rozendal, R. A.; Hamelers, H. V. M.; Molenkamp, R. J.; Buisman, C. J. N. Performance of single chamber biocatalyzed electrolysis with different types of ion exchange membranes. *Water Res.* 2007, *41*, 1984–1994.
- (32) Logan, B. E.; Hamelers, B.; Rozendal, R.; Schröder, U.; Keller, J.; Freguia, S.; Aelterman, P.; Verstraete, W.; Rabaey, K. Microbial fuel cells: Methodology and technology. *Environ. Sci. Technol.* 2006, *40*, 5181–5192.
- (33) Zhang, Y.; Angelidaki, I. Microbial electrolysis cells turning to be versatile technology: Recent advances and future challenges. *Water Res.* 2014, *56C*, 11–25.
- (34) Parameswaran, P.; Torres, C. I.; Lee, H. S.; Krajmalnik-Brown, R.; Rittmann, B. E. Syntrophic interactions among anode respiring bacteria (ARB) and Non-ARB in a biofilm anode: electron balances. *Biotechnol. Bioeng.* 2009, *103*, 513–523.
- (35) Tokash, J. C.; Logan, B. E. Electrochemical evaluation of molybdenum disulfide as a catalyst for hydrogen evolution in microbial electrolysis cells. *Int. J. Hydrogen Energy* 2011, *36*, 9439–9445.
- (36) Jeremiasse, A. W.; Bergsma, J.; Kleijn, J. M.; Saakes, M.; Buisman, C. J. N.; Cohen Stuart, M.; Hamelers, H. V. M. Performance of metal alloys as hydrogen evolution reaction catalysts in a microbial electrolysis cell. *Int. J. Hydrogen Energy* 2011, *36*, 10482–10489.
- (37) Ribot-Llobet, E.; Nam, J.-Y.; Tokash, J. C.; Guisasola, A.; Logan, B. E. Assessment of four different cathode materials at different initial pHs using unbuffered catholytes in microbial electrolysis cells. *Int. J. Hydrogen Energy* 2013, *38*, 2951–2956.
- (38) Call, D.; Logan, B. E. Hydrogen production in a single chamber microbial electrolysis cell lacking a membrane. *Environ. Sci. Technol.* 2008, *42*, 3401–3406.
- (39) Cusick, R.; Bryan, B.; Parker, D.; Merrill, M.; Mehanna, M.; Kiely, P.; Liu, G.; Logan, B. Performance of a pilot-scale continuous flow microbial electrolysis cell fed winery wastewater. *Appl. Microbiol. Biotechnol.* 2011, *89*, 2053–2063.
- (40) Rader, G. K.; Logan, B. E. Multi-electrode continuous flow microbial electrolysis cell for biogas production from acetate. *1st Iran. Conf. Hydrog. Fuel Cell* 2010, *35*, 8848–8854.
- (41) Gil-Carrera, L.; Escapa, A.; Mehta, P.; Santoyo, G.; Guiot, S. R.; Morán, A.; Tartakovsky, B. Microbial electrolysis cell scale-up for combined wastewater treatment and hydrogen production. *Bioresour. Technol.* 2013, *130*, 584–591.
- (42) Heidrich, E. S.; Dolfing, J.; Scott, K.; Edwards, S. R.; Jones, C.; Curtis, T. P. Production of hydrogen from domestic wastewater in a pilot-scale microbial electrolysis cell. *Appl. Microbiol. Biotechnol.* 2013, *97*, 6979–6989.

-
- (43) Liu, H.; Cheng, S.; Logan, B. E. Production of electricity from acetate or butyrate using a single-chamber microbial fuel cell. *Environmental Science and Technology*, 2005, 39, 658–662.
- (44) Strik, D. P. B. T. B.; Hamelers, H. V. M.; Snel, J. F. H.; Buisman, C. J. N. Green electricity production with living plants and bacteria in a fuel cell. *Int. J. Energy Res.* 2008, 32, 870–876.
- (45) Mu, Y.; Rozendal, R. A.; Rabaey, K.; Keller, J. Nitrobenzene removal in bioelectrochemical systems. *Environ. Sci. Technol.* 2009, 43, 8690–8695.
- (46) Rabaey, K.; Bützer, S.; Brown, S.; Keller, J.; Rozendal, R. A. High current generation coupled to caustic production using a lamellar bioelectrochemical system. *Environ. Sci. Technol.* 2010, 44, 4315–4321.
- (47) Mehanna, M.; Kiely, P. D.; Call, D. F.; Logan, B. E. Microbial electrodialysis cell for simultaneous water desalination and hydrogen gas production. *Environ. Sci. Technol.* 2010, 44, 9578–9583.
- (48) Jeremiasse, A. W.; Hamelers, H. V. M.; Buisman, C. J. N. Microbial electrolysis cell with a microbial biocathode. *Bioelectrochemistry* 2010, 78, 39–43.
- (49) Dennis, P. G.; Harnisch, F.; Yeoh, Y. K.; Tyson, G. W.; Rabaey, K. Dynamics of cathode-associated microbial communities and metabolite profiles in a glycerol-fed bioelectrochemical system. *Appl. Environ. Microbiol.* 2013, 79, 4008–4014.
- (50) Zhang, Y.; Angelidaki, I. Submersible microbial fuel cell sensor for monitoring microbial activity and BOD in groundwater: Focusing on impact of anodic biofilm on sensor applicability. *Biotechnol. Bioeng.* 2011, 108, 2339–2347.
- (51) Steinbusch, K. J. J.; Hamelers, H. V. M.; Schaap, J. D.; Kampman, C.; Buisman, C. J. N. Bioelectrochemical ethanol production through mediated acetate reduction by mixed cultures. *Environ. Sci. Technol.* 2010, 44, 513–517.
- (52) Clauwaert, P.; Verstraete, W. Methanogenesis in membraneless microbial electrolysis cells. *Appl. Microbiol. Biotechnol.* 2009, 82, 829–836.
- (53) Clauwaert, P.; Rabaey, K.; Aelterman, P.; De Schamphelaire, L.; Pham, T. H.; Boeckx, P.; Boon, N.; Verstraete, W. Biological Denitrification in Microbial Fuel Cells. *Environ. Sci. Technol.* 2007, 41, 3354–3360.
- (54) Cao, X.; Huang, X.; Liang, P.; Xiao, K.; Zhou, Y.; Zhang, X.; Logan, B. E. A New Method for Water Desalination Using Microbial Desalination Cells. *Environ. Sci. Technol.* 2009, 43, 7148–7152.

Part II: Materials and Methods

Chapter 1. Reactor designs and inoculation protocol

1.1. Reactor designs

Sed-MFC

Sed-MFC is based on sediment MFC, also known as benthic MFC. The concept of sediment MFC is quite simple: an anode is placed in an anaerobic sediment and it is electrically connected to a cathode placed in the liquid surface where oxygen is available. Sediments tested in the literature mainly include marine and lake sediments¹⁻⁴. Anaerobic digester sludge has also been presented as sediment in Sed-MFC by Ribot-Llobet et al.⁵.

The design presented by Ribot-Llobet was used in this work as an inoculation configuration (Figure 2.1.1). The Sed-MFC was constructed in a one liter capacity plastic vessel. The anode was a handmade graphite fiber brush constructed by twisting carbon fiber (70 mm diameter x 70 mm length, ~0.8 m² surface area, PANEX33 160K, ZOLTEK, Hungary) with a titanium wire. Once the brush was made, it was thermally treated at 450°C for 30 minutes to increase further microbial adhesion, which was enhanced by the micro fractures produced by the high temperature⁶. The titanium wire was protected with a plastic sheath to avoid direct contact with the cathode. The cathode was commercial steel wool connected to a copper wire. A high specific surface area for both electrodes compensated the overpotential losses associated to a non-catalyzed electrode.

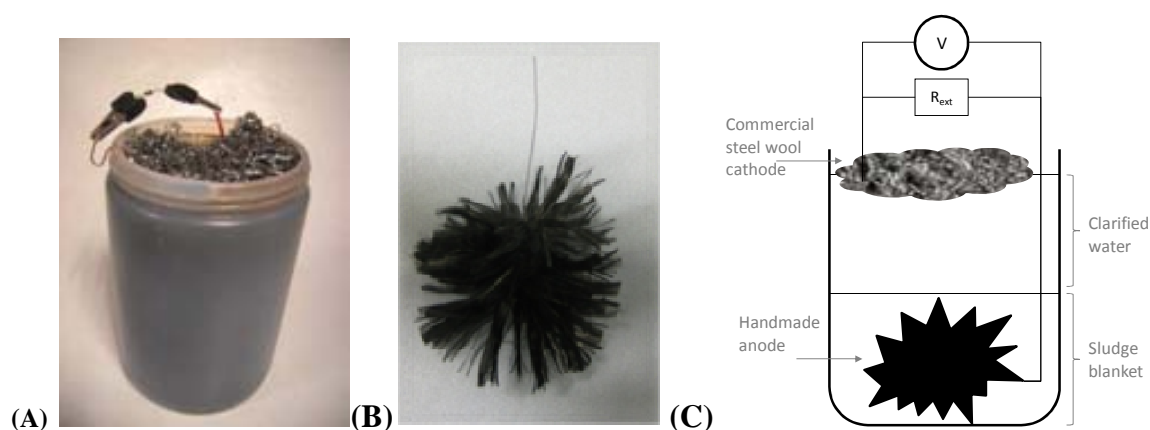


Figure 2.1.1. (A) Sed-MFC (B) Handmade graphite fiber brush (C) Sed-MFC schematics.

500 mL of anaerobic sludge from an anaerobic digester of an urban wastewater treatment plant (Manresa, Catalonia) were used to inoculate the system. Acetate as carbon source,

macronutrients, mineral medium containing micronutrients and a phosphate buffer solution (100 mM) were added. 2-bromoethanesulfonate was used to limit the methanogenic activity (10 mM). The final conductivity was to be between 15-25 mS cm⁻¹ and the pH around 7. The brush was introduced into the vessel with the homogeneous solution and it was left still for one day. After this period, it could be observed that the anaerobic sludge had settled down covering completely the graphite fiber brush. The steel wool was laid on the liquid surface in a manner that one half of it was in clear contact with water, and the other half was exposed to the atmosphere. Finally the circuit was closed connecting the titanium wire from the brush and the copper wire from the steel wool through an electrical resistance (1000 Ω unless otherwise stated).

As Ribot-Llobet reported, the brush anode can be considered to be inoculated after 30 days of fed-batch operation in Sed-MFC. Then the brush can be carefully washed to remove all bacteria that are not attached to the anode surface before the relocation to another MFC or MEC.

The advantages and drawbacks of this design have been listed next:

- + Cheap and simple procedure
- + Mechanical aeration of the cathode is not required
- + Easy accessibility to anaerobic digester sludge
- + Low electrodes activation losses due to high surface area
- Long inoculation period
- Medium evaporation
- Low robustness related to electrodes position and distance between each other
- Signal disturbance due to water or medium addition
- Low current densities due to high electrode specific surface

Y-MEC

Y-MECs were 700 mL glass bottles provided with two separate heads (Figure 2.1.2). Each head was capped with a stopper and a silicone septum, where the electrode connections were pierced through. This design avoided direct contact between the electrodes and therefore short circuit. The anode used in this design was a handmade graphite fiber brush as described for Sed-MFC. The cathode was a platinum plate (4 cm², Panreac Química SA). A nickel-stainless steel commercial steel wool cathode could also be used alternatively as low-priced

cathode. Nickel acts as a catalyst and therefore decreases the overpotential of the plain stainless steel cathode. The cathode was placed in a higher position than the anode favoring hydrogen removal and decreasing the chances for its microbial consumption. Gas samples could be taken directly sampling the headspace. Alternatively the caps could be substituted by gas tight caps which were connected to gas sampling bags (Ritter, Cali-5-bond, Germany). The Y-MEC was magnetically stirred. Both electrodes were connected to a power source (HQ Power, PS-23023) applying the desired potential. Current intensity production in MEC was measured quantifying the voltage drop across a $12\ \Omega$ external resistance serially connected to the circuit.

The advantages and drawbacks of this design have been listed next:

- + Stirring decreases internal resistance of the medium, decreasing mass transport limitations and avoiding local pH changes near the electrodes
- + A nickel-stainless steel commercial steel wool cathode can also be used, which offers a non-expensive cathode catalyst
- Low robustness related to electrodes position and distance between each other
- High hydrogen losses, even with gas tight caps
- Commercial steel wool cathode favors the hydrogen retention in the system and hence the growth of hydrogen scavengers
- Low volume utilization relative to electrode volume

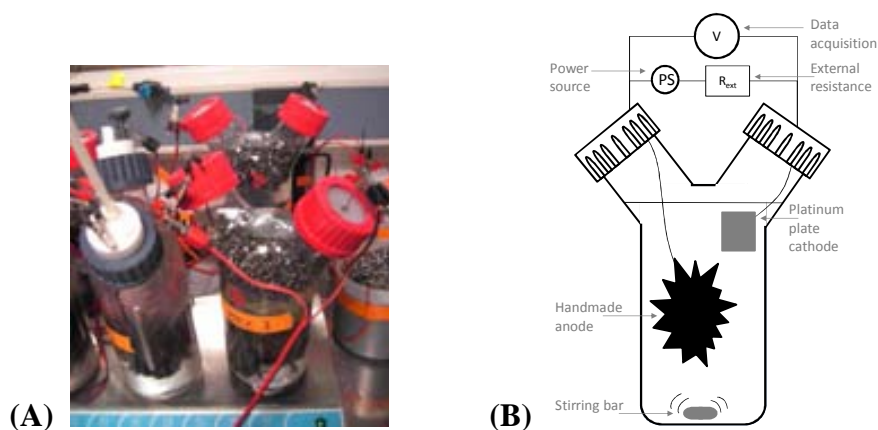


Figure 2.1.2. (A) Lab setup of Y-MEC (B) Y-MEC schematics.

Air cathode MFC (AC-MFC)

Double chamber MFCs have as drawback that external mechanical aeration is required in the cathodic chamber to provide oxygen for the reduction reaction on the cathode. Single

chamber air cathode MFC (AC-MFC) were designed to overcome this external aeration requirement^{7,8}. The basics of this design rely on the modification of the cathode, where a waterproof layer is applied without interfering in the oxygen diffusion into the cathode surface. Additionally a catalyst layer can also be applied in the inner cathode face to increase the cell performance⁸. The addition of an ionic exchange membrane allows to physically separate both the oxidation and the reduction reaction if desired.

In this work, AC-MFCs were single chamber membrane-less MFC (Figure 2.1.3). 400 mL glass vessels were provided with a lateral aperture (6.3 cm of diameter), where a PTFE diffusion layer applied on the outer face of the cathode permitted oxygen diffusion into the cell while preventing water leakage. The anode was a graphite fiber brush with a titanium wire core like the one described before. The titanium wire was pierced on a cap provided with a silicone septum that kept the anode surroundings anaerobic. The cathode consisted in a graphite fiber cloth (7.5 cm diameter) coated with platinum (5 mg Pt cm⁻², ElectroChem Inc., United States). The cathode was clamped in between the glass vessel and a perforated glass endplate with a protruding titanium wire to allow connections. The electrical connection was closed with an external resistance (1000 Ω unless otherwise stated).

The advantages and drawbacks of this design have been listed next:

- + External aeration is not required
- + Platinum increases MFC performance, because it decreases the voltage losses
- + Easy conversion to MEC by exchanging the perforated glass endplate by a non perforated one
- The anode is not in a fixed position, which varies the distance between each electrode
- Stirring is not recommended, since it favors the oxygen diffusion into the anode surroundings, and therefore homogeneity is compromised.

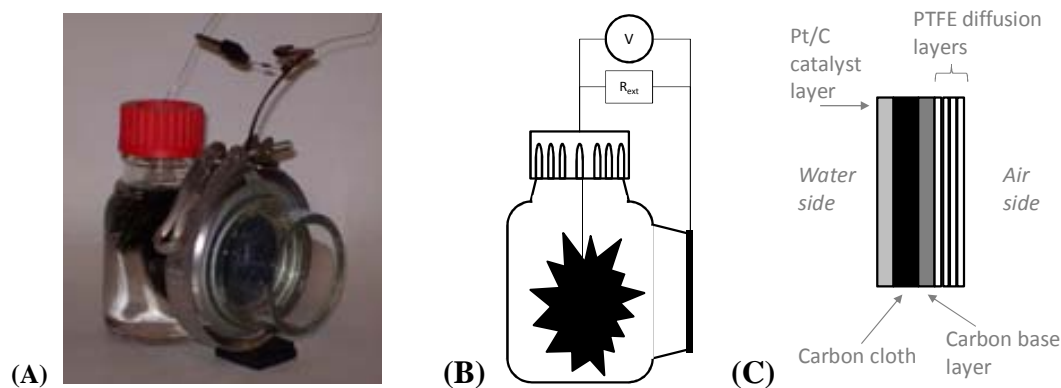


Figure 2.1.3. (A) Lab setup of AC-MFC (B) AC-MFC schematics (C) Cathode cross-cut schematics.

mAC-MFC

The basics of this design were identical to what has been discussed before, although some modifications made it more robust than the previously presented AC-MFC. This design was first presented by Liu and Logan⁹.

mAC-MFC was a 28mL detachable cylindrical methacrylate reactor that could be assembled or disassembled upon convenience (Figure 2.1.4). The body consisted in a methacrylate cube (5 cm x 5 cm x 4.5 cm) where a 3 cm hole was drilled on (Metacrilats Futura, Cornellà del Terri, Catalonia). The cell was assembled with two endplates joined to the body by means of rubber joints and gaskets that avoided liquid leakages. One of the end plates was perforated and clamped the modified carbon cloth cathode (3.8 cm diameter, 7 cm² total exposed area). Bolts and wing nuts kept all pieces together. The body was provided with two orifices to introduce the anode and a reference electrode, which stood tightly by means of a silicone septum. A lateral tiny orifice was used to introduce the protruding titanium wire that allowed the connection with the cathode. A drop of epoxy glue was used to keep the wire in place. In this design the graphite fiber brush anode was industrially made and therefore it had a complete regular shape (20 mm diameter x 30 mm length; 0.21 m², fibers of 7.2 μm diameter PANEX33 160K, ZOLTEK, Hungary). The titanium core of the anode was 2mm diameter, which made the brush completely rigid. Both electrodes were placed 2 cm apart.

The advantages and drawbacks of this design have been listed next:

- + External aeration is not required
- + Very robust design in terms of electrodes position
- + Small size allows to perform many replicates (low investment cost and reactant requirements per cell)

- + Easily convertible to double chamber MFC
- + Easily interchangeable position of electrodes and membranes
- Complicated adaptation to continuous flow operation
- Magnetic stirring is not possible due to the cylindrical shape of the body



Figure 2.1.4. (A) Lab setup of mAC-MFC (B) mAC-MFC schematics.

mMEC

mMEC was an adaptation of mAC-MFC (Figure 2.1.5) and was first presented by Call and Logan¹⁰. In this design, none of the endplates was perforated and, therefore, anaerobic conditions were enhanced. A glass cylinder tightly sealed with a Teflon rubber cap and an aluminum crimp was assembled at the top, which enabled gas collection. The system was filled up to 40 mL to guarantee water sealing on joints and to avoid gas leakage. The gas produced could be further collected in a gas-tight bag connected to the glass cylinder by means of a PVC hosepipe inserted into the rubber cap or by means of a hosepipe with needles on both ends that could be pierced in the MEC headspace and the gas bag.

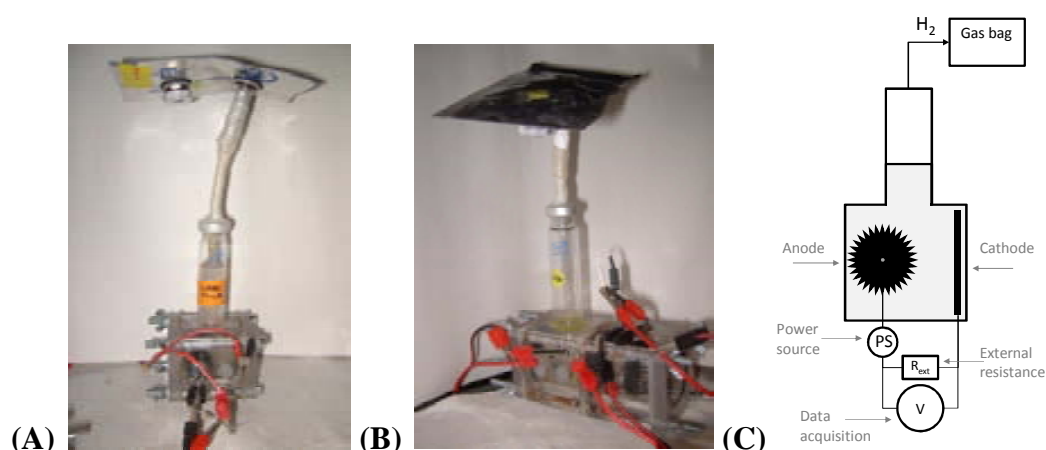


Figure 2.1.5. (A) Lab setup of single chamber mMEC (B) Lab setup of double chamber mMEC (C) Single chamber mMEC schematics.

The advantages and drawbacks of this design have been listed next:

- + Very robust design in terms of electrodes position
- + Small size allows to perform many replicates
- + Easily convertible to double chamber MEC
- + Easily interchangeable position of electrodes and membranes
- Complicated adaptation to continuous flow operation
- Magnetic stirring is not possible due to the cylindrical shape of the body

A common element in all designs defined before was the graphite fiber brush. Graphite is an interesting material for MFC and MEC because of being an inexpensive material with high conductivity. The brush shape allows a high surface area for the exoelectrogenic biofilm to develop. Nevertheless, it must be taken into account that not all the perimeter of the graphite fiber brush will be equally covered by the biofilm. Indeed, most biological density will most probably be found in the tips of those fibers where the distance to the cathode is the shortest possible. Alternatives to maximize the area of effective bioanode are: (i) working with half brush anode (ii) placing anode and cathode in a concentrically manner and (iii) working with a flat anode.

1.2. Inoculation protocol

Pure strains of exoelectrogenic bacteria have been isolated^{11–13}. However electroactivity has been observed to be lower in these pure cultures than for mixed cultures, where a synergy among microbial populations is most likely to contribute to higher outputs^{14–16}.

A variety of mixed culture sources have been used in the literature as successful inoculum for bioelectrochemical systems (marine and lake sediments, anaerobic digestion sludge, municipal wastewater...) indicating the ubiquitous presence of microorganisms with exoelectrogenic characteristics¹⁷. Anaerobic environments though, seem to offer a better location for exoelectrogenic bacteria to grow, since in absence of electron acceptors like oxygen, nitrate or sulphate the use of an external metallic compound can be one of the possible metabolic route left.

Inoculation with anaerobic digestion sludge was a common practice in this work. Such an inoculation source has as main drawback in this technology that methanogenic archaea are highly present, which in MFC can decrease the portion of substrate that is devoted to electricity production by anode respiring bacteria. On the other hand, methanogenic archaea

presence in MEC is a completely undesired situation, since they not only compete for the substrate (acetate) but also for the product (hydrogen).

Techniques to avoid methanogenic activity and growth will need to be applied when using anaerobic digestion sludge as inoculum, which at lab scale is most commonly addressed by adding methanogenic chemical inhibitors (e.g. sodium 2-bromoethanesulfonate).

Inoculation can also be expedited using as inoculum wastewater from an already running MFC. This allows a rapid bioaugmentation of the system, that can be further reinoculated until the signal response reaches its maximum. It must be noted that only microorganisms in suspension will be used as inoculum ($\sim 85 \text{ mg VSS} \cdot \text{L}^{-1}$ in a regular AC-MFC) and they will be cells that have been detached from the anodic biofilm, anode respiring bacteria that can use indirect electron transfer mechanisms (e.g. use of electron shuttles) and a mixed microbial population without electroactivity (heterotrophic bacteria, anaerobic and aerobic).

A consortium can also be developed so that a specific wastewater can be treated in bioelectrochemical systems. In this way, the system is bioaugmented in those microbial populations that, thanks to their synergistic interactions, allow the treatment of specific substrates. Fermentative bacteria able to hydrolyze and convert a substrate to volatile fatty acids can be cultured separately and then added to a bioelectrochemical system already enriched in exoelectrogenic bacteria.

Chapter 2. Media and analytical techniques

2.1. Synthetic media description

The synthetic medium used in this work was defined according to Parameswaran et al.¹⁸. It was intended that the macronutrients solution was not lacking for compounds like nitrogen and iron. Nitrogen was important in terms of its requirement in the protein structures, main structure in bacterial nanowires. Iron is the central atom in the group heme from cytochromes (Figure 2.2.1A), essential proteins for electron transfer. Electron transfer in bacterial nanowires has been reported to consist in a hopping/tunneling between cytochromes¹⁹ as schematized in Figure 2.2.1B. The reduced form of iron (Fe^{2+} instead of Fe^{3+}) and sulfur (S^{2-} instead of SO_4^{2-}) was added to avoid their use as electron acceptor.

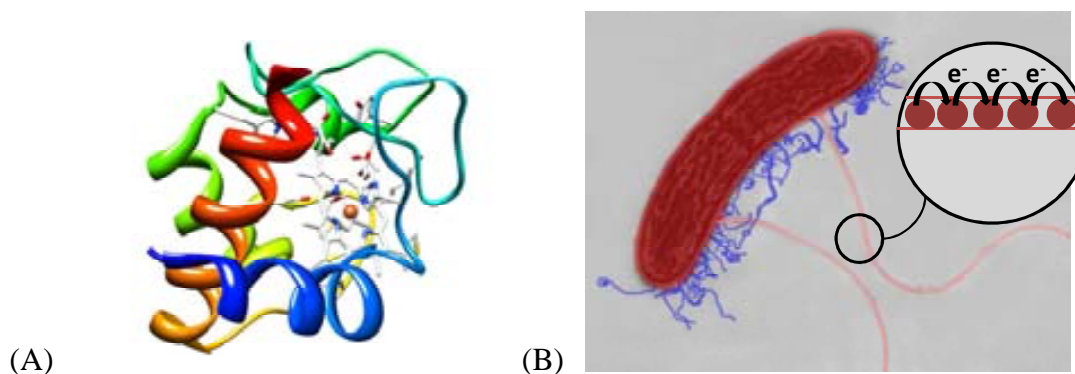


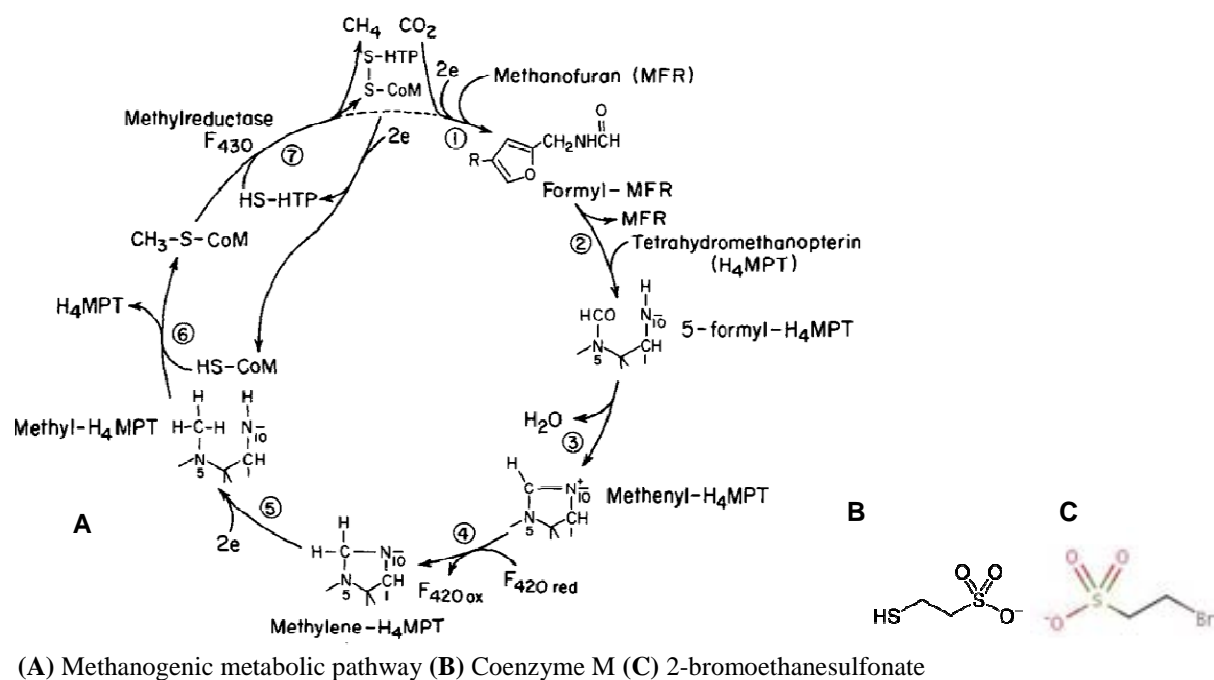
Figure 2.2.1. (A) Schematics of a cytochrome with the central iron atom (B) Schematics of a detail of a nanowire in *Geobacter sulfurreducens* (edited with permission of Dr. Lovley).

The **macronutrients solution** contained per liter: 0.2 g NH_4Cl , 4 mg FeCl_2 , 6 mg Na_2S , 5 mL of mineral media solution and 172 mL phosphate buffer solution (100 mM). 0.41 g L^{-1} NH_4Cl were added in the work of Parameswaran et al., but inhibition was observed with such concentration. Tests adding up to 0.28 g L^{-1} did not seem to inhibit the process. This solution was kept at 4°C once it prepared.

Sodium 2-bromoethanesulfonate (BES) was added when necessary to the macronutrient solution to chemically inhibit methanogenic growth and activity. Concentration ranged between 10 mM and 60 mM.

Box 2.1. | Methanogenesis inhibition by 2-bromoethanesulfonate^{20,21}

Methanogenic archaea have a unique coenzyme called coenzyme M (2-mercaptoethanesulfonic acid, HS-CoM), which is related to methyl transfer. Being of crucial importance in methanogens physiology, the reductive demethylation of one of its derivatives (2-methylthioethanesulfonic acid, CH₃-S-CoM) catalyzed by the enzyme methyl-CoM methylreductase is the methane-forming reaction in all methanogenic archaea. 2-bromoethanesulfonate binds to methylreductase (a membrane bound enzymatic system), avoiding methane formation. Several analogs have been found to be methylreductase inhibitors (e.g. 2-propanesulfonate), being the most efficient 2-bromoethanesulfonate.



The **mineral medium solution** contained per liter: 1 g EDTA, 0.164 g CoCl₂·6H₂O, 0.228 g CaCl₂·2H₂O, 0.02 g H₃BO₃, 0.04 g Na₂MoO₄·2H₂O, 0.002 g Na₂SeO₃, 0.02 g Na₂WO₄·2H₂O, 0.04 g NiCl₂·6H₂O, 2.32 g MgCl₂, 1.18 g MnCl₂·4H₂O, 0.1 g ZnCl₂, 0.02 g CuSO₄·5H₂O and 0.02 g AlK(SO₄)₂.

The stock **phosphate buffer solution (PBS)** contained per liter 70 g Na₂HPO₄ and 12 g KH₂PO₄. PBS stock solution was defined based on solubility of Na₂HPO₄ at 25°C (K_{ps} = 77 g L⁻¹). The buffer solution maintains its capacity for pH in between 6.5 and 8 as shown in Figure 2.2.2.

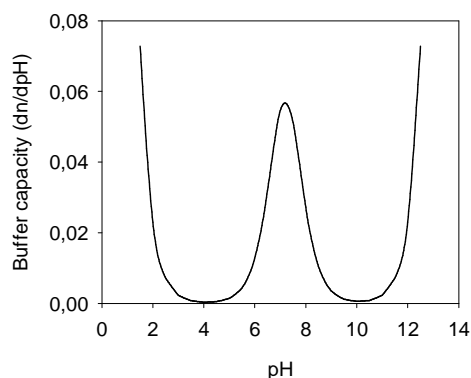


Figure 2.2.2. Buffer capacity for the phosphate buffer solution 100 mM ($\text{pK}_a (\text{H}_2\text{PO}_4^- \leftrightarrow \text{HPO}_4^{2-} + \text{H}^+) = 7.2$). n indicates the equivalents of strong acid or base added per liter of solution.

2.2. Analytical methods

Volatile fatty acids

VFAs concentration (acetate, propionate, butyrate and valerate) was analyzed with gas chromatography (Agilent Technologies, 7820-A) using a nitroterephthalic acid modified PEG capillary column (30 m x 250 μm x 0.25 μm ; length x internal diameter x film thickness) and a flame ionization detector. A sample of 1 μL was injected (liner 5183-4711, Agilent) at a temperature of 275°C under split conditions (29 psi). The carrier gas was helium with a split ratio of 10:1. The oven temperature was set to 85°C for 1min, followed by a first increase of 3°C min⁻¹ until the stable value of 130°C was reached and then 35°C min⁻¹ up to 220°C. The detector temperature was set at 275°C, with 350 mL min⁻¹ air, 40 mL min⁻¹ hydrogen and 30 mL min⁻¹ makeup gas (helium) supplied. The run time was 18 min.

In the procedure followed for sample preparation, 0.6 mL of sample was pipetted to a 1.5 mL glass vial. 0.15 mL of a preserving solution and 0.75 mL of deionized water were added to the vial, which was kept at -20°C until analyzed. The preserving solution added was meant to deproteinize the sample and to be used as internal standard. It contained per liter of solution: 2 g HgCl₂, 33.7 g orthophosphoric acid and 2 g of hexanoic acid. Sonication of the solution in an ultrasonic bath is recommended to obtain complete dissolution. Hexanoic acid acted as internal standard in the peaks quantification analysis.

Chemical Oxygen Demand

Chemical oxygen demand (COD) was analyzed by oxidation with potassium dichromate (catalyzed by silver sulphate) in acidic conditions at 150°C for 2 h (commercial test tubes,

LCK 714 100-600 mg O₂ L⁻¹, Hach Lange). The change in dichromate concentration was measured colorimetrically (spectrophotometer VIS DR 2800, Hach Lange).

Methanol, glycerol, glucose and lactate

Methanol concentration was determined by gas chromatography using an Innowax column (30 m x 250 µm x 0.25 µm; length x internal diameter x film thickness) and the flame ionization detector. A sample of 1 µL was injected at a temperature of 50°C under pulsed split conditions (15 psi). The carrier gas was helium with a split ratio of 20:1 at 1.2 psi, the column temperature was set at 45°C for the first 5 min, followed by an increase of 20°C min⁻¹ until the stable value of 110°C was reached. A cleaning step at 230°C during 5 min was used to remove any residue in the column. The detector temperature was set at 300°C. The run time was 20 min.

Glycerol concentration was quantified in 0.22 µm filtered samples by high performance liquid chromatography (HPLC, Dionex Ultimate 3000). The injection volume was 20 µL and a 6 mM sulphuric acid solution with a flow rate of 0.6 mL min⁻¹ was the mobile phase. The temperature was set to a constant value of 40°C. The instrument used an ionic exchange column (ICSep ICE-COREGEL 87H3, Transgenomic) and it was provided with a refractive index detector. The run time was 20 min.

Glucose and lactate were measured with YSI biochemistry analyzer (2700 SELECT Biochemistry Analyzer).

Hydrogen, oxygen, nitrogen and methane

Hydrogen and methane were also measured with gas chromatography using a HP-mole sieve column (30 m x 320 µm x 12 µm; length x internal diameter x film thickness) and a thermal conductivity detector. A sample of 1 mL was manually injected with a gas tight syringe (1 mL samplelock syringe, Hamilton) at a temperature of 200°C (liner 5183-4647, Agilent) under split conditions (7.2 psi). Hydrogen and helium possess very similar thermal conductivities, therefore the carrier gas was changed to argon (split ratio of 44:1). The oven temperature was set to a constant temperature of 40°C. The detector temperature was set at 220°C, with 20 mL min⁻¹ reference flow (argon) and negative polarity signal. The run time was 6 min.

Gas quantification was performed according to the procedure presented by Ambler and Logan²², following a double run methodology. In this methodology, the sample is analyzed in a first run, then a known volume of nitrogen is added as a reference compound and the resulting mixture is again analyzed. Mass balances calculations including the change in sample composition and the volume added allow the calculation of the initial gas volume as presented by Equation 2.1. A detailed development of the calculations has been included in Box 2.2.

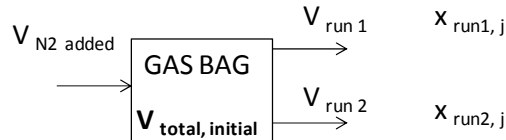
$$V_{\text{total,initial}} = \frac{V_{\text{added,N}_2}(1-x_{\text{run 2,N}_2}) + V_{\text{run 1}}(x_{\text{run 2,N}_2} - x_{\text{run 1,N}_2})}{x_{\text{run 2,N}_2} - x_{\text{run 1,N}_2}} \quad (\text{Equation 2.1})$$

where $V_{\text{total,initial}}$ is the initial total gas volume in the bag, $V_{\text{added,N}_2}$ is the known volume of nitrogen added, $V_{\text{run 1}}$ is the volume injected in the GC in the first analysis, and x is the molar fraction of nitrogen in the first analysis or the second as indicated on the subscript.

The output of gas chromatography analyses is the volumetric fraction (or molar fraction) per compound, thus, knowing the total initial volume, the initial volume per compound can be calculated.

Box 2.2. Equation development for gas quantification

The gas bag can be seen as:



where $V_{\text{run 1}}$ is the volume injected in the GC in the first analysis

$V_{\text{added,N}_2}$ is the known volume of nitrogen added

$V_{\text{run 2}}$ is the volume injected in the GC in the second analysis

$V_{\text{total,initial}}$ is the initial total gas volume in the bag

$x_{\text{run\#,j}}$ is the molar fraction of j compound in each analysis

The final volume of nitrogen in the gas bag can be expressed as:

$$V_{\text{final,N}_2} = V_{\text{initial,N}_2} + V_{\text{added,N}_2} - V_{\text{run1,N}_2} - V_{\text{run2,N}_2}$$

Dividing both sides of the equation by the final total volume of the gas ($V_{\text{total,final}}$):

$$\frac{V_{\text{final,N}_2}}{V_{\text{total,final}}} = x_{\text{run2,N}_2} = \frac{V_{\text{initial,N}_2} + V_{\text{added,N}_2} - V_{\text{run1,N}_2} - V_{\text{run2,N}_2}}{V_{\text{total,final}}}$$

The term of $V_{\text{total,final}}$ can be further developed:

$$x_{\text{final},N2} = \frac{V_{\text{initial},N2} + V_{\text{added},N2} - V_{\text{run1},N2} - V_{\text{run2},N2}}{V_{\text{total,initial}} + V_{\text{added},N2} - V_{\text{run1}} - V_{\text{run2}}}$$

The equation is rearranged in view of isolating $V_{\text{total,initial}}$:

$$x_{\text{run2},N2} [V_{\text{total,initial}} + V_{\text{added},N2} - V_{\text{run1}} - V_{\text{run2}}] = V_{\text{initial},N2} + V_{\text{added},N2} - V_{\text{run1},N2} - V_{\text{run2},N2}$$

where $V_{\text{initial},N2}$ can be expressed as: $V_{\text{initial},N2} = V_{\text{total,initial}} \cdot x_{\text{run1},N2}$

$$\begin{aligned} V_{\text{total,initial}} \cdot x_{\text{run2},N2} + V_{\text{added},N2} \cdot x_{\text{run2},N2} - V_{\text{run1}} \cdot x_{\text{run2},N2} - V_{\text{run2}} \cdot x_{\text{run2},N2} = \\ = V_{\text{total,initial}} \cdot x_{\text{run1},N2} + V_{\text{added},N2} - V_{\text{run1},N2} - V_{\text{run2},N2} \end{aligned}$$

$$\begin{aligned} V_{\text{total,initial}} (x_{\text{run2},N2} - x_{\text{run1},N2}) = \\ = V_{\text{added},N2} - V_{\text{run1},N2} - V_{\text{run2},N2} \\ - [V_{\text{added},N2} \cdot x_{\text{run2},N2} - V_{\text{run1}} \cdot x_{\text{run2},N2} - V_{\text{run2}} \cdot x_{\text{run2},N2}] \end{aligned}$$

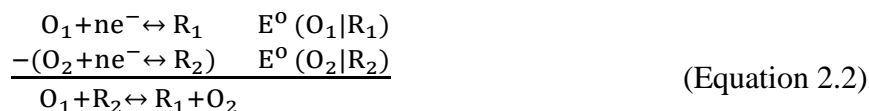
$$V_{\text{total,initial}} = \frac{V_{\text{added},N2} - V_{\text{run1},N2} - V_{\text{run2},N2} - V_{\text{added},N2} \cdot x_{\text{run2},N2} + V_{\text{run1}} \cdot x_{\text{run2},N2} + V_{\text{run2}} \cdot x_{\text{run2},N2}}{x_{\text{run2},N2} - x_{\text{run1},N2}}$$

Since $V_{\text{run2},N2} = V_{\text{run2}} \cdot x_{\text{run2},N2}$ both terms cancel, arriving to the expression presented in Equation 2.1.

Chapter 3. System thermodynamics and parameters to report system efficiency

3.1. Thermodynamics and the electromotive force

In an electrochemical system, a reduction reaction is coupled with an oxidation reaction:



where O is an oxidizing species that gains n electrons to become R, a reducing species. That the overall reaction $O_1 + R_2 \leftrightarrow R_1 + O_2$ occurs in one direction or the other depends on the system thermodynamics.

Thermodynamics of the overall reaction can be evaluated in terms of Gibbs free energy, which is a measure of the maximal work that can be derived from the reaction, calculated as:

$$\Delta G_r = \Delta G_r^0 + RT \ln(\Pi) \quad (\text{Equation 2.3})$$

where ΔG_r (J) is the Gibbs free energy for the specific conditions, ΔG_r^0 (J) is the Gibbs free energy under standard conditions (298.15 K, 1 atm and 1 M concentration for all species), R (8.31447 J mol⁻¹ K⁻¹) is the universal gas constant, T (K) is the absolute temperature and Π is the reaction quotient calculated as the activities of the products divided by those of the reactants. The standard reaction Gibbs free energy is calculated from tabulated energies of formation.

The overall cell electromotive force (emf), E_{emf} (V), is defined as the potential difference between the cathode and the anode:

$$E_{\text{emf}} = E_{\text{cathode}} - E_{\text{anode}} \quad (\text{Equation 2.4})$$

E_{emf} is related to the work produced by the cell, W(J), and thus the thermodynamics of the overall reaction as

$$W = E_{\text{emf}}Q = -\Delta G_r \quad (\text{Equation 2.5})$$

where Q is the charge transferred in the reaction (C). E_{emf} is positive for a thermodynamically favored process and vice versa.

The difference between the measured cell voltage and the cell emf is generally referred to as overvoltage or voltage losses and it is the sum of the overpotentials of the electrodes and the ohmic loss of the system.

$$E_{\text{cell}} = E_{\text{emf}} - (\Sigma\eta_a + |\Sigma\eta_c| + IR_{\Omega}) \quad (\text{Equation 2.6})$$

where $\Sigma\eta_a$ and $|\Sigma\eta_c|$ are the overpotentials of the anode and the cathode respectively, and IR_{Ω} is the sum of all ohmic losses which are proportional to the generated current intensity (I) and ohmic resistance of the system (R_{Ω}). The absolute value in cathode overpotentials takes into account the decrease in potential that this electrode experiences. In contrast anode potential increases as a result of voltage losses.

The cell voltage that is measured after some time in the absence of current intensity is known as open circuit voltage (OCV). OCV should approach the cell emf, but it is substantially lower due to current independent electrode overpotentials. The cell voltage can be thus described as:

$$E_{\text{cell}} = \text{OCV} - IR_{\text{int}} \quad (\text{Equation 2.7})$$

where IR_{int} is the sum of all internal losses, which are proportional to the generated current intensity (I) and the internal resistance of the system (R_{int}).

The potential of each half cell reaction, i.e. the oxidation and the reduction reaction separately, can be calculated according to Nernst equation:

$$E = E^{\circ} - \frac{RT}{nF} \ln (\Pi) \quad (\text{Equation 2.8})$$

where E° is the standard electrode potential (V), which by convention is reported as a reduction potential and can be found tabulated relative to the standard hydrogen electrode (SHE), which has a potential of zero at standard conditions ((298.15K, 1atm and $[H^+] = 1M$)). R ($8.31447 \text{ J mol}^{-1} \text{ K}^{-1}$) is the universal gas constant, T (K) is the absolute temperature, n is the number of electrons exchanged in the reaction, F is Faraday's constant ($96485.3 \text{ C mol}^{-1}$) and Π is the reaction quotient calculated as the activities of the products divided by those of the reactants.

3.2. Reporting system performance and efficiency

Cell intensity and power are calculated based on voltage monitored according to Ohm's law (Equations 2.9, 2.10):

$$I = V/R_{\text{ext}} \quad (\text{Equation 2.9})$$

$$P = V \cdot I \quad (\text{Equation 2.10})$$

where V is the voltage drop in the resistance (V), R_{ext} is the external resistance (Ω), I is the current intensity (A) and P is the power output (W). Maximum power output (P_{max}) is calculated with Equation 2.10 considering the maximum voltage reached during a batch cycle.

Coulombic efficiency (CE) defines the ratio of coulombs contained in the substrate consumed that are recovered as current intensity and it is calculated as stated in Equation 2.11:

$$CE = \frac{\int_{t_0}^t I(t) dt}{F \cdot b \cdot \Delta S \cdot V_R} \quad (\text{Equation 2.11})$$

where t is time (s), F is Faraday's constant (96485 C/mol- e^-), b is the stoichiometric number of electrons produced per mol of substrate (e.g. 8mol e^- /mol acetate), ΔS is the substrate consumption (mol/L) and V_R the liquid volume (L). For a mixed substrate CE can be calculated based on COD consumption ($b = 4\text{mol-}e^-/\text{mol O}_2$).

Cathodic gas recovery (r_{CAT}) is calculated as the ratio of moles of hydrogen measured and moles of hydrogen that can be produced based on current intensity measured, as presented in Equation 2.12:

$$r_{\text{CAT}} = \frac{n_{\text{H}_2}}{\frac{\int_{t_0}^t I(t) dt}{2F}} \quad (\text{Equation 2.12})$$

where n_{H_2} is the number of moles of hydrogen measured and is calculated according to the ideal gases law ($PV = nRT$) knowing the hydrogen volume measured. 2 is the number of moles of electrons per mole of hydrogen.

The overall efficiency (r_{H_2}) is calculated as stated in Equation 2.13:

$$r_{\text{H}_2} = r_{\text{CAT}} \cdot CE \quad (\text{Equation 2.13})$$

Energy recovery, i.e. the amount of energy added to the circuit by the power source and the substrate that is recovered as hydrogen, is calculated based on electricity input (η_w) and based on both electricity and substrate inputs (η_{ws}) according to Equations 2.14 and 2.15 respectively.

$$\eta_w = \frac{n_{\text{H}_2}}{n_{\text{in}}} \quad (\text{Equation 2.14})$$

where n_{in} is the number of moles based on electricity input, calculated as:

$$n_{in} = \frac{\int_{t_0}^t (I \cdot E_{ps} - I^2 R_{ext}) dt}{\Delta H_{H_2}}$$

where E_{ps} is the voltage applied (V), R_{ext} is the external resistance (Ω) and ΔH_{H_2} is the heat of combustion for hydrogen (286 kJ/mol). 286 kJ/mol is the upper heating value for hydrogen and it assumes water in the liquid phase, while a lower heating value of 242 kJ/mol is based on water in the gas phase.

$$\eta_{ws} = \frac{\Delta H_{H_2} \cdot n_{H_2}}{\int_{t_0}^t (I \cdot E_{ps} - I^2 R_{ext}) dt + \Delta H_S \cdot n_S} \quad (\text{Equation 2.15})$$

where ΔH_S is the heat of combustion of the substrate and n_S is the number of moles of substrate consumed during the period of time considered.

It must be noted that the different efficiencies presented here are considered as an average value in batch systems, whereas strictly they should be time dependant parameters.

Table 2.1 summarizes for different substrates used in this work the physicochemical properties that are used for the calculations described before.

Table 2.1. Summary of some physicochemical properties for different substrates

Substrate, S	b (mol e ⁻ /mol S)	$\Delta H_{C,S}$ (kJ/mol S) ²³	COD (gO ₂ /g S)	MW (g S/mol S)
Acetate	8	-870	1.084	59
Propionate	14	-1528	1.513	73.1
Methanol	6	-638	1.500	32
Glycerol	14	-1654	1.216	92.1
Glucose	24	-2812	1.067	180.1

Chapter 4. Electrochemical techniques

4.1. Polarization and power curve

MFC internal resistance (R_{int}) and maximum power output (P_{max}) are assessed from polarization curves. The polarization curve was performed allowing the cell (with substrate availability) to reach the open circuit voltage for a period of one hour and then progressively changing the external resistance (from high to low resistance) and measuring the cell voltage after 10 min. The voltage measured after 10 min was assumed to have reached a stationary response. The set of external resistances used for the polarization curves in this work were 470 k Ω , 218 k Ω , 44.2 k Ω , 24.1 k Ω , 12.1 k Ω , 6600 Ω , 3300 Ω , 2000 Ω , 1650 Ω , 1000 Ω , 825 Ω , 470 Ω , 250 Ω , 218 Ω , 100 Ω , 50 Ω and 25 Ω .

In a polarization curve three different trends of current intensity relative to cell voltage are observed (Figure 2.4.1A). These differences are due to voltage losses associated with phenomena of different nature. Part I of a polarization curve, at low current intensities, is mainly dominated by activation losses associated to the activation energy of the oxidation/reduction reactions; part II of a polarization curve is affected by ohmic losses associated to the resistance to the flow of electrons through the electrodes and electrical connections, and the resistance to the flow of ions through the ionic exchange membrane (if present) and the electrolytes; finally, part III of a polarization curve, for high current intensities, is mainly limited by the rate of mass transport to or from the electrode.

R_{int} was calculated as the slope in part II of a polarization curve, where cell voltage and current intensity follow a linear trend and voltage limitations are mainly caused by ohmic losses. Maximum attainable power output was estimated according to the power curve (Figure 2.4.1B).

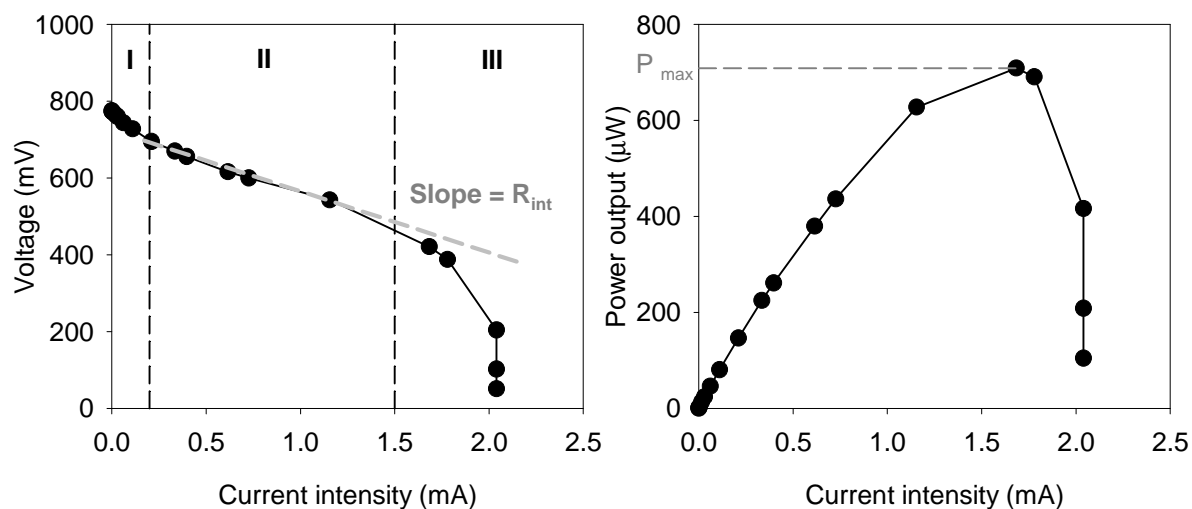


Figure 2.4.1. (A) Example of a polarization curve in a MFC (B) Example of a power curve in a MFC.

Box 2.3| Optimum external resistance coincides with internal resistance?

Assuming that voltage variation versus current intensity is linear in the part where voltage losses are dominated by ohmic losses being the slope R_{int} :

$$\frac{dV}{dI} = R_{int}$$

The variation of power vs. current intensity can be expressed as:

$$\frac{dP}{dI} = \frac{d(V \cdot I)}{dI} = I \cdot \frac{dV}{dI} + V \cdot \frac{dI}{dI} = I \cdot R_{int} + V$$

When $P = P_{max}$: $R_{int} = R_{ext}$?

$$\frac{dP}{dI} = 0 = I \cdot R_{int} + V$$

$$V = -I \cdot R_{int}$$

$$\frac{V}{I} = -R_{int}$$

According to Ohm's law $V = I \cdot R_{ext}$

$$\frac{V}{I} = R_{ext} = -R_{int}$$

$$|R_{ext}| = |R_{int}|$$

4.2. Cyclic voltammetry

Cyclic voltammetry is an electrochemical technique that is used to characterize the electron transfer process and is widely used in studies with bioelectrochemical systems to describe the biocatalyzed electrode/s^{24,25}. The method is commonly performed in a three electrode configuration, where the electrode to study is the working electrode, whose potential is varied

according to a reference electrode, and the response relative to a counter electrode is monitored. The cyclic voltammetry analysis consists in varying the working electrode potential in a ramped linear fashion with time (Figure 2.4.2A), and monitoring the system response in terms of current intensity (Figure 2.4.2B). The fact that this scan in electrode potential is performed in the two possible directions, i.e. increasing and decreasing the working electrode potential (forward and reverse scan), results in a cyclic response of current intensity (Figure 2.4.2C), that gives the name to the technique. Important parameters to set for this electrochemical analysis are the scan rate (mV/s) and the initial (E_i), the switching (E_s) and the final potentials (E_f)²⁶. If the scan rate is too fast, it can exceed the whole process rate, and the signal observed can be far from a steady response. In the final voltammogram a steady current intensity known as limit current intensity (I_{lim}) is achieved. Current intensity peaks can be observed in the forward and reverse scans which are result from the oxidation and reduction reactions. Oxidation and reduction peak position is related to the potential of the enzyme involved in the last step of the metabolic pathway (responsible of the extracellular electron transfer), which differs from one organism to another²⁷.

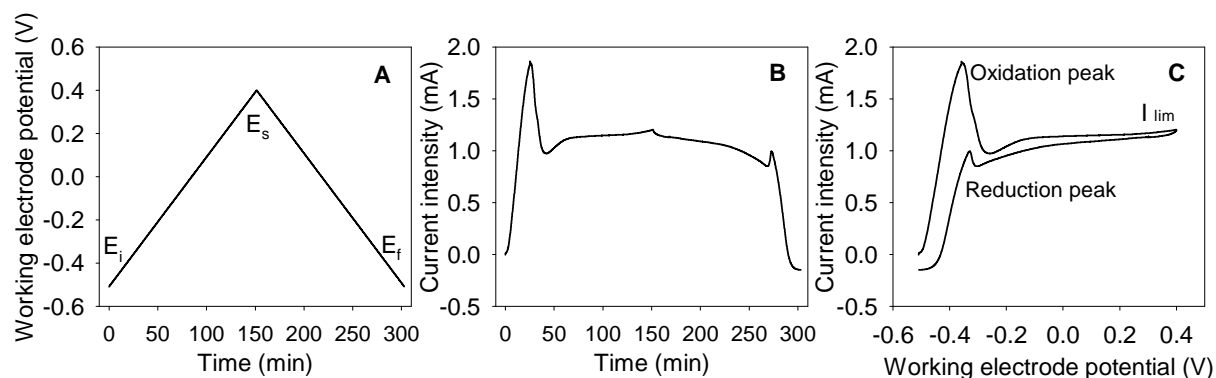


Figure 2.4.2. Example of a cyclic voltammetry analysis (A) Linear ramp sweep on the working electrode potential (B) Current intensity response vs. time (C) Cyclic voltammogram.

A silver-silver chloride reference electrode (NaCl 3 M, 209 mV vs. standard hydrogen electrode, SHE) was used to measure the electrode potential and also allowed to perform cyclic voltammetry analyses (CV) at a scan rate of 0.1 mV s^{-1} (Autolab Potentiostat/Galvanostat, The Netherlands). Prior to the CV, the medium was replaced to guarantee that the MFC was working under high substrate concentration conditions and the circuit was opened for 1 h. The initial potential was set to be the OCV of the electrode and

the switching potential was set to a potential where the integrity of the biofilm was not put at risk.

References for Part II: Materials and Methods

- (1) Reimers, C. E.; Tender, L. M.; Fertig, S.; Wang, W. Harvesting Energy from the Marine Sediment–Water Interface. *Environ. Sci. Technol.* 2001, 35, 192–195.
- (2) Dumas, C.; Mollica, A.; Féron, D.; Basséguy, R.; Etcheverry, L.; Bergel, A. Marine microbial fuel cell: Use of stainless steel electrodes as anode and cathode materials. *Electrochim. Acta* 2007, 53, 468–473.
- (3) Hong, S. W.; Chang, I. S.; Choi, Y. S.; Chung, T. H. Experimental evaluation of influential factors for electricity harvesting from sediment using microbial fuel cell. *Bioresour. Technol.* 2009, 100, 3029–3035.
- (4) Zhao, J.; Li, X.-F.; Ren, Y.-P.; Wang, X.-H.; Jian, C. Electricity generation from Taihu Lake cyanobacteria by sediment microbial fuel cells. *J. Chem. Technol. Biotechnol.* 2012, 87, 1567–1573.
- (5) Ribot-Llobet, E.; Montpart, N.; Ruiz-Franco, Y.; Rago, L.; Lafuente, J.; Baeza, J. A.; Guisasola, A. Obtaining microbial communities with exoelectrogenic activity from anaerobic sludge using a simplified procedure. *J. Chem. Technol. Biotechnol.* 2013, n/a–n/a.
- (6) Wang, X.; Cheng, S.; Feng, Y.; Merrill, M. D.; Saito, T.; Logan, B. E. Use of carbon mesh anodes and the effect of different pretreatment methods on power production in microbial fuel cells. *Environ. Sci. Technol.* 2009, 43, 6870–6874.
- (7) Cheng, S.; Liu, H.; Logan, B. E. Increased power generation in a continuous flow MFC with advective flow through the porous anode and reduced electrode spacing. *Environ. Sci. Technol.* 2006, 40, 2426–2432.
- (8) Cheng, S.; Liu, H.; Logan, B. E. Increased performance of single-chamber microbial fuel cells using an improved cathode structure. *Electrochem. commun.* 2006, 8, 489–494.
- (9) Liu, H.; Logan, B. E. Electricity generation using an air-cathode single chamber microbial fuel cell in the presence and absence of a proton exchange membrane. *Environ. Sci. Technol.* 2004, 38, 4040–4046.
- (10) Call, D.; Logan, B. E. Hydrogen production in a single chamber microbial electrolysis cell lacking a membrane. *Environ. Sci. Technol.* 2008, 42, 3401–3406.
- (11) Lovley, D. R. Bug juice: harvesting electricity with microorganisms. *Nat. Rev. Microbiol.* 2006, 4, 497–508.
- (12) Wei, J.; Liang, P.; Cao, X.; Huang, X. A new insight into potential regulation on growth and power generation of *Geobacter sulfurreducens* in microbial fuel cells based on energy viewpoint. *Environ. Sci. Technol.* 2010, 44, 3187–3191.

-
- (13) Geelhoed, J. S.; Stams, A. J. M. Electricity-assisted biological hydrogen production from acetate by *Geobacter sulfurreducens*. *Environ. Sci. Technol.* 2011, 45, 815–820.
- (14) Sun, D.; Call, D. F.; Kiely, P. D.; Wang, A.; Logan, B. E. Syntrophic interactions improve power production in formic acid fed MFCs operated with set anode potentials or fixed resistances. *Biotechnol. Bioeng.* 2012, 109, 405–414.
- (15) Qu, Y.; Feng, Y.; Wang, X.; Logan, B. E. Use of a coculture to enable current production by *geobacter sulfurreducens*. *Appl. Environ. Microbiol.* 2012, 78, 3484–3487.
- (16) Gao, Y.; Ryu, H.; Santo Domingo, J. W.; Lee, H.-S. Syntrophic interactions between H₂-scavenging and anode-respiring bacteria can improve current density in microbial electrochemical cells. *Bioresour. Technol.* 2014, 153, 245–253.
- (17) Coaxes, J. D.; Phillips, E. J. P.; Lonergan, D. J.; Jenter, H.; Lovley, D. R. Isolation of *Geobacter* species from diverse sedimentary environments. *Appl. Environ. Microbiol.* 1996, 62, 1531–1536.
- (18) Parameswaran, P.; Torres, C. I.; Lee, H.-S.; Rittmann, B. E.; Krajmalnik-Brown, R. Hydrogen consumption in microbial electrochemical systems (MXCs): The role of homo-acetogenic bacteria. *Spec. Issue Biofuels - II Algal Biofuels Microb. Fuel Cells* 2011, 102, 263–271.
- (19) Malvankar, N. S.; Lovley, D. R. Microbial nanowires for bioenergy applications. *Curr. Opin. Biotechnol.* 2014, 27, 88–95.
- (20) DiMarco, A. A.; Bobik, T. A.; Wolfe, R. S. Unusual coenzymes of methanogenesis. *Annu. Rev. Biochem.* 1990, 59, 355–394.
- (21) Ferry, J. G. *Methanogenesis: Ecology, physiology, biochemistry & genetics*; Ferry, J. G., Ed.; Chapman & Hall: New York, 1993.
- (22) Ambler, J. R.; Logan, B. E. Evaluation of stainless steel cathodes and a bicarbonate buffer for hydrogen production in microbial electrolysis cells using a new method for measuring gas production. *Int. J. Hydrogen Energy* 2011, 36, 160–166.
- (23) Green, D. W. *Perry's chemical engineers' handbook*; 8th ed.; McGraw-Hill: New York, etc., 2008.
- (24) Harnisch, F.; Freguia, S. A basic tutorial on cyclic voltammetry for the investigation of electroactive microbial biofilms. *Chem. Asian J.* 2012, 7, 466–475.
- (25) Marsili, E.; Rollefson, J. B.; Baron, D. B.; Hozalski, R. M.; Bond, D. R. Microbial biofilm voltammetry: direct electrochemical characterization of catalytic electrode-attached biofilms. *Appl. Environ. Microbiol.* 2008, 74, 7329–7337.
- (26) Rieger, P. H. *Electrochemistry*; Chapman & Hall: New York etc., 1994; Vol. 2, p. 483.

- (27) Fricke, K.; Harnisch, F.; Schroder, U. On the use of cyclic voltammetry for the study of anodic electron transfer in microbial fuel cells. *Energy Environ. Sci.* 2008, *1*, 144–147.

Part III: Results and Discussion

Chapter 1. Improving the inoculation process in MFC: what limits coulombic efficiency in microbial fuel cells?

Chapter Summary

A proper exoelectrogenic biofilm development is key to ensure better system efficiencies. The exoelectrogenic biofilm is usually developed in MFC configuration. Nevertheless coulombic efficiencies can be low in air-cathode MFC configuration, meaning that a large percentage of the available substrate is being consumed by non electroactive microorganisms. In this chapter, coulombic efficiency in MFC was considered to be an evaluation parameter to assess the inoculation process, and thus the aim was to increase it as much as possible. First, design parameters such as the area of cathode or the external resistance were studied, showing that an optimal area of cathode might exist and the importance of working at the optimal external resistance. Secondly, the cathodic biofilm was investigated, observing an oxygen barrier effect that maintains the anode in anaerobic conditions. Finally the role of the external resistance during the inoculation process was studied, seeing that the electroactivity of the biofilm was enhanced when inoculating at high external resistances.

1.1. Introduction

Coulombic efficiency (CE) is a common parameter used to describe the performance of a bioelectrochemical system. It is defined as the ratio between the amount of coulombs measured along the electrical circuit and the coulombs that could have been generated according to the amount of substrate consumed. Practical implementation of microbial fuel cells for wastewater treatment will require high efficiency when it comes to use the substrate available, or what is the same, high CE. CEs reported in the literature are usually higher than 50%¹⁻³, meaning that more than half of the substrate is devoted to current intensity generation. Different aspects in the design and configuration of MFC can have a direct effect on CE and therefore the system performance. Figure 3.1.1 schematizes an AC-MFC and highlights some of the elements that can influence CE, introduced next.

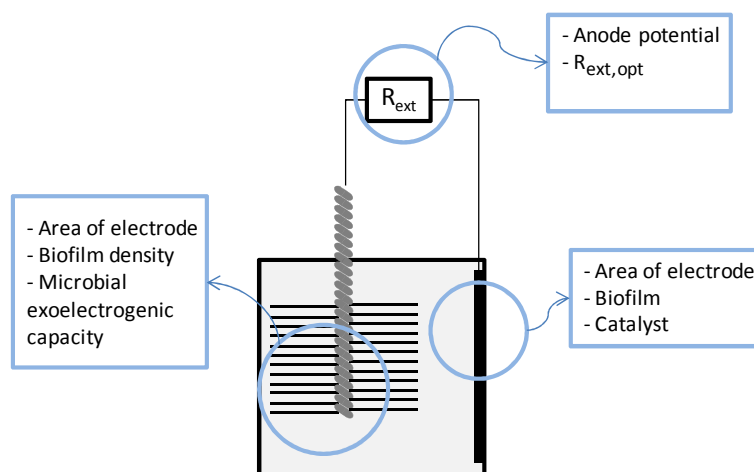


Figure 3.1.1. Elements influencing CE in AC-MFC

The *external resistance* (R_{ext}) used in MFC to close the electrical circuit affects CE^{1,4-6}. On the one hand the R_{ext} can be chosen to coincide with R_{int} so that power output is maximized, defining an optimum external resistance ($R_{ext,opt}$). On the other hand it indirectly poises an anode potential, and thus enhances the growth of different anode microbial populations⁷. The anode potential determines the capability of ARB to use it as electron acceptor, and influences anode potential losses. In fact, the anode potential is a key parameter in bioelectrochemical systems, since it determines the energy gain for the bacteria. The higher the difference between the redox potential of the substrate and the anode potential, the higher the possible metabolic energy gain for the bacteria, but the lower the MFC response^{8,9}. Hence R_{ext} could become a parameter to control the cell performance, enhancing either selection or

growth of ARB just by adjusting or selecting the right R_{ext} . Changes in the anodic biofilm community that develops or changes in the biofilm morphology have been reported after a change in R_{ext} ^{10–12}. Actually, *anode potential* can also be controlled using a potentiostat. This costly device varies the electrode potential by changing the electrical energy input of the instrument. In contrast, R_{ext} simply regulates the anode potential and the current without any energy input¹², having an insignificant cost when compared to a potentiostat.

Electroactive surface area, i.e. the active electrode area, has also influence on CE^{13–15}, since it can be limiting the redox reactions taking place in either electrode. In bioelectrochemical systems, the active anode area is tightly related to the anodic biofilm that develops on its surface. Hence CE will be dependent on how much colonized on ARB the anode is and their energy gain requirements. Regarding the cathode, in an AC-MFC configuration, its area should be large enough not to limit the reduction reaction but not too large to avoid oxygen diffusion into the anode surroundings where anaerobic conditions are required.

Lower values of CEs may be due to the presence of *bacteria other than ARB* that compete for the carbon source, such as methanogenic *archaea* or other aerobic consuming bacteria wherever oxygen is available^{1,16,17}.

The observation of a naturally appearing *biofilm on the cathode* surface is common in a single chamber MFC like AC-MFC. Such biofilm develops because in the cathodic environment both the carbon source and oxygen are fully available, reaching a thickness about 2-3mm in less than one month. Given the competition for the carbon source with ARB, the suppression of this biofilm should result in a CE increase. Opposed observations have been reported in the literature, attributing the decrease in CE to oxygen crossover from the cathode to the anode^{17,18}. Hence the presence of the cathodic biofilm seems to avoid oxygen diffusion towards the anode surroundings, avoiding the possibility that ARB use the oxygen that diffuses as electron acceptor.

Also, the fact that these heterotrophic bacteria are growing on the cathode surface make them eligible to have some sort of electroactivity, which somehow could catalyze the reduction reaction on the cathode, lowering the electrode overpotential (η) and therefore increasing the system performance. This possible catalytic behavior could present an alternative to the use of expensive noble *catalysts*, like platinum.

In this chapter the role of the area of cathode and the external resistance was investigated in an AC-MFC which barely reached 20% CE with the default configuration. Particularly AC-MFC was not expected to have such low CE, since oxygen was fully available on the cathode and the system was catalyzed by platinum.

The effects on CE of the biofilm growing on the cathode of an AC-MFC were also studied. Both the oxygen barrier effect and its possible catalytic character were considered to understand its role in the overall efficiency of the cell.

Finally it was aimed at studying the effect of R_{ext} in the performance of MFC throughout the inoculation, taking into account its influence on the anode potential. A set of AC-MFC operating with different R_{ext} were studied and their response to a change to a common R_{ext} were analyzed.

1.2. Materials and methods

Reactors were operated with sodium acetate as sole carbon source in fed-batch mode (0.1-1 g L⁻¹ initial concentration). BES was used as methanogenic activity inhibitor at a concentration of 10 mM. The cell content was completely replaced with fresh media when voltage response showed a sharp decrease, meaning that substrate was about to be completely depleted. Samples for VFA analyses at the beginning and at the end of the cycle allowed the quantification of substrate consumption.

To explore the role of the area of cathode in AC-MFC performance different areas of electrode were tested and the respective CE was assessed. The area of cathode was progressively changed covering the total area of cathode with a high-density polyethylene layer (1mm thickness) provided with different apertures. Aperture diameters were set to 0 mm (area of cathode fully covered), 5 mm, 11 mm, 20 mm, 30 mm, 36 mm, 50 mm and 63 mm (area of cathode fully uncovered).

The effects on CE of the biofilm growing on the cathode were explored in two different configurations of air cathode MFC: AC-MFC and mAC-MFC. Oxygen barrier effects of the cathodic biofilm were studied by measuring dissolved oxygen (DO) with a dissolved oxygen microsensor (Ox-11706, Unisense) that allowed the obtainment of DO profiles both in the bulk liquid and inside the cathodic biofilm. In order to introduce the oxygen microsensor into the cell a modification in the mAC-MFC design was necessary, providing the cell with an orifice that allowed the microsensor to move perpendicularly to the cathode surface. Oxygen diffusion in this aperture was minimized by a water column of 8 cm (Figure 3.1.2). In AC-MFC a DO probe was used (WTW, Oxi 340i).

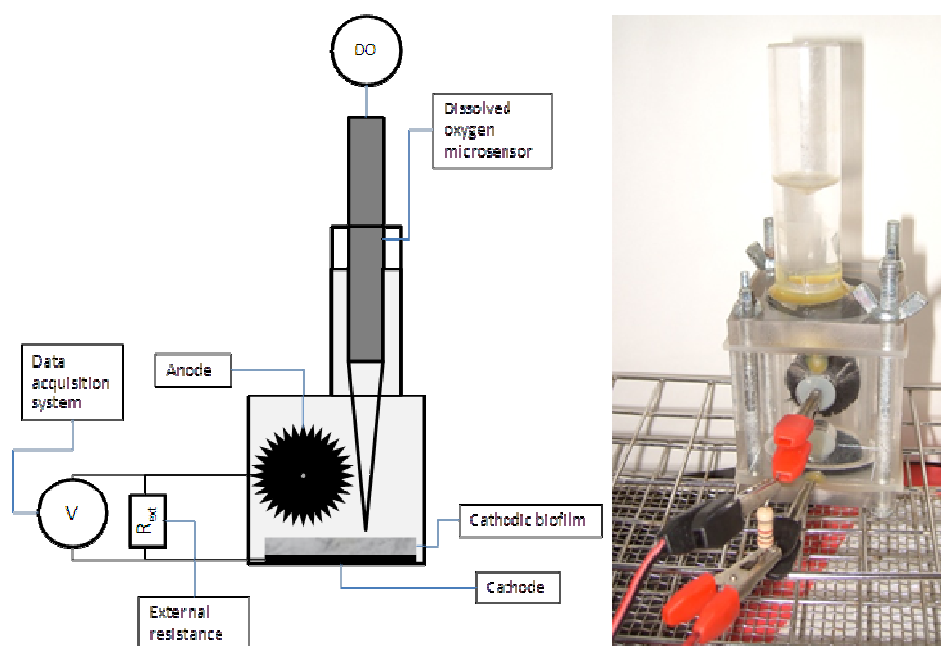


Figure 3.1.2. Modification in mAC-MFC design to allow the insertion of the dissolved oxygen microsensor.

Samples for SEM analysis were collected and fixed with 2.5% glutaraldehyde and 2% para-formaldehyde, followed by a treatment with osmium tetra-oxide, dehydration with ethanol and drying at critical point with carbon dioxide (BAL-TEC CPD030; Bal-Tec). Then the samples were coated with few nanometers of Au-C (E5000 Sputter Coater) to increase signal detection. They were visualized on a Scanning Electron Microscope (Hitachi S-70). Fixation, metallization and following visualization were performed in the Microscopy Service at Universitat Autònoma de Barcelona. In order to see a sensitive difference in population density the graphite fiber brush samples were collected just before the change of R_{ext} and one month later.

1.3. Results and discussion

1.3.1. The role of the area of cathode and the external resistance

1.3.1.1. Finding the optimal cathodic area

The AC-MFC of this study were operated for several cycles with the default configuration of full cathode area and $560\ \Omega\ R_{\text{ext}}$. The CE of these systems was generally lower than 20%, what in other words would mean that less than 20% of the substrate available was being devoted to current generation. One possibility to explore was the oxygen diffusion towards the anode surroundings, which would decrease the cell efficiency because (i) strict anaerobic ARB could be damaged (ii) the anode would not be the only electron acceptor accessible for facultative ARB and (iii) aerobic consumption of acetate by other microorganisms present in the cell could be possible.

This hypothesis was corroborated by measuring DO concentration in the AC-MFC bulk liquid during its operation. Actually, significant DO was detected near the anode when the substrate was depleted (Figure 3.1.3), meaning that previously the substrate was also aerobically consumed in the cell. Therefore, oxygen diffusion to the anode negatively affected MFC performance, because an alternative electron acceptor was available for facultative ARB or other bacteria and the substrate was consequently aerobically consumed, decreasing CE¹⁹.

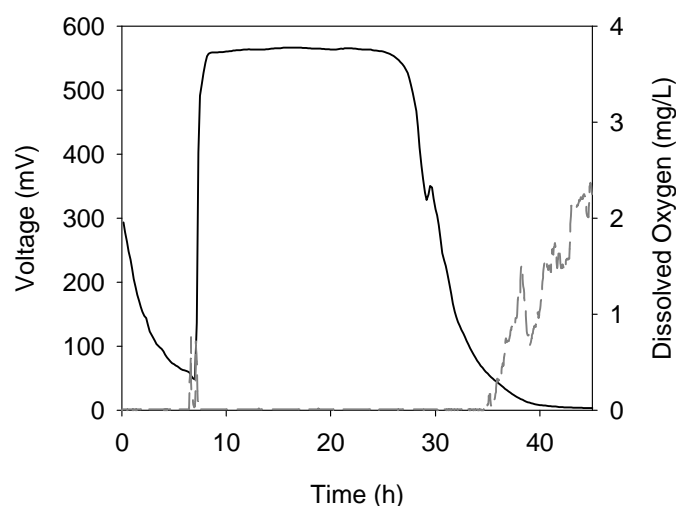


Figure 3.1.3. Voltage (solid) and DO (dashed) near the anode for a batch cycle of AC-MFC (without biofilm on the cathode).

The observation that oxygen was diffusing into the anode surroundings implied that the area of cathode had been overdimensioned. This area should be large enough to prevent limitations by insufficient area of cathode to carry out the reduction reaction but not too large to avoid limitations by excessive oxygen diffusion into cell and the anode. Hence, there should be an optimal area, A_{cat}^{CEmax} , where both factors were correctly balanced and hence the performance of the cell was maximized. To find the aforementioned area, several cycles of the AC-MFC were operated using different cathode areas. Figure 3.1.4 shows the AC-MFC performance in terms of CE and power output versus the cathode area for these experiments. For each aperture diameter, the cell was operated for two batch cycles (~1-2 days per batch cycle) and CE was assessed in the second one. The biofilm grown on the cathode was removed every time the diameter was changed to avoid a dynamic response of the AC-MFC due to its growth.

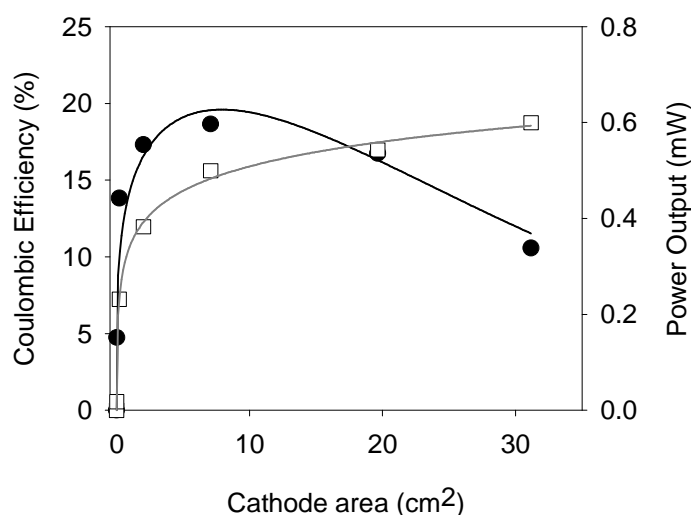


Figure 3.1.4. CE (●), fitted CE curve (solid), maximum power output (□) and maximum power output fitted curve (grey solid) for different cathode apertures.

According to the CE results, A_{cat}^{CEmax} was obtained for an area of 7 cm² (diameter of 3 cm), having a cathode area per cell volume and per anode area of 1.76 m² m⁻³ and 9·10⁻⁴ m² m⁻² respectively. These results also indicated that the area of cathode in these AC-MFCs when working with complete area was overdimensioned 4.4-fold. The effect of using A_{cat}^{CEmax} involved almost doubling the CE in these operational conditions from 10 to 19%. Lower areas of cathode would entail limitations in the reduction reaction, whereas higher areas would enhance oxygen diffusion to the anode surroundings. Finally, the maximum power output had a growing trend with cathode area, indicating that cathode area was limiting such

parameter. According only to the power output in these experiments, the cathode area should be as high as possible. Nevertheless, a negative impact of larger cathode areas on power output cannot be neglected, as some inhibition of ARB is foreseeable due to a very increased DO diffusion.

1.3.1.2. Finding the optimal external resistance

Regarding the external resistance, it was periodically changed to the optimum external resistance ($R_{\text{ext,opt}}$) in another AC-MFC. $R_{\text{ext,opt}}$ was tracked so that the AC-MFC could operate at maximum power output and CE could further increase. Figure 3.1.5 shows the polarization curves, power curves and the $R_{\text{ext,opt}}$ assessed for two months of operation. $R_{\text{ext,opt}}$ was estimated according to the polarization and power curves once per week. Every two batch cycles it was considered that the response had had time to reach a new steady state and a new $R_{\text{ext,opt}}$ was again estimated. A slight decrease in the polarization curve slope is perceived, indicating a decrease in R_{int} . Power output also experienced a growing trend. It can be seen that $R_{\text{ext,opt}}$ decreased during the first month of operation and remained constant afterwards at $50\ \Omega$. The decreasing trend in $R_{\text{ext,opt}}$ throughout was consistent with what was expected, since R_{int} should also decrease as anode biofilm grew. Also CE rose up to 87%, which represents a 3.5-fold increase from the initial operation. Such an increase points out the importance of working at $R_{\text{ext,opt}}$ in these systems.

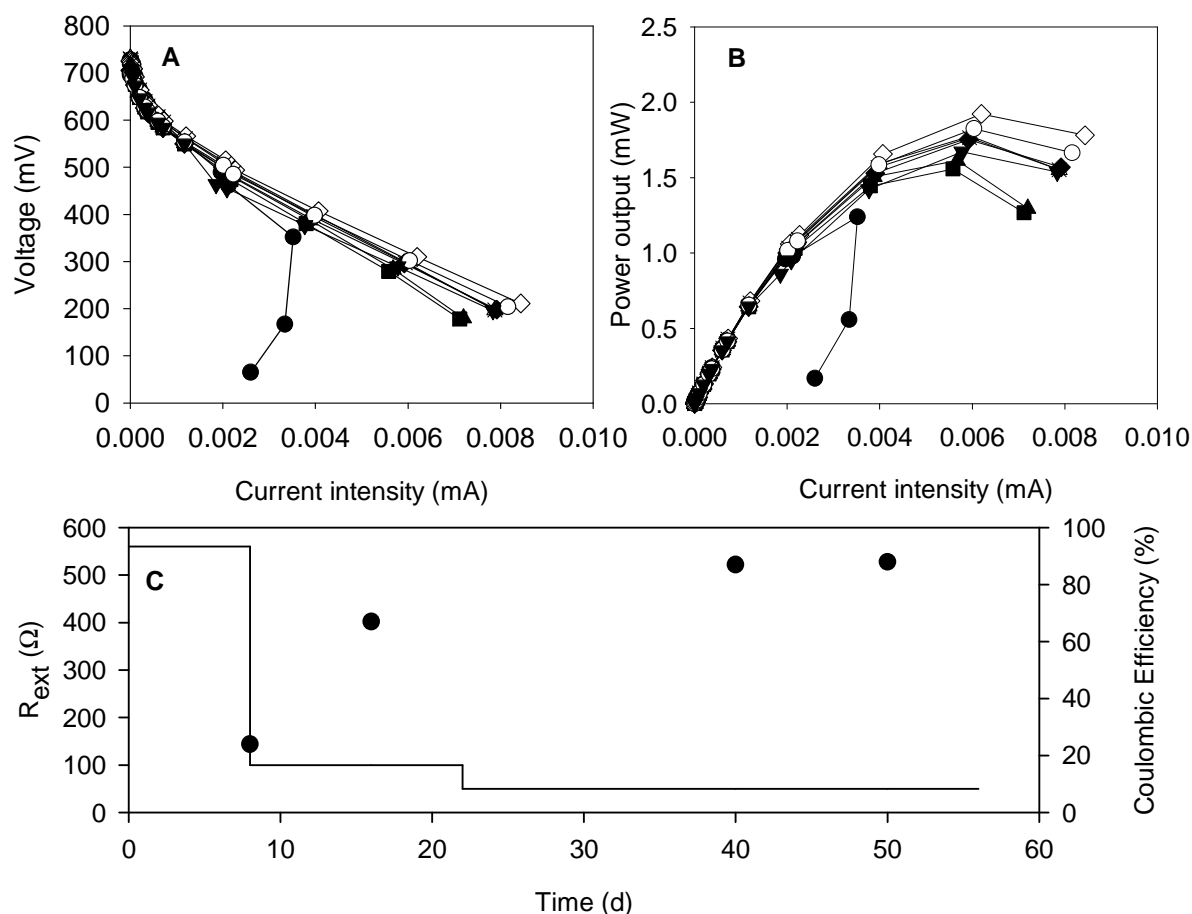


Figure 3.1.5. A and B Evolution along time of the polarization curves and power curves performed on AC-MFC (about 9 weeks operation). Curves are plotted from the first week to the ninth according to $\bullet, \Delta, \blacksquare, \blacktriangle, \times, \diamond, \circ, \blacktriangledown$. **C.** Optimum external resistance evolution (solid) and CE (\bullet).

1.3.1.3. Final performance assessment: combined effect of area and external resistance

Finally, the area of cathode and the external resistance that independently maximized the performance of the cell were applied simultaneously in the same AC-MFC. The batch reached a CE of 52% in the first batch (Figure 3.1.6), which was lower than the 87% obtained for $R_{ext,opt}$ because by reducing the area of cathode also $R_{ext,opt}$ was affected, i.e. the AC-MFC was probably no longer working on its $R_{ext,opt}$. In any case, CE kept rising in the following batches up to 70%, which could be an effect of the progressive growth on the anode. Also the growth of the naturally growing biofilm on the cathode could have favored such increase in CE, since, although it consumes a part of the substrate available, it could further prevent oxygen diffusion into the anode surroundings.

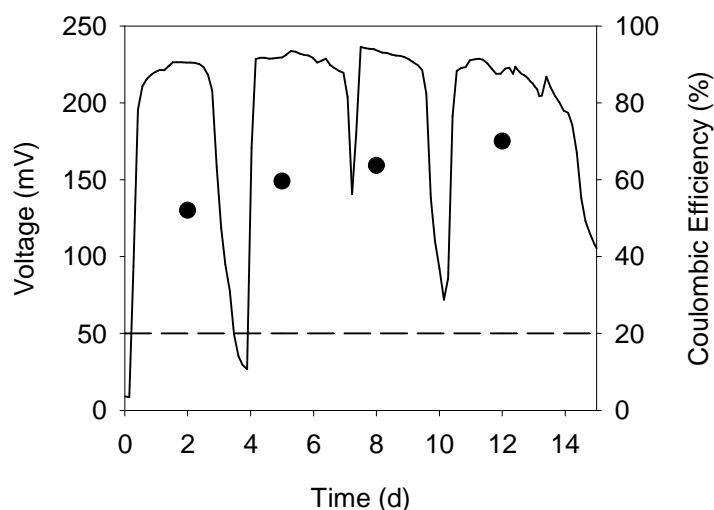


Figure 3.1.6. Voltage (solid), initial CE (dashed) and CE (●) in consecutive batch cycles after combining both the cathode area reduction and operation at $R_{\text{ext,opt}}$.

1.3.2. Cathodic biofilm effects

1.3.2.1. Preliminary results

The low CE of AC-MFC with the default configuration (lower than 20%) and the fact that the biofilm growing on the cathode (Figure 3.1.7 A) was an acetate sink, motivated the removal of the biofilm to minimize substrate consumption by aerobic heterotrophs and thus increase CE. However, a repetitive decrease in CE was experienced when it was removed (Figure 3.1.7 B). An equivalent observation was made by Ahmed et al.¹⁸, who showed a consistent decrease in CE when the cathodic biofilm was removed in a single chamber MFC, attributing this fact to an increase in oxygen crossover from the cathode to the anode. Accordingly also Oh et al.¹⁷ stated that oxygen diffusion from the cathodic chamber to the anodic chamber was decreasing CE, since oxygen was also being used as electron acceptor.

Such a decrease in CE after removing the cathodic biofilm could be a result of oxygen diffusion into the anode surroundings, as already suggested, of a loss in biocatalytic activity or a result of both effects. The possibility that when removing the biofilm also some catalyst (platinum) had been lost could also be considered. However, the fact that CE was again increasing in the following cycles after removing the cathodic biofilm ruled out this option.

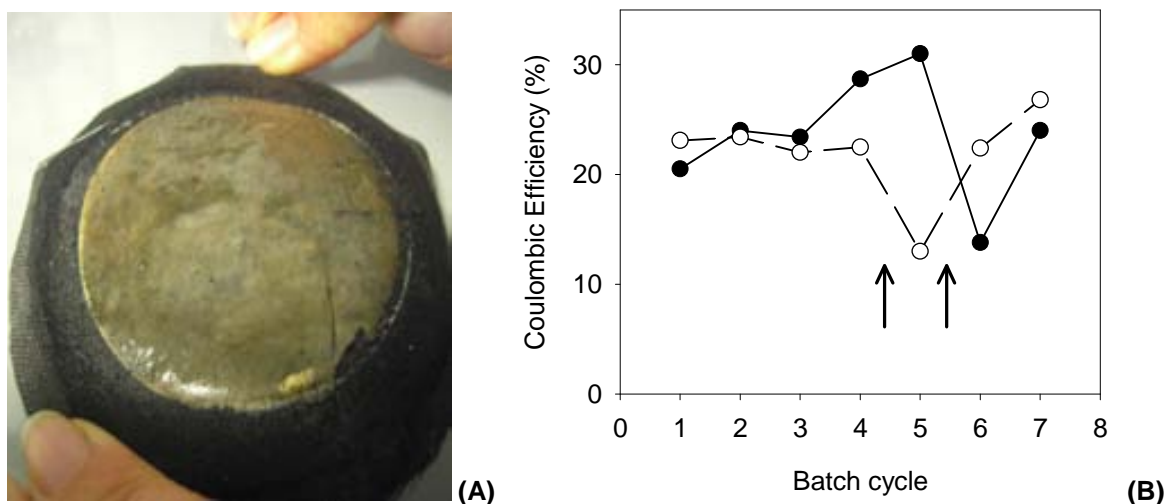


Figure 3.1.7. (A) Biofilm grown on the cathode surface of an AC-MFC. (B) Consecutive batch cycles of two AC-MFC working under the same conditions. Arrows indicate the washout of the biofilm grown on the cathode for each system

Given that oxygen diffusion into the anode surroundings was considered a possible cause of such CE drop, a test to understand the effects of oxygen exposure on MFC cell potential and the electrodes potentials was performed. As presented in Figure 3.1.8 when the MFC was fed, and therefore there was current intensity production, the anode potential decreased to its operation value (-520 mV vs. Ag|AgCl). During Period I the cell was sparged with synthetic air, which resulted in a sharp decrease in cell potential and an increase in anode potential (-50 mV vs. Ag|AgCl). This denoted that in this period oxygen was being used as preferred electron acceptor by facultative ARB and that it inhibited anaerobic ARB. In period II, the oxygen was stripped out by sparging nitrogen gas for few minutes, recovering the use of the anode as electron acceptor.

In the following tests the oxygen barrier effects and biocatalytic activity of the cathodic biofilm were further investigated and discussed.

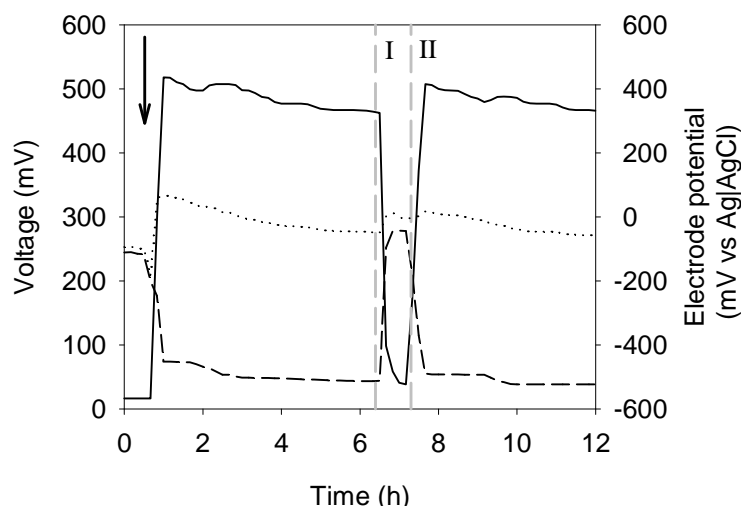


Figure 3.1.8. MFC cell potential (solid), anode (dashed) and cathode potential (dotted) for a batch cycle where in period I the reactor was sparged with synthetic air and in period II with nitrogen gas. Arrow indicated addition of substrate in the medium.

1.3.2.2. Oxygen effects

Oxygen in the bulk liquid

Measurements of DO concentration in the AC-MFC bulk liquid during its operation corroborated the hypothesis that the biofilm was preventing oxygen diffusion to the anode. Indeed DO was negligible near the anode when the biofilm was present on the cathode, even after substrate depletion (Figure 3.1.9). These results indicated the barrier effect of the biofilm for oxygen. Even when acetate is not available for the heterotrophic biomass, these microorganisms are able to consume the oxygen transferred through the cathode surface using its endogenous activity. Unlike this, significant DO was detected near the anode when the biofilm had been removed and substrate was depleted as presented in section 1.3.1 (Figure 3.1.3). Oxygen diffusion to the anode negatively affected MFC performance, because an alternative electron acceptor was available for facultative ARB and the substrate was consequently aerobically consumed, decreasing CE.

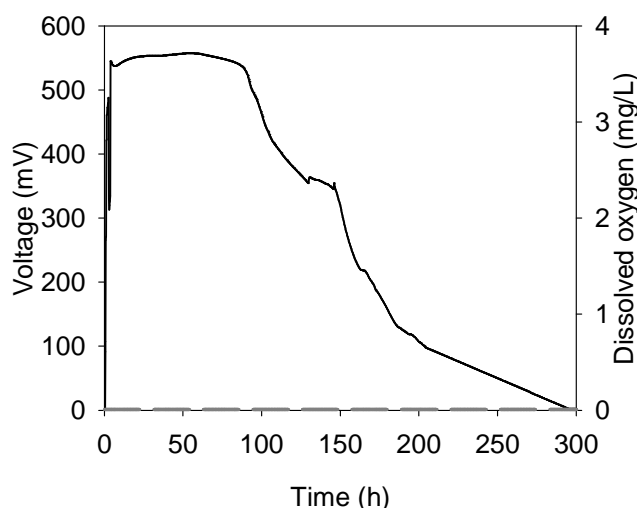


Figure 3.1.9. Voltage (solid) and DO (dashed) near the anode for a batch cycle of AC-MFC with biofilm on the cathode.

DO was also measured in the bulk liquid at different positions relative to the cathode in the mAC-MFC (Figure 3.1.10). It could be seen that oxygen could diffuse into the cell when there was not a biofilm on the cathode surface. DO concentration had a decreasing trend when distancing the cathode and was zero before reaching the anode (placed 2 cm apart from the cathode). This behavior coincided both when substrate was available and when it was not. However, when substrate was available, oxygen was exhausted after the first millimeters from the cathode, whereas it reached higher values when substrate was not available. The difference of behavior of the 28 mL (mAC-MFC) and 400 mL (AC-MFC) systems when no substrate was present was attributed to an overdimensioned cathode area for the 400 mL system as presented in section 1.3.1. In fact, the ratio of cathode area to anode area was higher for AC-MFC than for mMFC. This highlights the advantages of the design proposed by Cheng and Logan²⁰, i.e. mMFC, which ensures anaerobic conditions in the anode surroundings even after substrate depletion when a cathodic biofilm has not been developed yet. Nevertheless, it must be noted that the ratio of electrode areas should consider the electroactive electrode areas to provide a fully comparable parameter.

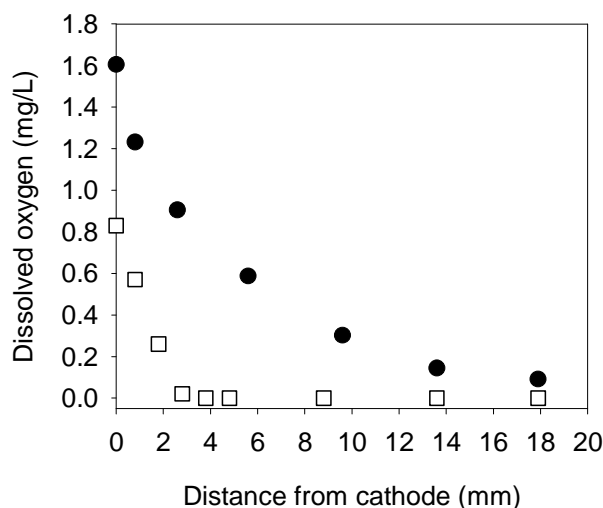


Figure 3.1.10. DO at different depths in the bulk liquid for a batch cycle of mAC-MFC without biofilm on the cathode with (□) and without acetate (●).

Given the fact that the biofilm naturally grows on the cathode surface and that its presence ensures anoxic conditions near the anode, it was considered that the oxygen profile inside the biofilm could be more interesting.

Oxygen in the biofilm

DO throughout the biofilm thickness was also measured to inquire into its oxygen barrier role. In fact the cathodic biofilm was most probably avoiding oxygen inlet into the cell because of both a diffusion decrease and microbial oxygen consumption.

Figure 3.1.11 shows the oxygen profile inside the biofilm under different working conditions (with and without acetate and in open and closed circuit conditions). It can be seen that most changes in oxygen concentration happened in the first tenths of millimeter of the biofilm. It was observed that when acetate was available and the electrical circuit was closed no oxygen at all was detected (cross symbols). In this situation multiple effects were taking place: oxygen diffusion, oxygen consumption in the cathodic biofilm and, most importantly, oxygen reduction to water. A current intensity of 0.5 mA was detected in these conditions. In contrast, when no carbon source was available and the cell was in open circuit configuration (black circle symbols) only diffusional effects were possible. As a result of closing the circuit (white square symbols) diffusion of oxygen experienced a little increase. A low current intensity of 0.04 mA was detected in these conditions, indicating some endogenous consumption in the anode. Finally, when acetate was available and the cell was working in open circuit conditions (grey triangle symbols) not only the diffusion of oxygen through the

biofilm was being detected, but also the oxygen consumption in the cathodic biofilm itself. In this situation oxygen was detected in a narrower section.

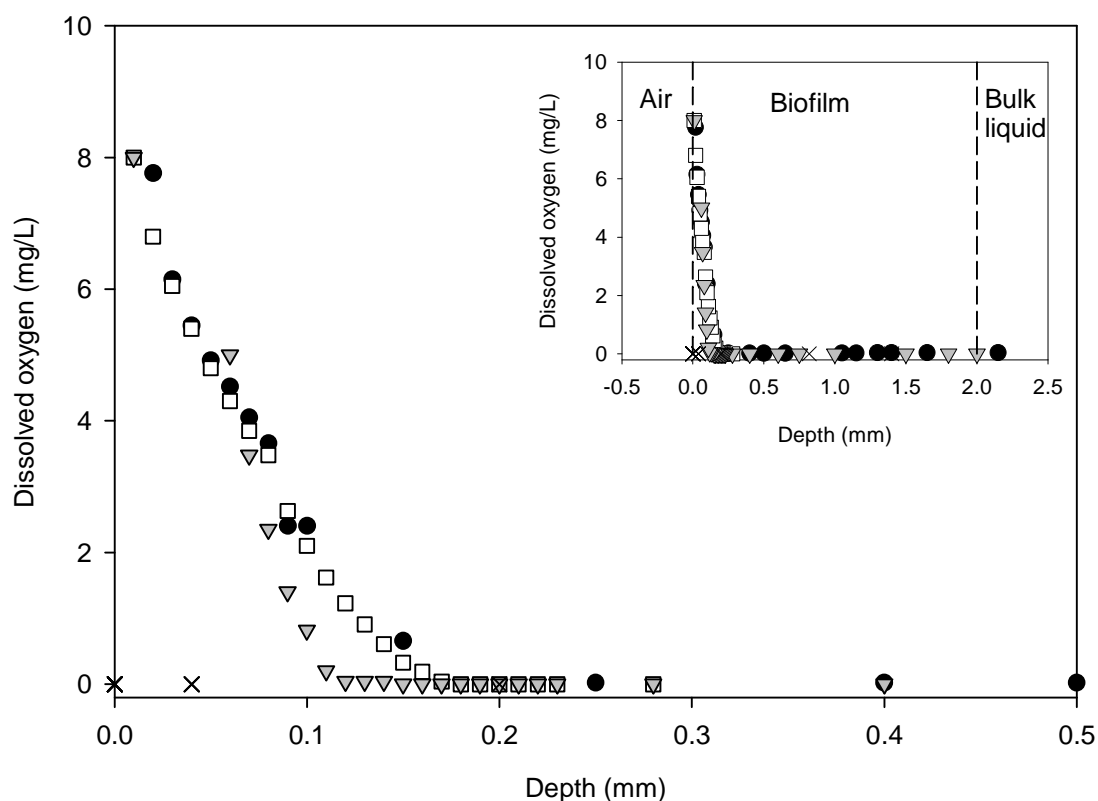


Figure 3.1.11. Dissolved oxygen profile in the cathodic biofilm when no substrate was available (open circuit, ●, and closed circuit, □) and when acetate was available (open circuit, ▼, and closed circuit, ×)

1.3.2.3. Evaluation of the catalytic activity of the biofilm

The possible catalytic role of the cathodic biofilm was evaluated by means of CV analyses and measuring the open circuit potential of the electrode ($OCP_{cathode}$) for different cathode conditions. The cell content was replaced prior to the analysis to guarantee high substrate concentration and the cell was left for one hour in open circuit conditions. CV analyses were meant to reveal a more catalyzed situation for the highest absolute current intensity (the physical meaning of the negative current intensity is the occurrence of a cathodic process, where electrons arrive to the electrode). In an open circuit state, when current dependent voltage losses are discarded, the measurement on both anode and cathode potential allows the assessment of the electrode overpotentials (Figure 3.1.12), being able to distinguish between a more or less catalyzed situation.

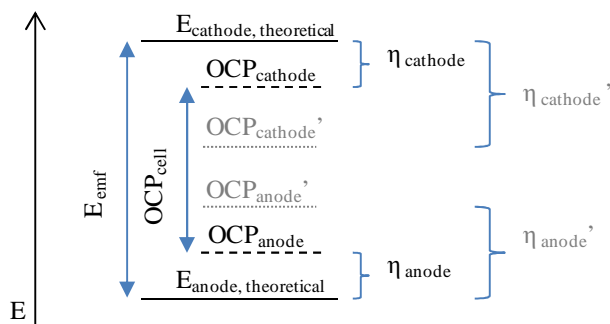


Figure 3.1.12. Scheme of potentials in a microbial fuel cell in open circuit. According to thermodynamics a maximum of E_{emf} can be achieved. In practice voltage losses comprising electrode overpotentials and ohmic losses lower the thermodynamically attainable potential. In open circuit, only voltage losses related to the electrode overpotentials (η) are accounted. The higher the $OCP_{cathode}$ the more catalyzed and vice versa.

CV analyses were performed for five different cathodes: (i) catalyzed with platinum with a mature biofilm (3 mm thickness), (ii) catalyzed with platinum with a fresh biofilm (1 mm thickness) (iii) catalyzed with platinum without any biofilm, (iv) without any platinum catalyst and (v) without platinum with biofilm (in this case barely visible to the naked eye). Figure 3.1.13A presents the results obtained for these tests. The results showed a difference in terms of current intensity, reaching the highest current intensities (in absolute value) the cathode catalyzed only by platinum, followed by the cathode with both platinum and a fresh biofilm, then the cathode with platinum and a mature biofilm, following the cathode without any catalyst and finally the cathode without platinum catalyst with the hardly visible biofilm. The fact that cathodes amended with platinum had higher current intensities was consistent with the behavior expected, since for a catalyzed situation the electron flow should be favored.

Comparing the cathodes provided with platinum, the biofilm grown on the cathode was detrimental for the electroactivity of the electrode. Indeed, the effects of a fresh biofilm slowed down the current intensity response (generally reaching lower current intensities, less negative, for the same scan potential considered), whereas for a mature biofilm current intensity decreased in the presence of the biofilm. Such an effect could be caused by protons mass transport limitations from the bulk liquid to the cathode surface, which would increase for a thicker biofilm.

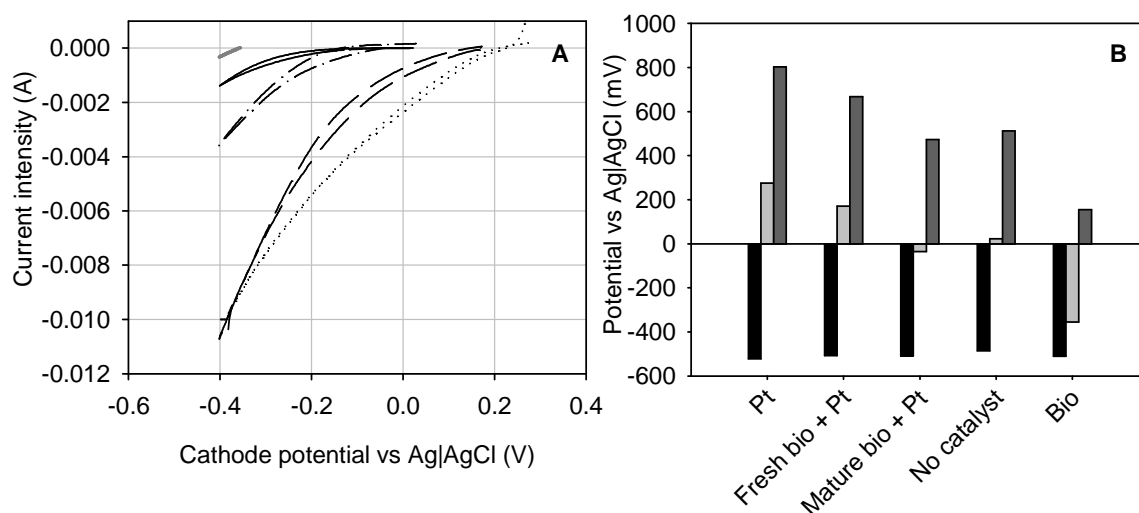


Figure 3.1.13. A: Cyclic voltammograms for cathodes catalyzed by platinum without biofilm (dotted), catalyzed by platinum with a fresh biofilm (dashed), catalyzed by platinum with a mature biofilm (dashed-dotted), a non-catalyzed cathode (solid black) and a non-catalyzed cathode with biofilm (barely visible to the naked eye) (solid grey). B: OCP_{anode} (black), OCP_{cathode} (light grey) and OCP_{cell} (grey) for different cathode conditions.

Before the electrochemical analyses, the cell was in open circuit operation for one hour. Figure 3.1.13B presents the open circuit potentials for the cathode, the anode and the cell for each test studied. Higher values of OCP_{cathode} show a more catalyzed situation. As expected, the highest OCP_{cathode} was observed for the cathode amended with platinum (+275 mV), which experienced a decrease when a fresh biofilm grew on the cathode (+171 mV). Even lower OCP_{cathode} was measured for the cathode coated with platinum when a mature biofilm developed (-36 mV). In a non-catalyzed cathode the OCP_{cathode} was much lower than for those electrodes containing platinum (+22 mV), a trend that was expected. However, when a biofilm began growing on it, the OCP_{cathode} reached the lowest value (-355 mV). The general decrease in OCP_{cathode} when the biofilm is grown showed that the overpotential associated with it increased. Such an increase in the overpotential might, again, be a consequence of the protons transport limitations through the biofilm, which agreed with the fact that it increased for a mature biofilm.

Interestingly, the cathode non-catalyzed by platinum experienced a progressive decrease in power output throughout the time that the biofilm was allowed to grow (around 35 days) even though no biofilm formation was visible to the naked eye. This was accompanied with the sharp drop in OCP_{cathode} observed in Figure 3.1.13B. Such a behavior was observed in multiple occasions, giving consistency to this observation. One possible explanation to the increase in cathode overpotential could be the biological growth inside the plain carbon cloth

lattice, which progressively could either avoid oxygen diffusion or decrease the conductivity of the electrode.

All the aforementioned observations suggest that no catalytic effects can be attributed to the biofilm that naturally grows on the cathode surface, which generally increases the cathode overpotential.

The results obtained here contradict the observations reported in the literature. Bergel et al. proved the catalytic effect on oxygen reduction of the cathodic biofilm grown in a fuel cell, showing an increase in OCP_{cathode} when the system was biocatalyzed²¹. In the work of Cristiani et al. it was shown that the performance of the cathode improved after the biofilm growth (higher absolute current intensity in CV analyses), but no significant differences were observed when assessing the effects of the biofilm growth on a platinum catalyzed and a platinum free cathode. In that case no differences were observed in cathode open circuit potential after six months operation²². In a double chamber configuration, with a mechanically aerated cathodic chamber, also Chung et al. observed such a decrease in MFC performance after the cathodic biofilm was removed. Indeed electrochemical analyses on the cathode also revealed an enhancement of the electroactivity when the biofilm was grown²³.

Here, the increase in cathode overpotentials was hypothesized to be a consequence of the protons transport limitations through the biofilm. This agrees with the observations from Ahmed et al.¹⁸, Cheng et al.²⁰ and Cristiani et al.²², where a negative impact in power generation was observed when the biofilm had developed on the cathode surface, which they attributed to the pH influence, that changed inside the biofilm as a result of the protons diffusion towards the cathode both in double chamber MFC and AC-MFC. This parameter was not measured in this study but it is proposed as a future work to fully understand the chemical flows in the biofilm.

1.3.2.4. Biofilm microbial composition

A sample of the cathodic biofilm was analyzed to determine its microbial composition since it was expected that, at least regarding oxygen toleration, it would present some differences. The microbial distribution that was obtained by pyrosequencing the cathodic biofilm sample showed a broad microbial diversity (Figure 3.1.14). As could be expected aerobic microorganisms were found (e.g. *Pseudomonas sp.*). Also facultative aerobic bacteria were

present (e.g. *Desulfovibrio sp.*). Most interestingly anaerobic microorganisms were detected, which agrees with the fact that oxygen was only detected in the first tenths of millimeter of the biofilm (*Thauera sp.* and *Fusibacter sp.*). Seeing the metabolic diversity present in the biofilm it seems reasonable to hypothesize that this microbial community is growing on layers depending on the oxygen availability, although a crosswise cut should be processed to confirm it.

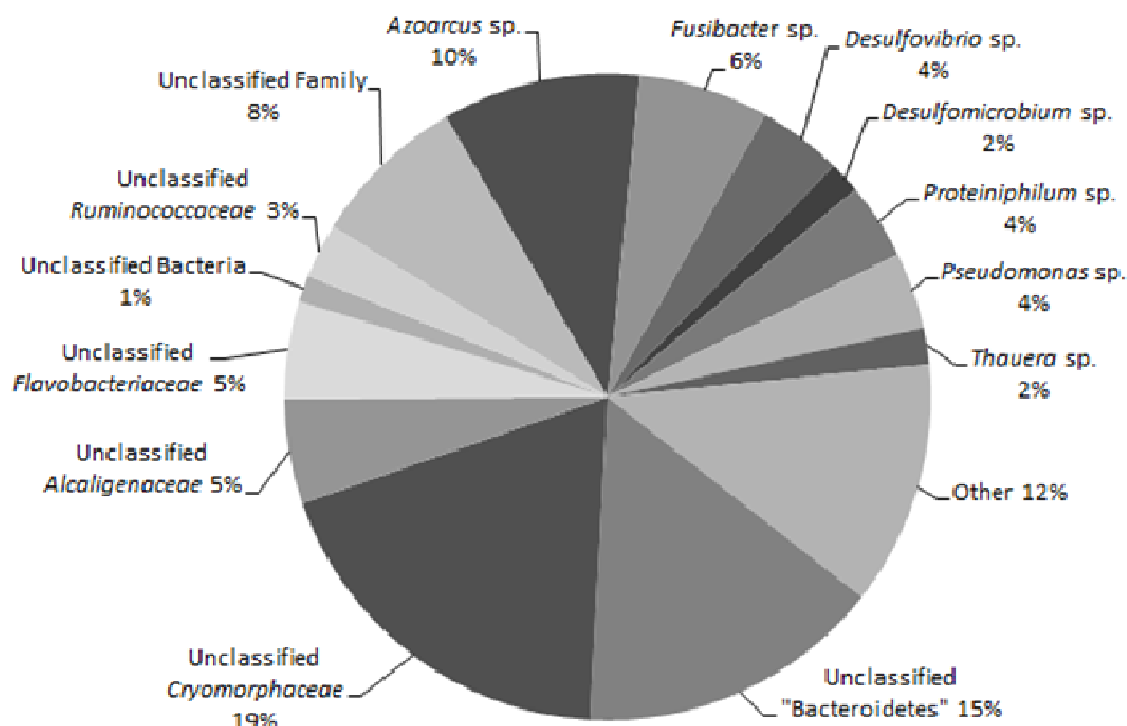


Figure 3.1.14. Microbial distribution by genus in the biofilm grown on the cathode of AC-MFC (with permission of Laura Rago).

1.3.3. External resistance effects during inoculation in MFC

R_{ext} is an effective variable to modulate anode potential, as it is shown in Figure 3.1.15. As it is observed, the higher R_{ext} the lower the anode potential up to a limit value where it keeps on a rather constant anode potential value, approaching the redox potential of the substrate being oxidized, acetate in Figure 3.1.15.

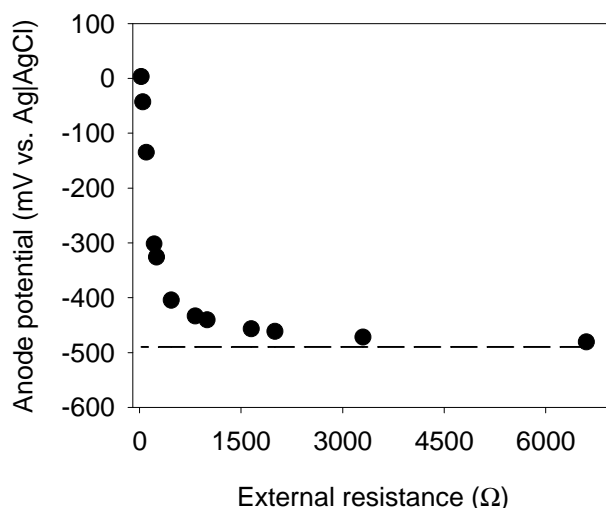


Figure 3.1.15. Anode potential variation with external resistance in an AC-MFC consuming acetate (●) and acetate redox potential (dashed).

In order to study the effect of R_{ext} during the inoculation in the performance of MFC, a set of AC-MFC operating with different R_{ext} were studied and their response to a change to a common R_{ext} were analyzed. The set of four AC-MFC worked with R_{ext} of 12, 50, 470 and 1000 Ω (AC-MFC₁₂, AC-MFC₅₀, AC-MFC₄₇₀ and AC-MFC₁₀₀₀). The anodes had been previously inoculated in a Sed-MFC with the respective R_{ext} mentioned. The four AC-MFC were operated for four months at the aforementioned R_{ext} and then these resistances were replaced by a common external load of 50 Ω .

Figure 3.1.16 shows the performance of the set of AC-MFC working with different R_{ext} one month before the change to a common R_{ext} of 50 Ω and one month later. Current intensity and power output for most cells had reached a steady state before the R_{ext} change (day 26). The only cell that experienced a perturbation in response was AC-MFC₅₀, showing a decrease in response from day 10.

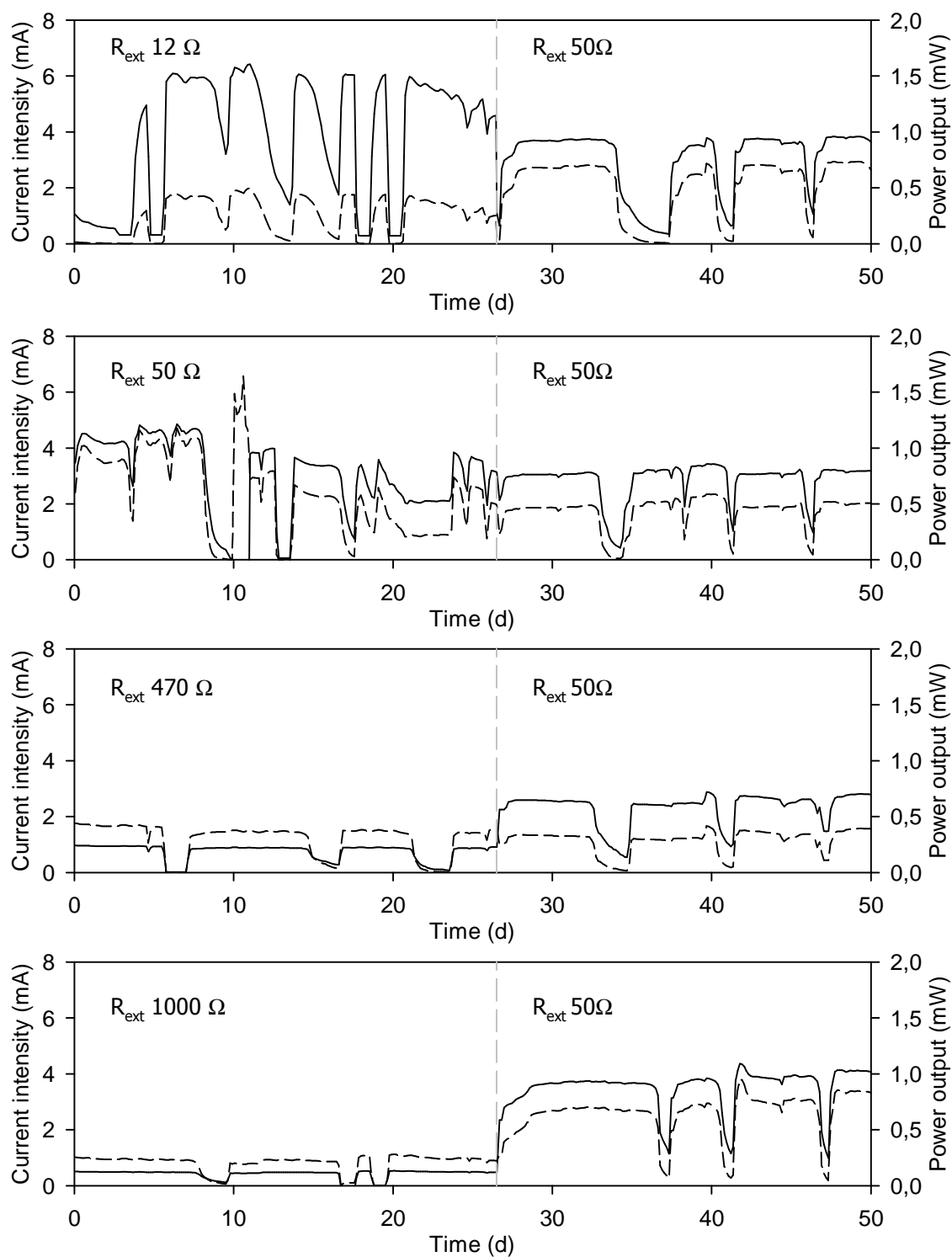


Figure 3.1.16. Evolution of current intensity (solid) and power output (dashed) for the set of AC-MFC studied. Grey dashed line indicates the change to a common resistance of 50Ω .

The anode potential measured throughout all the operational period is presented in Figure 3.1.17. It is seen that during the first weeks of operation at different R_{ext} anode potential ranged between -150 and -450 mV, whereas after two months of operation this difference

narrowed converging within values around -400 and -450 mV. High R_{ext} , 470 Ω and 1000 Ω , kept the anode potential around -450 mV throughout. This effect would give more growth time to ARB able to grow at lower anode potentials in those AC-MFCs operating at high R_{ext} . On the other hand, there was a progressive decrease in anode potential in the low R_{ext} operating AC-MFCs as the electrode was being colonized by all sorts of ARB. After the change to a common resistance of 50 Ω , anode potentials did not vary significantly, although AC-MFC₄₇₀ presented an unexpected increase.

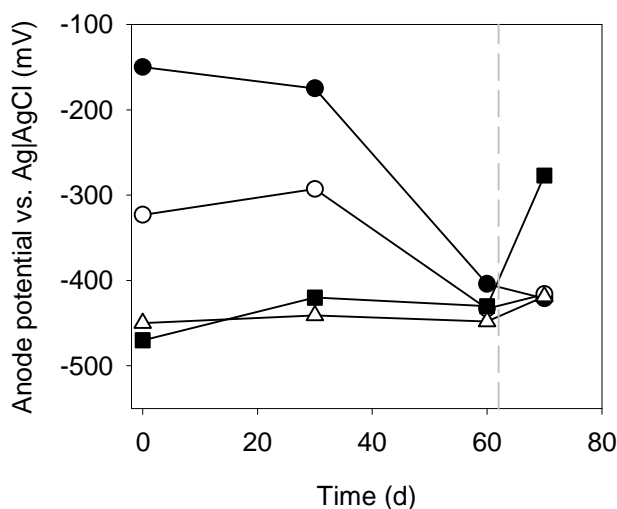


Figure 3.1.17. AC-MFC anode potential evolution. ● AC-MFC₁₂, ○ AC-MFC₅₀, ■ AC-MFC₄₇₀ and △ AC-MFC₁₀₀₀. Dashed line indicates the change to a common resistance of 50 Ω .

According to the results having an R_{ext} of 50 Ω favored power output, reaching up to 1 mW, (Figure 3.1.16, until day 10) and, potentially, this load was the one that could give the highest current intensity as was gathered from CV analyses (Figure 3.1.18). That was the reason why 50 Ω was decided to be the new R_{ext} for the other cells. Nevertheless, the low biomass density in AC-MFC₅₀ showed that growth was not especially enhanced in this cell unlike what could be expected according to current intensity (Figure 3.1.19). It must be taken into account that even though samples for SEM were intended to be as uniform as possible, homogeneity in sampling in such support could not be fully guaranteed, restricting the conclusions that could be taken from SEM images.

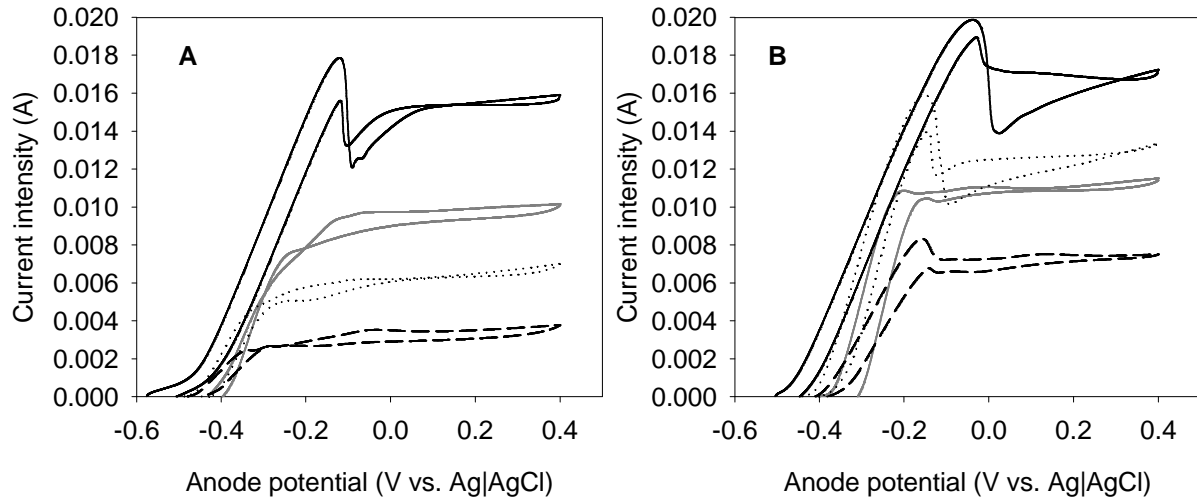


Figure 3.1.18. (A) Voltammograms performed on AC-MFC operating with different external resistances. (B) Voltammograms performed on AC-MFC operating at a common external resistance of 50 Ω . Grey: AC-MFC₁₂, black: AC-MFC₅₀, dashed: AC-MFC₄₇₀ and dotted: AC-MFC₁₀₀₀. CV were performed one month before and one month after the change to 50 Ω .

CE did not show any clear trend according to the initial R_{ext} , although an increase in CE for those AC-MFCs that had been growing at R_{ext} higher than 50 Ω was observed after the change to a this common resistance (Table 3.1.1).

Table 3.1.1. Average CE before and after the change to a common R_{ext}

Initial R_{ext}	Average CE with initial R_{ext}	Average CE after change to R_{ext} 50 Ω
12	31 ± 5	35 ± 4
50	64 ± 9	60 ± 6
470	20 ± 4	25 ± 3
1000	41 ± 6	50 ± 1

After the change in R_{ext} not only there was an increase in CE but also in current intensity of those AC-MFCs that had been growing at 470 and 1000 Ω . Actually AC-MFC₁₀₀₀ increased power output more than three-fold and current intensity almost 8-fold. An increase in power output was also expected for AC-MFC₄₇₀, but the increase in anode potential could have limited its response. A similar study where two very different R_{ext} were exchanged suggested that R_{ext} do not sensitively change the power output of a MFC, inferring from this that changing the R_{ext} was useless¹⁰. However, the results obtained here, together with the results presented in section 1.3.1 regarding operation at $R_{\text{ext,opt}}$ and other studies found in the literature show the opposite^{4,6,24}, giving consistency to the results obtained in this study.

SEM analyses after the change to the common R_{ext} again showed odd-looking results (Figure 3.1.20). For instance, AC-MFC₅₀, prior and after, seemed to show an increase in microbial

density, which could only be explained by ARB growth between one analysis and the other. On the other hand those AC-MFCs that had been growing at R_{ext} higher than 50 Ω appeared to have more biomass attached to the anode than before, unlike AC-MFC₁₂. In these cases an increase would not be only consequence of the time difference but also the change in the R_{ext} . The low biomass density in AC-MFC₁₂ was not consistent with the growth expected at high anode potentials, a situation with more energy gain for bacteria and therefore more growth possibilities.

Regarding CV, a clear trend in limit current intensity was observed. Initially, lower R_{ext} were allowing higher limit current intensity, being the highest for 50 Ω . In contrast, a significant increase was experienced for AC-MFC₁₀₀₀ and also AC-MFC₄₇₀ increased after the change of R_{ext} to 50 Ω . As could be expected no significant variations were observed for AC-MFC₁₂ and AC-MFC₅₀. Regardless of the high increase in the signal for AC-MFC₁₀₀₀, the signal for AC-MFC₅₀ could not be surpassed.

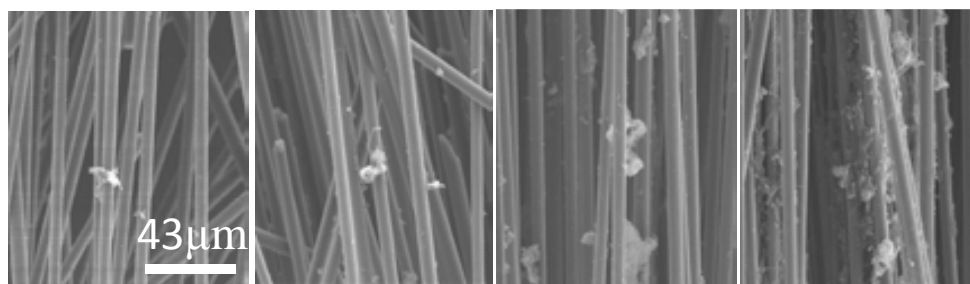


Figure 3.1.19. SEM analyses of the anodes working on AC-MFC with different external resistances: External resistance of 12, 50, 470 and 1000 Ω (rightwards).

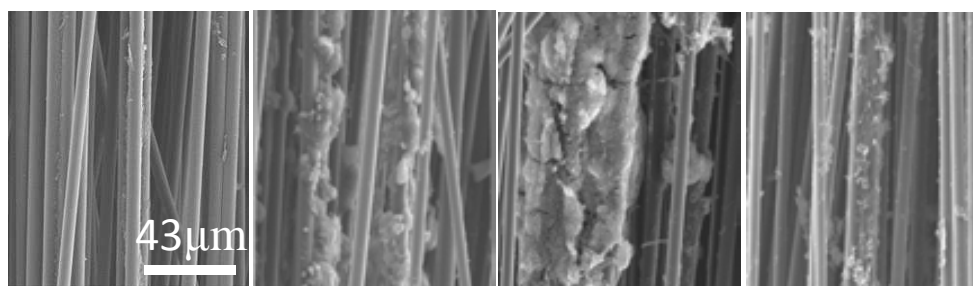


Figure 3.1.20. SEM analyses of the anodes working on AC-MFC with 50 Ω external resistance, performed one month after the change to the common R_{ext} : Previous external resistance of 12, 50, 470 and 1000 Ω respectively (rightwards).

The interpretation of the results was decided to be based on voltammetric and amperometric analyses rather than based on SEM images because of being more reliable in this particular study. In fact, it is thought that initially few ARB could be able to live at a very low anode

potential, whereas a higher diversity could be developing in an anode at more positive potential. As time passed and cells grew, more growth was expected in the anode where initially more bacteria could develop, progressively lowering the anode potential. When AC-MFC were working at similar anode potentials and the R_{ext} was switched to a low value, those ARB grown at very low anode potential throughout the operational time could increase their electroactivity, increasing in a large extent the power output (Figure 3.1.21). Nevertheless the fact that somehow the growth at very low anode potential had been restrained and less ARB would be available, would explain the still lower or similar current intensities. The work from Aelterman et al. also showed a similar behavior, reaching higher current generation per amount of biomass with an anode poised at low potential (-400 mV vs. Ag|AgCl) when compared to another inoculated at high potential (0 mV vs. Ag|AgCl)²⁵.

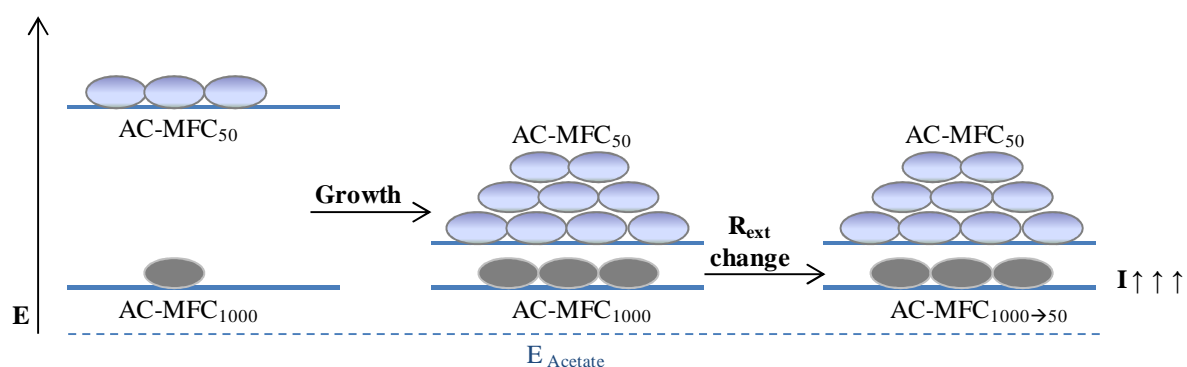


Figure 3.1.21. Qualitative scheme of the external resistance effects on the anode potential, cell growth and power production.

1.4. Conclusions

In this chapter, the influence on CE and MFC performance of the area of cathode, the external resistance and the cathodic biofilm were explored.

The cathode surface area and R_{ext} in AC-MFC were observed to be important parameters when designing a new configuration or scaling up an existing bioelectrochemical system, because they have a direct effect on CE. Actually, in this study, it was managed to increase the CE of an AC-MFC from 20% to 70% by simultaneously working at the area of cathode that maximized cell performance and working with an R_{ext} close to $R_{ext,opt}$. In this system, the cathode area per cell volume maximizing cell performance was estimated to be $1.76 \text{ m}^2 \text{ m}^{-3}$ and a R_{ext} of 50Ω was set as stationary $R_{ext,opt}$.

In the system studied in this work, an overdimensioned cathode design contributed to such a low initial CE. Indeed, the area of cathode was so much larger than required (4.4-fold larger than the assessed $A_{cat}^{CE_{max}}$) that too much oxygen was diffusing into the cell, not allowing to fully maintain anaerobic conditions close to the anode.

It must be taken into account that both parameters were studied independently. However, when applied simultaneously in the system, an influence between both exists. As a consequence these setting values, when applied together, might not be the ones maximizing the response anymore. If this had been the aim of the work a more detailed study on multivariable optimization should have been performed, but these tests are more time-consuming and with the procedure followed in this work the final response of the system was already satisfactory, having a significant increase in CE.

It is also important to point out that a MFC is a dynamic system, hence the parameters maximizing CE may vary along time. For instance, the development and growth of the anodic biofilm will increase CE up to some extent, where the system will begin being limited by insufficient area of cathode available to carry out the reduction reaction.

It was also shown that the cathodic biofilm that naturally grows in AC-MFC prevents oxygen diffusion into the anode surroundings allowing to reach higher CE and therefore increasing the system performance. The prevention of oxygen diffusion into the anode surroundings is particularly interesting in the case of systems where the cathodic area has been overdimensioned or in the start-up phase of the reactor, when the anode has not been fully

colonized yet and the surplus of oxygen that cannot react on the cathode can diffuse into the bulk liquid. In any case, the presence of the cathodic biofilm always ensures anoxic conditions on the anode surroundings.

In terms of the catalytic effects of the biofilm grown on the cathode, a systematic increase of cathode overpotential was observed when the biofilm could develop, meaning that no catalytic effects could be attributed to this biofilm at all. The pH profile inside the cathodic biofilm should also be assessed to verify it as a possible cause of the increase in overpotential.

Regarding inoculation of the anode at different R_{ext} , it was presented as a strategy to modulate the anode potential. Indeed, current intensity results seemed to show an enhancement in electroactivity when inoculating at high R_{ext} , i.e. at low anode potentials, and decreasing this resistance to a lower value afterwards. For example a MFC inoculated at 1000 Ω increased by three times its power output and almost eight times its current intensity when the external resistance was changed to 50 Ω . In agreement to this observation it was decided to apply this procedure in all further inoculation of MFC, i.e. to inoculate at high R_{ext} and later on decrease it. This procedure would improve CE and the overall cell performance, becoming of interest in view of a low cost start-up or in view of the scale-up of a bioelectrochemical system.

Chapter 2. Biomass selection and bioaugmentation in MXC

Chapter summary

In a biological system, enhancing the growth and activity of those organisms that carry out the task of interest is crucial. Selection of biomass that efficiently deals with the energy input would be interesting in bioelectrochemical systems because electrode overpotentials decrease and the overall efficiency increases. Such a selection could be expedited up by setting the electrode potential or, as discussed in Chapter 1, operating with a specific external resistance. Different external resistances were used to inoculate the anode and their capability to work in MEC under low applied potential was tested. In view of a real use of bioelectrochemical systems treating wastewater, it is also of interest obtaining a microbial community that ensures the degradation of a broad spectrum of substrates. A consortium between fermentative bacteria and ARB was therefore developed and used to bioaugment the system, managing effective current generation in MFC from all complex substrates tested. Codegradation of different complex substrates enhanced the system performance.

The content of this chapter has been partially submitted for publication in Water Research as “Complex carbon sources as electron donors for bioelectrochemical systems” by Nuria Montpart, Juan Antonio Baeza and Albert Guisasola (April 2014).

2.1. Introduction

The use of wastewater to drive bioelectrochemical systems is an interesting alternative for wastewater treatment and valorization. Selection and bioaugmentation of an adequate microbial community seems a good approach to sort out some of the hurdles that the future implementation of this technology may face, such as the high energy requirements for hydrogen production in MEC, or a limited substrate degradation capacity due to the wide range of carbon sources with different biodegradability that wastewater contains.

In Chapter 1, it was concluded that inoculation at high external resistances could enhance the electroactivity of the biomass grown on the anode. It still remained as a question, though, if this also means that bacteria developed under these conditions were more energetically efficient, i.e. that bacteria managing the energy flows better off were being selected. A direct consequence of this more energetically efficient metabolism in MEC operation could be the achievement of a similar system performance with lower energy inputs, which obviously would increase the energy yield of the system and would increase the chances of this technology to reach a future application.

In terms of the degradation capacity in bioelectrochemical systems, lab scale studies have broadly studied bioelectrochemical systems fed with synthetic wastewater containing readily biodegradable substrates, mainly acetic acid, which is easily metabolized by ARB. In systems where a complex substrate is used, an initial hydrolysis and fermentation step is necessary in order to break macromolecules to simpler ones and to convert them to acetate and other readily biodegradable substrates, which will be further degraded by exoelectrogenic bacteria. Hence a syntrophic consortium between fermentative and exoelectrogenic bacteria needs to develop.

Studies on bioelectrochemical systems fed with complex substrates as sole carbon source show the necessity to develop such syntrophy in the system^{26–30} and present the hydrolysis and fermentation step as the limiting one²⁸. They also show that a preacclimation to single products improves later degradation in a complex mixture and increases hydrogen yield²⁶. In general, the substrates that have been tested so far in bioelectrochemical systems include synthetic wastewater containing starch^{28,31–33}, cellulose^{26,29}, glycerol^{34–37}, methanol³⁸, phenol³⁹, landfill leachates⁴⁰, municipal wastewater^{41,42} and industrial wastewater from dairy industry^{43,44}, brewery⁴⁵ and biodiesel wastewater⁴⁶.

The selection of efficient exoelectrogenic bacteria able to operate at low applied voltage in MEC by means of the external resistance was aimed in a first section in this chapter. To do so anodes were inoculated with anaerobic sludge under different external resistances and they were later on transferred to MEC. Operating at two different applied voltages, their performance in terms of current intensity and hydrogen production was analyzed.

In a second section of this chapter, the aim was bioaugmenting bioelectrochemical systems with syntrophic consortia to increase the treatment opportunities of different complex substrates in these systems. Milk, starch and glycerol were chosen as carbon sources in view of their differences in composition and therefore biodegradability. In this sense, glycerol was chosen for being a short chain fermentable substrate, starch a large polysaccharide and milk a mixture of sugars, fats and proteins. Also the advantages of codigesting the three substrates at the same time were explored.

2.2. Materials and methods

The possibility to select ARB with different energy requirements by inoculating at different external resistances was studied with two different set of experiments. Firstly, the set of tests A was conducted in Sed-MFC. When the anode was considered to be enriched, after at least 30 days operation⁴⁷, the anode was gently washed with water and transferred to MEC (400 mL). In a second test (set of tests B), in order to improve repeatability, the anodes were inoculated in mAC-MFC and later on transferred to mMEC. In both cases anaerobic sludge was used as inoculum.

Throughout the experiment acetate and water were added to Sed-MFC to ensure cathode contact with the liquid medium and substrate availability. As for mAC-MFC, 50% of the reactor volume was replaced by fresh media every time the cell voltage signal decreased as a result of substrate depletion. When the cell reached a stationary response, the cell content was completely replaced by fresh medium at the end of each batch (initial concentration of 1 g L⁻¹ acetate and 10 mM BES).

The cells differed in the external resistance throughout the inoculation in MFC. For the set of tests A the external resistances used during the inoculation process were 12, 218, 560, 1000, 1470, 4000 and 22100 Ω . For the set of tests B the external resistances used were changed to 12, 50, 560, 1000 and 4000 Ω . In MEC operation a 12 Ω external resistance was used to quantify the current intensity in the system.

The gas produced in MEC was collected by means of a gas collection bag, which was connected to the headspace of the MEC by means of a hosepipe with needle ends that pierced both the gas bag septum and the MEC septum. As an initial supposition it was considered that the gas composition in the gas bag and in the headspace were identical.

The development of consortia that enabled the degradation of substrates other than acetate in bioelectrochemical systems was pursued in a second stage. Each consortium able to degrade a specific complex substrate was obtained by separately growing both communities, i.e. fermentative and ARB, in culture flasks and in mAC-MFC respectively. Next, both communities were joined in mAC-MFC.

Culture flasks were 100 mL glass bottles tightly capped with PTFE rubber septa and an aluminum crimp top. Bottles were filled up to 70 mL, they were magnetically stirred and kept

in a 37°C room. 45 mL of anaerobic digester sludge (Municipal wastewater treatment plant of Manresa, Catalonia) was used as inoculum in each culture flask. The culture flasks were operated under fedbatch mode with cycles of five days duration. Every time the system was fed, the mixed liquor was centrifuged (4 minutes at 5000 rpm) to enhance biomass retention, the supernatant medium was discarded, and the sludge was then resuspended in fresh medium. Before closing the bottles, nitrogen was sparged to ensure anaerobic conditions.

Each culture flask treated a different substrate (glycerol, milk and starch) independently. Glycerol and starch were analytical grade reactants (1.216 g COD g glycerol⁻¹ and 1.185 g COD g starch⁻¹ respectively). Milk was commercial powder milk (1 g COD g milk⁻¹). 50 mM BES was used to inhibit the methanogenic activity. VFA and COD were measured to assess the development of the fermenting community and gas analyses from the headspace allowed to ensure that no methane was being produced. pH was also measured. Additionally, also lactate and glucose were measured for those systems working with starch or milk.

mAC-MFC consumed independently each complex substrate (glycerol, milk and starch) in fed-batch mode and at room temperature, with an initial concentration per compound of 0.5 g L⁻¹ that was later increased to 1 g L⁻¹. Only during MFC inoculation both acetate and propionate were used as carbon sources. During the first four weeks of the work, BES was used as methanogenic activity inhibitor at a concentration of 50 mM. The cell content was completely replaced with fresh medium when voltage response decreased below half the maximum signal. Samples for COD and VFA were taken at the beginning, at the middle and at the end of each cycle, accounting for a maximum of 10% of the total reactor volume. pH was measured at the beginning and at the end of each batch cycle.

For culture flasks, the *j* metabolite concentration was calculated in COD units relative to the initial COD, obtaining in total the percentage of complex substrate degradation, as presented in Equations 3.1 and 3.2.

$$\text{Normalized metabolite concentration (t)} = \frac{\text{COD}_{j,t}}{\text{COD}_{t=0}} 100 \quad (\text{Equation 3.1})$$

$$\text{Complex substrate degradation (t)} = \frac{\sum_{j=1}^n \text{COD}_{j,t}}{\text{COD}_{t=0}} 100 \quad (\text{Equation 3.2})$$

2.3. Results and discussion

2.3.1. Evaluation of ARB selection inoculating at different R_{ext}

The possibility to select ARB with different energy requirements by inoculating at different external resistances was studied with two different set of experiments. The first allowed the obtainment of preliminary results and the second intended to sort out the difficulties found in the previous test.

Firstly, the set of tests A was conducted in Sed-MFC (Figure 3.2.1A). When the anode was considered to be enriched, it was transferred to MEC (400 mL). In a second test (set of tests B), in order to improve repeatability, the anodes were inoculated in mAC-MFC and later on transferred to mMEC (Figure 3.2.1B). In both cases anaerobic sludge was used as inoculum. Throughout inoculation in MFC the cells differed in the external resistance. Experiments were conducted in triplicate in the set of tests A, whereas in B the tests were performed in duplicate.

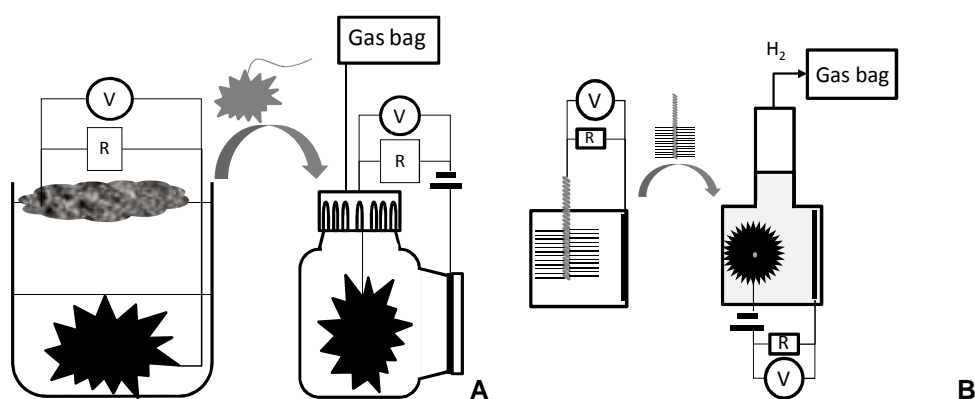


Figure 3.2.1. Schematics of the process and configurations used in this study where (A) anode is inoculated in Sed-MFC and transferred to MEC (400 mL) (*set of tests A*) and (B) anode is inoculated in mAC-MFC and transferred to mMEC (*set of tests B*).

2.3.1.1. Set of tests A: inoculation in Sed-MFC

In the set of tests A, inoculation of the anodes at different R_{ext} was conducted in Sed-MFC. As shown in Figure 3.2.2, the growing trend of a set of Sed-MFC indicated the progressive growth of a biofilm in the surface of the anode. Abrupt variations in response were due to the addition of water or substrate to the cell and are normal in this type of MFC. It is observed that low and very high resistances required longer acclimation times, although for very high loads (22100 Ω) biomass did not seem to grow. Prior to cell disassembling to transfer the

anode to MEC, the anode potential for each Sed-MFC was measured (Figure 3.2.3) and it had the expected decreasing trend, approaching the acetate reduction potential as the R_{ext} increased.

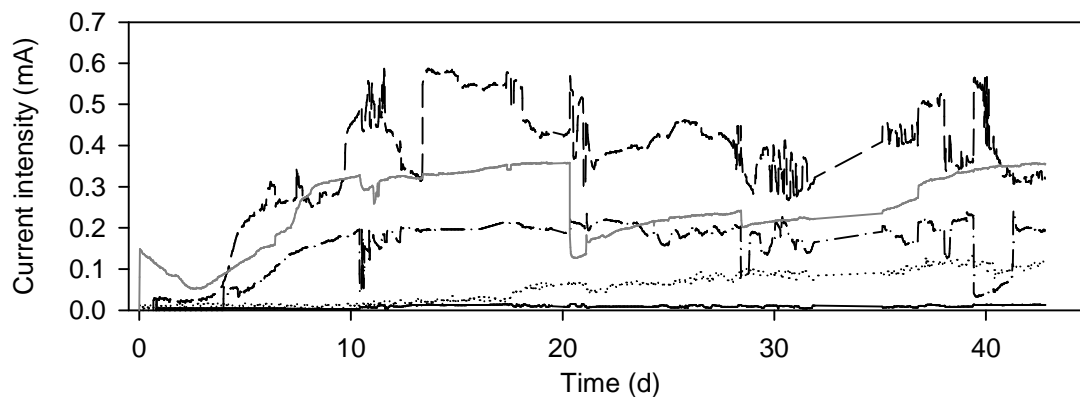


Figure 3.2.2. Current intensity of Sed-MFCs operating at different external resistances (Monitoring data for 12 Ω and 4000 Ω was not recorded): 218 Ω (dotted), 560 Ω (dashed), 1000 Ω (dash-dotted), 1470 Ω (grey solid) and 22100 (black solid).

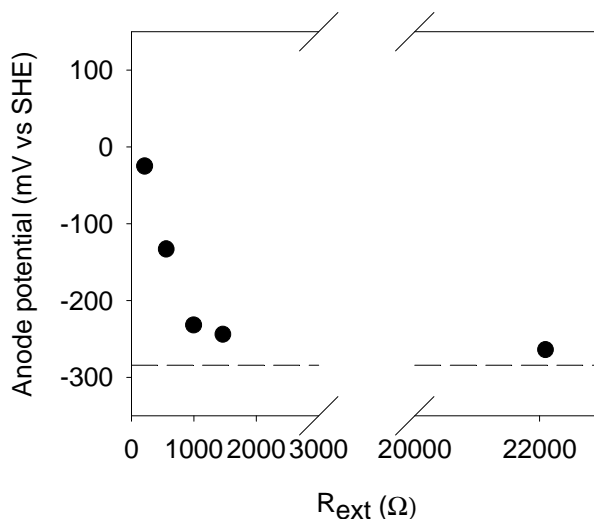


Figure 3.2.3. Anode potentials of Sed-MFC before cell disassembling. Dashed line indicates acetate redox potential.

Even though the electroactive biofilm was growing in all Sed-MFC, the low robustness of the system avoided repeatability in cell signal, as shown in Figure 3.2.4. This fact was already restricting the repeatability in further MEC operation with the anodes inoculated in Sed-MFC. The differences observed for the three replicates were most probably caused by differences in brush size and anode position relative to cathode, which are common limitations of Sed-MFC.

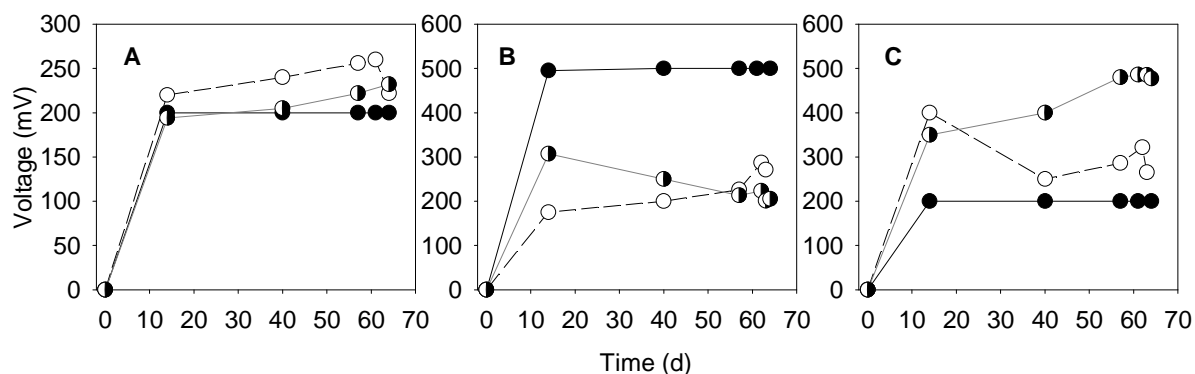


Figure 3.2.4. Cell potential evolution in Sed-MFC for three replicate tests (A) inoculating at 1000 Ω , (B) 1470 Ω and (C) 22100 Ω .

The anodes inoculated with a Sed-MFC at different R_{ext} were then transferred to MECs. Initially the applied potential was kept at 0.4 V and after a period of seven days it was changed to 0.8 V. Only a seven days period at 0.4 V was chosen not to influence the next period at 0.8 V. Figure 3.2.5 summarizes the average current intensity measured in Sed-MFC and in MEC. No clear trends were obtained in either system. In Sed-MFC the best performance in terms of current intensity was reached inoculating the anode at 560 Ω , obtaining 0.4 mA. As it was expected when inoculating at 22100 Ω , very low signal was detected, since it was a working condition close to the open circuit scenario.

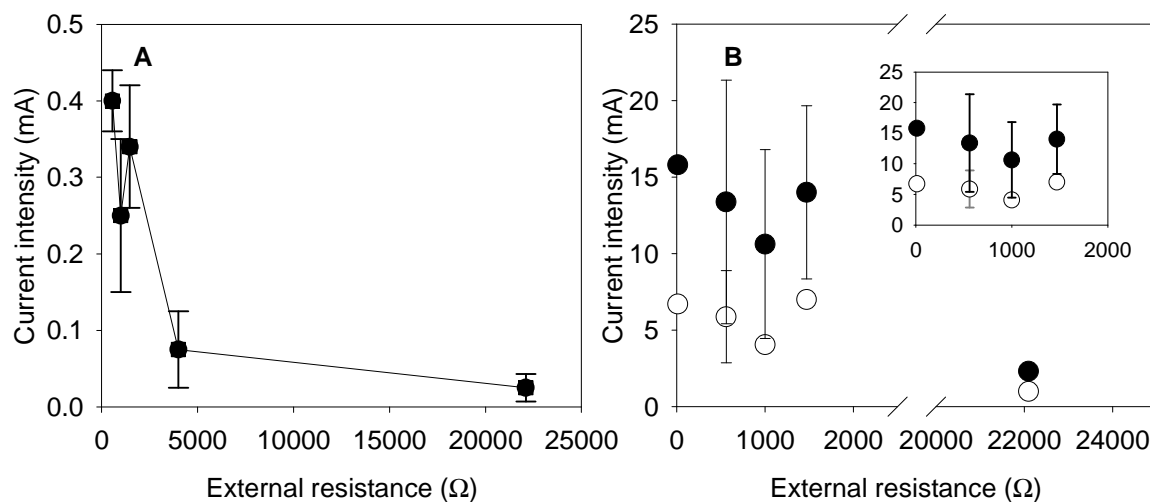


Figure 3.2.5. Current intensity response in systems inoculated at different R_{ext} (A) Sed-MFC and (B) MEC at 0.4V applied voltage (white circles) and 0.8V applied voltage (black circles).

Regarding MEC, current intensity achieved did not show significant differences for anodes inoculated at R_{ext} lower than 1470 Ω , reaching values around 5 mA at an applied voltage of 0.4 V. Average values ranging between 10 and 15 mA were obtained when the system was

operated at 0.8 V applied voltage, but a large variability in response was detected as can be noted by the wide error bars.

Measured hydrogen production was much lower than expected, being 1-4% of theoretical hydrogen produced based on substrate consumption and 0.3-1% based on current intensity measured. It was also observed that hydrogen production calculation based on current intensity was in all cases higher than hydrogen production based on substrate consumed, or in other words that CE was higher than 100%, what was indicative of the presence of other processes contributing to current intensity generation, such as the use of hydrogen as electron donor by ARB. Hence, low hydrogen production was measured as consequence of hydrogen-recycling phenomena, caused by the metabolism of H_2 -oxidizing ARB and homoacetogenic bacteria. Gas leakages through connections could also be responsible for the low hydrogen production.

It was decided to perform the Set of Tests B because of the low robustness on the results (low repeatability in cell signal, lack of trends in terms of inoculation at different R_{ext}) and because of the fact that MEC could only be analyzed in terms of current intensity but not in terms of hydrogen production.

2.3.1.2. Set of tests B: inoculation in mAC-MFC

Inoculation at different R_{ext} in mAC-MFC produced repeatable signals (Figure 3.2.6). A steady state response was achieved in about one week for the highest resistances tested (560, 1000 and 4000 Ω), whereas it took between 2-3 weeks for the lowest (12 and 50 Ω). Current intensity had a decreasing trend as R_{ext} increased as it is shown in Figure 3.2.7A, reaching a maximum of 2 mA on average when the system had been inoculated at 50 Ω . However such a trend was not observed when the anodes were switched to mMEC (Figure 3.2.7B). In fact, as already suggested by the results in the Set of Tests A, no significant difference was detected in terms of current intensity for anodes inoculated at different external resistances neither at 0.4 V nor 0.8 V of applied potential.

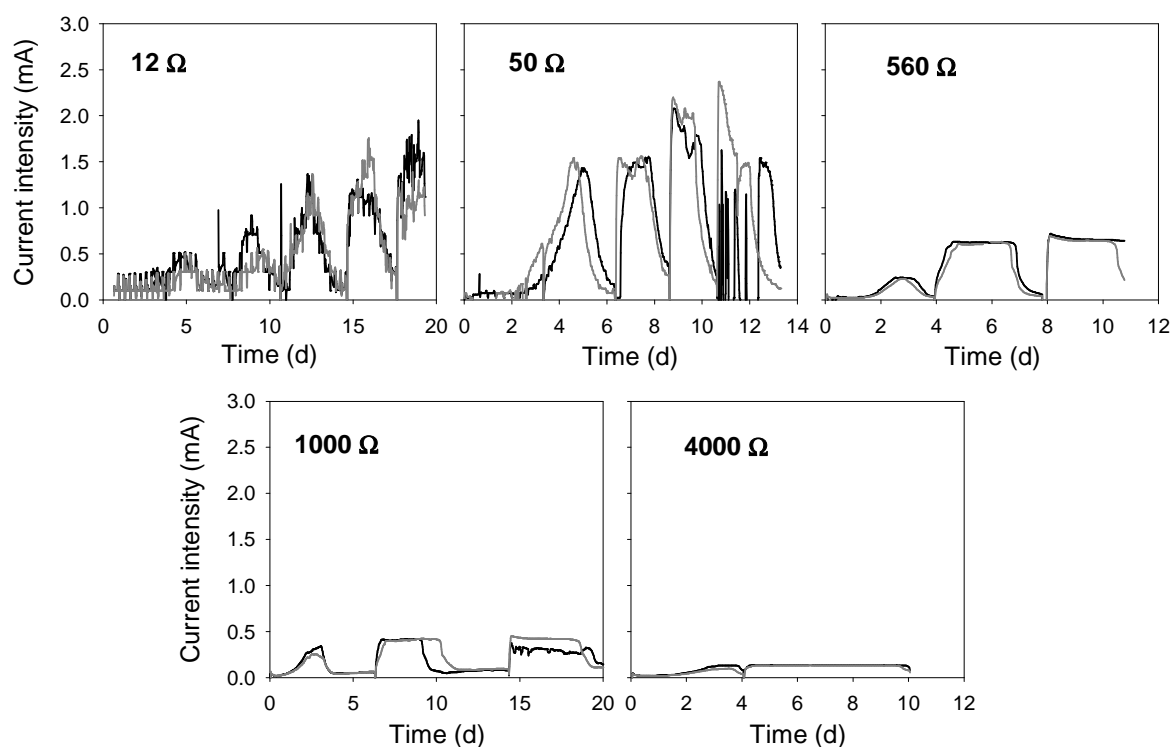


Figure 3.2.6. Current intensity throughout the inoculation of mMFC-AC with anaerobic sludge.

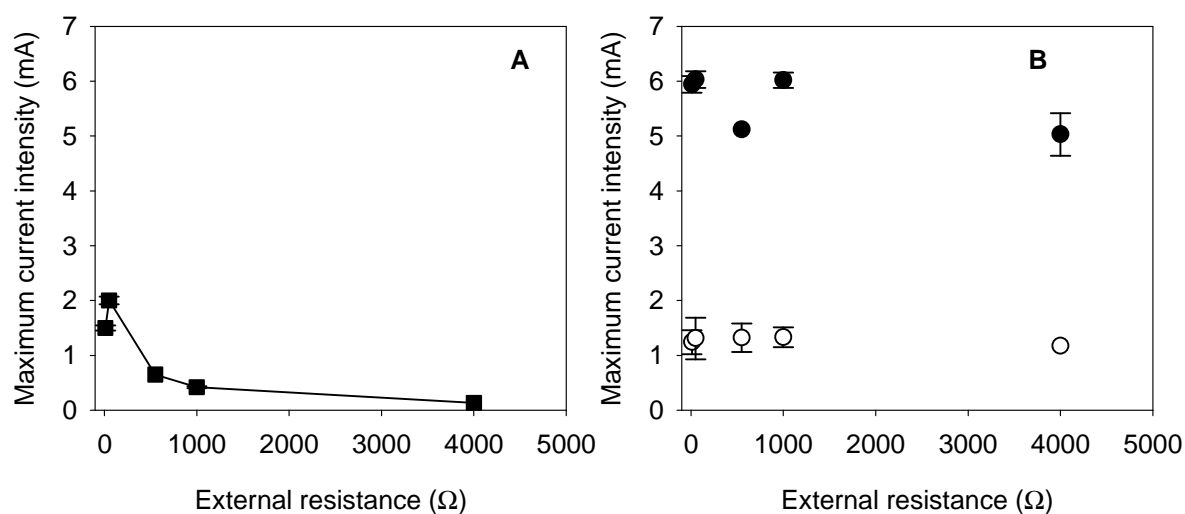


Figure 3.2.7. Current intensity response in (A) mAC-MFC and (B) mMEC at 0.4 V applied voltage (white circles) and 0.8 V applied voltage (black circles).

Hydrogen production in MEC was systematically measured analyzing the gas bag content. Unfortunately a double analysis performed in the gas bag and in the MEC headspace revealed that gas composition was not homogeneous, which had been assumed initially, quantifying less than 5% of total hydrogen volume produced if only the gas bag was considered in the analyses. This fact introduces a large uncertainty in the results, which cannot be used quantitatively. However it is supposed that the higher the hydrogen production and therefore

the higher hydrogen concentration in the headspace the higher should be the hydrogen detection in the gas bag. This allows to use the results qualitatively, assessing a trend in hydrogen production for the different systems considered.

Regarding cathodic efficiency and energy yield, higher recoveries were calculated for anodes inoculated at low external resistances, both for low and high applied potentials (Figure 3.2.8). It should be noted that energy yield should have a minimum value of 100%, so that at least the energy input is recovered. Such a threshold was not reached. Taking into account that hydrogen production was underestimated due to headspace-gas bag differences in composition it is assumed that energy yields presented in Figure 3.2.8 were minimum values. Even though they represent minimum values, interestingly energy yield reached 70% at an applied voltage of 0.4 V and 97% at 0.8 V for an anode inoculated at 50 Ω .

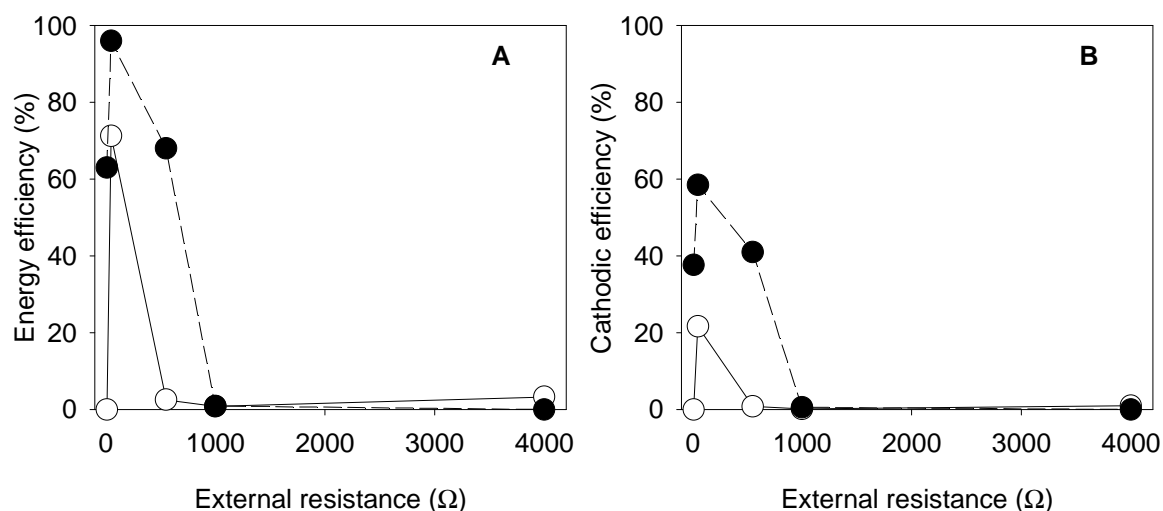


Figure 3.2.8. (A) Energy efficiency relative to electrical input and (B) cathodic efficiency in MEC working with anodes inoculated at different R_{ext} and applying 0.4V (○) or 0.8V (●).

Comparing the response of Sed-MFC and mAC-MFC it can be seen that the latter had a higher response in terms of current intensity and current density, reaching a maximum of 0.4 mA (0.5 mA m^{-2}) in Sed-MFC and 2 mA in mAC-MFC (9 mA m^{-2}). These differences are attributed to (i) the differences in cathode materials, since Sed-MFC has a simple steel wool cathode whereas mAC-MFC has a cathode catalyzed with platinum and (ii) anode position relative to the cathode, being shorter for mAC-MFC than for Sed-MFC. Another aspect to take into consideration is that mAC-MFC has its medium replaced regularly, washing out from the system a large portion of microorganisms without electroactivity that compete with ARB for the substrate and therefore enhancing its growth.

2.3.1.3. Comparison with other works

The results obtained in this study have been listed together with results reported in the literature for MEC working at different applied potentials (Table 3.2.1). Note that studies that apply less than 0.6 V in MEC are scarce in the literature.

Table 3.2.1 Current intensity normalized to reactor volume, current density and energy efficiency in MEC under different applied potential.

System	R_{ext} in MFC inoculation	Inoculum	ΔV applied (V)	I_V (A/m ³)	J (A/m ²)	η_w (%)	Reference
Double chamber, carbon cloth anode	1000	Wastewater	0.4 0.8	ND ND	0.3 0.85	ND ND	Liu et al, 2005 ⁴⁸
Double chamber, graphite felt anode	NA	Previous MEC effluent	0.5	2.8	0.2	169	Rozendal et al, 2006 ⁴⁹
Single chamber cube shaped, graphite brush anode	1000	Wastewater	0.4 0.6 0.8	103 186 292	0.013 0.024 0.037	351 254 194	Call et al, 2008 ⁵⁰
Single chamber, carbon cloth anode	1000	Wastewater	0.4 0.6	19.1 43.4	4.1 9.3	267 204	Hu et al, 2008 ⁵¹
Single chamber cube shaped, graphite brush anode	1000	Wastewater	0.6	143	0.018	187	Nam et al., 2011 ⁵²
Continuous membrane-less, carbon felt anode.	NA	Anaerobic sludge	0.4	40	0.4	ND	Tartakovsky et al., 2011 ⁵³
mMEC, graphite brush anode	50 50 1000 1000	Anaerobic sludge	0.4 0.8 0.4 0.8	46.8 214.3 47.5 215	0.006 0.027 0.006 0.027	71.3 96 0 0	This work

A direct comparison can be stated with studies working with cube shaped MEC (equivalent to mMEC) and a graphite fiber brush anode (Call et al., 2008 and Nam et al., 2011). Lower current intensities were obtained here regardless of the external resistance used in the inoculation of MFC, although they were of the same order of magnitude when 0.8 V were applied. Current intensities achieved applying 0.4 V were one order of magnitude lower in this study.

The differences observed when 0.4V were applied could be a consequence of a still transitory response of MEC. In fact, the batch cycle was prolonged at 0.4 V of applied voltage as a result of lower current intensities. Therefore a 7 days period could have not been enough to

reach a stationary response at such applied voltage. Nonetheless a stable current intensity response was observed throughout the period.

The inoculum source was also different in both cases, being anaerobic sludge in this work and municipal wastewater in the others. In fact, it was expected that anaerobic sludge would contain a higher percentage of ARB than wastewater and therefore higher current intensities would be enhanced.

The results for the rest of works that are presented in Table 3.2.1 are very dependent on the system configuration, since low anode surface favors high current densities and low reactor volumes favor volumetric current intensities. In terms of installation costs a comparison in terms of volumetric current intensities is more coherent.

In works performed fixing an anode potential it is not common to provide the energy input from the potentiostat and therefore they have not been included in Table 3.2.1

In this work, no significant effects were observed regarding the selection of more energetically efficient ARB in MEC at higher external resistances.

2.3.2. Bioaugmentation of bioelectrochemical systems with microbial consortia

Bioaugmentation of bioelectrochemical systems with syntrophic consortia that would allow exoelectrogenesis from complex substrates was aimed. With this objective a fermenting population and an exoelectrogenic population were initially grown separately. Anaerobic digestion sludge was used as inoculum in the development of the fermenting population, since it contains microorganisms responsible of the hydrolysis of complex substrates to simpler subunits and fermenting microorganisms that perform the conversion of these simpler subunits to VFA by acidogenesis, which are further metabolized to acetic acid, hydrogen and carbon dioxide by acetogenesis. The fact that BES was dosed, though, inhibited the methanogenesis step. Hence, when both fermenting and exoelectrogenic bacteria would be joint, acetic acid would be consumed by ARB (Figure 3.2.9).

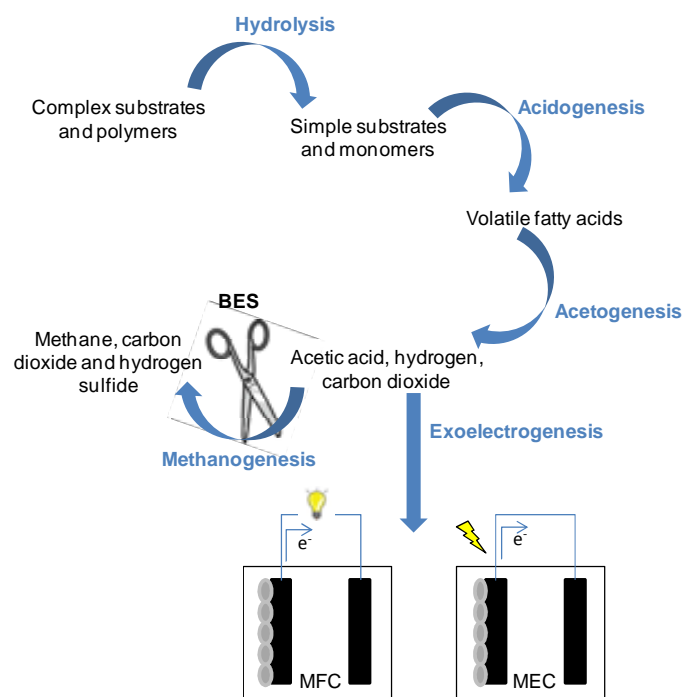


Figure 3.2.9. Process scheme to obtain a syntrophic consortium to consume complex substrates in bioelectrochemical systems inoculating with anaerobic digestion sludge.

2.3.2.1. Selection and growth of fermenting and exoelectrogenic populations

The growth of a fermenting population able to degrade each complex substrate (glycerol, milk and starch) was assessed by periodically monitoring the metabolites concentration in the culture flask. Figure 3.2.10 presents the metabolites concentration profile (normalized to initial COD and expressed as a percentage) in a conventional batch cycle for each substrate studied. A progressive accumulation of VFA was observed, especially acetic and propionic acids. Lactate, glucose, valeric acid and butyric acid were present in low concentrations (lower than 15 mg L^{-1} for all the period) and were, therefore, plotted together for glycerol and starch culture flasks. On the contrary milk-culture flask showed an increasing profile for almost all the intermediates measured. For the starch-culture flask, the fact that these fermentation intermediates were present at low concentrations for all the period could suggest that they were being rapidly metabolized or that they were not an important degradation product in the system.

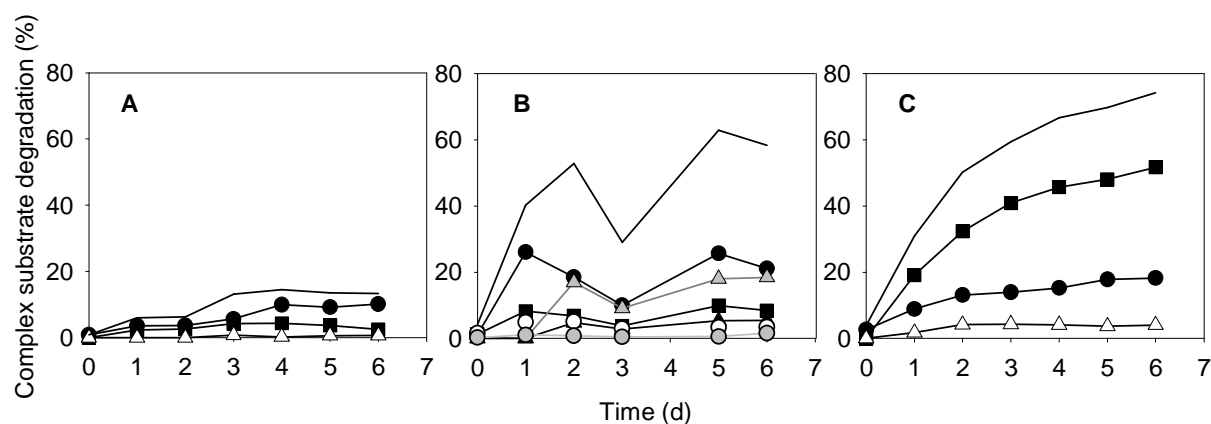


Figure 3.2.10. Metabolites concentration profiles normalized to initial COD for a batch cycle in the culture flasks: **A** glycerol-culture flask; **B** milk-culture flask and **C** starch-culture flask. ● Acetate, ■ Propionate, △ Sum of butyrate, valerate, lactate and glucose, ▲ butyrate, ▲ valerate, ● lactate and ○ glucose. Solid line: complex substrate degradation.

The glycerol-culture flask presented the lowest fermentation ability, reaching a maximum of 15% degradation of the initial COD, whereas milk and starch-culture flasks could degrade 60 and 70% respectively. The trend for milk and starch-culture flasks seemed to show that a complete degradation from the initial COD could be possible for a longer batch cycle. In contrast, glycerol-culture flask exhibited a slow degradation profile. In that case, much longer cycle time could be needed for complete degradation. Inhibitory effects due to pH changes were excluded, not observing a pH decrease of more than 0.2 units regardless of the VFA accumulation. Methane was not detected, indicating that methanogenesis was effectively inhibited.

In parallel, the enrichment of the anodic biofilm on ARB was assessed by monitoring the voltage generation in mAC-MFC (Figure 3.2.11). Propionic acid and acetic acid were used as carbon source in view of the future syntrophy with a fermenting population, which would degrade the more complex substrates to VFA. The analyses performed at the end of each batch cycle showed that both acetate and propionate were being consumed by ARB. Maximum current intensity achieved increased with time until a steady state was reached (~0.45 mA). Accordingly, CE progressively increased, achieving a steady CE of 15% from day 12. At this point it was considered that the mAC-MFC were ready to be inoculated with the fermenting community and to be fed with the complex substrate as a sole carbon source.

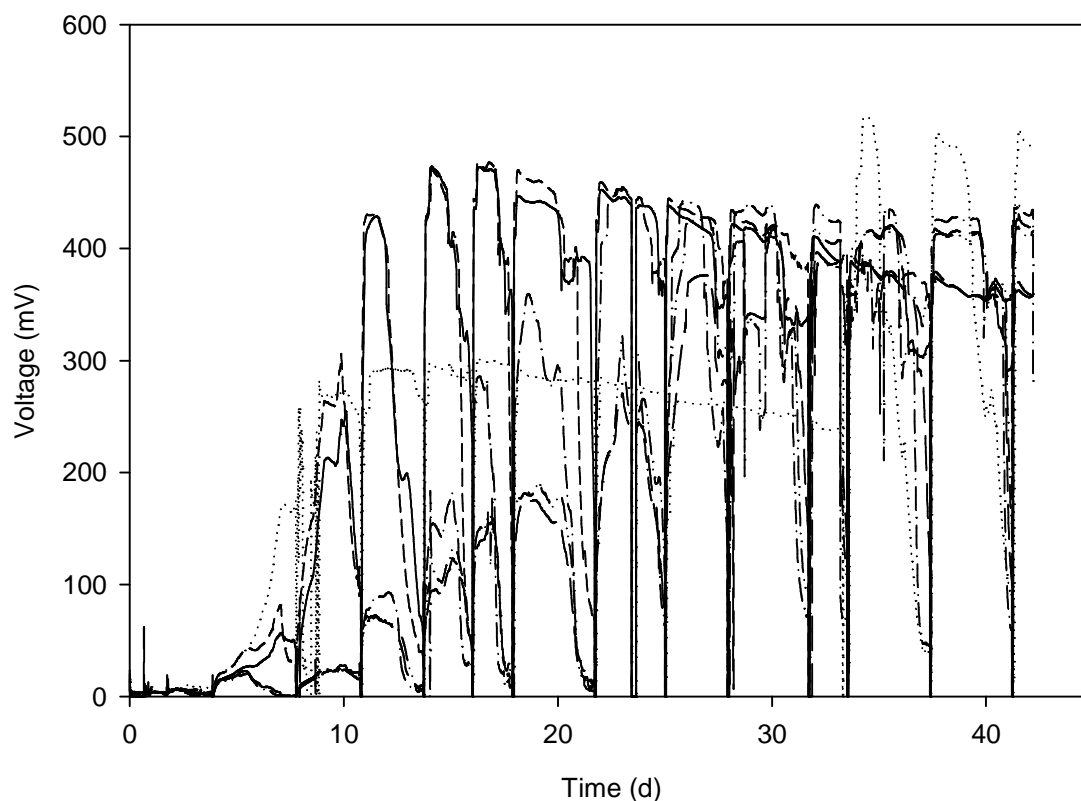


Figure 3.2.11. Evolution of voltage during the start-up of a set of six mMFC fed with acetate and propionate (R_{ext} 1000 Ω). Inoculum was taken from a previously working MFC.

2.3.2.2. Complex substrates in MFC: Development of an anodic syntrophic consortium

Each mAC-MFC was inoculated with sludge from the corresponding culture flask (Figure 3.2.12A), accounting for the 25% of the total reactor volume. From this moment on, the system was fed exclusively with glycerol, milk or starch as sole carbon source (MFC-glycerol, MFC-milk and MFC-starch). Figure 3.2.12B presents the current intensity response for the three cells operating with different substrates since the inoculation. The fermenting community was initially in suspension in mAC-MFC, which would not be interesting in view of a fed batch or continuous operation, since fermenting microorganisms could be washed out from the system. The growth of fermenting bacteria on the anode surface would be an ideal situation in view of the syntrophy required with ARB. An initial step-wise replacement of the media was designed to enhance the growth on the anodic biofilm as a syntrophic consortium, i.e. the percentage of media replaced by fresh one was gradually increased until a moment when it was totally replaced (day 30 since inoculation). Current intensity achieved during this period was sustained, denoting that the substrate degradation was maintained and, therefore, that the syntrophic consortium was effectively growing on the anode surface. The possibility

to immobilize the syntrophic consortia in the anode introduces an operational improvement in the system, since a pre-treatment tank to perform hydrolysis and fermentation of complex substrates would not be required.

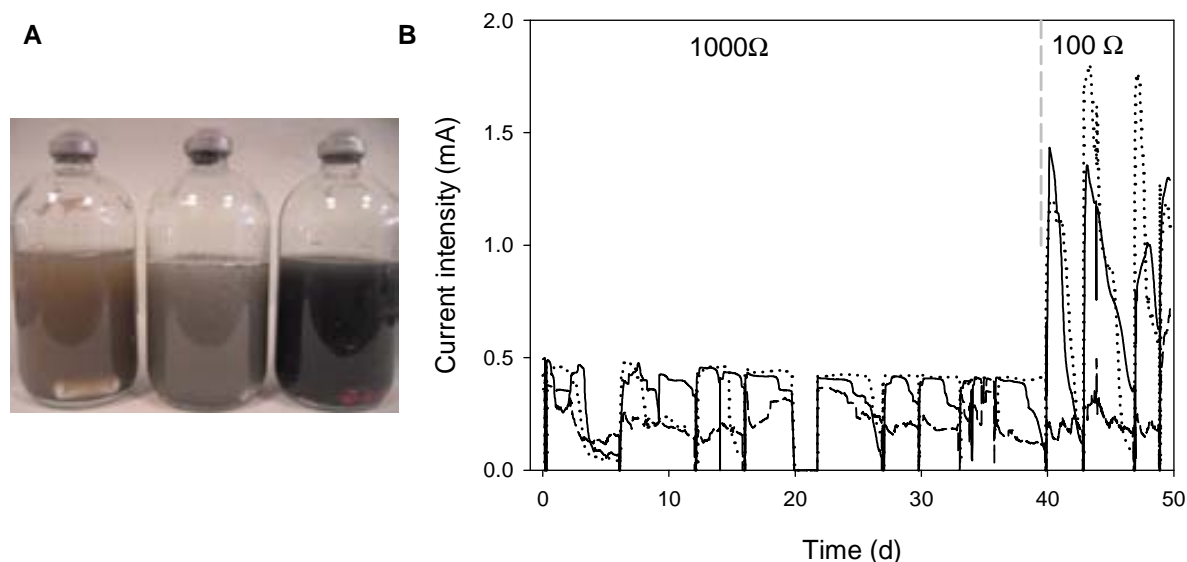


Figure 3.2.12. A. Culture flasks fed with glycerol, milk and starch B. Current intensity profiles for MFC fed with complex substrates: glycerol (solid line), milk (dotted line) and starch (dashed line). Time 0 represents MFC inoculation with the fermenting population grown in the respective culture flask.

The possibility of enhancing the degradation of the three complex substrates by codigesting them was explored in the so called MFC-mixed. In this case, to inoculate MFC-mixed with a fermenting community, sludge from the three culture flasks was used accounting in total for a 25% of the reactor volume and the reactor was fed with the three complex substrates (Figure 3.2.13).

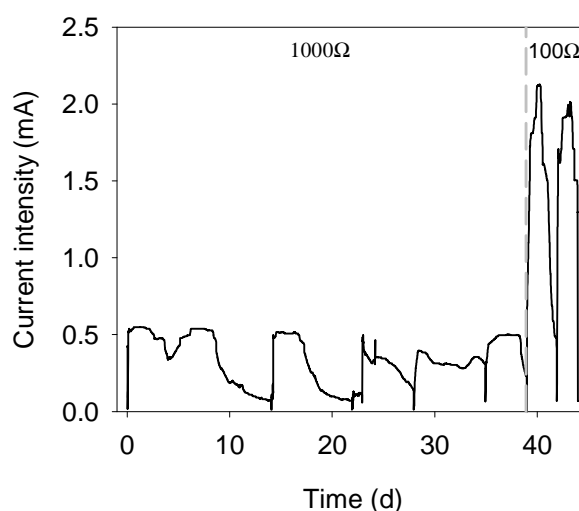


Figure 3.2.13. Current intensity profile for MFC-mixed treating simultaneously glycerol, milk and starch. Time 0 represents MFC inoculation with the three fermenting populations grown in the culture flasks.

As discussed in Chapter 1, a high R_{ext} of 1000 Ω was only used during the inoculation period to ensure working at a low anode potential. R_{ext} were decreased on day 40 from 1000 Ω to 100 Ω to enhance biomass electroactivity, resulting in a significant increase in current intensity for MFC-glycerol, MFC-milk and MFC-mixed.

Table 3.2.2 shows the coulombic efficiencies for each substrate used. The syntrophy between fermenting bacteria and ARB in general resulted in better CE than when only acetate and propionate were used. However, CE lower than 50%, indicated that still less than a half of the substrate available was being recovered as current intensity and therefore consumed by ARB. Changing over to a lower R_{ext} generally produced an increase in CE, which was more important for MFC-milk and MFC-mixed. Only MFC-starch was negatively affected by the change.

Table 3.2.2. Average coulombic efficiency for mAC-MFC before and after the change of R_{ext}

Substrate	CE (R_{ext} 1000 Ω)	CE (R_{ext} 100 Ω)
Glycerol	32% \pm 10	35% \pm 8
Milk	36% \pm 4	52% \pm 6
Starch	28% \pm 10	15% \pm 3
Mixed	12.5 %	28.8 %

Polarization and power curves were performed not only to estimate the internal resistance of the system but also to identify the limiting step in the power production from a complex substrate (Figure 3.2.14). With this aim, the curves were first obtained for the three mAC-MFCs running with the actual complex substrate and they were repeated for acetate as sole carbon source. According to Figure 3.2.14 only for MFC-starch power production would be limited by the fermenting community, obtaining up to 1.3 mA when acetate was fed and barely reaching 0.4 mA when starch was fed. On the contrary, glycerol and milk-fed MFC did not show a significant difference neither in terms of maximum power output nor in current intensity achieved when they were operating with the complex substrate or acetate. In their case power production would be limited by ARB community. The profiles obtained with 100 Ω R_{ext} were analogous to the ones with 1000 Ω , again showing limitations due to the fermentation step only for MFC-starch.

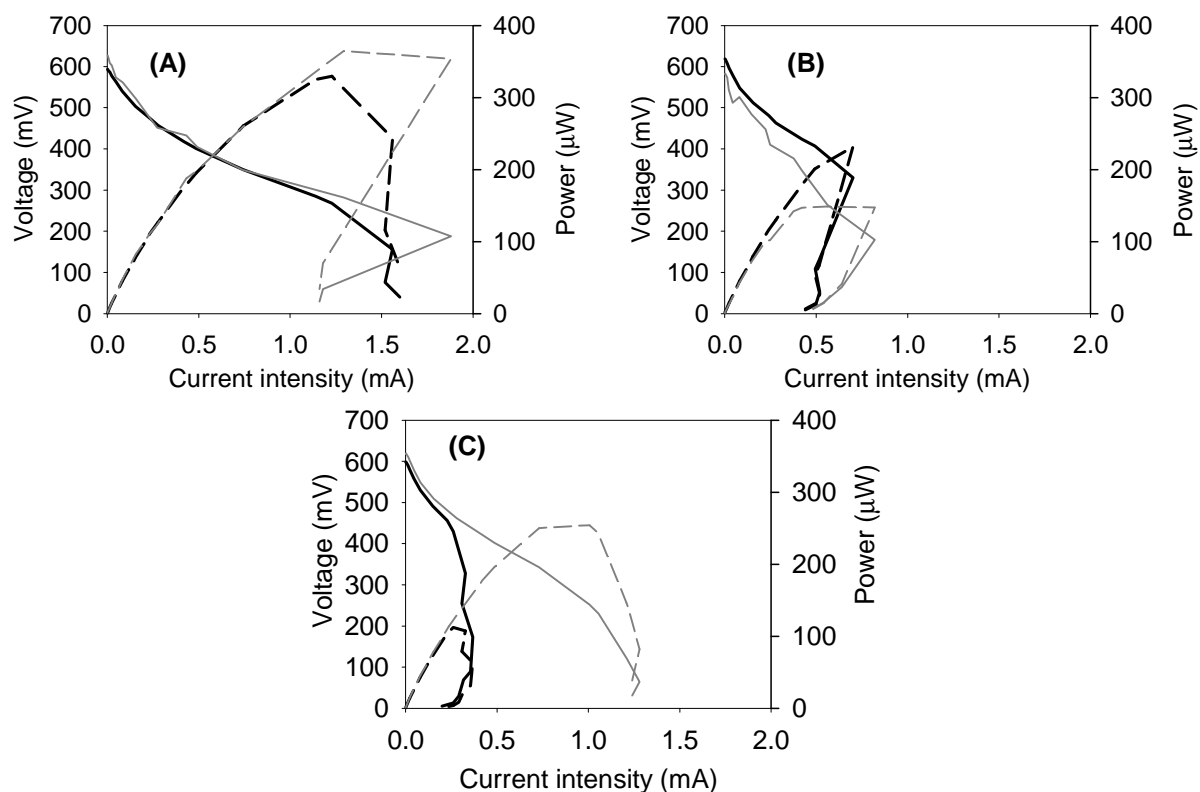


Figure 3.2.14. Polarization curves (solid) and power curves (dashed) for MFC operating with 1000 Ω external resistance with (A) glycerol, (B) milk and (C) starch. Thick line: actual complex substrate. Thin line: acetate.

Table 3.2.3 summarizes the results obtained from the polarization and power curves when the system was fed with the complex substrate. From the first period at 1000 Ω, according to OCV values, potential losses did not differ much for the different carbon sources. For comparison purposes, Table 3.2.3 also includes data obtained in an additional MFC with equivalent configuration which was always fed with acetate. In such system both OCV and P_{\max} exceeded the results obtained for any complex substrate indicating lower potential losses. It is worth mentioning that, as it can be seen in Figure 3.2.14, OCV values for the complex substrates did not show significant difference with the values obtained when acetate was fed, presumably because the fermentation step was not limiting under OCV operation and hence acetate was available in all the cases. R_{int} , which should coincide with R_{ext} to maximize power output ($R_{\text{ext,opt}}$), was lower than the actual R_{ext} for all MFC for the period operating at 1000 Ω. Nevertheless a value closer to 1000 Ω was obtained for MFC-starch, probably as a consequence of being limited by the fermentation step. This higher resistance would be indicating that decreasing the external load to 100 Ω would definitely not enhance power production in MFC-starch, as confirmed with the results obtained for the second period at 100 Ω, where MFC-starch showed a significant increase in R_{int} .

Table 3.2.3. Summary of the main results obtained from power and polarization curves in complex substrate fed-MFC. Results for an additional acetate fed MFC in an equivalent configuration have been included for comparison purposes.

Substrate	Operation at 1000 Ω			Operation at 100 Ω		
	OCV	P_{\max} (mW)	R_{int} (Ω)	OCV	P_{\max} (mW)	R_{int} (Ω)
Acetate	681	0.75	218			
Glycerol	594	0.34	218	558	0.22	252
Milk	618	0.24	355	543	0.19	330
Starch	595	0.10	730	587	0.07	1190

Maximum power output also presented some differences for both periods, but unlike R_{int} , P_{\max} was calculated with a discrete data point obtained for a given resistance, which intrinsically introduces some error in its estimation. Anyway, according to these estimations lower P_{\max} were obtained for the second period at 100 Ω . Regardless of the lower P_{\max} , current intensity was clearly boosted after the change of R_{ext} as seen in Figure 3.2.12, which would be more interesting in view of operating later on in MEC.

CV analyses (Figure 3.2.15) evidenced a clear difference in each system behavior. Not only maximum current intensity achieved differed significantly from one system to the other, but also oxidation and reduction peaks appeared at different anode potentials. From these voltammograms the suitability of each complex substrate to be treated in bioelectrochemical systems could be discussed, appearing to be glycerol the substrate that could offer the highest outputs.

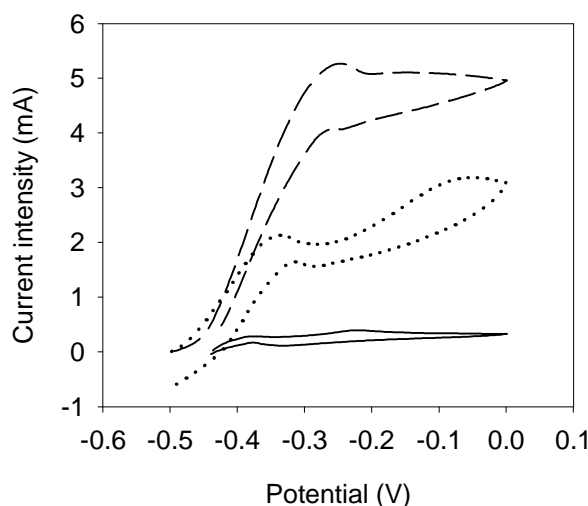


Figure 3.2.15. Voltammograms for mMFC working with complex substrates. Dashed line: MFC-glycerol. Dotted line: MFC-milk. Solid line: MFC-starch.

Peaks position is related to the potential of the enzyme involved in the last step of the metabolic pathway (responsible of the extracellular electron transfer), which differs from one organism to another⁵⁴. Therefore it could also be inferred that the electroactive microbial community that evolved in each system was different, which would be consistent with the fact that the fermentation products of each substrate vary in nature and composition and therefore different ARB or metabolic pathways for ARB would be favored.

Table 3.2.4 presents common parameters to assess MFC performance (current intensity, CE, COD removal) obtained in this work together with similar works from the literature. A direct comparison can be stated with single chamber systems inoculated with a source already containing the specific substrate, e.g. industrial wastewater, since they will most probably already contain a fermentative population able to degrade it. Nevertheless other cases have also been included to have a broader view.

Table 3.2.4. Comparison of this work with others studies dealing with complex substrates in MFC

Carbon source	Reactor configuration	Inoculation	Current intensity ¹ (A/m ³)	Coulombic efficiency (%)	COD removal	Reference
Crude glycerol	Single chamber	Domestic WW	43.71*	18	90	Feng et al., 2011 ⁴⁶
Glycerol	Single chamber	<i>Bacillus subtilis</i>	1	23	-	Nimje et al., 2011 ³⁴
Dairy WW	Annular single chamber	Dairy WWTP activated sludge	42.2*	27	91	Mardanpour et al., 2012 ⁴³
Dairy WW	Double chamber	Dairy WW	-	17	91	Elakkiya et al., 2013 ⁴⁴
Proteins (meat extract, peptone)	Double chamber	Anaerobic sludge	1.5 ^{1,*}	12	50	Liu et al., 2009 ⁵⁵
Proteins (bovine serum albumin)	Single chamber	Meat processing Plant WW	27.5*	20	90	Heilmann et al., 2006 ⁵⁶
Starch WW	Single chamber	Starch processing WW	5.25*	8	98	Lu et al., 2009 ³¹
Starch	Single chamber	Primary clarifier effluent	3.5*	19	60	Velasquez-Orta et al., 2011 ²⁸
Glycerol	Single chamber	Fermentative population	50	35	100	This work
Starch		and water	9	15	85.1	
Milk		from already working MFC	62.5	52	73.5	
Mixed			71.4	28.8	99	

¹ Current intensity is normalized by anodic chamber volume

* Parameter calculated from the data presented in the specific publication

The results obtained in terms of current intensity generation per reactor volume and CE were better than those reported in other studies. Thus, bioaugmenting the anode with a syntrophic consortium was advantageous in such systems. Indeed, comparable results were obtained when the system was inoculated with the very same wastewater⁵⁶, or with activated sludge treating the same kind of substrate⁴³ as the inoculum was probably already containing the proper fermentative population. In the case of MFC-starch, results were one order of magnitude lower, but they were also comparable with those found by Lu³¹ in a system fed with starch wastewater and inoculated with wastewater from a starch processing plant.

Concerning substrates complexity, it was observed that starch was the most difficult substrate to degrade and effectively convert to electricity, which was probably related to the necessity to hydrolyze such a big macromolecule, implying an important role of fermentative

populations, and related to its low solubility, introducing an accessibility limitation to the substrate. In contrast, milk seemed to allow the highest power production regardless of the variety of its content, containing sugars, fats and proteins. Regarding glycerol, results were comparable to other works, where conditions were stricter and even crude glycerol (biodiesel waste) was used as carbon source⁴⁶.

In terms of COD removal, milk was the substrate with the lowest efficiency. Nevertheless when all the substrates were fed together in MFC-mixed, the organic matter was practically totally degraded. In fact, in MFC-mixed, not only COD removal was better than for mAC-MFC with single substrates, but also current intensity was boosted.

2.4. Conclusions

The role of the external resistance during the inoculation on selection of more energetically efficient bacteria in MEC was evaluated in two different set-ups. Taking into account the variability observed in bioelectrochemical system performance, no significant effects were observed regarding the selection of more energetically efficient ARB in MEC at higher external resistances: current intensity achieved at 0.4 V and 0.8 V of applied voltage did not show significant differences. In terms of cathodic efficiency and energy efficiency in MEC there seemed to be a higher recovery for lower external resistances.

Regarding bioaugmentation with consortia that enable the use of complex substrates in bioelectrochemical systems, which require the presence of fermentative bacteria and ARB, the development of such consortium on the anode surface enhanced the electroactivity of the system, avoiding any prefermentation treatment. Glycerol, starch and milk were explored as complex substrates for current generation in a single chamber MFC configuration.

In terms of current generation in mAC-MFC after bioaugmenting the system with the syntrophic consortium, higher current intensities and coulombic efficiencies were reached in this work when compared to previous reports, validating the methodology proposed.

The simultaneous degradation of the three complex substrates in MFC-mixed seemed to stand out against MFC-single substrates, confirming the advantages of codegrading substrates of very different nature. In fact current intensity, power generation and COD removal in MFC-mixed overcame any MFC-single substrate.

The fact that the syntrophic consortium can grow as a biofilm on the anode surface, being therefore immobilized, is interesting in view of practical implementation of bioelectrochemical systems, because (i) a pretreatment tank to perform hydrolysis and fermentation of complex substrates can be omitted (ii) slow growing biomass in the biofilm is protected against washout when operating at low hydraulic retention times (iii) operation at low hydraulic retention time would decrease the chances for other non-desired communities such as methanogenic *archaea* to grow.

Chapter 3. Methanogenic population control

Chapter summary

One of the main bottlenecks in single chamber microbial electrolysis cells is the growth of methanogenic *archaea* that compete with ARB for substrate and product. Addition of chemical inhibitors of methanogenesis is not economically feasible in view of future scale-up of the process. A strategy to avoid methanogenesis in MEC by reducing the hydrogen retention time is presented in this chapter. The procedure presented is tested for both readily biodegradable synthetic wastewater and complex synthetic wastewater. The first is oriented to test the strategy in conditions favoring methanogenic activity, whereas the later has the purpose of testing it in conditions closer to reality regarding substrate complexity and operation. The strategy was effective for MEC fed with readily biodegradable synthetic wastewater but presented limitations depending on the complex substrate consumed.

The content of this chapter was partially registered by Sociedad Española de Carburos Metálicos SA in the European Patent Office with the name “Process for methanogenesis inhibition in single chamber microbial electrolysis cells” in 2012.

3.1. Introduction

MEC are anaerobic environments and, therefore, anaerobic microorganisms like methanogenic *archaea* can develop. In single chamber MEC methanogenic *archaea* are favored, since they are able to consume both acetate and hydrogen. Affinity for acetate differs for acetoclastic methanogens and ARB, having values of the half saturation constant of 0.85-7 mM for the first and 0.04 mM for the later, specifically for *Geobacter* spp.⁵⁷⁻⁶¹. Accordingly methane has been observed to be associated to current generation and hydrogenotrophic methanogenesis⁶². Also, the fact that anaerobic digestion sludge is often the inoculum for bioelectrochemical systems entails that ARB have to grow among an already rich methanogenic population. This leads to the need of using chemical inhibitors or operational parameters that enable ARB to outcompete methanogens. On the contrary, if any strategy to reduce methane production is used, studies performed at pilot scale with single chamber configurations and under continuous flow conditions showed that these systems ended up producing a gas mostly composed of methane^{45,63}.

BES dosage to bioelectrochemical systems to inhibit methanogenic *archaea* is accepted at lab scale studies⁶⁴. However its utilization is a non-economically feasible alternative at higher scales due to its high cost (~ 600 euros per kg, laboratory grade). There is not a general agreement on how much BES is required, i.e. what is the minimum amount that allows methanogens inhibition and how long the inhibition lasts. Nollet et al.⁶⁵ reduced methane production in rumen by more than 90% using 10 μ M BES. In terms of tests on the effect of BES in bioelectrochemical systems, Chae et al.⁶⁶ claimed that 286 μ M BES dosage retained inhibitory effects even after ten batch cycles (1 day cycle⁻¹) and Parameswaran et al.⁶⁷ stated that 50 mM BES was required to selectively inhibit methanogens (acetoclastic and hydrogenotrophic methanogens).

Several proposals that try to come up with an operational procedure that avoids methanogens growth in MEC are discussed in the literature. Temperature was reported not to be an efficient procedure^{1,62}. The effects of low pH (lower than pH 6), which a priori should cause a sharp drop in methane production rate, were also explored, not seeing a decrease in methane production^{1,51,62}. A periodic exposure of the anode to air or the periodic sparging with air was also investigated, obtaining better results for the former. The effectiveness of air exposure, though, was observed to be dependent on the time of exposure, reaching 98% reduction of

methane production after 120h of air exposure^{1,68}. Air exposure of the cathode was also considered, taking into account that it is an ideal support for hydrogenotrophic methanogens to grow⁵¹. Applied voltage and anode potential were also studied as parameters influencing methanogenic growth. It was observed that by limiting ARB growth at very low anode potentials methanogens had greater chances to proliferate⁴ and that methane production was lower applying higher potentials, where current densities were higher and cycles were shorter^{51,62}. Higher turbulence in the media also showed an increase in hydrogen production relative to methane⁶⁸. Other operational parameters negatively affected hydrogen production as a result of methanogenic growth, such as high organic loading rates and long batch cycles²⁶, suggesting that rapidly removing hydrogen from the system could increase the system performance. With this aim, the reactor design could be engineered so that hydrogen is easily driven out of the system and it is not accessible to neither methanogens nor other H₂-consuming microorganisms (homoacetogenic bacteria and H₂-oxidizing ARB). For example, Lee et al. operated a continuous upflow cathode-on-top MEC resulting in an increased efficiency⁶⁹.

Most strategies studied were just partially investigated and, if working, they did not represent a complete suppression of methanogenic activity, but a mere decrease. Also, they were carried out for a short time, and thus are not representatives in a fed-batch or continuous system.

Given the high costs of BES, its continuous dosage is not an option, especially if MEC are to be applied in a continuous mode or at a larger scale. For this reason studies addressed to decreasing BES dosage are interesting for a future scale-up. In this lab scale work, the effect of both BES addition and hydrogen stripping with nitrogen were studied for a long period of time under different approaches. BES was supposed to inhibit methanogenic growth whereas nitrogen sparging was used to strip hydrogen from the system, i.e. to reduce its retention time, so that hydrogen consuming methanogens growth was prevented or minimized.

The same procedure was tested for both readily biodegradable synthetic wastewater (containing acetate as carbon source) and complex synthetic wastewater in single chamber MEC. The first was oriented to test the strategy in conditions favoring methanogenic activity, since acetate was used as sole carbon source and the system operated under long hydraulic retention time conditions. The later had the purpose of testing the strategy in conditions

closer to reality in terms of substrate complexity and operation. With this aim, the system was fed with complex synthetic wastewater to account for the heterogeneity and complexity of real wastewater and hydraulic retention time was adapted according to the degradation rate, which was interesting in view of its practical use in a future scaled up system.

3.2. Materials and methods

Y-MEC were used to test methanogenic control strategies in single chamber MEC fed with readily biodegradable synthetic wastewater. Y-MEC that had been working from the very beginning with BES (12 mM) were run in batch mode (0.8 V applied potential). The cathode was a platinum plate (4 cm², Panreac Química SA, Castellar del Vallès, Catalonia), which was periodically sandpapered.

Acetate was used as sole carbon source (100 mg L⁻¹ initial concentration). Cycle duration was around 24 hours. At the end of the cycle a pulse of acetate was fed again. Throughout the experiment, the entire content of the MEC was replaced with fresh medium every three weeks (hydraulic retention time 21 days). Reactors were magnetically stirred and kept at room temperature during all the operational period.

Nitrogen sparging was tested as a strategy to decrease hydrogen retention time and thus avoid methanogenic *archaea* proliferation. A nitrogen inlet was connected to MEC, and the gas was finely sparged by means of a gas diffuser. Acetate concentration remained constant in a blank test with nitrogen sparging and without biomass, indicating that the substrate would not be stripped along with hydrogen when sparging the MEC. Nitrogen sparging periods were programmed in the same software developed in LabWindows CVI 2010 used for voltage monitoring, where the signal was sent to an electrovalve connected to the system. Nitrogen flow rate supplied was not monitored.

In a second stage of the study, the nitrogen sparging strategy to control methanogenic population growth was tested for different complex synthetic wastewater. Glycerol, milk and starch were used as carbon sources. The three anodes where a consortium of fermenting bacteria and ARB had developed (presented in Chapter 2) were transferred to single chamber mMEC operation. Glycerol, milk and starch were fed independently in each system in fed-batch mode and at room temperature, with an initial concentration per compound of 1 g L⁻¹. MEC-mixed was also assembled and it was fed with the three substrates simultaneously (1 g L⁻¹ of each). Only during the first four weeks of MFC operation, BES was used as methanogenic activity inhibitor at a concentration of 50 mM. When MEC were assembled the anodes had been working for 20 days without BES. The cell content was completely replaced with fresh medium when voltage response decreased below half the maximum signal. MEC were sparged with nitrogen for 20 minutes after feeding to maintain anaerobic conditions.

Throughout this section the reactors will be identified as MEC-glycerol, MEC-milk, MEC-starch and MEC-mixed.

Nitrogen was continuously sparged to mMEC by means of a needle pierced on a lateral septum after methane activity was detected in the system.

Hydrogen relative composition was calculated as the ratio of hydrogen to the total amount of hydrogen and methane and was calculated as presented in Equation 3.3.

$$\text{Relative composition}_{\text{H}_2} = \frac{v_{\text{H}_2}}{v_{\text{H}_2} + v_{\text{CH}_4}} \quad (\text{Equation 3.3})$$

where v_{H_2} and v_{CH_4} represent the volume fraction for H_2 and CH_4 respectively.

Carbon dioxide was not included in the relative hydrogen composition calculation because analyses of the headspace showed a rather negligible amount in the gas.

3.3. Results and discussion

3.3.1. Methanogenic population control in readily biodegradable synthetic wastewater

3.3.1.1. Nitrogen sparging strategies to decrease hydrogen retention time

Nitrogen sparging was tested as a strategy to decrease hydrogen retention time and thus avoid methanogenic *archaea* proliferation. Different scenarios were studied to reduce methanogenic activity: (A) the medium, containing 12 mM BES, was replaced with fresh one without BES and during the next cycles the cell was sparged with nitrogen for 20 minutes at the end of each batch cycle, in order to strip the remaining hydrogen (B and C) in a cell where methanogenic activity was very high, BES was progressively added to the system until hydrogen production was recovered and suddenly added (D) in a cell where methanogenic activity was very high, hydrogen was stripped out of the system with nitrogen sparging, which was continuously on (E) in a cell where methanogenic activity was very high hydrogen was stripped out of the system with nitrogen sparging, which was 24 hours on and 24 hours off (F) in a high hydrogen producing cell nitrogen sparging time was reduced but performed more frequently, 15 minutes every 6 hours (G) in a cell where methanogenic activity was very high, discontinuous sequential air and nitrogen sparging

A) Initial 12mM BES dosage and nitrogen sparging at the end of the batch cycle

A MEC that had been working for several weeks with 12 mM BES, had its medium replaced with fresh one without BES. During the next batch cycles the cell was sparged with nitrogen for 20 minutes at the end of each batch cycle in order to strip the remaining hydrogen. With the combined strategy of initial BES dosage and nitrogen sparging after each batch cycle methanogenic activity was kept under control for a period of 110 days (Figure 3.3.1A). This suggested that in single chamber MEC under batch operation methanogenic activity could be controlled by periodically sparging nitrogen, i.e. after each batch cycle, and dosing BES once in a while. In fact, methane was not detected for a period of four months from the last BES dosage using this strategy. Even though BES addition was not suppressed, with this procedure its dosage was significantly reduced, decreasing operational costs of this technology.

B and C) Methanogenic activity reduction with increased BES concentration

Taking into consideration that large scale MEC studies converged to methane production rather than hydrogen^{45,63}, the effectiveness of BES dosage in MEC in the worst scenario was tested, i.e. when methanogenic activity did not allow hydrogen detection in the system. Consecutive feeding cycles without nitrogen sparging enhanced this situation. When a high methanogenic activity was observed (values close to 0% of hydrogen relative composition in the MEC headspace), BES was progressively added up to a concentration of 60 mM, which was the one required to finally recuperate the system (more than 150 days required), i.e. to almost totally eliminate methanogenic activity (Figure 3.3.1B). The same test was repeated dosing 60 mM BES at once and methane production was completely inhibited in only five days (Figure 3.3.1C). The differences between these two tests might well be a consequence of methanogenic *archaea* adaptation to BES when it is being added gradually. Adaptation of methane producers to BES has already been reported⁷⁰⁻⁷³.

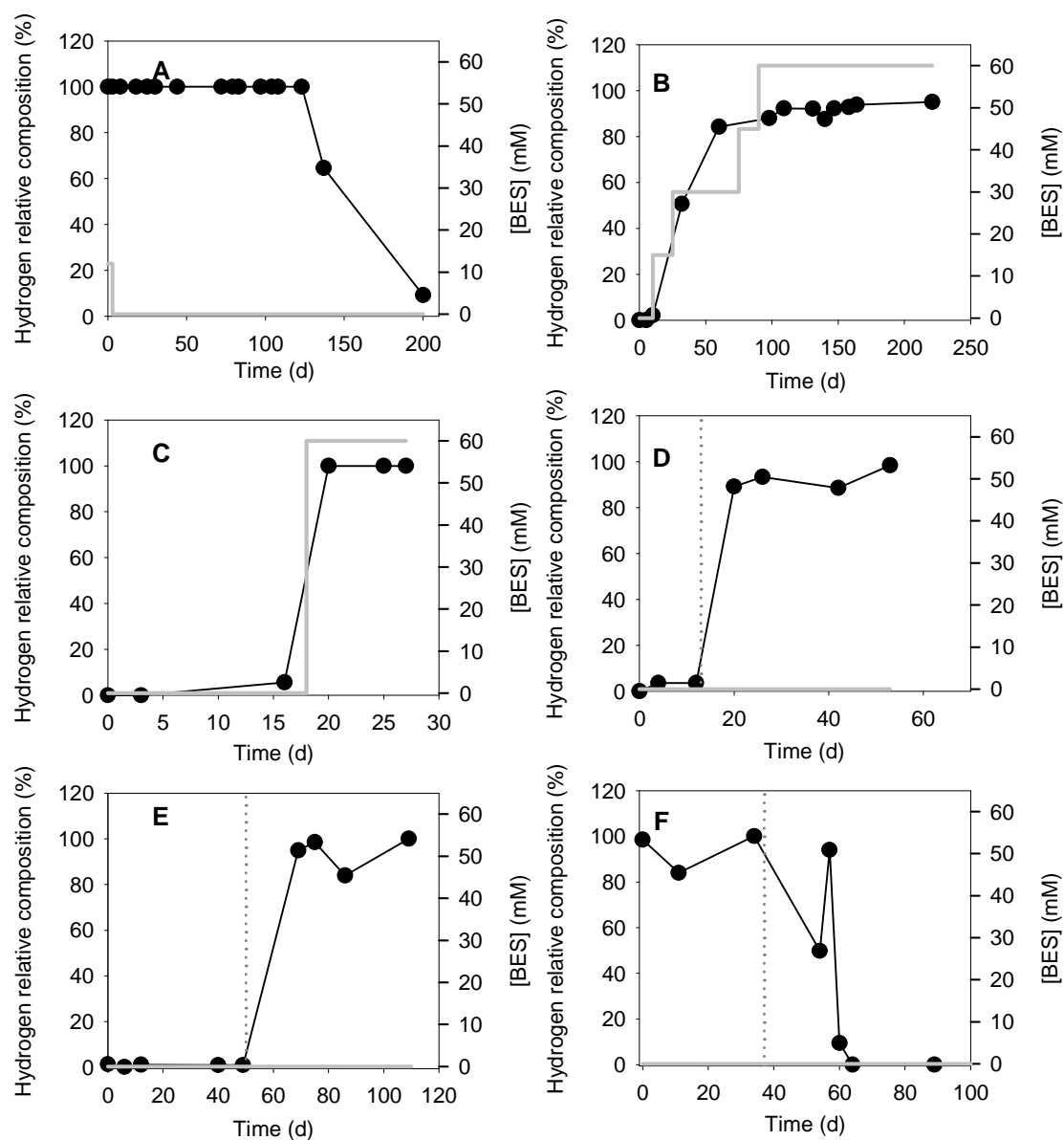


Figure 3.3.1. Hydrogen relative composition following different strategies for methanogenic activity reduction. **A.** Initial 12 mM BES dosage and nitrogen sparging at the end of the batch cycle. **B.** Progressive increase in BES concentration. **C.** Sudden increase in BES concentration. **D.** Continuous nitrogen sparging. **E.** Discontinuous nitrogen sparging, 24 hours stripping cycle. **F.** Discontinuous nitrogen sparging, 15 minutes stripping every 6 hours. Dotted lines indicate the start of the nitrogen sparging strategy

BES addition to an MEC where methanogenic *archaea* have already grown does not seem effective, since high inhibitor concentration is required to completely rid MEC of methanogens.

D) Methanogenic activity reduction with continuous nitrogen sparging

With the same intention as in the last scenario presented, nitrogen was continuously sparged into the cell so that hydrogen was removed from the MEC as it was being produced at the cathode (Figure 3.3.1D). Methane production was reduced and eventually not detected, what implies that before nitrogen stripping methane was being produced by hydrogenotrophic methanogens and that acetoclastic methanogens were not active in the system. Indeed, low contribution on methane production could be expected from acetoclastic methanogens in MEC given that their affinity for acetate is lower than for ARB, and therefore their growth should be less favored. Taking into account that hydrogenotrophic methanogens are reported to have very low half saturation constant for hydrogen^{59,61} and that acetoclastic methanogens are unfavored, methane is expected to be mainly produced by hydrogenotrophic methanogens in these systems.

E and F) Methanogenic activity reduction with discontinuous nitrogen sparging

Bearing in mind that stripping of hydrogen by nitrogen sparging implies a supplementary cost regarding pumping and separation, it was intended to reduce nitrogen supply. Nitrogen was continuously sparged for 24 hours and it was stopped for next 24 hours. Then the stripping cycle was again repeated. Results showed that a practically total decrease in methane production was reached (Figure 3.3.1E).

Seeing that the previous strategy was effective for methanogenic activity reduction, the sparging time was further reduced to 15 minutes stripping every 6 hours in the same cell. However this procedure allowed methanogenic activity to rise again (Figure 3.3.1F). Apparently hydrogen consuming microorganisms were able to resist the period of lack of substrate and once the hydrogen stripping was off they could consume it and grow, whereas the 24 hours stripping cycle might slowly have caused starvation and decay of hydrogenotrophic methanogens.

Even though in the initial operating point little methanogenic activity was detected, methanogenic *archaea* remained in the cell and eventually were able to consume hydrogen and produce methane. A continuous operation mode could possibly wash out hydrogen consuming microorganisms from the system and then reducing the nitrogen sparging time would be possible.

G) Methanogenic activity reduction with discontinuous sequential air and nitrogen sparging

Nitrogen sparging as a strategy to limit methanogenic activity was also tested in a new MEC-1.3 L configuration (Figure 3.3.2A, single chamber, anode and cathode placed concentrically, nickel and steel wool cathode, graphite fiber brush anode, batch operation). In such a system hydrogen was easily trapped in the cathode surface due to its high porosity, enhancing the growth and activity of hydrogen consuming microorganisms. This configuration favored methanogenesis and therefore it was more conservative to test the 24 hours cycle discontinuous sparging strategy, which had decreased considerably methane production in the previous tests presented. Beginning from complete methanogenic activity (no hydrogen detection) the sparging strategy was not able to increase hydrogen relative composition, showing that this was not an effective strategy in this configuration.

A new approach was tried. A sequential sparging of air (30 min) and nitrogen (3 h) was then applied at the beginning of each batch cycle, similarly to in Call and Logan⁵⁰. Oxygen aimed at inhibiting methanogenic *archaea* whereas nitrogen ensured anaerobic conditions for ARB. A sharp decrease in methane activity was observed (Figure 3.3.2B), which was maintained even after increasing the batch cycle duration, indicating that methanogenic *archaea* could not get through the inhibition induced by the air exposure period. No detrimental effects on ARB were observed, however a progressive decrease in current intensity was probably caused by nickel oxidation due to aeration, which progressively would be increasing cathode overpotentials.

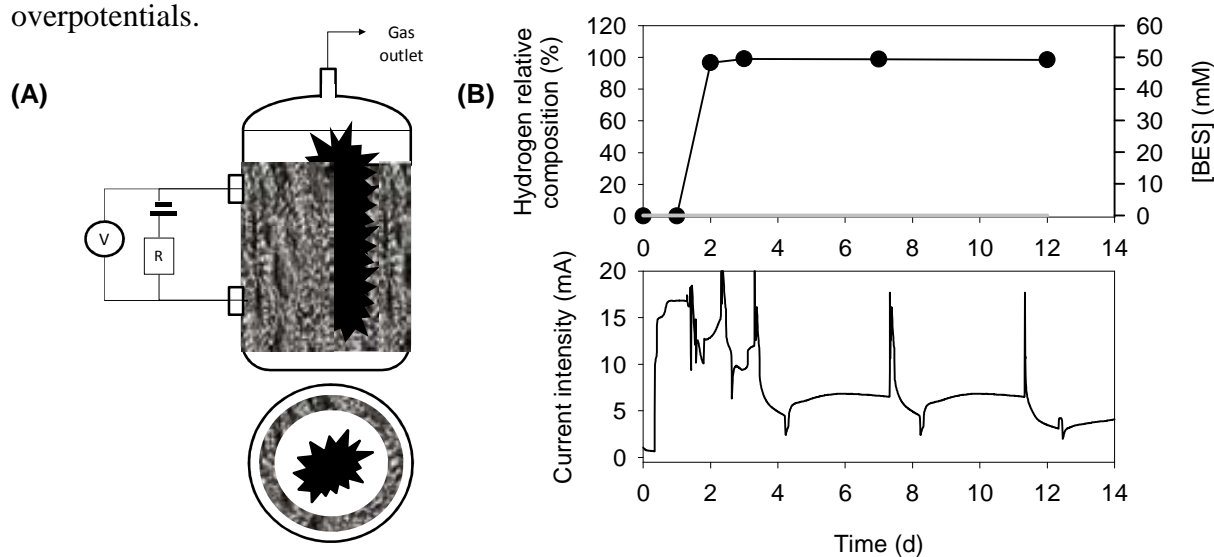
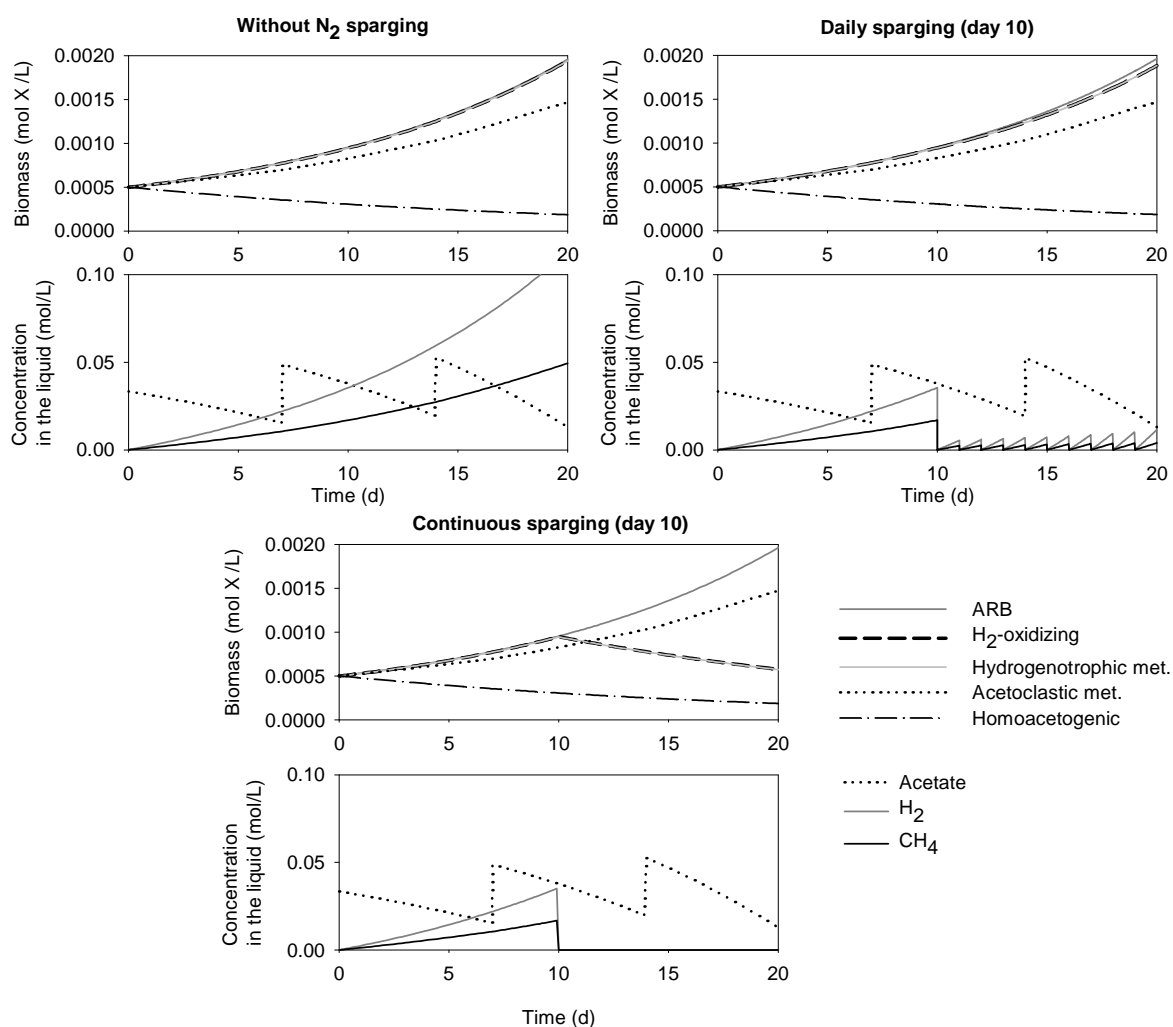


Figure 3.3.2. (A) Schematics of MEC-1.3L, front and crosscut upper view. (B) Hydrogen relative composition for MEC-1.3L sparging air (30 min) and nitrogen (3 h) at the beginning of the batch cycle.

Box 3.1| Simulation of MEC response to nitrogen sparging

Nitrogen sparging in MEC could be a strategy to further optimize and develop control systems that maintain and enhance hydrogen production. In order to test the opportunities of this strategy a model was developed to simulate the competition of ARB with other microorganisms and the rest of processes occurring in MEC. The model included all possible biological reactions considering that acetate was the carbon source (acetate oxidation by ARB, hydrogen oxidation by H_2 -oxidizing ARB, methane production from acetate by acetoclastic methanogens, methane production from hydrogen by hydrogenotrophic methanogens and acetate production by homoacetogenic bacteria) and chemical equations considering equilibrium and mass transport phenomena. Kinetic parameters were gathered from the literature and from other models for anaerobic processes^{58–60,74,75}. However some growth and decay parameters as well as diffusion coefficients were unknown, limiting the use of the model. Therefore, the model never was calibrated and validated, although it could give a qualitative vision of the system response to processes like substrate addition or nitrogen sparging. The model has been included in the Appendix of this document. The assumptions and simplifications taken included: maximum growth rate, substrate-biomass yields and decay rate were considered the same for all microorganisms, no inhibition was taken into account and all gas compounds remained in solution unless there was nitrogen sparging.

Different nitrogen sparging strategies were simulated with the model developed: (i) without nitrogen sparging (ii) daily nitrogen sparging (instantaneous stripping considered) and (iii) continuously nitrogen sparging. The output of a simulation is presented next:



- (i) Without nitrogen sparging: The model predicts the progressive growth of methanogenic populations along with ARB.
- (ii) Daily nitrogen sparging (day 10): A tiny decrease is observed in methanogenic *archaea* growth, progressively becoming the gas produced richer in hydrogen.
- (iii) Continuous nitrogen sparging (day 10): This scenario allows the decrease in hydrogen scavengers, but methane would still be produced by acetoclastic methanogens.

3.3.2. Methanogenic population control with complex synthetic wastewater

Nitrogen sparging strategy to limit methanogenic population growth was tested for different complex synthetic wastewater (glycerol, milk and starch). The three anodes where a consortium of fermenting bacteria and ARB had developed (presented in Chapter 2) were transferred to single chamber mMEC operation. When MEC were assembled the anodes had been working for 20 days without BES. The cell content was completely replaced with fresh medium when voltage response decreased, allowing a lower hydraulic retention time than Y-MEC presented in section 3.3.1, and the removal of hydrogen at the end of the batch cycle. Sparging of nitrogen to eliminate the methanogenic population was to be applied once methane was produced in the system.

3.3.2.1.MEC operation with complex synthetic wastewater

Throughout a period of more than three months, single chamber MEC fed with glycerol, milk, starch and a mixture of the three last were run without any BES addition for hydrogen production. For MEC-glycerol, MEC-milk, MEC-starch and MEC-mixed, the performance of the systems in terms of current intensity, CE and hydrogen relative composition is presented in Figure 3.3.3. Hydrogen relative composition was measured at the end of each batch cycle.

The highest current intensity in MEC fed with a single complex substrate during the first 50 days of operation was observed for MEC-glycerol, reaching about 4 mA. 2.6 mA were measured on average for MEC-milk. Current intensity observed for MEC-starch was lower, barely reaching a maximum of 2 mA. Regarding MEC-mixed, current intensity reached 5 mA, the highest value of all carbon sources tested.

The trend observed in terms of current intensity for the four systems correlated with the behavior observed in MFC operation in Chapter 2, i.e. higher exoelectrogenic activity was measured for MEC-glycerol and when the three substrates were being fed simultaneously in MEC-mixed some sort of advantage in the codigestion of the three substrates was experienced.

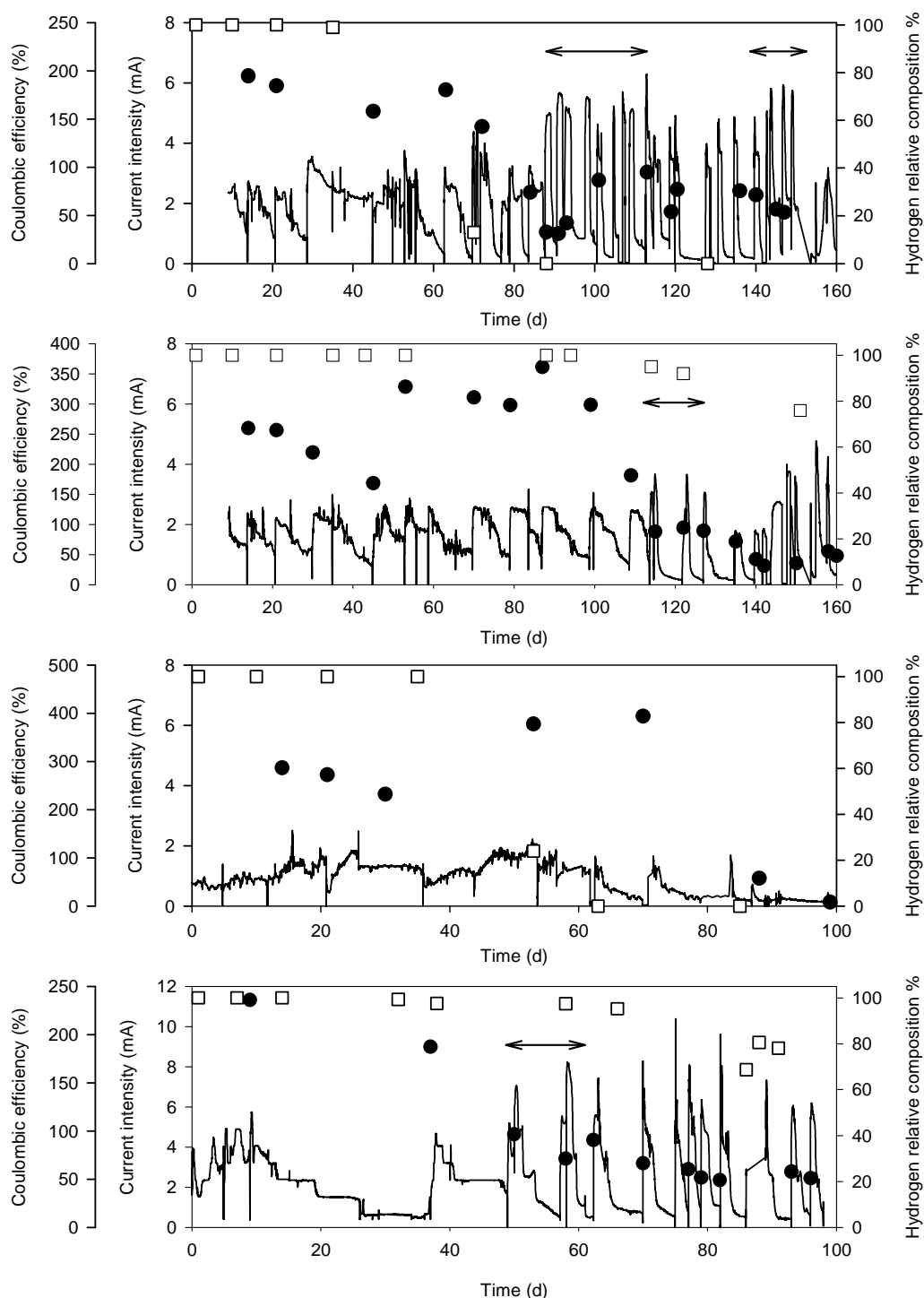


Figure 3.3.3. Current intensity, coulombic efficiency and hydrogen relative composition evolution throughout the operational period. Respectively downwards: MEC-glycerol, MEC-milk, MEC-starch and MEC-mixed. Solid: Current intensity, \square Hydrogen relative composition, \bullet coulombic efficiency. Arrows indicate nitrogen sparging periods.

Regarding gas production, it was quickly observed for the tree complex substrates, with a hydrogen relative composition of 100% even though BES was not used. Nevertheless the long term stability of hydrogen production was only demonstrated for MEC-milk and MEC-mixed, producing a gas with about 80% of hydrogen volumetric content.

CE followed a similar trend in all the systems: it was initially much higher than 100%, indicating electron recycling, and it decreased up to values ranging from 50 to 70%. Such a decrease in CE coincided with the loss of biogas purity, which, starting from 100% relative composition of hydrogen, ended up enriched with methane. In fact for MEC-glycerol and MEC-starch, the composition of the gas collected for the last batch cycles exclusively contained methane. Although no final net hydrogen production was being observed, hydrogen was being produced as the monitoring of the gas composition during the batch cycle indicated (Figure 3.3.4). Therefore, hydrogen was being used by hydrogenotrophic methanogenic *archaea*.

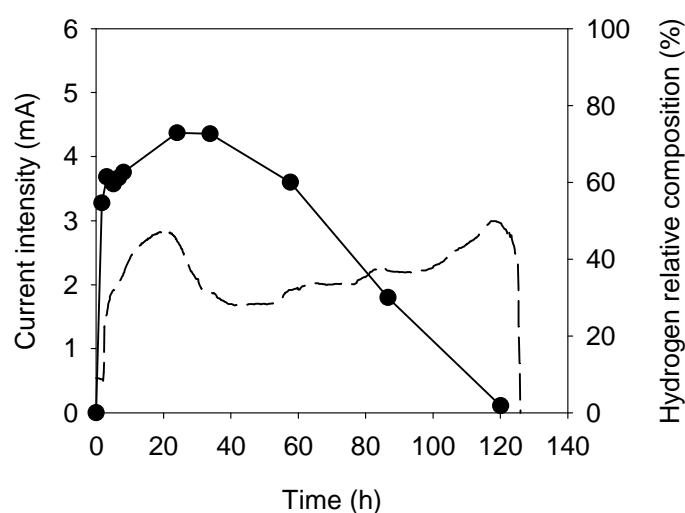


Figure 3.3.4. Hydrogen relative composition in the headspace (●) and current intensity (dashed line) for one batch cycle in MEC-glycerol (day 170).

Figure 3.3.5 shows the evolution of hydrogen relative composition for different batch cycles throughout MEC operation, where a clear difference in gas composition can be observed after 24 h of operation and at the end of the cycle for MEC-glycerol and MEC-starch. In these two systems, MEC-glycerol and MEC-starch, hydrogen was being produced and mainly consumed by hydrogenotrophic methanogens. Although the activity of other hydrogen scavengers could not be completely ruled out, the decrease in CE indicated that they were less favored.

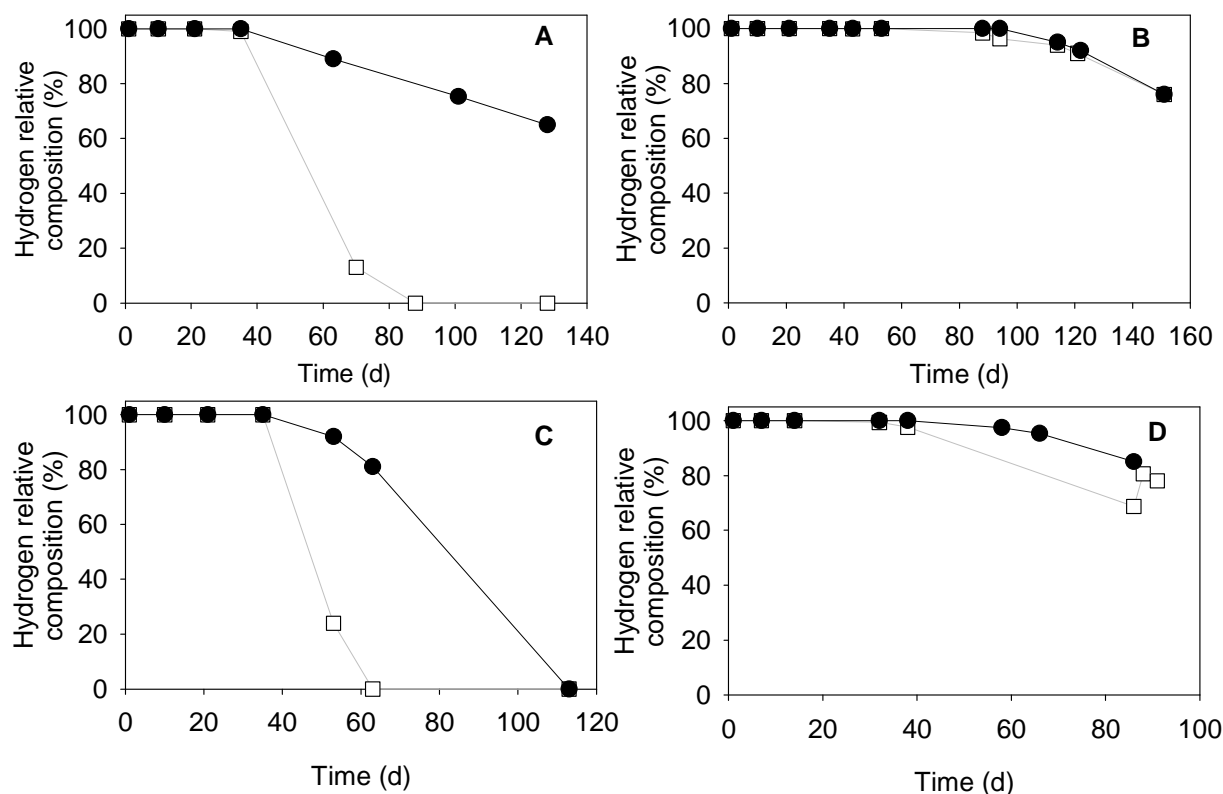


Figure 3.3.5. Evolution of hydrogen relative composition after 24 h from the beginning of the cycle (●) and at the end of the cycle (□) for MEC fed with (A) glycerol (B) milk (C) starch and (D) mixture of glycerol, milk and starch.

Unlike MEC-glycerol and MEC-starch, methane detection for MEC-milk took longer, and when it was finally detected, it accounted for less than 25% of the total biogas collected, i.e. the gas kept being richer in hydrogen than in methane. Similarly, MEC-mixed also experienced this lag time in methane production. In these two systems, pH did not change significantly, ruling out the possibility of a decrease in methanogenic activity due to pH effects. It rather seemed that an intermediate in milk metabolism was partially inhibiting methane production.

MEC-starch experienced a loss of electroactivity that explains the loss of hydrogen producing capacity of the system. A washout of starch fermenting could have been the cause as revealed a sudden increase in current intensity when a pulse of acetate was fed (not shown), i.e. ARB were still active in the system.

Similarly to the sparging of nitrogen in Y-MEC at the end of each batch, that lowered hydrogen retention time, short hydraulic retention time in mMEC sustained the initial BES

dosage effects for one month in MEC-glycerol and MEC-starch, whereas its effect was prolonged for 2 and 3 months for MEC-mixed and MEC-milk respectively.

The before mentioned CE trend implied that a shift in hydrogen scavengers occurred. A significant activity of homoacetogenic bacteria was initially observed and they were slowly replaced by a methanogenic population. This behavior between both communities was already discussed by Parameswaran et al.⁶⁰ and Ruiz et al.⁷⁶, proving that homoacetogenesis was only significant when methanogenesis was not active. It should be noted that hydrogen oxidizing exoelectrogenic bacteria could also have participated in the initial electron recycling situation. Equations 3.4 to 3.9 (Table 3.3.1) present the most probable reactions taking place in the system once the complex substrate has been fermented to VFA (only acetate and propionate oxidation reactions are shown, since it is considered that fermentative acetogenic bacteria will mainly end up in such compounds).

Table 3.3.1. Potential biological reactions in the MEC after fermentation of the complex substrate

Reaction	Group of microorganisms	Location	Equation
$\text{CH}_3\text{COO}^- + 4\text{H}_2\text{O} \rightarrow 2\text{HCO}_3^- + 9\text{H}^+ + 8\text{e}^-$	ARB	Anode	(Eq. 3.4)
$\text{CH}_3\text{CH}_2\text{COO}^- + 7\text{H}_2\text{O} \rightarrow 3\text{HCO}_3^- + 16\text{H}^+ + 14\text{e}^-$	ARB	Anode	(Eq. 3.5)
$\text{H}_2 \rightarrow 2\text{H}^+ + 2\text{e}^-$	H_2 -oxidizing ARB	Anode	(Eq. 3.6)
$2\text{HCO}_3^- + 4\text{H}_2 + \text{H}^+ \rightarrow \text{CH}_3\text{COO}^- + 4\text{H}_2\text{O}$	Homoacetogenic bacteria	Bulk liquid	(Eq. 3.7)
$4\text{H}_2 + \text{CO}_2 \rightarrow \text{CH}_4 + 2\text{H}_2\text{O}$	Hydrogenotrophic methanogens	Bulk liquid	(Eq. 3.8)
$\text{CH}_3\text{COO}^- + \text{H}_2\text{O} \rightarrow \text{CH}_4 + \text{HCO}_3^-$	Acetoclastic methanogens	Bulk liquid	(Eq. 3.9)

The fact that hydrogen was consumed by hydrogen scavengers throughout implies that very low cathodic recoveries were obtained (less than 13%), initially due to homoacetogenic bacteria and finally to methanogenic *archaea*. Although cathodic recovery is indicating the actual performance of the system in terms of net hydrogen production, other parameters to differentiate the fraction of current intensity generated from the substrate added or the one from hydrogen recycling could be calculated to give a fairer view of the activity of ARB, such as the ones proposed by Ruiz et al.⁷⁷. Analogously to cathodic recoveries net hydrogen production remained at low values, reaching a maximum of $0.08 \text{ m}^3 \text{ H}_2 \text{ m}^{-3} \text{ reactor d}^{-1}$ for MEC-milk.

3.3.2.2. Methanogenic activity reduction with continuous nitrogen sparging

A continuous feeding of nitrogen was supplied to the MEC once methane was detected (sparging period is indicated as horizontal arrows in Figure 3.3.3) so that hydrogen could be continuously stripped out of the system, leaving hydrogen scavengers without substrate.

The direct effect of sparging nitrogen was the observation of shorter cycles and higher current intensities, which was consequence of reducing R_{int} of the system due to the stirring created with the nitrogen bubbling. During the sparging period, a cycle without stripping was periodically performed to assess the evolution of the gas composition. Depending on the output of the test, the MEC kept stripping hydrogen with nitrogen or was normally closed and connected to a gas collection bag.

MEC-glycerol experienced a decrease in CE once methanogenic activity appeared (day 70). Initially CE had values much above 100% indicating the existence of hydrogen recycling phenomena. A continuous nitrogen sparging period began when no hydrogen production was detected at the end of the cycle (day 87, CE 35%). Throughout this period CE slowly rose up to 100% presumably as a result of both the stirring effect created by nitrogen sparging and the washout of acetate consumers. The later could have been favored by the operation at lower hydraulic retention time in this period, given that at higher current intensities the substrate was degraded faster and therefore the fedbatch cycle was shortened. After the nitrogen sparging period, CE decreased to values around 70% and the gas collected at the end of each batch cycle still contained exclusively methane (day 127). This showed that methanogens had not been washed out, as before suggested.

MEC-milk also showed a decrease in CE when methane was initially detected, decreasing from about 300 to 170%, which indicated that still the hydrogen recycling phenomena was far more active than methanogenesis. In this point, nitrogen sparging was supplied continuously to avoid hydrogen consuming metabolisms (day 113). CE values of about 100% were directly favored by the stirring effects, lowering up to 50% afterwards. After one week with continuous nitrogen sparging, hydrogen relative composition kept decreasing. As opposed to MEC-glycerol, hydrogen relative composition did not differ after 24h from the beginning of the batch cycle and at the end. This could be indicating that methane origin was not related to hydrogen but acetate. A very similar trend to MEC-milk was observed for MEC-mixed.

It is important bearing in mind that nitrogen stripping is only effective against those hydrogen consuming metabolisms, like hydrogenotrophic methanogenesis, homoacetogenesis or hydrogen oxidation by ARB. Methanogenesis could still be possible through acetoclastic methanogenesis, even though their affinity for acetate is lower than for ARB.

As mentioned before, methane was detected both in MEC-milk and MEC-glycerol even after a nitrogen sparging period. Some tests in open circuit configuration were performed with the aim of assessing the origin of methane. Methane formation from electrochemically produced hydrogen was not possible under these conditions, but still hydrogen could be produced during fermentation. In order to rule out this hydrogen input, only acetate and propionate were used as carbon source in these tests. A second set of tests was performed aiming at assessing hydrogenotrophic methanogenesis. Hydrogen was initially bubbled in the open circuit MEC configuration and sodium carbonate was added in the medium (no acetate or propionate added). With this last test, methane could only be produced by hydrogenotrophic methanogens. Excess initial substrate concentration was assumed in all cases. Figure 3.3.6 shows the methane production rate during these tests and compares them to the methane production rates in the ordinary MEC configuration, when the complex substrate was fed. It was clearly seen that methane production from hydrogen was much lower than from acetate or propionate. Nevertheless, the methane production rate in a regular MEC with the usual carbon source was higher than the total methane from both hydrogen and acetate or propionate, which only accounted for 60% of the methane detected in MEC. This difference could also be attributed to the fermentation step, which also gives some hydrogen that can be converted to methane. The contribution of hydrogen obtained in the fermentation step was not experimentally assessed. Alternatively an estimate of hydrogen yield per mole of glycerol could have been used, but this can widely vary in a mixed culture system. When comparing these production rate values, it must be noted that maximum reaction rates are assumed. Far from expecting a quantitative result, these tests qualitatively confirmed that hydrogen stripping with nitrogen alone could not be effective in terms of methane control, because, whereas hydrogenotrophic methanogens and other hydrogen scavengers would be affected, acetoclastic methanogens could proliferate. A rough contribution of hydrogen to methane formation could be calculated, being around 25% for MEC-glycerol and around 20% for MEC-milk.

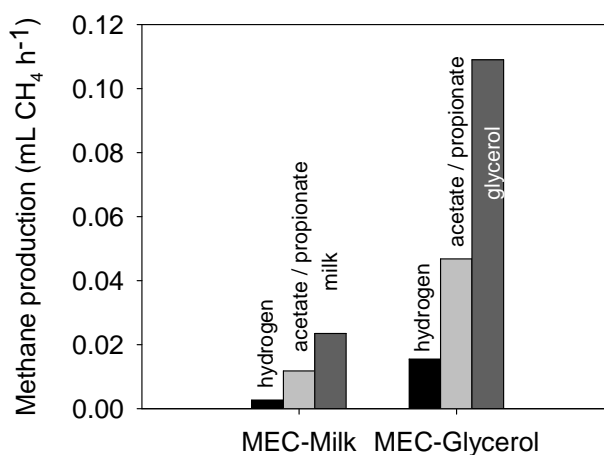


Figure 3.3.6. Qualitative estimation of methane origin in MEC-milk and MEC-glycerol.

Regardless of the methane origin, the volume produced of both hydrogen and methane was compared to the theoretical values. Theoretical values of hydrogen production based on current intensity were calculated for a batch cycle with continuous stripping of hydrogen. By doing so, the effects of electron recycling due to homoacetogenesis or hydrogen oxidizing ARB were ruled out, hence only the coulombs that could effectively derive in hydrogen or methane were measured. Hydrogen consumed to methane was calculated considering the relative contribution of hydrogen to methane formation (from Figure 3.3.6) and the stoichiometry presented by Equation 3.8. Figure 3.3.7 presents the contribution of both gases measured in ordinary MEC operation, expressed as moles of hydrogen, on the theoretical moles of hydrogen produced in absence of the recycling phenomenon. It can be seen that for MEC-glycerol most hydrogen participated in the hydrogen recycling phenomenon, whereas gas leakages seemed to be the main reason for hydrogen loss for MEC-milk, as the comparison of the coulombs measured with and without hydrogen stripping revealed.

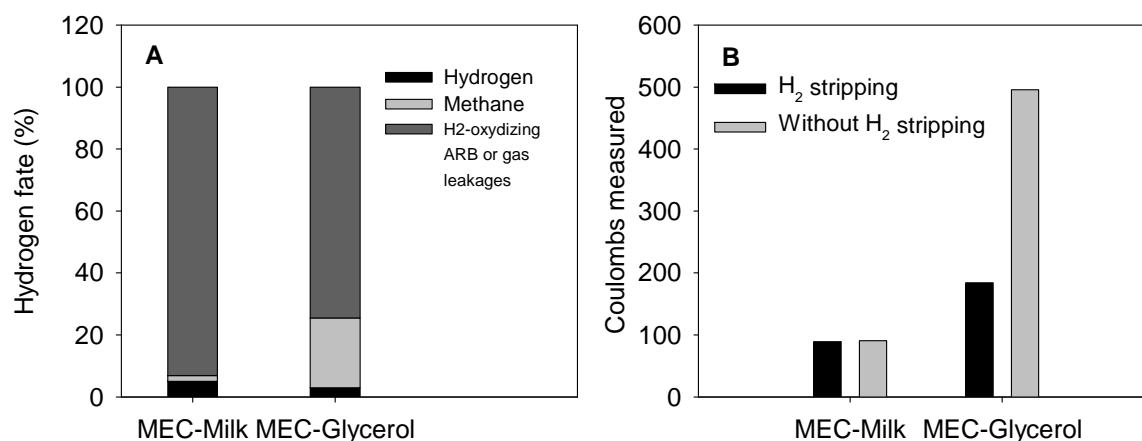


Figure 3.3.7. (A) Contribution of hydrogen and methane measured, expressed as moles of hydrogen, on the theoretical moles of hydrogen produced in a MEC batch cycle. (B) Comparison of the coulombs measured in two consecutive batch cycles in MEC with and without hydrogen stripping.

Finally, Table 3.3.2 compares the results obtained in this work with results reported on complex substrates for hydrogen production in MEC. Single chamber MEC studies are directly comparable to this work, but also other configurations have been included in the list since their comparison is also interesting. It can be stated that similar results in terms of current intensities were obtained in this work. However very low hydrogen production values are evidenced here, mainly due to hydrogen use by methanogenic *archaea* and H₂-oxidizing ARB in the system or to gas leakages as previously discussed. Only MEC-mixed showed a different behavior, recovering up to 90% of the hydrogen produced, and obtaining a biogas mainly composed by hydrogen (80% hydrogen content), even after 100 days operation. Again MEC-mixed seemed to stand out against MEC-single substrates, confirming the advantages of codigesting substrates of very different nature.

Table 3.3.2. Comparison of this work with others studies dealing with complex substrates in MEC

Carbon source	Reactor configuration and operation	Current intensity (A/m ³)	Hydrogen production (m ³ /m ³ ·d)	Cathodic gas recovery (%)	Biogas composition (% H ₂)	Reference
Glycerol	Single chamber,	221	2	79	88	Selembo et al., 2009 ⁷⁸
Crude glycerol	V _{app} 0.9V	87	0.41	65	87	
Glycerol	Single chamber, V _{app} 0.6V	238	1.3	-	-	Chignell and Liu, 2011 ³⁷
Glycerol	Single chamber, gas phase cathode V _{app} 1V 57 days	10.7	0.6	100	98	Escapa et al., 2009 ³⁵
Cellulose	Single chamber, 2 stage process, <20 days*	1.15	1.11	86	84	Lalaurette et al., 2009 ²⁶
Proteins	Single chamber	236	0.42	35	100	Lu et al., 2010 ⁷⁹
Domestic WW	Double chamber	308*	-	40	100	Ditzig et al., 2007 ⁸⁰
Domestic WW	Multi cassette, double chamber, 3 months	0.135*	0.015	60	≈100	Heidrich et al., 2013 ⁴²
Domestic WW	Single chamber, gas phase cathode	18.6*	0.05	-	100	Gil-Carrerra et al., 2013 ⁸¹
Winery WW	Multi module, single chamber, 3 months	7.4	0.19	-	14	Cusick et al., 2011 ⁴⁵
Glycerol	Single chamber	100	0.021	4	5	This work
Starch	V _{app} 0.8V	25	0	0	0	
Milk	100 days	75	0.086	12.7	76	
Mixed		150	0.94	91	80	

Index “*” indicates that the parameter has been calculated from the data presented in the specific publication. Biogas composition measured at the end of the batch.

In terms of gas composition, i.e. hydrogen concentration, also MEC-milk presented an interesting behavior, reaching about 75% of hydrogen purity after 100 days operation, unlike MEC-glycerol or MEC-starch, which could not avoid the proliferation of hydrogen scavengers.

Although other works managed net hydrogen production using glycerol, long-term stability of these systems has not been reported. Selembo et al. (2009) produced hydrogen from glycerol and crude glycerol reaching cathodic recoveries higher than 70% and gas purities higher than 85%. A periodic exposure to air was applied to maintain under control methanogenic *archaea*. However the period of time that the systems were working was not stated. Also Chignell and Liu (2011) and Escapa et al. (2009) reached net hydrogen

production from glycerol, nevertheless Escapa used a system with a gas phase cathode that avoided hydrogen uptake. Chignell and Liu did not mention the length of the study.

Works focused on hydrogen production out of starch-like substrates also managed net hydrogen production²⁶. In fact, in this study, MEC-starch initially performed better in terms of current intensity but it slowly lost its degradation capacity, which was most probably due to a fermentative bacteria washout (as revealed by a sudden current intensity increase in a test with acetate as sole carbon source).

Concerning milk-like substrates, protein containing wastewater was also tested by Lu et al (2010) with high efficiencies and hydrogen recovery. In this case also a periodic exposure to air was applied to maintain under control methanogenic *archaea*, but the period of time that the system was working was not stated. Therefore it is complicated to discern about the hydrogen production potential of proteins.

Studies on hydrogen production in MEC with domestic wastewater as substrate^{42,80,81} have also been included to account for the heterogeneity of the mixture, typically containing a wide range of substrates with different biodegradability and therefore being somehow analogous to MEC-mixed. The three systems presented, though, have as advantage versus MEC-mixed that they have double chamber configuration or work with a gas phase cathode.

When it comes to the length of the study and the proliferation of methanogenic *archaea*, it is interesting to have a look to the works of Cusick et al. (2011) and Heidrich et al. (2013). Also the work from Escapa et al. (2009) is comparable to the previous ones in terms of the length of the study. In these works, there is a clear difference in gas composition in the long term operation depending on the system configuration. In this sense, a single chamber MEC would seem to offer low chance of hydrogen production. Nevertheless, in this work it was managed to produce a gas richer in hydrogen than methane for MEC-milk and MEC-mixed in a long term operation.

This section shows the possibility of effectively producing hydrogen in a single chamber MEC for given wastewaters containing dairy industry substrates, which in the long term operation do not enhance complete methanogenic *archaea* proliferation. Even though this is already an important achievement, tests with real dairy wastewater should be done to confirm this potential. It should be also a focus of study the development of a gas tight system that

allows collection and quantification of the gas produced, since gas leakages limit the practical implementation of this technology.

3.3.3. Practical implications

As shown in this study, sparging a single chamber MEC with nitrogen decreases hydrogen retention time and therefore the growth of methanogens is less favored. This strategy for methanogenic population control has some practical implications that will be discussed next.

Only methanogenic populations were considered in the assessment of the potential of this strategy. Nevertheless the reduction of the hydrogen retention time would not only affect the growth of hydrogenotrophic methanogens, but also homoacetogenic bacteria. Furthermore hydrogen oxidation by ARB would also be avoided. The fact that these two last metabolisms would not be favored would avoid the hydrogen recycling phenomena, which also limits hydrogen production in MEC in a single chamber configuration.

The gas collected in MEC will be a mixture of mainly hydrogen and nitrogen. Downstream processes will determine the gas post-treatment needs. When hydrogen is to be used as fuel the MEC gas outlet stream can be directed to a combustion turbine, where only hydrogen will be oxidized (Figure 3.3.8A). Nitrogen will not react and can therefore be recycled into the MEC for sparging. Drawbacks of this situation are the larger piping and compressing capacity needed as a result of higher gas flow rates, and the decrease of energy yield as a result of heat loss, since heat produced will be gained by nitrogen warming it up. The use of a hydrogen selective membrane prior to the combustion turbine would be a nice option to sort out these disadvantages. Alternatively, this size selective membrane that specifically separates hydrogen⁸³ gives the possibility to obtain it as a reactant with high purity. In this case also nitrogen can be recycled to the MEC (Figure 3.3.8B). Regarding carbon dioxide, it is commonly separated from mixtures containing hydrogen and nitrogen by means of a CO₂-selective membrane.

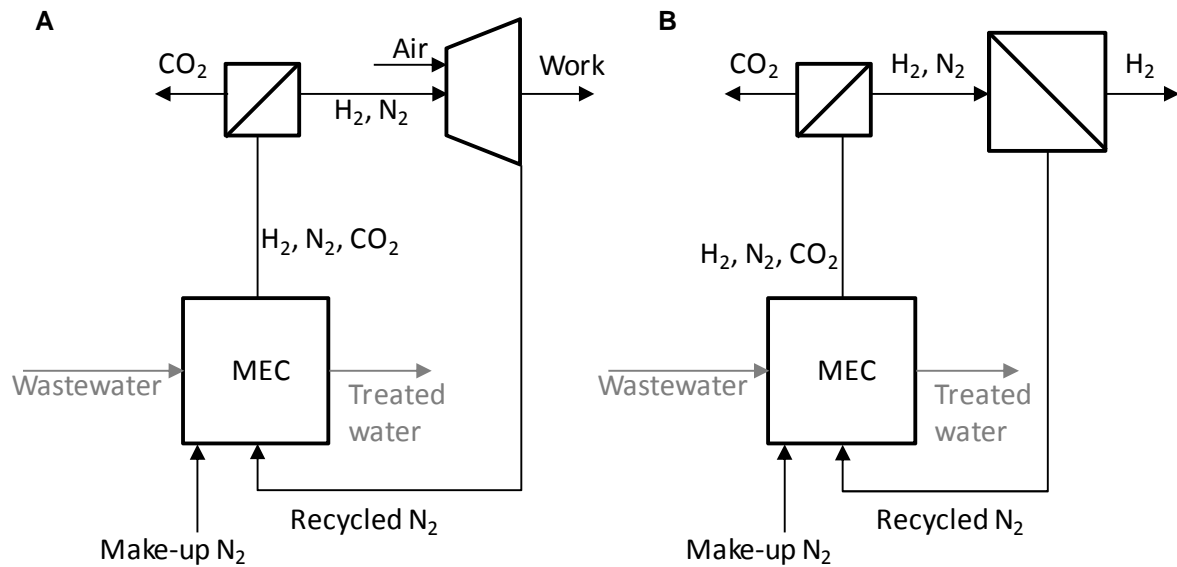


Figure 3.3.8. Nitrogen recycling in MEC coupled to a (A) combustion turbine (B) hydrogen selective membrane.

The fact that nitrogen could be recycled to the system compensates the costs of feeding it in MEC. Only a make-up nitrogen stream would be necessary to account for possible gas losses. Nevertheless the economical feasibility of the process should be studied in detail.

Finally it is important to point out that methane production could still be possible in MEC even with low hydrogen retention time conditions, since acetoclastic methanogens could be active in the system. BES addition to MEC would not be feasible in continuous flow operation, but hydraulic retention time could be adapted to allow the washout of acetoclastic methanogens, which a priori would be found mainly in suspension. Additionally, a periodical sequential exposure of air and nitrogen could eventually avoid the methanogenic *archaea* proliferation.

3.4. Conclusions

It was found that by periodically sparging a single chamber MEC with nitrogen one can decrease BES dosage to the system. With this procedure the effect of the chemical inhibitor was prolonged up to four months when feeding a readily biodegradable substrate under fedbatch operation with high hydraulic retention time. The effectiveness of the strategy proposed is of relevance, since working conditions that favored methanogenesis evolution were met: (i) acetate was used as sole carbon source and (ii) operation at high hydraulic retention time. Nitrogen sparging was also an effective strategy to reduce methane production when initially there was significant methanogenic activity. However, the system response was dependant on the nitrogen sparging time frequency, being more effective for long sparging periods rather than short but more frequent sparging periods.

Regarding MEC fed with complex carbon sources, net hydrogen production (meaning by net that hydrogen was not being scavenged by any microorganism) was only achieved for MEC-milk and MEC-mixed even after more than three months MEC operation without addition of any methanogenesis chemical inhibitor. In fact, MEC-mixed showed the best results in terms of current intensity, hydrogen production and gas recovery. On the contrary, glycerol and starch as substrates in MEC could not avoid the complete proliferation of hydrogen scavengers, even under low hydrogen retention time conditions.

The results obtained indicated that nitrogen sparging as a strategy to control methanogenic activity was not equally efficient for all substrates. Carbon sources limit the populations that can develop and therefore the possibility for methanogenic *archaea* to proliferate could also be different. In MEC-milk and MEC-mixed methane build-up took longer than for MEC-glycerol, which seemed to be a consequence of some metabolite intermediate rather than other effects like pH. Therefore substrates containing milk derivates are presented as an interesting option in these systems, although tests with real dairy waste water should be performed in further studies.

After a period of continuous nitrogen supply a switch in methane producers was observed, having acetoclastic methanogens a contribution of 70-75% on total methane production. Nevertheless hydrogenotrophic methanogens were still active in the system.

Therefore, nitrogen sparging as a method to restrain methane production by limiting its retention time should not be addressed as a sole strategy in single chamber MEC. In terms of system operation, hydraulic retention time will also play a key role, i.e. low hydraulic retention time will eventually allow the washout of non favored microorganisms. Also a periodical exposure to air could easily inhibit methane producers, which according to single chamber MEC studies allows enrichment in hydrogen, at least in a short term.

It should be taken into account that by sparging nitrogen into the system hydrogen purity decreases, that nitrogen sparging increases investment costs and that BES might still be needed.

To sum up, this study gives a step forward to continuous mode operation and especially to future process scale-up of single chamber MEC, but still further research on methanogenic activity minimization and reduction is required. For instance, the development of an optimized nitrogen sparging time depending on the system response could give more opportunities to the strategy presented.

Chapter 4. On-line monitoring of hydrogen production

Chapter summary

A fuel cell was tested as a low cost monitoring tool for biohydrogen producing systems at lab scale. The signal obtained with the device was proved to correlate with hydrogen supplied and was equally efficient as other reference analytical methodologies such as gas chromatography. Signal was repeatable and did not show interferences by the presence of other biogas compounds. The fuel cell was coupled to a microbial electrolysis cell to test its applicability on a biohydrogen producing system. The use of this system as an alternative to more complex and more expensive devices is expected to increase the chances for biohydrogen producing systems, lowering investment and operational costs and allowing the implementation of control and optimization strategies.

4.1. Introduction

Investment costs in biohydrogen producing technologies, like MEC, should be minimized in order to fully become economically feasible technologies. Analytical methods to monitor the system performance in terms of hydrogen production may represent an important portion of such costs, especially in lab scale studies. Thus, finding new methodologies to monitor hydrogen production gains interest.

Offline measurements on a gas chromatograph (GC) or the coupling of the system with an online GC is a common practice in lab scale studies when aiming at hydrogen production monitoring^{50,67,81}. Both methodologies also require the connection of a flow-meter to fully quantify the production^{84,85}. Gas production can also be measured sparing a flow-meter with a double GC analysis strategy as presented by Ambler and Logan⁸⁶. Other analytical techniques described in the literature comprise the use of membrane inlet mass spectrometry together with a flow-meter system⁴² or specific hydrogen sensors⁸⁷. These techniques are notably expensive and require regular maintenance. The development of low cost and simple online monitoring techniques are interesting, like the real-time monitoring strategy proposed by Kana et al. for biohydrogen evolution estimation based on conductivity measurements⁸⁸.

A low cost strategy for hydrogen monitoring is presented in this chapter. A fuel cell was examined to work as a sensor for hydrogen quantification and, therefore, its potential to give a fast and stable response, a long lifetime and easy calibration and operation was tested. The possibility of monitoring hydrogen production with the system proposed in this work was tested coupling it with a single chamber MEC.

4.2. Materials and methods

A single reversible fuel cell provided with a proton exchange membrane was used in this work (Figure 3.4.1.A, 54 mm x 54 mm x 17 mm, SKU 63200, Fuel Cell Store, USA). A needle was tightly connected to the anodic chamber inlet port, which allowed the connection to gas collection bags or to the system headspace. Epoxy glue (Araldit, Ceys) was used in joints to minimize leakages. The cathodic inlet port was left uncapped to permit free air diffusion into the cathode. Two fuel cells were used in parallel in the tests performed in this work to account for the device variability, observing no significant differences.

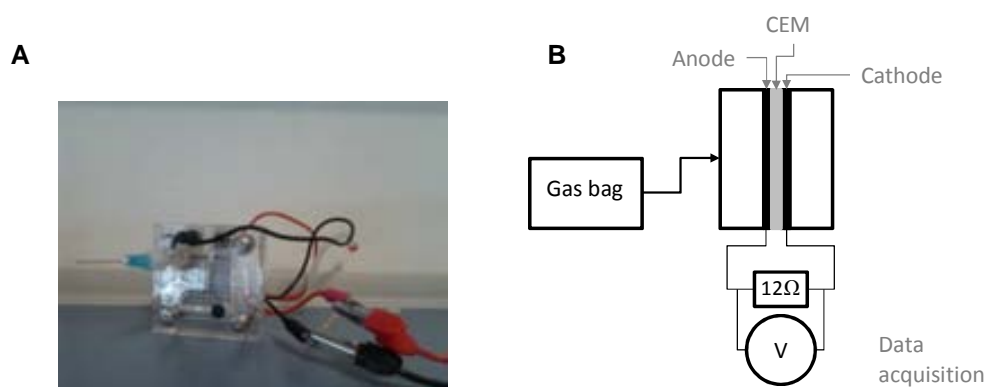


Figure 3.4.1. (A) Fuel cell with connection modification in the anodic chamber inlet port. (B) Schematics of a fuel cell connected to a gas bag (side view).

Gas bags with low hydrogen permeability (Ritter, Cali-5-Bond, 100 mL and 500 mL) were used to supply the gas sample to the fuel cell (Figure 3.4.1.B). A Teflon rubber septum permitted the connection with the needle from the fuel cell. Additionally, a valve with olive fitting allowed the connection with a hosepipe coming from the hydrogen producing system when needed. The bags were rinsed three times with nitrogen gas and emptied with a vacuum pump prior to gas sample introduction. The gas sample was introduced to the gas bag via a gas tight syringe (Samplelock Syringe, 1 mL and 10 mL, Hamilton, USA). High purity gases (hydrogen, nitrogen, carbon dioxide and methane, Air Products, Inc) were used to prepare the gas samples.

The charge circulated in the system was calculated as presented in Equation 3.10:

$$\text{Charge (Coulombs)} = \int_{t_i}^{t_f} I(t)dt \quad (\text{Equation 3.10})$$

Coulombs supplied to the fuel cell could be estimated from the volume of hydrogen supplied to the fuel cell as presented in Equation 3.11:

$$\text{Charge (Coulombs)}_{\text{H}_2} = n_{\text{H}_2} \cdot 2 \cdot F \quad (\text{Equation 3.11})$$

Where n_{H_2} is the moles of hydrogen, calculated with the ideal gas law at room temperature, 2 are the moles of electrons available per mole of hydrogen and F is Faraday's constant (96485C/mol e^-).

Coulombic recovery was calculated as the ratio of coulombs measured by the fuel cell (from Equation 3.10) and the theoretical coulombs to be obtained from hydrogen supplied (from Equation 3.11).

Gas chromatography was used as reference method for hydrogen analysis. Gas quantification was performed according to the procedure presented by Ambler and Logan⁸⁶, following a double run methodology (Equation 2.1). Standard mixtures of hydrogen and nitrogen were used. They contained 10 mL hydrogen. Nitrogen was added according to the final concentration desired.

The fuel cell sensor was tested on a real biohydrogen production system coupling it with a mMEC. It operated with a hold up volume of 35mL, under fedbatch mode with acetate as sole carbon source and at an applied voltage of 0.8V (unless otherwise stated). 50mM BES was used to inhibit methane production. Maximum attainable hydrogen production per batch based on substrate supplied was 25mL (to ensure a measurement comprised in the range of gas volume calibrated).

4.3. Results and discussion

4.3.1. Instrument characterization and calibration

4.3.1.1. Description of the system

The ability of the fuel cell to work as a sensor was initially tested. For each test, the fuel cell was connected to a gas bag containing a known volume of hydrogen gas (Figure 3.4.2.A). Hydrogen supplied diffused to the anodic chamber where it was oxidized. Protons migrated through the proton exchange membrane whereas the electrons flowed along the electrical circuit to the cathode translating in a voltage signal. In the cathodic chamber, oxygen was reduced to water. Voltage reached a maximum in the first minutes of the test and decreased progressively. For an identical external resistance, the more volume it was supplied the higher voltage it was observed and the longer it took to reach again the base signal. Figure 3.4.2B shows the response with different external resistances (12, 100 and 350 Ω) for an identical hydrogen volume supplied. As can be observed, the system experienced less current intensity response limitation for an external resistance of 12 Ω , reaching higher values of current intensity. Apparently the resistance to the flow of electrons did not differ significantly for an external resistance of 100 and 350 Ω .

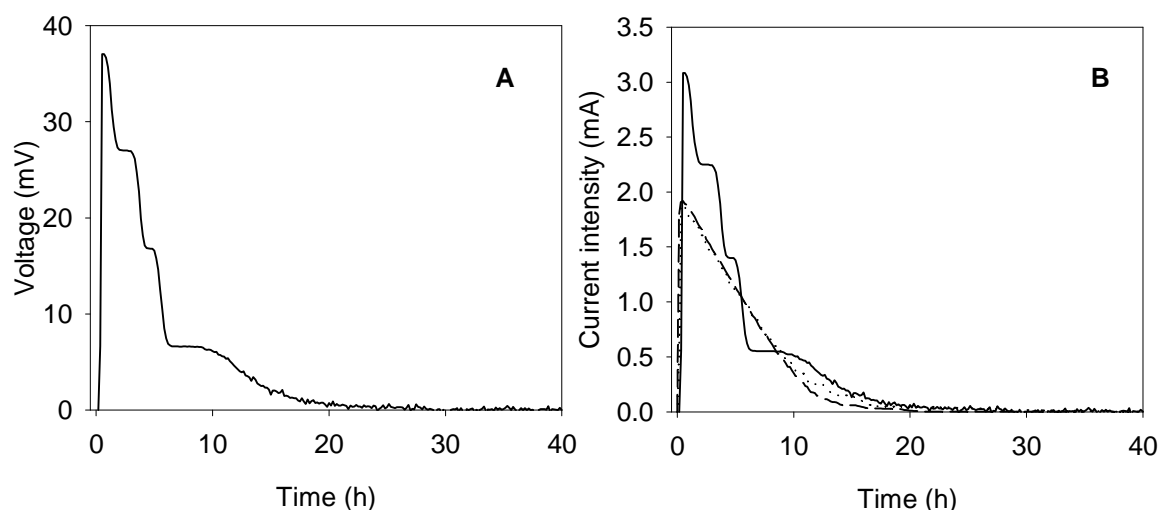


Figure 3.4.2. (A) Voltage monitored for the fuel cell after supplying 10 mL of hydrogen (external resistance of 12 Ω) (B) Current intensity for the fuel cell after supplying 10 mL of hydrogen for external resistance of 12 Ω (solid), 100 Ω (dashed) and 350 Ω (dashed-dotted).

From a chemical engineering point of view, the fuel cell operation is a reaction driven by a non-porous heterogeneous catalyst and hence there is external mass-transfer limitation of

hydrogen from the bulk gas to the catalyzer surface and chemical reaction with its three steps of reactant (hydrogen) adsorption, surface reaction and product (protons) desorption. In addition to the classical heterogenic catalysis, the external resistance of the fuel cell limits the maximum rate of the surface reaction, reducing the electron flow through the electric circuit. Regarding the experiments performed with different external resistance, the current intensity profiles obtained with 100 and 350 ohm seem to indicate that the high external resistance is limiting the surface reaction and hence no external mass transfer limitation exists (i.e. hydrogen transfer by diffusion to the catalyzer surface is faster than the chemical reaction). The constant decrease of current intensity observed is related to the decrease of hydrogen concentration in the gas bag (i.e. current intensity seems to be proportional to the bulk hydrogen concentration). On the other hand, the results for the external resistance of 12 ohm show that external mass transfer seems to be limiting the observed reaction rate. The shape of the current profile depends on the diffusion of hydrogen from the bulk gas of the bag through the needle and the inlet port of the fuel cell to the surface of the catalyzer, where different zones are exposed to different hydrogen concentration and these zones are changing with the decrease of bulk hydrogen concentration during the operation of the cell. Other factors as water accumulation in the anode that decreases the catalytic surface may be also modifying the fuel cell response⁸⁹.

4.3.1.2. Decreasing external resistance limitations

When the fuel cell is conceived to work in series with another device, for example if it is to be used as a sensor like in this work, it is crucial that the fuel cell is not the limiting step of the process. The rate at which the electrochemical reactions take place in a fuel cell is dependent on the external resistance that is used to close the electrical circuit. Hence, a set of external resistances were tested to evaluate which load would offer the maximum quantification of the volume of hydrogen supplied to the fuel cell (Figure 3.4.3). Such quantification was determined in terms of percentage of coulombs recovered, i.e. coulombs measured referred to as hydrogen supplied in units of coulombs.

As shown in Figure 3.4.3, higher external loads resulted in lower coulombic recoveries, which were also more dispersed. These observations were most probably caused by the electrical current limitations mentioned before, since under these conditions diffusion losses may be more probable to occur. The highest coulombic recovery was achieved with a 12 Ω

external resistance, allowing an average recovery of 71%. This value can be considered high because the usual efficiency reported for fuel cells is around 40-60% of useful output energy versus total input energy⁹⁰. This optimized resistance was used in the following tests as the design configuration.

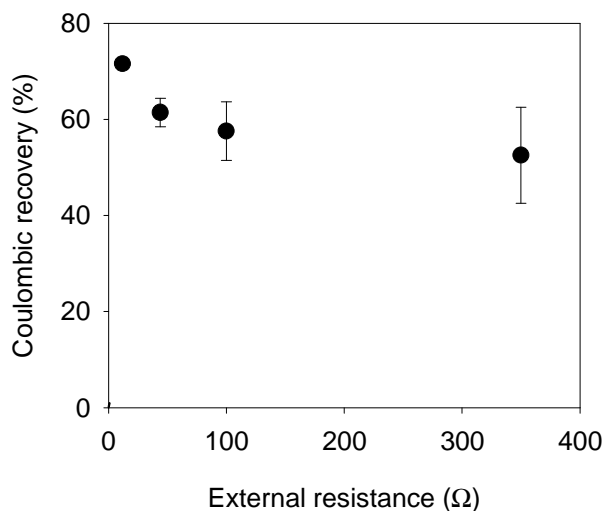


Figure 3.4.3. External resistance optimization to quantify the maximum volume of hydrogen (in units of coulombs). Error bars indicate standard deviation, which was calculated based on triplicate tests.

Even though current intensity was dependent on the external resistance, reaching lower values for higher loads, a signal response was immediately detected in all the cases. A fast response is needed in a measuring device, so that a corrective control action can be quickly applied. However a slower response of the measuring instrument can be accepted for biological dynamics as in a MEC.

4.3.1.3. Fuel cell calibration

Once the adequate external resistance was set, the fuel cell was calibrated to get a correlation between the coulombs measured in the fuel cell and the actual hydrogen volume supplied. As shown in Figure 3.4.4 a good linear correlation with high repeatability was obtained for the quantification. A little variability can be observed for the highest volumes tested. Higher hydrogen volumes and thus longer analyses time favor hydrogen diffusion besides from increasing the human error probability when sampling the gas, increasing the standard deviation of the results.

In terms of hydrogen volume, also a lower detection limit for the fuel cell was of interest. Indeed, 4 mL of hydrogen was found to be the lowest volume that permitted its quantification at the highest attainable coulombic recovery, i.e. 71%.

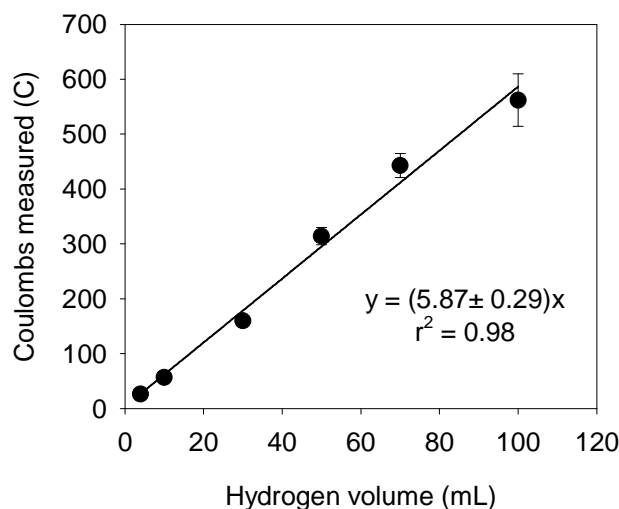


Figure 3.4.4. Fuel cell sensor calibration for hydrogen volume supplied vs. coulombs measured. Error bars indicate standard deviation, which was calculated based on triplicate tests.

A total of 12 experiments (containing 10 mL of hydrogen each) were used to assess the repeatability of the fuel cell as an electrochemical sensor. The fuel cell quantified an average of 71.09 C, with a relative standard deviation of 0.023 or a variation coefficient of 2.3%. Values for the variation coefficient lower than 5% are generally describing high repeatability.

4.3.1.4. Validation of the fuel cell sensor with a method of reference

As already mentioned, gas chromatography is the most common analytical technique to quantify hydrogen production. Hence it was considered as a reference method to compare with the one presented in this work.

Standard mixtures of hydrogen and nitrogen were quantified in triplicate by gas chromatography and with the fuel cell. A strong positive correlation (slope very close to the unity) was obtained when comparing both methods, indicating that both methodologies were analogous when it comes to hydrogen quantification (Figure 3.4.5). Nevertheless more variability was observed for the analyses with the fuel cell as observed with the wider error bars associated to the method.

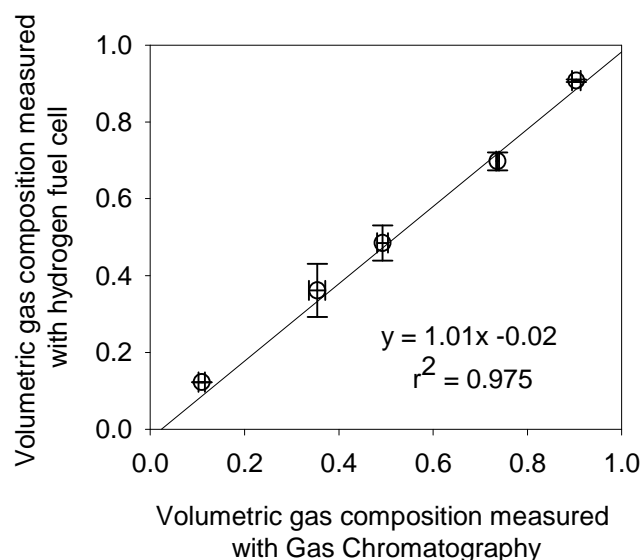


Figure 3.4.5. Comparison of fuel cell as hydrogen monitoring device with a reference method (gas chromatography). Average values from triplicate tests are presented. Error bars indicate standard deviation from the triplicate tests.

4.3.1.5. Signal interferences from other biogas compounds

Methane and carbon dioxide were tested independently in the device to check that they were not interfering and therefore no electrical signal was being detected. Neither methane nor carbon dioxide allowed current generation on the fuel cell, indicating that they did not react and no interference existed. Although no interference in terms of signal was expected from methane or carbon dioxide, a verification test was performed afterwards to confirm that no catalytic damages were caused by these compounds. In both cases the signal was totally matching the signal before the tests with carbon dioxide or methane, and therefore no catalytic loss was experienced in the system. Methane and carbon dioxide are therefore regarded to be inert.

Carbon dioxide was proven to be inert when fed independently in the fuel cell. However, mixtures of carbon dioxide with hydrogen were also tested to investigate about the possible poisoning effects of carbon monoxide, which can be produced by the reverse water gas shift reaction ($\text{H}_2 + \text{CO}_2 \leftrightarrow \text{H}_2\text{O} + \text{CO}$). Carbon monoxide is reported to adsorb on the catalyst, decreasing the efficiency of the fuel cell^{91–93}. Nevertheless, no catalytic loss was observed in the system studied, although such an effect could be limiting the system in the long term operation.

Regarding the lifetime of the device, the system was tested for a period of four months without seeing any loss in its measuring capacity. A periodical control analysis and, if necessary, a calibration of the device would be recommended. An option to avoid catalytic loss by carbon monoxide formation includes the possibility of trapping carbon dioxide in a sodium hydroxide solution before the gas mixture arrives to the fuel cell.

4.3.2. Implementation in MEC: online monitoring of hydrogen production

A last validation test was performed connecting in series the fuel cell with a microbial electrolysis cell, which was possible on a direct connection configuration or incorporating a gas bag between both systems (Figure 3.4.6). As shown in Figure 3.4.7 the fuel cell signal followed a similar trend as the MEC current intensity response, and the total hydrogen produced could be quantified.

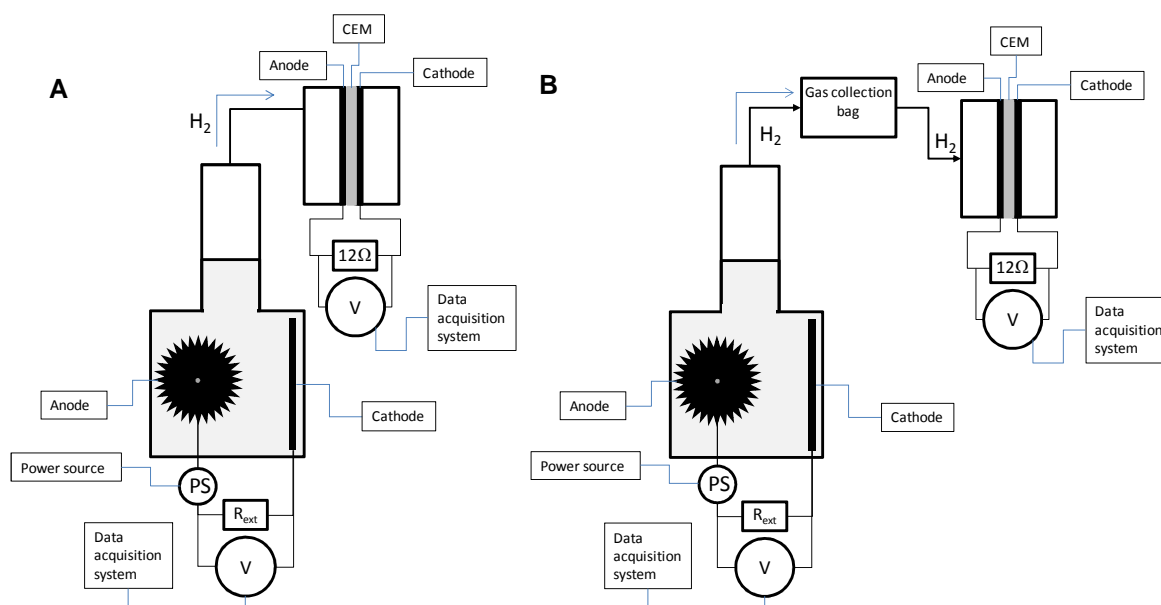


Figure 3.4.6. Experimental setups for the implementation in MEC of the fuel cell as an online hydrogen production monitoring tool. **(A)** Direct connection MEC-fuel cell **(B)** Connection MEC-gas bag-fuel cell.

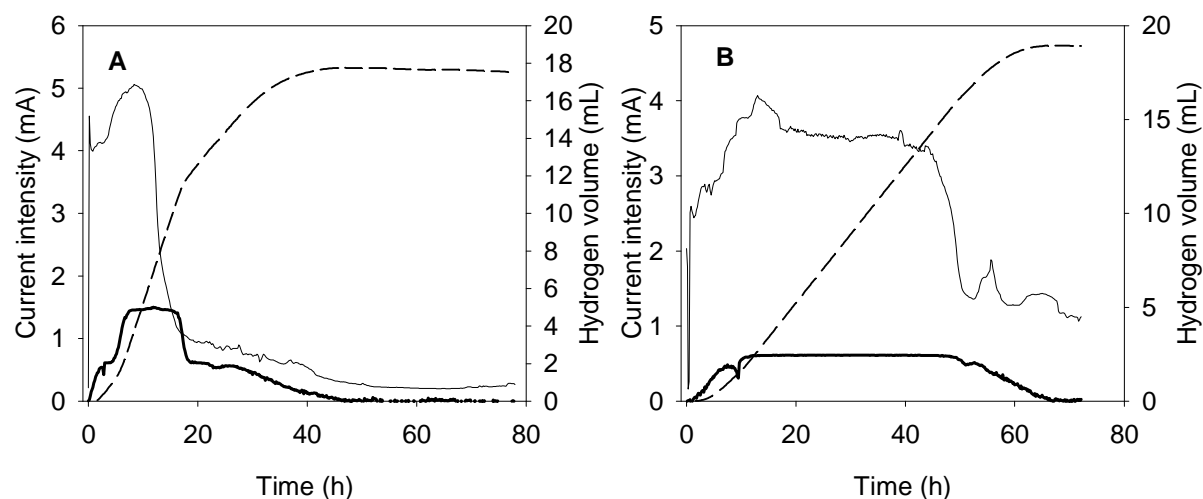


Figure 3.4.7. Microbial electrolysis cell current intensity signal (thin), fuel cell current intensity response (thick) and cumulative hydrogen volume measured (dashed). **(A)** Direct connection MEC-fuel cell **(B)** Connection MEC-gas bag-fuel cell.

A slower response of the fuel cell than MEC response was observed initially, since the hydrogen produced had to accumulate first in the headspace or the gas bag before diffusing into the fuel cell. Such a lag time should not affect the gas quantification, and in any case it would not be relevant in a continuous mode operation.

Based on the coulombs measured in MEC, the coulombs recovered in the fuel cell accounted for a 15% of the total with the MEC-gas bag-fuel cell configuration (21% based on substrate), and reached a 35% of the total with the MEC-fuel cell setup (40% based on substrate). It is important bearing in mind that a 100% recovery would only be possible if also cathodic coulombic recovery in the MEC would be of 100%. However, the results denoted the presence of gas losses, which were more important with the MEC-gas bag-fuel cell configuration. It was also observed that in terms of current intensity MEC was giving higher signal than the fuel cell, indicating a limitation in the fuel cell performance. Such a limitation was most probably caused by low hydrogen diffusion rate, which could be related to gas leakages or microbial hydrogen utilization as electron donor.

Seeing that higher recovery was obtained in the direct connection MEC-fuel cell, it was decided to use this configuration to try to improve the method quantification. To do so the fuel cell limitations were compensated by decreasing the MEC hydrogen production rate (decreasing the initial substrate concentration and changing the applied voltage to 0.6V). With these changes a 50% recovery of coulombs measured in the fuel cell with respect to the coulombs that were measured in MEC was obtained (60% based on substrate).

In following tests, unfortunately, the fact that hydrogen had been accumulating in the headspace rather than in a gas bag became a hurdle in the system quantification, since hydrogen accessibility for hydrogen scavengers (H_2 oxidizing ARB and homoacetogenic bacteria) was favored. This was noted by the increase in CE, which rose from 115% to 200%. Also a decrease in the coulombs recovered in the fuel cell based on the coulombs available in the substrate supplied was indicative of such phenomena, varying from 60% to 43%.

These tests were a proof of concept that the fuel cell can effectively quantify the hydrogen produced in MEC. Nevertheless, it is crucial that the gas leakages are minimized for a precise quantification, especially when a gas bag is incorporated between the MEC and the fuel cell. It is important mentioning that the incorporation of a gas bag is believed to have an important role in the hydrogen recycling phenomena, since it avoids an increase in the headspace hydrogen partial pressure, and therefore it does not enhance that hydrogen is in solution, accessible for hydrogen scavengers.

4.3.3. Practical implications

In this work the use of a fuel cell at lab scale to monitor hydrogen production is presented as an alternative to more complex analytical methods, such as gas chromatography. There are advantages and drawbacks for both systems, but at the end the possibility of using one or another is highly dependent on the system to be monitored (configuration, use, location, budget, etc).

Regarding GC, the advantages of the system include the possibility to detect more than one gas compound, not only hydrogen, and the availability of commercial online GC. Nevertheless, the device is notably expensive (thousands of euros) and it requires the consumption of utility gases. Also, when it comes to the analysis per se, a double analysis is required in order to be able to quantify the volume produced (as in Ambler and Logan⁸⁶). Alternatively the system can be connected to a flow-meter to measure total gas production, increasing the costs.

On the other hand, the fuel cell as a device to monitor the hydrogen produced represents a completely affordable instrument, which can easily be set online with the system to monitor. Being selective for hydrogen, it can be a perfect option in systems where pure hydrogen is produced (such as double chamber microbial electrolysis cells). In other anaerobic systems,

only the hydrogen produced or its relative composition can be measured. Finally, the time to perform the analysis can be quite long when using it offline, in the range of few hours, since hydrogen would only arrive to the reacting surface by diffusion.

At lab scale the fact that the fuel cell will consume the product of interest is not an important drawback. In larger systems just a little percentage of the gas produced can be directed to the fuel cell, and the installation of a mass flow-meter prior to the fuel cell will allow monitoring the hydrogen production.

Finally, it is worth mentioning that having a device able to monitor with high reliability and with an analogical signal the hydrogen produced also eases the implementation of control strategies, which can end up improving the whole performance of the system.

4.4. Conclusions

A low cost fuel cell is presented in this chapter as an alternative, transportable and robust methodology to monitor hydrogen production in MEC at lab scale. Tests revealed the high repeatability of the system as a monitoring tool, showing high correlation of the system signal with hydrogen supply. A strong correlation was also obtained when comparing the methodology presented here with gas chromatography as a reference method. In addition, no interferences or loss of catalytic activity were observed for other biogas compounds.

Although the use of a fuel cell as a hydrogen monitoring device has only been tested at lab scale in this work, the system has prospects to be easily scaled up, which would lower the costs of biohydrogen production in MEC. Besides of becoming more economically competitive, this monitoring system introduces the possibility to incorporate control strategies that would enhance the system optimization.

Chapter 5. Case study: treatment of biodiesel industry wastewater with bioelectrochemical systems

Chapter summary

Arise in biodiesel production in the last decades has caused a drop in glycerol price, lowering the added value of this subproduct in biodiesel industry. The use of glycerol contained in biodiesel industry wastewater as a substrate for bioelectrochemical systems is therefore interesting. In this chapter, the opportunities for crude glycerol to produce electricity and hydrogen in single chamber MXC were explored. The role of methanol in crude glycerol was also studied, since it is commonly found in biodiesel industry wastewater. Whereas electricity production was feasible in single chamber MFC, its applicability in single chamber MEC for hydrogen production was constraint as a result of homoacetogenic bacteria metabolism. Electrofermentation of synthetic glycerol was also studied as a possible technology to give an added value to biodiesel industry wastewater by enhancing the production of 1,3-propanediol.

The content of this chapter was partially published in International Journal of Hydrogen Energy with the name “Methanol opportunities for electricity and hydrogen production in bioelectrochemical systems” by N. Montpart, E. Ribot-Llobet, Vijay Kumar Garlapati, L. Rago, A. Baeza and A. Guisasola (2014).

The study on electrofermentation of glycerol was carried out in the Laboratory of Microbial Ecology and Technology (LabMET) in Universiteit Gent under the supervision of Prof Dr Korneel Rabaey and Dr Jan Arends.

5.1. Introduction

The increase in biodiesel fuel production in the last decades has caused a surplus production of the main subproduct of this industry, glycerol. Glycerol has decreased its market price and, hence, finding alternative applications to valorize this waste stream is interesting. Bioelectrochemical systems are presented as an option to produce electricity or other products with more added value like hydrogen or 1,3-propanediol from glycerol.

Biodiesel is made by chemically reacting lipids (vegetable oils, animal fats...) with an alcohol producing fatty acid esters. As a subproduct, about 10% of the total biodiesel fuel production is obtained as crude glycerol. In the production process, methanol is often used for the esterification reaction because of being the cheapest alcohol available. Therefore its presence in crude glycerol is common. Crude glycerol as a raw material for processes such as bioelectrochemical systems for hydrogen production was reported to be an interesting carbon source^{35,82} but Chignell and Liu³⁷ observed a decrease in hydrogen production yield when methanol was present in this waste stream in a single chamber MEC.

Synthetic glycerol was proved to be a possible substrate in single chamber MEC as presented in Chapter 3, although there was methane build-up in the system and the hydrogen recycling phenomena was observed. In a first section of this chapter, the opportunities of crude glycerol from an industrial biodiesel production plant to produce hydrogen in a single chamber MEC were explored.

Besides from hydrogen, microbially assisted electrosynthesis offers the possibility to drive the chemical synthesis of other products in anodic or cathodic environments depending on whether the metabolic pathway leading to the desired product requires oxidizing or reducing power. In terms of cathodic bioproduction, such processes are linked to the electron uptake by microorganisms. The reducing power provided by the electrode can either redirect fermentation pathways or can be directly used in the microbial metabolism. The electron transfer from electrodes to the microorganisms is thought to follow different pathways: through hydrogen as intermediate in the whole process, by means of electron shuttles, by direct catalysis and by the intermediate biological formation of an initial building block, such as formate, which can be further used by other microorganisms⁹⁴.

In processes of redirection of fermentation pathways (also known as electrofermentation) the current flow influences the ability for cells to regenerate NADH. The NAD^+/NADH ratio is therefore altered and the change in the redox status of the cell can end in the enhancement of certain metabolic processes.

Microbial electrofermentation has been reported in the literature^{95–99} but this technology still faces some operational hurdles that should be addressed before considering these processes at a realistic scale. In this sense, the selectivity towards the desired end product, product inhibition and recovery, pH gradients that can limit the biocathode activity and the biofilm-electrode interactions should be focus of interest¹⁰⁰.

Cathode surface modification is regarded to improve the cell adherence and thus the biofilm development, which in plain cathodes is not enhanced. Indeed, the negatively charged cathode results in a repulsive effect with the negatively charged bacterial cell membrane. Taking into account that the microbial cell wall is charged, the option of initially polarizing the cathode to enhance the cell attachment and therefore the electrode inoculation is studied in this chapter.

Glycerol surplus as a result of biodiesel production has lowered its economical value, however fermentation products of glycerol are economically interesting. This is the case of 1,3-propanediol, used in the production of polyurethanes and polyesters. Electrofermentation offers the possibility to enhance the production yield of 1,3-propanediol from glycerol.

Glycerol fermenting microorganisms are not expected to have electroactive abilities and therefore their growth on the electrode is not favored. The growth of a glycerol fermenting mixed culture on a plain cathode surface was pursued in a second section of this chapter. The possibility to initially polarize the cathode to enhance the cell attachment during the inoculation process was tested.

5.2. Materials and methods

5.2.1. Hydrogen production in single chamber MEC with biodiesel industry wastewater

A mMFC able to use synthetic glycerol as sole carbon substrate was inoculated following the methodology presented in Chapter 2. The substrate was afterwards switched to crude glycerol (Biodiesel Peninsular-Stocks del Vallès, Barcelona), which in the raw solution had a concentration of 203 g L⁻¹ glycerol and 23.4 g L⁻¹ methanol, 282 g COD L⁻¹. The system was operated in fedbatch with an initial concentration of 200 mg L⁻¹ and was increased up to 1800 mg L⁻¹. BES was only added during the two first weeks of operation with crude glycerol (50 mM). After characterizing the electroactivity of the system the configuration was changed to work in single chamber mMEC mode.

The role of methanol in biodiesel industry wastewater was also tested. Methanol was used as the sole carbon source in mMFC and mMEC. The methanol synthetic medium contained per liter: 1.6 g methanol, 172 mL PBS stock solution, 2.925 g KHCO₃ and 12.5 mL mineral media. BES was used at a concentration of 50 mM.

5.2.2. Glycerol electrofermentation

The electrofermentation reactor consisted of two plastic frames separated by a cationic exchange membrane (CEM, Ultrex CMI-7000, Membranes International Inc, USA) and sandwiched between two plastic endplates leaving a volume of 200mL per chamber. The CEM was soaked overnight in a 4% NaCl solution before use. Rubber gaskets were used to create a watertight seal. An iridium oxide mesh was used as stable anode and carbon felt as cathode (20 cm x 5 cm x 0.3 cm, Alfa Aesar, Germany). A stainless steel mesh was placed next to the cathode to favor the current collection and connections. The cathode was situated next to the CEM, at a separation distance of 2 cm from the anode. Liquid connections were provided by means of the endplates. A potentiostat (VSP, Biologic, France) was used to control the potential of the cathode, using a Ag|AgCl reference electrode (RE-1B, Biologic, France) inserted in the cathodic chamber endplate.

The system was run in batch mode with continuous recirculation of both catholyte and anolyte. The catholyte contained per liter 8.5 g Na₂HPO₄·7H₂O, 3 g KH₂PO₄, 0.5 g NaCl, 1 g

NH_4Cl , 0.24 g MgSO_4 , 1 mL CaCl_2 stock solution of 11 g $\text{CaCl}_2 \text{ L}^{-1}$, 1 mL of trace element solution and 10 g L^{-1} of glycerol. Trace element solution contained per liter 1 g $\text{FeSO}_4 \cdot 7\text{H}_2\text{O}$, 70 mg ZnCl_2 , 100 mg $\text{MnCl}_2 \cdot 4\text{H}_2\text{O}$, 6 mg H_3BO_3 , 130 mg $\text{CaCl}_2 \cdot 6\text{H}_2\text{O}$, 2 mg $\text{CuCl}_2 \cdot 2\text{H}_2\text{O}$, 24 mg $\text{NiCl}_2 \cdot 6\text{H}_2\text{O}$, 36 mg $\text{Na}_2\text{MoO}_4 \cdot 2\text{H}_2\text{O}$ and 238 mg $\text{CoCl}_2 \cdot 6\text{H}_2\text{O}$. The anolyte was a solution with 100 mM H_2SO_4 and 5 mM Na_2SO_4 . Initial pH was about 1.5 and 6.5 for the anolyte and the catholyte respectively and never changed more than one unit at the end of the batch.

The carbon felt cathode was initially inoculated with a glycerol fermenting community coming from a continuously stirred glycerol culture flask (800 mL liquid volume) operated in fed-batch mode, with a hydraulic retention time of 2 days and initial substrate concentration of 10 g glycerol L^{-1} (organic loading rate of 5 g glycerol $\text{L}^{-1} \text{ d}^{-1}$), which was kept at 34°C. The reactor was a gas tight 1 L Schott bottle whose gas outlet was connected to a gas measuring cylinder, where a sampling port was available. The initial inoculum was a mixture of conventional anaerobic digestion sludge, wastewater from a SHIME[®] reactor (Simulator of Human Intestinal Microbial Ecosystem reactor) and sludge from brewery wastewater fermentation.

After inoculation, the electrofermentation reactor ran in batch operation under galvanostatic mode (i.e. current supplied) for 16 hours, fixing current intensity at -100 mA to favor the reductive process. Under these conditions the cathode potential stabilized to a steady state potential ($E_{\text{we,ss}}$). After this period the catholyte was replaced by a fresh catholyte solution and the operation mode was changed to potentiostatic mode for 24 hours, setting the cathode potential ($E_{\text{we,sp}}$) at 50 mV lower than the $E_{\text{we,ss}}$ previously reached, and reaching at the end of the period a steady state current intensity (I_{ss}).

Blank tests were carried out in absence of biomass, after running 1 M NaOH along the reactor setup for 24 hours to sterilize the system and rinsing it afterwards by running demineralized water. Media were autoclaved. In a first test the same experimental procedure abovementioned was followed, i.e. initial galvanostatic operation following a potentiostatic operation period. In a second test, a manual chronoamperometry was performed, setting the working electrode potential at those values set in each experiment during the potentiostatic operation.

Following the potentiostatic mode operation a cyclic voltammetry was performed for all tests. Potential limits and scan rate were set to -0.4 V, 0 V and 0.5 mV s⁻¹. Change of catholyte or feeding glycerol prior to CV was required to guarantee substrate availability.

Cell attachment on the carbon felt surface was evaluated using flow cytometry, which should allow the assessment of the decrease in cell count of the filtrate. Samples for cell count assessment with the flow cytometer (CyAn AFP, DakoCytomation) were taken regularly along the filtration, and kept at -20°C until analyzed. For the counting of bacterial cells with flow cytometry analyses, the samples were diluted 100 times with deionized water (0.22 µm filtered) and they were stained with a live/dead staining solution (containing two fluorescent dyes: SYBR® Green I and propidium iodide). EDTA was added to avoid cells aggregation and a known volume of counting beads allowed the cell concentration determination. The stained sample was incubated for 5 minutes in the dark prior to flow cytometric analysis. Cells concentration should be between 10⁴ and 10⁶ cells mL⁻¹. Too much dilution would mask the cell count with background signal and too much cell concentration would increase the chances that several particles are detected as one. Taking into account that samples had to be frozen before flow cytometry analysis, total cell count (sum of alive and dead count) was considered. No significant differences in total cell count were observed between a fresh sample and a frozen sample.

Glycerol and its metabolites concentrations were analyzed. Gas chromatography fitted with a polar capillary column and a flame ionization detector was used to assess VFA concentration. An external lab analyzed the samples in a HPLC with a refractive index detector for glycerol and 1,3-propanediol. COD analyses were performed using COD reagent ampules (commercial test tubes, Hach Lange). pH of both electrolytes was also evaluated. Samples were filtered (0.22 µm) and kept at -20°C until analyzed.

Gas composition was analyzed with gas chromatography (compact GC, Global Analyzer Solutions, The Netherlands). A double column system allowed detection of hydrogen, oxygen, nitrogen, methane and carbon dioxide in a single run.

5.3. Results and discussion

5.3.1. Hydrogen production in single chamber MEC with biodiesel industry wastewater

5.3.1.1. Crude glycerol in single chamber MFC

Synthetic glycerol was observed to be a possible substrate in single chamber MFC as presented in Chapter 2, offering higher power generation than other complex substrates. Wastewater from the biodiesel industry contains other substances besides glycerol. Its composition varies depending on the process, i.e. catalyst, biodiesel removal efficiency, feedstock impurities and alcohol used. The fact that wastewater from the biodiesel industry, here called crude glycerol, contains other substances besides glycerol might limit its use in bioelectrochemical systems.

A mMFC able to use synthetic glycerol as sole carbon substrate was inoculated following the methodology presented in Chapter 2. The substrate was afterwards switched to crude glycerol (203 g L⁻¹ glycerol and 23.4 g L⁻¹ methanol in the raw solution). Figure 3.5.1A presents the mMFC current intensity profile from the moment that crude glycerol was fed. A stable maximum current intensity of 0.4 mA was obtained from the beginning, not significantly lower than when synthetic glycerol was used (0.45 mA, Figure 3.2.12A). According to Chapter 1, the external resistance of the system was lowered from 1000 Ω to 100 Ω to enhance the system electroactivity, reaching afterwards up to 1.6 mA. The system seemed to be limited by substrate concentration, since the more loaded the fresh medium the higher the current intensity achieved. The substrate concentration was slowly increased up to 1800 mg L⁻¹, but a maximum steady response was obtained from 1200 mg L⁻¹. Crude glycerol resulted in better results than those found with synthetic glycerol. Table 3.5.1 summarizes the performance of MFC-crude glycerol and it is compared to MFC-synthetic glycerol (presented in Chapter 2, Table 3.2.4). Crude glycerol as a carbon source in MFC allowed higher CE and current intensity, although COD removal was lower, which was attributed to products other than glycerol or methanol contained in the wastewater, since glycerol was being completely depleted as shown in Figure 3.5.1B.

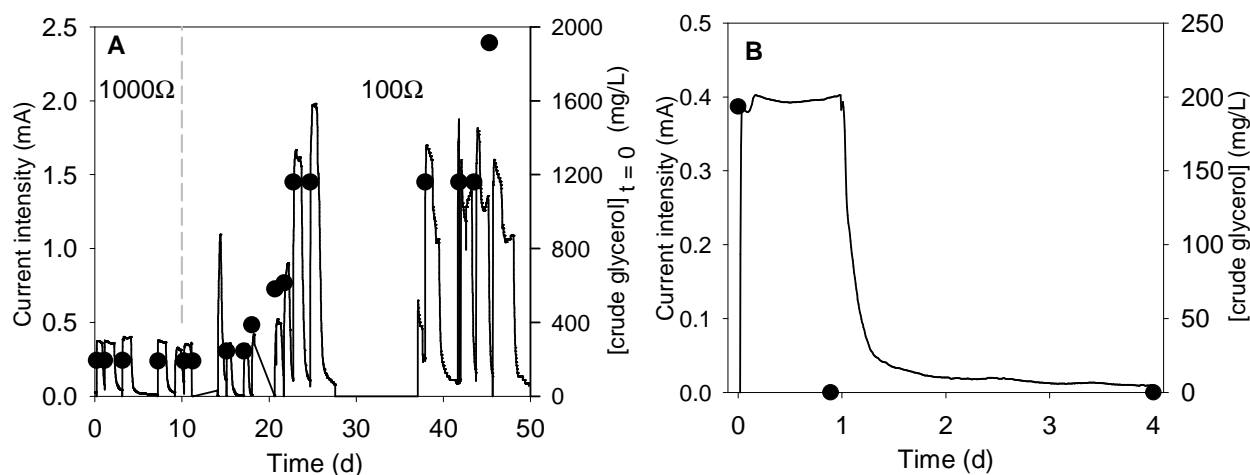


Figure 3.5.1. (A) Current intensity profile (solid line) and initial crude glycerol concentration (●) for MFC-crude glycerol. Dashed line indicates the change of R_{ext} from 1000 to 100 Ω . (B) Current intensity (solid) and crude glycerol concentration (●) in a fedbatch cycle in MFC-crude glycerol (methanol initial concentration 15 mg L^{-1}).

Table 3.5.1. Single chamber MFC performance with glycerol and crude glycerol

	Current intensity (A m^{-3})	CE (%)	COD removal (%)
Synthetic glycerol	50	35	100
Crude glycerol	57.1	39.4	57

5.3.1.2. Crude glycerol in single chamber MEC

The anode acclimated to work in MFC-crude glycerol was changed to a mMEC configuration. From the first cycle tested, the cycle exhibited a very long current intensity response and no hydrogen was detected (Figure 3.5.2). Methane was neither detected, although no BES had been dosed for one month. This behavior was indicative of an electron recycling situation, which was corroborated by an average CE of 240%. Electron recycling could be a consequence of the presence of H_2 -oxidizing ARB or homoacetogenic bacteria. The initial existence of these microorganisms in the system was only expected as a result of hydrogen production from glycerol fermentation. However, the fact that methanol was present in crude glycerol enhanced the presence of homoacetogenic bacteria in the system and the electron recycling situation, since acetogenic bacteria are responsible of metabolizing C1-compounds, such as CO_2 and methanol, to acetate^{101,102}. The metabolism of homoacetogenic bacteria was even more favored than methanogenic metabolism, even without inhibiting their growth with BES. As Chignell and Liu³⁷ also observed a decrease in

hydrogen production from crude glycerol when methanol was present in the waste stream, it was decided to determine the potential of methanol per se to produce hydrogen in MEC.

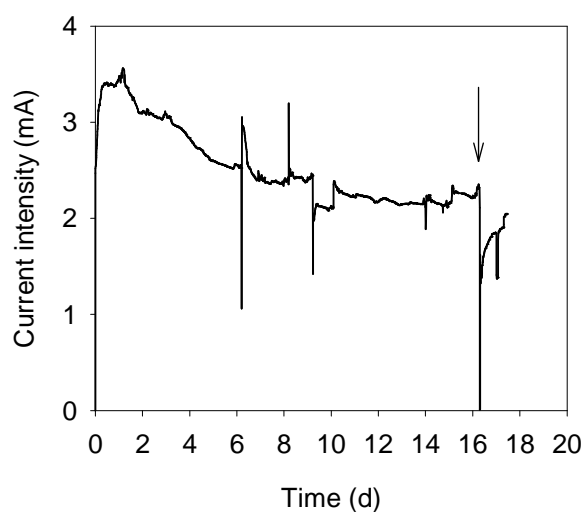


Figure 3.5.2. Current intensity profile for a conventional cycle in MEC fed with crude glycerol. Arrow indicates change of media.

5.3.1.3. The role of methanol in biodiesel industry wastewater in single chamber MEC

The presence of methanol was observed to favor the electron recycling situation, avoiding net hydrogen production in single chamber MEC. However, the use of methanol in MEC was further explored to investigate about its other possible positive or negative effects: methanol could simply be innocuous in the system, it could potentially have an inhibitory or toxic effect on ARB, or it could even improve the system performance due to a possible syntrophy. Indeed, direct utilization of methanol for operation of bioelectrochemical systems was attempted by Kim et al.¹⁰³ studying the feasibility of alcohols (ethanol and methanol) for power generation using two chambered MFC, succeeding with ethanol and reporting non-appreciable electricity generation with methanol. Regarding MEC, direct methanol utilization had never been reported.

The methanol-driven mMEC was started up with the anode of a methanol-driven mMFC inoculated following the syntrophic consortium strategy presented in Chapter 2. Figure 3.5.3 presents the voltage profile of the last batch cycle performed in that mMFC. Previous cycles had also shown that methanol could be used as substrate in MFC. As it can be observed, methanol degradation was fast whereas acetate concentration was low indicating that the

process was not limited by ARB, i.e. the fermentation products were rapidly consumed by ARB. However, the presence of other acetate sinks different from ARB could not be ruled out. The low acetate presence in the bulk was consistent with the fact that the growth of the consortium as anodic biofilm was enhanced throughout the cell operation, since after every batch cycle the media was completely replaced by fresh one. Thus, only the acetate that had not been consumed by ARB in the biofilm could diffuse into the bulk.

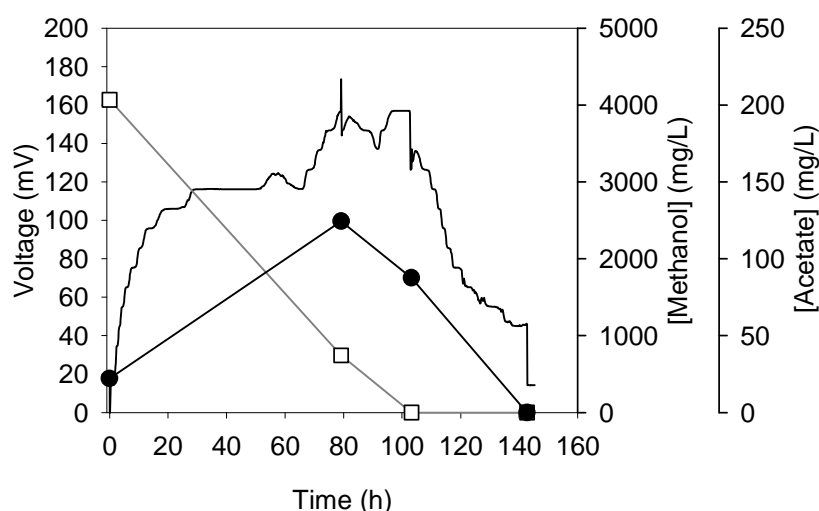


Figure 3.5.3. Voltage and metabolites evolution in a methanol driven mMFC. Solid line: Voltage, ●: acetate and □: methanol concentration.

The results when operating as mMEC for hydrogen production (Figure 3.5.4) showed a similar trend to crude glycerol; CE was 296%, the cycle was remarkably long (about 28 days) and, despite the significant current density obtained (5.7 mA m^{-2}), again no hydrogen was detected during all the batch cycle. These observations again evidenced the occurrence of electron recycling from the cathode to the anode, i.e. hydrogen recycling phenomena.

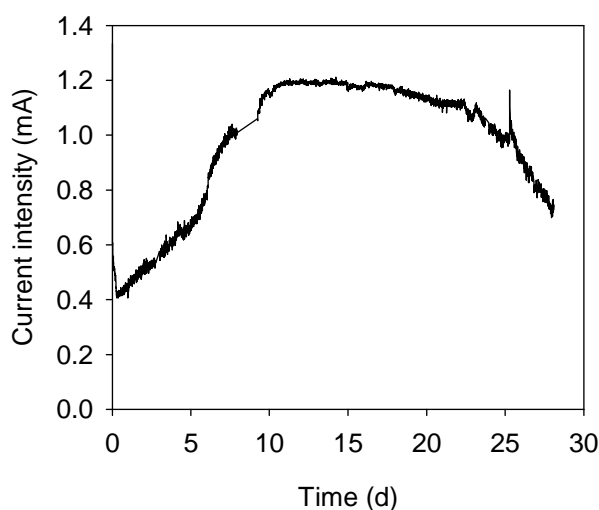
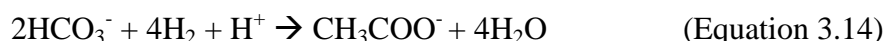


Figure 3.5.4. Current intensity evolution in a single chamber methanol-driven MEC.

Equations 3.12 to 3.15 present the most probable chemical reaction scheme occurring in this mMEC. Equation 3.12 describes the methanol conversion to acetate, which is further oxidized by ARB to bicarbonate (Equation 3.13). Equation 3.14 describes the hydrogen consumption by homoacetogenic bacteria and finally Equation 3.15 shows the possible hydrogen utilization by ARB. The last two reactions are responsible for the electron recycling scenario.



In this case, methanogenic *archaea*, although being potential hydrogen consumers, could be ruled out since i) BES was used, ii) methane was never detected and iii) their metabolic activity would not have caused such an electron recycling effect.

The presence of homoacetogenic bacteria in these methanol-fed systems was assessed and confirmed with microbiological techniques³⁸, detecting *Acetobacterium sp* and *Desulfovibrio sp* (Figure 3.5.5).

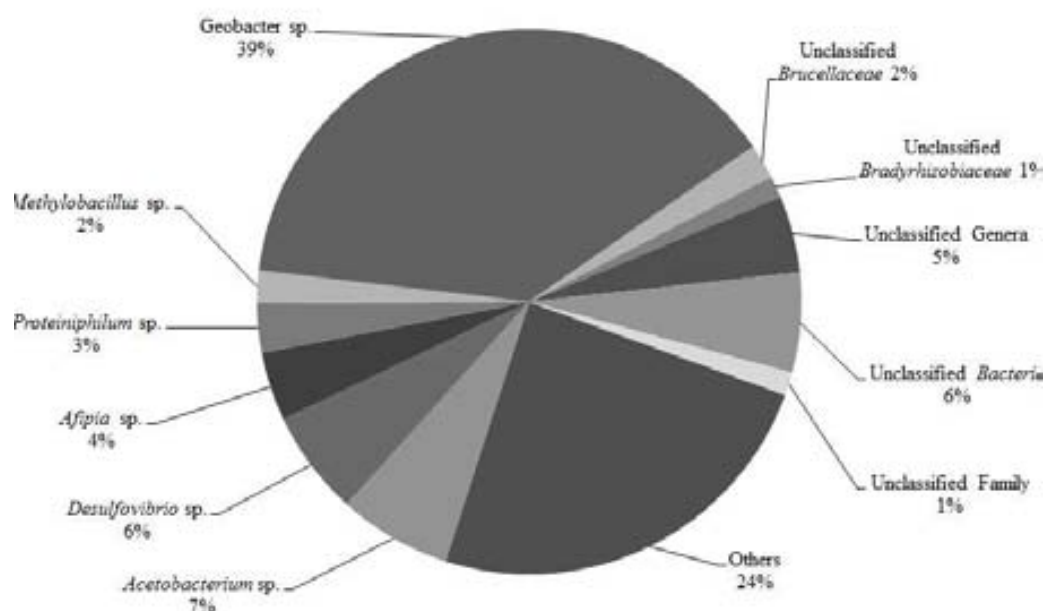


Figure 3.5.5. Anodic genus microbial distribution through high-throughput 16S rRNA gene pyrosequencing. Genera making less than 1 % of total sequences were classified as others (With permission of Laura Rago).

Moreover, an extra test was performed in MFC configuration in order to further study whether the electron recycling was consequence of the presence of H_2 oxidizing ARB or it was only caused by homoacetogenic bacteria (Figure 3.5.6). In Period I, during the first 22 hours, the circuit was opened, the cell was fed with fresh medium without methanol and sparged during 5 minutes with hydrogen. At the end of the period, acetate was detected in the medium but at a very low concentration (less than 5 mg L^{-1}). In Period II, fresh medium without methanol was fed and the circuit was closed in MFC configuration, achieving a stable voltage of 20 mV after one hour. Hydrogen was then sparged into the system as in Period I. A lag time of about ten hours was required for observing a voltage increase, in agreement with hydrogen not being directly used as electron donor. In the same way, when no more substrate was available (presumably acetate rather than hydrogen) the response of the cell decreased to 0 mV. According to the experimental results, the existence of this lag-time indicates that H_2 -oxidizing ARB activity was minimal. The cell voltage monitored at the very beginning of Period II could be a sign of homoacetogenic bacteria presence in the anodic biofilm, where the acetate produced in Period I could have remained in the biofilm and eventually be consumed by ARB. Again this would be consistent with the fact that biofilm growth was enhanced along all the cell operation.

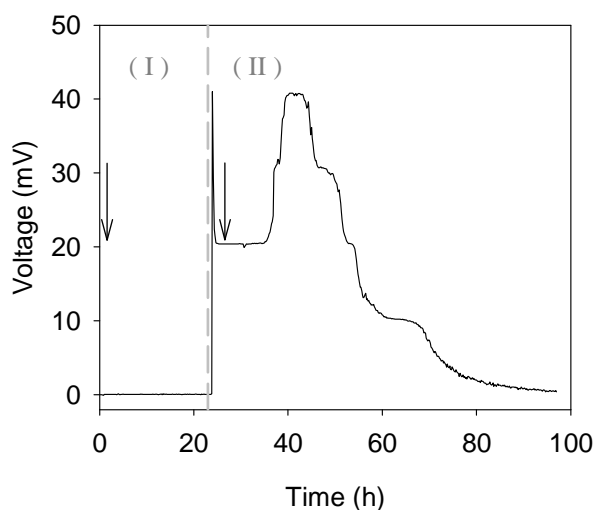


Figure 3.5.6: Homoacetogenic detection in a MFC fed with hydrogen and carbonate. Period I open circuit. Period II closed circuit. Arrows indicate hydrogen sparging.

Thus, hydrogen production from methanol in a single chamber MEC was not possible due to the presence of homoacetogenic bacteria, which could not be avoided since they were in charge of methanol conversion to acetate, a preferred substrate for ARB.

To avoid the problem of electron recycling, the system was changed to work as a mMEC in double chamber configuration. Under this arrangement a clear current intensity profile was obtained for each batch cycle (Figure 3.5.7), i.e. the cell experienced a current intensity increase as methanol was being converted to acetate and it decreased when the substrate was being depleted. This evidenced that electron recycling was avoided. Also hydrogen was detected during this period and CE was assessed to be lower than 100% for each batch cycle. Throughout the double chamber operational period, maximum current intensity achieved in every batch cycle increased, obtaining at the steady state a CE of 90%, r_{CAT} of 40% and r_{H_2} of 28%, with a production of $0.1 \text{ m}^3 \text{ H}_2 \text{ m}^{-3} \text{ reactor d}^{-1}$. Energy recovery based on electricity input stabilized around 60% and energy recovery based on both electricity and substrate input was only around 20%, still being far from considering the system energetically feasible. In any case, methanol-driven hydrogen production using bioelectrochemical systems was not found to be reported before.

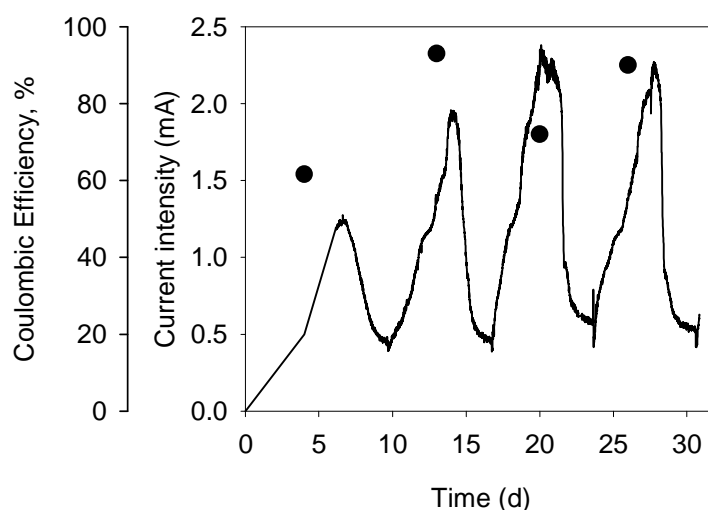


Figure 3.5.7. Current intensity evolution in a double chamber methanol-driven MEC. Solid: current intensity; ●: CE.

When working in a double chamber configuration, current density doubled reaching a stable response of 10.7 mA m^{-2} despite the membrane inclusion, which should have increased the cell internal resistance. However, as a consequence of physically separating both anolyte and catholyte a pH change was observed. pH decreased in the anolyte (final pH about 6.5), where protons were produced, and increased in the catholyte (final pH about 11), where hydroxides were produced. Methanol was not detected when the cycle was over, i.e. when current density decreased. During the cycle, maximum current intensity remained rather constant, inferring

from this that the decrease in current density was not a consequence of the change in pH but of the complete depletion of the substrate.

Seeing the results presented before, it was expected that net hydrogen production from crude glycerol could also be possible in a double chamber configuration regardless of the presence of methanol and methanol metabolizing bacteria. In fact, methanol would be effectively used as substrate in MEC in this configuration, which had never been reported before and therefore reinforces the scientific contribution of the study.

5.3.2. Other possibilities in BES for glycerol: Redirection of glycerol fermentation pathways in a microbially catalysed electrochemical cell

Nowadays fermentation products of glycerol are more economically interesting than glycerol itself. This is the case of 1,3-propanediol, whose production could be enhanced from electrofermentation of glycerol. Nevertheless, glycerol fermenting microorganisms are not expected to have electroactive abilities and therefore their growth on the electrode of the electrofermentation reactor is not favored. The possibility to initially polarize the cathode to enhance the attachment of a glycerol fermenting mixed culture during the inoculation process was tested.

The glycerol fermenting community to inoculate the carbon felt cathode was grown in a continuously stirred glycerol culture flask (Figure 3.5.8A) operated in fed-batch mode, at 34°C, with an organic loading rate of 5 g glycerol L⁻¹d⁻¹. A high organic loading rate was convenient to favor VFA production that could limit methanogenesis. It was also interesting in view of favoring fast growing glycerol fermenting bacteria. The mixed culture growth was estimated following the optical density of the liquid media and adjusting the curve to an exponential growth function. A duplication time of 7.3 h was estimated.

The growth of a glycerol fermenting community was to be evidenced by means of glycerol concentration analyses, VFA analyses and gas analyses. Hydrogen was produced throughout whereas methane was only detected during the first days of operation. No methanogenic activity was observed in the long term (more than three months operation). However a steady production of hydrogen was not reached. Regarding glycerol and 1,3-propanediol concentration, the results from HPLC were not consistent, but the analyses could not be repeated. Although both compounds were detected, mass balances were not matching and

therefore its use was ruled out. Acetic acid and propionic acid were also detected in the glycerol culture flasks, reaching high concentrations. The accumulation of these VFA dropped the pH of the system up to 4.5-5, allowing to keep under control methanogenic *archaea*. COD analyses at the beginning of the batch and at the end did not differ significantly, indicating that the substrate was being mainly fermented rather than totally oxidized to carbon dioxide. The fact that a wide range of metabolites was being detected in the analyses indicated that various metabolic routes from glycerol were taking place in the system, which seems coherent in a mixed culture.

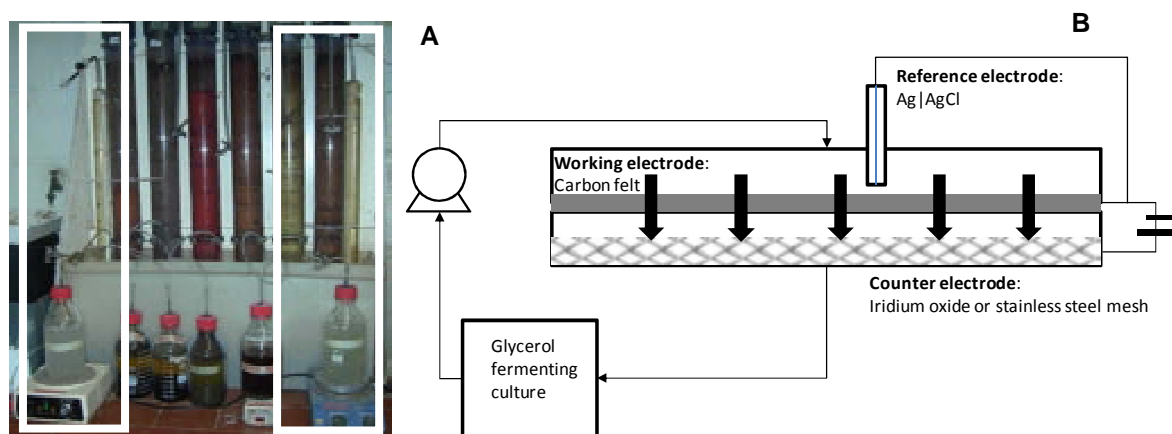


Figure 3.5.8. (A) Glycerol fed culture flasks connected to gas measuring cylinders. (B) Setup schematics during the inoculation of the carbon felt by filtration.

The effluent from the glycerol fed culture flasks was used to inoculate by filtration the carbon felt cathode. The inoculation process consisted in a so called filtration of 400 mL of glycerol fermenting culture through the brand new carbon felt (Figure 3.5.8B). Cell attachment on the carbon felt surface was evaluated using flow cytometry, which should allow the assessment of the decrease in cell count of the filtrate. The system setup during the inoculation was placed horizontally and lacked the CEM so that the media could freely flow from one chamber to the other. The media was continuously recycled to the system (50 mL min^{-1}) during the 2 h that the filtration lasted. The filtration time was chosen to avoid excessive cell growth, which would mask the cell attachment evaluation with flow cytometry.

The electrode was polarized at a different potential for each filtration test, expecting a difference in cell adherence by modifying the surface properties (duplicate tests performed). Polarization potentials tested were -570 mV, -250 mV, -100 mV, 100 mV, 500 mV and 800 mV vs. SHE. For those tests where the carbon felt was positively polarized the counter electrode was changed to a stainless steel mesh in order to avoid loss of electrocatalytic

activity of the iridium oxide electrode. A test without polarizing the electrode was performed as well. Figure 3.5.9A presents the cell count in the filtrate throughout the filtration normalized to the initial cell count for three of the tests (-570 mV, -100 mV and 100 mV vs. SHE). According to the results, it was observed that cell attachment was enhanced the most for a positively polarized cathode (100 mV), as can be inferred from the decrease of almost 90% in cell count in the cell suspension filtered. Polarizing the cathode at -100 mV allowed a decrease in cell count of 40%, whereas at -570 mV no cell attachment was evidenced. Oscillations could be a consequence of little differences in temperature and light conditions, which can affect flow cytometry output (Figure 3.5.9B), as well as possible cell growth during the 2 hours process, given that glycerol could still be available in the filtrating medium (coming from the glycerol fermenting culture flask). The fact that cell growth could still be possible strengthens the observation made for the filtration on the positively polarized cathode, where the cells were being trapped on the electrode regardless of any growth.

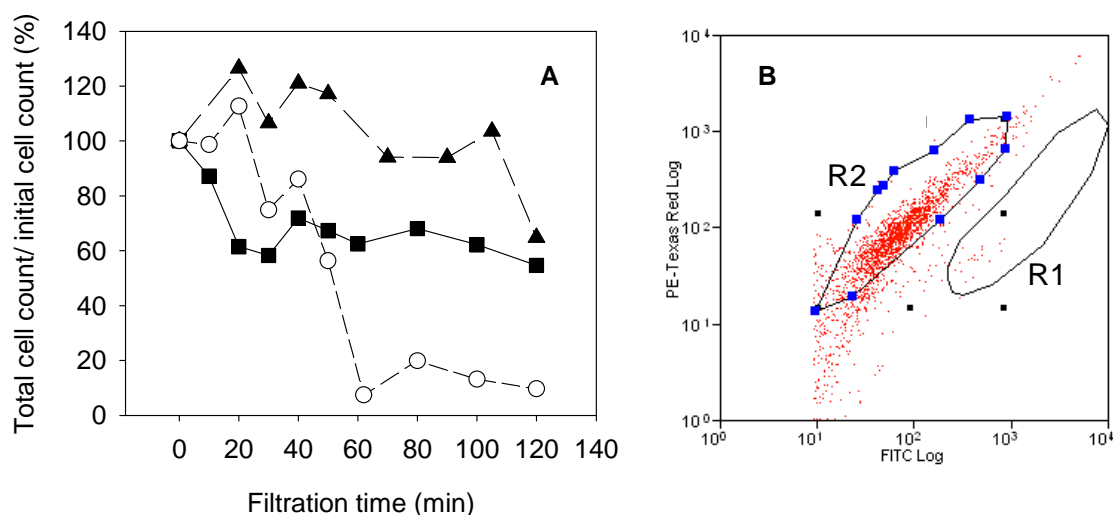


Figure 3.5.9. (A) Cell content in filtrate during the filtration normalized to initial cell count. Electrode polarized at: \blacktriangle -570, \blacksquare -100 and \circ 100 mV vs. SHE. (B) Example of flow cytometric analysis output, where R1 and R2 are the regions indicating live and dead cells respectively.

After the inoculation of the cathode by filtration of the glycerol fermenting community, both chambers were rinsed with demineralized water and the CEM was introduced in the setup, which was now placed vertically. The assembling time of the electrofermentation reactor was about one hour, in which the system was in open circuit conditions. Each chamber was respectively connected to the corresponding electrolyte with an ascendant flow. Two recirculation pumps continuously feeding the electrolyte to each chamber (50 mL min^{-1}) favored the homogeneity of the mixture.

The electrofermentation reactor (Figure 3.5.10) ran for 16 hours under galvanostatic mode fixing current intensity at -100 mA to favor the reductive process. Figure 3.5.11A shows the cathode potential reached at the end of this period at galvanostatic mode ($E_{we,ss}$), when a steady potential was achieved, for the different polarization conditions during inoculation. The results seemed to indicate that for a set current intensity $E_{we,ss}$ was less negative when the inoculation took place in a more positively polarized cathode, which might well be a consequence of being more biocatalysed. This would match with the aforementioned fact that more cells had been trapped on the electrode in the inoculation process as seen in Figure 3.5.9.

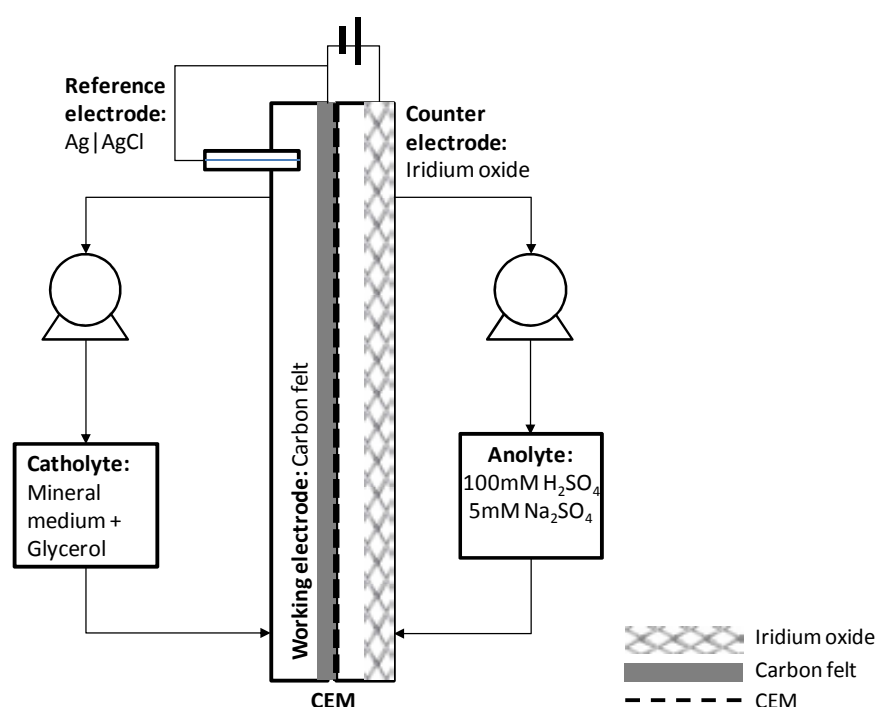


Figure 3.5.10. Schematics of the BES experimental setup for the electrofermentation of glycerol.

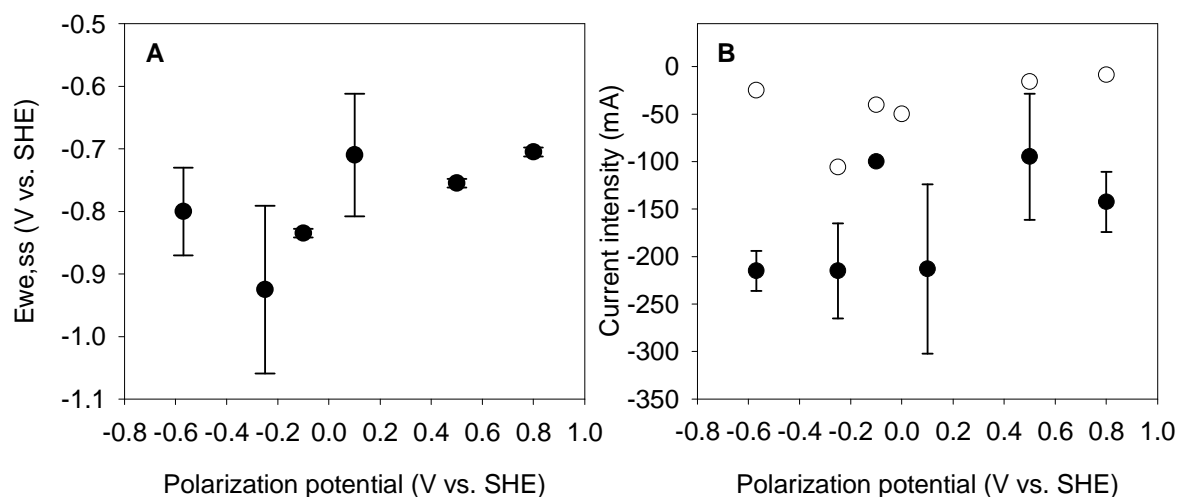


Figure 3.5.11. For different polarization potentials of the electrode during the inoculation: **A)** Potential of the working electrode at the steady state, $E_{we,ss}$ (current intensity set at -100mA) **B)** ● Current intensity (Working electrode potential set at 50mV lower than $E_{we,ss}$), ○ Current intensity for blank chronoamperometry (working electrode potentials set at the same values than the actual tests).

Once $E_{we,ss}$ had been assessed, the electrofermentation reactor stopped operating at galvanostatic mode, the catholyte was replaced by a fresh catholyte solution, and the reactor started to run under potentiostatic mode for 24 hours, setting a cathode potential 50 mV lower than $E_{we,ss}$ reached. Lowering the cathode potential the electron uptake by the microorganisms could be further favored, because higher energy gain for them would be possible and the driving force, i.e. the difference in potential, would increase. At the end of the period, a steady state current intensity (I_{ss}) was achieved. Figure 3.5.11B presents I_{ss} achieved in these conditions for the different polarization potentials during inoculation. In Figure 3.5.11B, I_{ss} are also compared to current intensities for a blank chronoamperometry test, where cathode potentials were set at the same values tested for the inoculated tests. For example, the cathode inoculated polarizing it at -0.57 V reached a $E_{we,ss}$ of -0.8 V on average; when it was operated under potentiostatic mode 50 mV lower, at -0.85 V, current intensity reached on average -220 mA, whereas the blank test with the cathode potential poised at -0.85 V reached -25 mA. It was observed that current intensities were higher (in absolute values) for a catalysed cathode than for a blank, and thus noncatalysed cathode. Low cathode potentials for noncatalysed cathodes could have evolved in hydrogen production whereas glycerol electrofermentation fermentation could have been the main process occurring in the system in those that were catalysed. Cathodic hydrogen production was detected for all tests, which was reasonable given the low electrode potentials.

Glycerol was in excess concentration throughout the 24 hours that the system was left under potentiostatic operation. Under these conditions an initial decrease in current intensity was observed and a steady response was achieved. Only in the case of a cathode inoculated polarizing the electrode at +100 mV a depletion of glycerol was inferred (Figure 3.5.12) (beginning the substrate limitation at 11 hours from the start). This showed that the observed current intensity response of the electrofermentation reactor was due to glycerol consumption. A coulombs balance confirmed that changes in current intensity were due to glycerol depletion (glycerol analysis was not possible). This was consistent with the fact that the cathode had been positively polarized during the filtration process and that more glycerol fermenting cells had been trapped on the cathode.

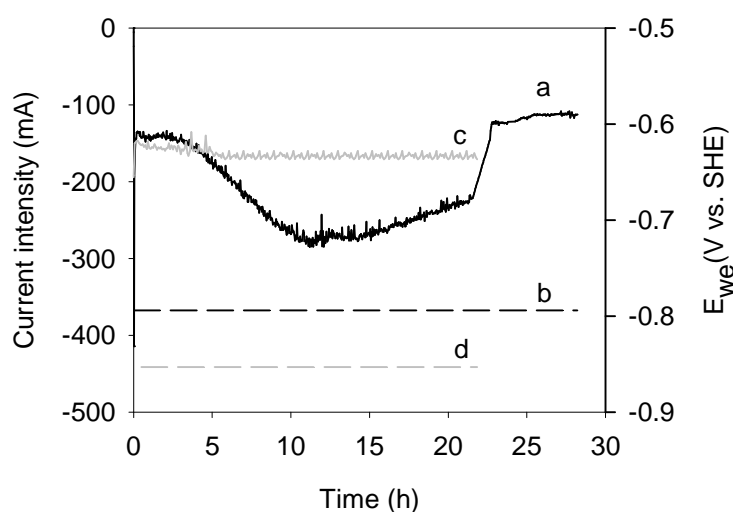


Figure 3.5.12. Current intensity response under potentiostatic operation for a cathode inoculated at +100 mV (line a) and the respective cathode potential (line b). Current intensity response under potentiostatic operation for a blank test (line c) and the respective cathode potential (line d).

During the batch tests performed, COD did not differ significantly at the beginning and at the end of the batch cycle, indicating that almost no organic matter was mineralized to carbon dioxide and hence that the fermentation conditions were favorable. VFA were not detected as opposed to the glycerol fed culture flasks. These observations could be a sign of the redirection of glycerol fermentation to a narrower range of metabolites, but the lack of glycerol and 1,3-propanediol data does not allow a clear vision of what was really occurring in the system.

Following the potentiostatic mode operation the catalytic activity of the cathodes inoculated at different electrode potentials was also explored by means of CV analyses. Change of catholyte or feeding glycerol prior to CV guaranteed substrate availability. Voltammograms are plotted in Figure 3.5.13 together with the electrode potential that allowed reaching -100

mA according to the analyses. A clear trend was not obtained and only the voltammogram for the blank test was consistent with the expected behaviour, reaching lower current intensities (in absolute value) than any other biotic system, which were supposed to be biocatalyzed. The open circuit potential of the cathode before the galvanostatic mode test started was also investigated. Higher cathodic OCP were expected for more biocatalyzed cathodes, however no clear differences were observed due to the high variability in results (Figure 3.5.14).

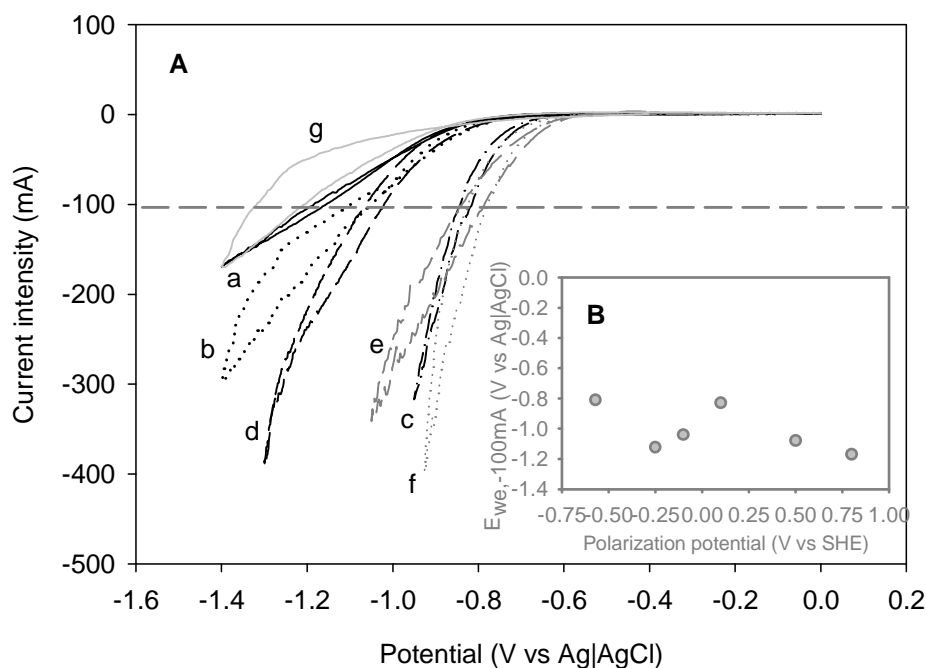


Figure 3.5.13. (A) Cyclic voltammograms (CVs) for the carbon felt inoculated at different polarization potentials: +800 mV (line a), +500 mV (line b), +100 mV (line c), -100 mV (line d), -570 mV (line e), non polarized filtration (line f) and blank test (line g). Dashed line cuts CVs at the potentials which achieve -100 mA current intensity (B) Average potentials that achieve -100 mA current intensity according to CVs.

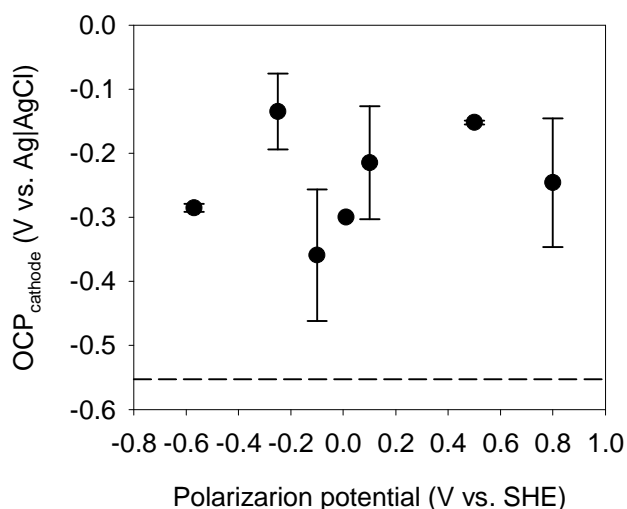


Figure 3.5.14. Cathodic OCP after the filtration at different polarization conditions. Dashed line indicated the cathodic OCP for the blank experiment.

The lack of repeatability in electrochemical analyses did not allow to conclude about the possible catalytic effects induced by the differences in the inoculation step. The variability observed could have been a consequence of the initial inoculum used, in which it could not be demonstrated that the glycerol fermenting culture had reached a steady state during all the experimental period.

5.4. Conclusions

Crude glycerol from the biodiesel industry wastewater often contains unreacted methanol from the esterification reaction. Methanol can be metabolized to acetate by acetogenic bacteria, which offered an opportunity to MFC to treat crude glycerol containing methanol. However, the use of crude glycerol containing methanol was constrained in MEC. Hydrogen produced in single chamber MEC was consumed by homoacetogenic bacteria leading to a hydrogen recycling situation, avoiding the possibility to have net hydrogen production. On the contrary, net hydrogen production from crude glycerol could be possible in a double chamber configuration regardless of the presence of methanol and methanol metabolizing bacteria. In fact, methanol could be effectively used as substrate in MEC in this configuration. In addition, in the double chamber MEC neither the build-up of methane or other hydrogen scavengers could limit the use of biodiesel industry wastewater.

Regarding methanol, it was proved to be a possible substrate for bioelectrochemical systems, both for power generation in single chamber MFC and for hydrogen production in MEC, which had never been reported before.

The electrofermentation of glycerol was explored as an alternative to hydrogen production in MEC from biodiesel industry wastewater. The enhancement of the inoculation step for a glycerol electrofermentation process was intended by initially polarizing the cathode. With the results observed in this study it could be hypothesized that the inoculation of non electroactive fermenting bacteria could be enhanced polarizing the cathode positively, which was supported by flow cytometry analyses and less negative cathode potentials ($E_{we,ss}$) that suggested more biocatalyzed cathodes. Current intensity was also observed to be related to glycerol consumption for a cathode positively polarized during the inoculation.

The redirection of glycerol fermentative pathways could not be demonstrated because of the inconsistency of glycerol and 1,3-propanediol analyses. Nevertheless a difference in the range of metabolites detected was observed when comparing the glycerol fed culture flasks and the electrofermentation reactor, inferring from this that a narrower range of fermentation pathways were being favored.

References for Part III: Results and Discussion

- (1) Chae, K.-J.; Choi, M.-J.; Kim, K.-Y.; Ajayi, F. F.; Park, W.; Kim, C.-W.; Kim, I. S. Methanogenesis control by employing various environmental stress conditions in two-chambered microbial fuel cells. *Bioresour. Technol.* 2010, *101*, 5350–5357.
- (2) Borole, A. P.; Hamilton, C. Y.; Vishnivetskaya, T. A. Enhancement in current density and energy conversion efficiency of 3-dimensional MFC anodes using pre-enriched consortium and continuous supply of electron donors. *Bioresour. Technol.* 2011, *102*, 5098–5104.
- (3) Wang, X.; Feng, Y.; Liu, J.; Lee, H.; Ren, N. Performance of a batch two-chambered microbial fuel cell operated at different anode potentials. *J. Chem. Technol. Biotechnol.* 2011, *86*, 590–594.
- (4) Jung, S.; Regan, J. M. Influence of external resistance on electrogenesis, methanogenesis, and anode prokaryotic communities in microbial fuel cells. *Appl. Environ. Microbiol.* 2011, *77*, 564–571.
- (5) Pinto, R. P.; Srinivasan, B.; Guiot, S. R.; Tartakovsky, B. The effect of real-time external resistance optimization on microbial fuel cell performance. *Water Res.* 2011, *45*, 1571–1578.
- (6) Premier, G. C.; Kim, J. R.; Michie, I.; Dinsdale, R. M.; Guwy, A. J. Automatic control of load increases power and efficiency in a microbial fuel cell. *J. Power Sources* 2011, *196*, 2013–2019.
- (7) Torres, C. I.; Krajmalnik-Brown, R.; Parameswaran, P.; Marcus, A. K.; Wanger, G.; Gorby, Y. A.; Rittmann, B. E. Selecting anode-respiring bacteria based on anode potential: Phylogenetic, electrochemical, and microscopic characterization. *Environ. Sci. Technol.* 2009, *43*, 9519–9524.
- (8) Logan, B. E.; Hamelers, B.; Rozendal, R.; Schröder, U.; Keller, J.; Freguia, S.; Aelterman, P.; Verstraete, W.; Rabaey, K. Microbial fuel cells: Methodology and technology. *Environ. Sci. Technol.* 2006, *40*, 5181–5192.
- (9) Schröder, U. Anodic electron transfer mechanisms in microbial fuel cells and their energy efficiency. *Phys. Chem. Chem. Phys.* 2007, *9*, 2619–2629.
- (10) Lyon, D. Y.; Buret, F.; Vogel, T. M.; Monier, J.-M. Is resistance futile? Changing external resistance does not improve microbial fuel cell performance. *Bioelectrochemistry* 2010, *78*, 2–7.
- (11) Zhang, L.; Zhu, X.; Li, J.; Liao, Q.; Ye, D. Biofilm formation and electricity generation of a microbial fuel cell started up under different external resistances. *J. Power Sources* 2011, *196*, 6029–6035.

-
- (12) Jung, S.; Regan, J. M. Influence of external resistance on electrogenesis, methanogenesis, and anode prokaryotic communities in microbial fuel cells. *Appl. Environ. Microbiol.* 2011, 77, 564–571.
- (13) Oh, S.; Min, B.; Logan, B. E. Cathode performance as a factor in electricity generation in microbial fuel cells. *Environ. Sci. Technol.* 2004, 38, 4900–4904.
- (14) Freguia, S.; Rabaey, K.; Yuan, Z.; Keller, J. Non-catalyzed cathodic oxygen reduction at graphite granules in microbial fuel cells. *Electrochim. Acta* 2007, 53, 598–603.
- (15) Logan, B. E.; Cheng, S.; Watson, V.; Estadt, G. Graphite Fiber Brush Anodes for Increased Power Production in Air-Cathode Microbial Fuel Cells. - *Environ. Sci. Technol.* 2007, 41, 3341–3346.
- (16) Liu, H.; Logan, B. E. Electricity generation using an air-cathode single chamber microbial fuel cell in the presence and absence of a proton exchange membrane. *Environ. Sci. Technol.* 2004, 38, 4040–4046.
- (17) Oh, S. E.; Kim, J. R.; Joo, J. H.; Logan, B. E. Effects of applied voltages and dissolved oxygen on sustained power generation by microbial fuel cells. *Water Sci. Technol.* 2009, 60, 1311–1317.
- (18) Ahmed, J.; Kim, S.-H. Effect of Cathodic Biofilm on the Performance of Air-Cathode Single Chamber Microbial Fuel Cells. *Bull. Korean Chem. Soc.* 2011, 32, 3726–3729.
- (19) Harnisch, F.; Schröder, U. Selectivity versus mobility: Separation of anode and cathode in microbial bioelectrochemical systems. *ChemSusChem* 2009, 2, 921–926.
- (20) Cheng, S.; Liu, H.; Logan, B. E. Increased performance of single-chamber microbial fuel cells using an improved cathode structure. *Electrochem. commun.* 2006, 8, 489–494.
- (21) Bergel, A.; Féron, D.; Mollica, A. Catalysis of oxygen reduction in PEM fuel cell by seawater biofilm. *Electrochem. commun.* 2005, 7, 900–904.
- (22) Cristiani, P.; Carvalho, M. L.; Guerrini, E.; Daghighi, M.; Santoro, C.; Li, B. Cathodic and anodic biofilms in Single Chamber Microbial Fuel Cells. *Bioelectrochemistry* 2013, 92, 6–13.
- (23) Chung, K.; Fujiki, I.; Okabe, S. Effect of formation of biofilms and chemical scale on the cathode electrode on the performance of a continuous two-chamber microbial fuel cell. *Bioresour. Technol.* 2011, 102, 355–360.
- (24) Pinto, R. P.; Srinivasan, B.; Guiot, S. R.; Tartakovsky, B. The effect of real-time external resistance optimization on microbial fuel cell performance. *Water Res.* 2011, 45, 1571–1578.

-
- (25) Aelterman, P.; Freguia, S.; Keller, J.; Verstraete, W.; Rabaey, K. The anode potential regulates bacterial activity in microbial fuel cells. *Appl. Microbiol. Biotechnol.* 2008, 78, 409–418.
- (26) Lalaurette, E.; Thammannagowda, S.; Mohagheghi, A.; Maness, P.-C.; Logan, B. E. Hydrogen production from cellulose in a two-stage process combining fermentation and electrohydrogenesis. *Int. J. Hydrogen Energy* 2009, 34, 6201–6210.
- (27) Gómez, X.; Fernández, C.; Fierro, J.; Sánchez, M. E.; Escapa, A.; Morán, A. Hydrogen production: Two stage processes for waste degradation. *Bioresour. Technol.* 2011, 102, 8621–8627.
- (28) Velasquez-Orta, S. B.; Yu, E.; Katuri, K. P.; Head, I. M.; Curtis, T. P.; Scott, K. Evaluation of hydrolysis and fermentation rates in microbial fuel cells. *Appl. Microbiol. Biotechnol.* 2011, 90, 789–798.
- (29) Cheng, S.; Kiely, P.; Logan, B. E. Pre-acclimation of a wastewater inoculum to cellulose in an aqueous-cathode MEC improves power generation in air-cathode MFCs. *Bioresour. Technol.* 2011, 102, 367–371.
- (30) Sun, D.; Call, D. F.; Kiely, P. D.; Wang, A.; Logan, B. E. Syntrophic interactions improve power production in formic acid fed MFCs operated with set anode potentials or fixed resistances. *Biotechnol. Bioeng.* 2012, 109, 405–414.
- (31) Lu, N.; Zhou, S.; Zhuang, L.; Zhang, J.; Ni, J. Electricity generation from starch processing wastewater using microbial fuel cell technology. *Biochem. Eng. J.* 2009, 43, 246–251.
- (32) Herrero-Hernandez, E.; Smith, T. J.; Akid, R. Electricity generation from wastewaters with starch as carbon source using a mediatorless microbial fuel cell. *Biosens. Bioelectron.* 2013, 39, 194–198.
- (33) Ghosh, S.; Chatterjee, S.; Chatterjee, M.; Ghosh, S.; Basumallick, I. N. A Microbial Fuel Cell for Starch Oxidation. *ECS Trans.* 2012, 41, 37–43.
- (34) Nimje, V. R.; Chen, C.-Y.; Chen, C.-C.; Chen, H.-R.; Tseng, M.-J.; Jean, J.-S.; Chang, Y.-F. Glycerol degradation in single-chamber microbial fuel cells. *Bioresour. Technol.* 2011, 102, 2629–2634.
- (35) Escapa, A.; Manuel, M.-F.; Morán, A.; Gómez, X.; Guiot, S. R.; Tartakovsky, B. Hydrogen production from glycerol in a membraneless microbial electrolysis cell. *Energy and Fuels* 2009, 23, 4612–4618.
- (36) Reiche, A.; Kirkwood, K. M. Comparison of *Escherichia coli* and anaerobic consortia derived from compost as anodic biocatalysts in a glycerol-oxidizing microbial fuel cell. *Bioresour. Technol.* 2012, 123, 318–323.
- (37) Chignell, J. F.; Liu, H. Biohydrogen production from glycerol in microbial electrolysis cells and prospects for energy recovery from biodiesel wastes. In *ASME 2011*

- International Manufacturing Science and Engineering Conference, MSEC 2011*; 2011; Vol. 1, pp. 693–701.
- (38) Montpart, N.; Ribot-Llobet, E.; Garlapati, V. K.; Rago, L.; Baeza, J. A.; Guisasola, A. Methanol opportunities for electricity and hydrogen production in bioelectrochemical systems. *Int. J. Hydrogen Energy* 2014, *39*, 770–777.
- (39) Song, T.-S.; Wu, X.-Y.; Zhou, C. C. Effect of different acclimation methods on the performance of microbial fuel cells using phenol as substrate. *Bioprocess Biosyst. Eng.* 2014, *37*, 133–138.
- (40) Mahmoud, M.; Parameswaran, P.; Torres, C. I.; Rittmann, B. E. Fermentation pretreatment of landfill leachate for enhanced electron recovery in a microbial electrolysis cell. *Bioresour. Technol.* 2014, *151*, 151–158.
- (41) Escapa, A.; Gil-Carrera, L.; García, V.; Morán, A. Performance of a continuous flow microbial electrolysis cell (MEC) fed with domestic wastewater. *Bioresour. Technol.* 2012, *117*, 55–62.
- (42) Heidrich, E. S.; Dolfing, J.; Scott, K.; Edwards, S. R.; Jones, C.; Curtis, T. P. Production of hydrogen from domestic wastewater in a pilot-scale microbial electrolysis cell. *Appl. Microbiol. Biotechnol.* 2013, *97*, 6979–6989.
- (43) Mardanpour, M. M.; Nasr Esfahany, M.; Behzad, T.; Sedaqatvand, R. Single chamber microbial fuel cell with spiral anode for dairy wastewater treatment. *Biosens. Bioelectron.* 2012, *38*, 264–269.
- (44) Elakkiya, E.; Matheswaran, M. Comparison of anodic metabolisms in bioelectricity production during treatment of dairy wastewater in Microbial Fuel Cell. *Bioresour. Technol.* 2013, *136*, 407–412.
- (45) Cusick, R.; Bryan, B.; Parker, D.; Merrill, M.; Mehanna, M.; Kiely, P.; Liu, G.; Logan, B. Performance of a pilot-scale continuous flow microbial electrolysis cell fed winery wastewater. *Appl. Microbiol. Biotechnol.* 2011, *89*, 2053–2063.
- (46) Feng, Y.; Yang, Q.; Wang, X.; Liu, Y.; Lee, H.; Ren, N. Treatment of biodiesel production wastes with simultaneous electricity generation using a single-chamber microbial fuel cell. *Bioresour. Technol.* 2011, *102*, 411–415.
- (47) Ribot-Llobet, E.; Montpart, N.; Ruiz-Franco, Y.; Rago, L.; Lafuente, J.; Baeza, J. A.; Guisasola, A. Obtaining microbial communities with exoelectrogenic activity from anaerobic sludge using a simplified procedure. *J. Chem. Technol. Biotechnol.* 2013, DOI: 10.1002/jctb.4252.
- (48) Liu, H.; Grot, S.; Logan, B. E. Electrochemically assisted microbial production of hydrogen from acetate. *Environ. Sci. Technol.* 2005, *39*, 4317–4320.

- (49) Rozendal, R.; Hamelers, H.; Euverink, G.; Metz, S.; Buisman, C. Principle and perspectives of hydrogen production through biocatalyzed electrolysis. *Int. J. Hydrogen Energy* 2006, *31*, 1632–1640.
- (50) Call, D.; Logan, B. E. Hydrogen production in a single chamber microbial electrolysis cell lacking a membrane. *Environ. Sci. Technol.* 2008, *42*, 3401–3406.
- (51) Hu, H.; Fan, Y.; Liu, H. Hydrogen production using single-chamber membrane-free microbial electrolysis cells. *Water Res.* 2008, *42*, 4172–4178.
- (52) Nam, J.-Y.; Tokash, J. C.; Logan, B. E. Comparison of microbial electrolysis cells operated with added voltage or by setting the anode potential. *Int. J. Hydrogen Energy* 2011, *36*, 10550–10556.
- (53) Tartakovsky, B.; Mehta, P.; Santoyo, G.; Guiot, S. R. Maximizing hydrogen production in a microbial electrolysis cell by real-time optimization of applied voltage. *Int. J. Hydrogen Energy* 2011, *36*, 10557–10564.
- (54) Fricke, K.; Harnisch, F.; Schroder, U. On the use of cyclic voltammetry for the study of anodic electron transfer in microbial fuel cells. *Energy Environ. Sci.* 2008, *1*, 144–147.
- (55) Liu, Z.; Liu, J.; Zhang, S.; Su, Z. Study of operational performance and electrical response on mediator-less microbial fuel cells fed with carbon- and protein-rich substrates. *Biochem. Eng. J.* 2009, *45*, 185–191.
- (56) Heilmann, J.; Logan, B. E. Production of electricity from proteins using a microbial fuel cell. *Water Environ. Res.* 2006, *78*, 531–537.
- (57) Esteve-Núñez, A.; Rothermich, M.; Sharma, M.; Lovley, D. Growth of *Geobacter sulfurreducens* under nutrient-limiting conditions in continuous culture. *Environ. Microbiol.* 2005, *7*, 641–648.
- (58) Kato Marcus, A.; Torres, C. I.; Rittmann, B. E. Conduction-based modeling of the biofilm anode of a microbial fuel cell. *Biotechnol. Bioeng.* 2007, *98*, 1171–1182.
- (59) Parameswaran, P.; Torres, C. I.; Lee, H. S.; Krajmalnik-Brown, R.; Rittmann, B. E. Syntrophic interactions among anode respiring bacteria (ARB) and Non-ARB in a biofilm anode: electron balances. *Biotechnol. Bioeng.* 2009, *103*, 513–523.
- (60) Parameswaran, P.; Zhang, H.; Torres, C. I.; Rittmann, B. E.; Krajmalnik-Brown, R. Microbial community structure in a biofilm anode fed with a fermentable substrate: the significance of hydrogen scavengers. *Biotechnol. Bioeng.* 2010, *105*, 69–78.
- (61) Balmant, W.; Oliveira, B. H.; Mitchell, D. A.; Vargas, J. V. C.; Ordonez, J. C. Optimal operating conditions for maximum biogas production in anaerobic bioreactors. *Appl. Therm. Eng.* 2014, *62*, 197–206.

- (62) Wang, A.; Liu, W.; Cheng, S.; Xing, D.; Zhou, J.; Logan, B. E. Source of methane and methods to control its formation in single chamber microbial electrolysis cells. *Int. J. Hydrogen Energy* 2009, *34*, 3653–3658.
- (63) Rader, G. K.; Logan, B. E. Multi-electrode continuous flow microbial electrolysis cell for biogas production from acetate. *1st Iran. Conf. Hydrog. Fuel Cell* 2010, *35*, 8848–8854.
- (64) Liu, H.; Wang, J.; Wang, A.; Chen, J. Chemical inhibitors of methanogenesis and putative applications. *Appl. Microbiol. Biotechnol.* 2011, *89*, 1333–1340.
- (65) Nollet, L.; Demeyer, D.; Verstraete, W. Effect of 2-bromoethanesulfonic acid and *Peptostreptococcus productus* ATCC 35244 addition on stimulation of reductive acetogenesis in the ruminal ecosystem by selective inhibition of methanogenesis. *Appl. Environ. Microbiol.* 1997, *63*, 194–200.
- (66) Chae, K.-J.; Choi, M.-J.; Kim, K.-Y.; Ajayi, F. F.; Chang, I.-S.; Kim, I. S. Selective inhibition of methanogens for the improvement of biohydrogen production in microbial electrolysis cells. *3rd Asian Bio Hydrog. Symp.* 2010, *35*, 13379–13386.
- (67) Parameswaran, P.; Torres, C. I.; Lee, H.-S.; Rittmann, B. E.; Krajmalnik-Brown, R. Hydrogen consumption in microbial electrochemical systems (MXCs): The role of homo-acetogenic bacteria. *Spec. Issue Biofuels - II Algal Biofuels Microb. Fuel Cells* 2011, *102*, 263–271.
- (68) Ajayi, F. F.; Kim, K.-Y.; Chae, K.-J.; Choi, M.-J.; Kim, I. S. Effect of hydrodynamic force and prolonged oxygen exposure on the performance of anodic biofilm in microbial electrolysis cells. *Int. J. Hydrogen Energy* 2010, *35*, 3206–3213.
- (69) Lee, H.-S.; Torres, C. I.; Parameswaran, P.; Rittmann, B. E. Fate of H₂ in an upflow single-chamber microbial electrolysis cell using a metal-catalyst-free cathode. *Environ. Sci. Technol.* 2009, *43*, 7971–7976.
- (70) Smith, M. R. Reversal of 2-bromoethanesulfonate inhibition of methanogenesis in *Methanosarcina* sp. *J. Bacteriol.* 1983, *156*, 516–523.
- (71) Santoro, N.; Konisky, J. Characterization of bromoethanesulfonate-resistant mutants of *Methanococcus voltae*: Evidence of a coenzyme M transport system. *J. Bacteriol.* 1987, *169*, 660–665.
- (72) Immig, I.; Demeyer, D.; Fiedler, D.; Van Nevel, C.; Mbanzamihiho, L. Attempts to induce reductive acetogenesis into a sheep rumen. *Arch. Anim. Nutr. fur Tierernahrung* 1996, *49*, 363–370.
- (73) De Graeve, K. G.; Grivet, J. P.; Durand, M.; Beaumatin, P.; Demeyer, D. NMR study of ¹³CO₂ incorporation into short-chain fatty acids by pig large-intestinal flora. *Can. J. Microbiol.* 1990, *36*, 579–582.

- (74) Batstone, D. J.; Keller, J.; Newell, R. B.; Newland, M. Modelling anaerobic degradation of complex wastewater. I: model development. *Bioresour. Technol.* 2000, 75, 67–74.
- (75) Parameswaran, P.; Torres, C. I.; Kang, D.-W.; Rittmann, B. E.; Krajmalnik-Brown, R. The role of homoacetogenic bacteria as efficient hydrogen scavengers in microbial electrochemical cells (MXCs). *Water Sci. Technol.* 2012, 65, 1–6.
- (76) Ruiz, Y.; Baeza, J. A.; Guisasola, A. Revealing the proliferation of hydrogen scavengers in a single-chamber microbial electrolysis cell using electron balances (Submitted), 2013.
- (77) Ruiz, Y.; Baeza, J. A.; Guisasola, A. Revealing the proliferation of hydrogen scavengers in a single-chamber microbial electrolysis cell using electron balances. *Int. J. Hydrogen Energy* 2013, 38, 15917–15927.
- (78) Selembo, P. A.; Perez, J. M.; Lloyd, W. A.; Logan, B. E. Enhanced hydrogen and 1,3-propanediol production from glycerol by fermentation using mixed cultures. *Biotechnol. Bioeng.* 2009, 104, 1098–1106.
- (79) Lu, L.; Xing, D.; Xie, T.; Ren, N.; Logan, B. E. Hydrogen production from proteins via electrohydrogenesis in microbial electrolysis cells. *Biosens. Bioelectron.* 2010, 25, 2690–2695.
- (80) Ditzig, J.; Liu, H.; Logan, B. Production of hydrogen from domestic wastewater using a bioelectrochemically assisted microbial reactor (BEAMR). *Int. J. Hydrogen Energy* 2007, 32, 2296–2304.
- (81) Gil-Carrera, L.; Escapa, A.; Mehta, P.; Santoyo, G.; Guiot, S. R.; Morán, A.; Tartakovsky, B. Microbial electrolysis cell scale-up for combined wastewater treatment and hydrogen production. *Bioresour. Technol.* 2013, 130, 584–591.
- (82) Selembo, P. A.; Perez, J. M.; Lloyd, W. A.; Logan, B. E. High hydrogen production from glycerol or glucose by electrohydrogenesis using microbial electrolysis cells. *Int. J. Hydrogen Energy* 2009, 34, 5373–5381.
- (83) Scholes, C. A.; Stevens, G. W.; Kentish, S. E. Membrane gas separation applications in natural gas processing. *Fuel* 2012, 96, 15–28.
- (84) Logan, B. E.; Oh, S.-E.; Kim, I. S.; Van Ginkel, S. Biological Hydrogen Production Measured in Batch Anaerobic Respirometers. *Environ. Sci. Technol.* 2002, 36, 2530–2535.
- (85) Datar, R.; Huang, J.; Maness, P.; Mohagheghi, A.; Czernik, S.; Chornet, E. Hydrogen production from the fermentation of corn stover biomass pretreated with a steam-explosion process. *Int. J. Hydrogen Energy* 2007, 32, 932–939.

- (86) Ambler, J. R.; Logan, B. E. Evaluation of stainless steel cathodes and a bicarbonate buffer for hydrogen production in microbial electrolysis cells using a new method for measuring gas production. *Int. J. Hydrogen Energy* 2011, *36*, 160–166.
- (87) Babu, M. L.; Subhash, G. V.; Sarma, P. N.; Mohan, S. V. Bio-electrolytic conversion of acidogenic effluents to biohydrogen: an integration strategy for higher substrate conversion and product recovery. *Bioresour. Technol.* 2013, *133*, 322–331.
- (88) Gueguim Kana, E. B.; Schmidt, S.; Azanfack Kenfack, R. H. A web-enabled software for real-time biogas fermentation monitoring – Assessment of dark fermentations for correlations between medium conductivity and biohydrogen evolution. *Int. J. Hydrogen Energy* 2013, *38*, 10235–10244.
- (89) Strahl, S.; Husar, A.; Riera, J. Experimental study of hydrogen purge effects on performance and efficiency of an open-cathode Proton Exchange Membrane fuel cell system. *J. Power Sources* 2014, *248*, 474–482.
- (90) U.S. Department of Energy, E. E. F. C. T. P.
http://www1.eere.energy.gov/hydrogenandfuelcells/fuelcells/pdfs/fc_comparison_chart.pdf.
- (91) De Bruijn, F. A.; Papageorgopoulos, D. C.; Sitters, E. F.; Janssen, G. J. M. The influence of carbon dioxide on PEM fuel cell anodes. *J. Power Sources* 2002, *110*, 117–124.
- (92) Janssen, G. J. M. Modelling study of CO₂ poisoning on PEMFC anodes. *J. Power Sources* 2004, *136*, 45–54.
- (93) Yan, W.-M.; Chu, H.-S.; Lu, M.-X.; Weng, F.-B.; Jung, G.-B.; Lee, C.-Y. Degradation of proton exchange membrane fuel cells due to CO and CO₂ poisoning. *J. Power Sources* 2009, *188*, 141–147.
- (94) Rabaey, K.; Rozendal, R. A. Microbial electrosynthesis - revisiting the electrical route for microbial production. *Nat. Rev. Microbiol.* 2010, *8*, 706–716.
- (95) Nevin, K. P.; Woodard, T. L.; Franks, A. E.; Summers, Z. M.; Lovley, D. R. Microbial electrosynthesis: feeding microbes electricity to convert carbon dioxide and water to multicarbon extracellular organic compounds. *MBio* 2010, *1*.
- (96) Dennis, P. G.; Harnisch, F.; Yeoh, Y. K.; Tyson, G. W.; Rabaey, K. Dynamics of cathode-associated microbial communities and metabolite profiles in a glycerol-fed bioelectrochemical system. *Appl. Environ. Microbiol.* 2013, *79*, 4008–4014.
- (97) Marshall, C. W.; Ross, D. E.; Fichot, E. B.; Norman, R. S.; May, H. D. Long-term operation of microbial electrosynthesis systems improves acetate production by autotrophic microbiomes. *Environ. Sci. Technol.* 2013, *47*, 6023–6029.

- (98) Steinbusch, K. J. J.; Hamelers, H. V. M.; Plugge, C. M.; Buisman, C. J. N. Biological formation of caproate and caprylate from acetate: fuel and chemical production from low grade biomass. *Energy Environ. Sci.* 2011, *4*, 216.
- (99) Choi, O.; Um, Y.; Sang, B.-I. Butyrate production enhancement by *Clostridium tyrobutyricum* using electron mediators and a cathodic electron donor. *Biotechnol. Bioeng.* 2012, *109*, 2494–2502.
- (100) Desloover, J.; Arends, J. B.; Hennebel, T.; Rabaey, K. Operational and technical considerations for microbial electrosynthesis. *Biochem. Soc. Trans.* 2012, *40*, 1233–1238.
- (101) Diekert, G. Metabolism of homoacetogens. *Antonie Van Leeuwenhoek* 1994, *66*, 209–221.
- (102) Heijthuijsen, J. H. F. G. Interspecies hydrogen transfer in co-cultures of methanol-utilizing acidogens and sulfate-reducing or methanogenic bacteria. *FEMS Microbiol. Lett.* 1986, *38*, 57–64.
- (103) Kim, J. R.; Jung, S. H.; Regan, J. M.; Logan, B. E. Electricity generation and microbial community analysis of alcohol powered microbial fuel cells. *Bioresource Technology*, 2007, *98*, 2568–2577.

Part IV: General Conclusions and Future Perspectives

This last section gives an overview of the main achievements of this work and points out the topics for future research derived from this thesis.

Studies with single chamber microbial fuel cells and microbial electrolysis cells with mixed cultures were performed to investigate on those aspects that can favor a future scale-up of this technology.

Inoculation in MFC

Favoring conditions throughout the inoculation process improve the anodic biofilm development and electroactivity. Maintenance of anaerobic conditions and the electrode potential have a key role in this process. In this regard it can be stated that:

- The area of cathode is an important design parameter in air-cathode microbial fuel cells. When it has been overdimensioned excessive oxygen diffusion can decrease the system performance in terms of coulombic efficiency. Nevertheless, in such a dynamic system, the optimum area of cathode can vary according to the anodic biofilm growth.
- The cathodic biofilm that grows on air-cathode microbial fuel cells prevents oxygen intrusion into the anode surroundings improving the cell performance in terms of coulombic efficiency. No catalytic effects on the oxygen reduction can be attributed to this biofilm. Overpotential related to protons diffusion might exceed the possible catalytic effects of the biofilm.
- Inoculation at high external resistance stimulates the growth at low anode potentials enhancing the electroactivity of the system. A general inoculation procedure consisting in a first inoculation at high external resistance and a later shift to a low resistance can be generally applied.

The pH profile in the cathodic biofilm could reveal the origin of the increase in cathodic overpotential when the cathodic biofilm has grown.

Methanogenesis control

Methanogens and hydrogen scavengers proliferation is the main drawback in single chamber MEC configuration. With regard to strategies that decrease the hydrogen

retention time to control the growth and activity of these populations it can be stated that:

- Net hydrogen production in single chamber MEC is restrained by hydrogen scavengers that favor the conversion of hydrogen to methane or cause the hydrogen recycling phenomena.
- The reduction of hydrogen retention time by nitrogen sparging delays the growth of methanogenic archaea, prolonging the effects of 2-bromoethanesulfonate.
- Hydrogen oxidizing ARB and homoacetogens cannot be active if hydrogen is continuously stripped along with nitrogen, however acetoclastic methanogens are still active.

Continuous operation of single chamber MEC should be tested with nitrogen sparging strategy to keep under control hydrogen scavengers.

Operational improvements

Operational improvements concerning instrumentation and control can ease the scale-up and future implementation of bioelectrochemical systems. In view of online hydrogen monitoring it can be stated that:

- Hydrogen production can be monitored online using a low-cost fuel cell with the same precision as gas chromatography. Hydrogen relative composition can be measured coupling a flow-meter to measure the total gas volume produced.

A control strategy could be implemented using the fuel cell and a flow-meter as measuring instruments and the supply of nitrogen as control action, where sparging time could be controlled according to the system performance in terms of hydrogen composition in the gas. The development of the MEC mathematical model would allow testing control strategies to optimize the process at lab scale.

Hydrogen leakages are a big limitation of hydrogen producing microbial electrolysis cells. Big efforts should be made to improve gas tightness. Fast use or storing could diminish hydrogen losses.

Opportunities of different substrates in single chamber MEC

For practical implementation of bioelectrochemical systems to treat wastewater, the study of the potential of substrates with different biodegradability is essential. Concerning the opportunities of different substrates in single chamber MEC it can be stated that:

- Different substrates imply different growth trends for methanogenic archaea in MEC. Milk derivatives limited the growth of methanogenic archaea for the longest period.
- Crude glycerol from the biodiesel industry often contains methanol, which enhances the hydrogen recycling phenomena in single chamber MEC and avoids net hydrogen production.
- Codegradation of multiple substrates enhances power output and COD removal in single chamber MFC. In single chamber MEC higher current intensity, hydrogen production and gas recovery than for single substrates are obtained.
- Microbial electrofermentation offers an alternative to hydrogen production in MEC.

The opportunities for real dairy wastewater should be tested in single chamber MEC to confirm its potential to produce hydrogen without methanogenic archaea proliferation.

Part V: Appendix

Appendix A: Code of the mathematical model for MEC

```

function MEC1_continuous_sparging
clear, close all

%Initial values (molar concentration) -----
EA0=0.1/200; EH0=0.1/200; MH0=0.1/200; MA0=0.1/200; HA0=0.1/200;
A0=2/60; H0=0; CH40=0; CO20=0.05; HG0=0; CH4G0=0; CO2G0=0;
opcions=odeset('AbsTol', 1e-10, 'RelTol',1e-5);

% Differential equations resolution -----
[t,y]=ode45(@fmec,[0 7],[EA0 EH0 MH0 MA0 HA0 A0 H0 CH40 CO20 HG0 CH4G0 CO2G0],
opcions);

y(end,6)=y(end,6)+2/60; %Acetate addition at day 7-----
[t2,y2]=ode45(@fmec,[7 10],y(end,:),opcions);

y2(end,7)=0; %hydrogen stripping with nitrogen sparging at day 10-----
y2(end,8)=0; % methane stripping with nitrogen sparging
[t3,y3]=ode45(@fmec_N2continuous,[10 20],y2(end,:),opcions);
t=[t;t2;t3];
y=[y;y2;y3];
xlswrite('y_continuous_spargingN2',y)
xlswrite('t_continuous_spargingN2',t)

% graphs-----
% figure(1)
subplot(2,1,1)
plot(t,y(:,1:5))
%legend('EA','EH','MH','MA','HA','location','best');
legend('ARB','H2-oxidizer ARB','Hydrogenotrophic methanogens','Acetoclastic
methanogens','Homoacetogens','location','best');
xlabel('Time (d)'); ylabel('Biomass concentration (mol X/L)'); grid;
% figure(2)
subplot(2,1,2)
plot(t,y(:,6:9))
%legend('A','H','CH4','CO2','location','best');
legend('CH3COO-','H2','CH4','CO2','location','best');
xlabel('Time (d)'); ylabel('Concentration liquid phase (mol/L)'); grid;axis([0 20 0 0.1])
% figure(3)
% plot(t,y(:,10:12))
% legend('H','CH4','CO2','location','best');
% xlabel('Time (d)'); ylabel('Concentration gas phase'); grid;

% Equations-----
function dydt=fmec(t,y)
EA=y(1); %ARB (acetate --> H2): CH3COO- + 4 H2O --> 2 HCO3- + 9 H+ + 8e-
EH=y(2); %H2-oxidizing bacteria (H2 --> H2): H2-->2H+ + 2e- --> H2
MH=y(3); %hydrogenotrophic methanogens (H2 --> CH4): 4H2 + CO2 --> CH4 + 2H2O
MA=y(4); %acetoclastic methanogens (acetate --> CH4): CH3COOH --> CH4 + CO2
HA=y(5); %homoacetogenic bacteria (H2 --> acetate):
% HCO3- + 2H2 + 0.5H+ --> 0.5CH3COO- + 2H2O
A=y(6); %acetate
H=y(7); %hydrogen in solution
CH4=y(8); %methane in solution
CO2=y(9); %CO2 in solution
HG=y(10); %H2 in gas phase
CH4G=y(11); %CH4 in gas phase

```

$CO_2G=y(12)$; %CO₂ in gas phase
 % maximum growth rate
 $\mu_{EAmax}=0.132$; %mmol/mgX·d
 $\mu_{EHmax}=\mu_{EAmax}$; $\mu_{MHmax}=\mu_{EAmax}$; $\mu_{MAmax}=\mu_{EAmax}$;
 $\mu_{HAmax}=0$;
 % half saturation constant
 $K_{sEA}=3e-5$; %mmol/cm³, mol/L
 $K_{sMH}=40e-6$; %mol/L 1-80 micromol/L
 $K_{sEH}=K_{sMH}$; %mol/L
 $K_{sMA}=4e-3$; %mol/L 0.85-7 mmol/L
 $K_{sHA}=K_{sMA}$;
 $K_{sCO_2}=0.01$;
 $MoCO_2=CO_2/(K_{sCO_2}+CO_2)$;
 % Monod, specific growth rate
 $\mu_{EA}=\mu_{EAmax} \cdot A/(K_{sEA}+A) \cdot MoCO_2$; $\mu_{EH}=\mu_{EHmax} \cdot H/(K_{sEH}+H) \cdot MoCO_2$;
 $\mu_{MH}=\mu_{MHmax} \cdot H/(K_{sMH}+H) \cdot MoCO_2$; $\mu_{MA}=\mu_{MAmax} \cdot A/(K_{sMA}+A) \cdot MoCO_2$;
 $\mu_{HA}=\mu_{HAmax} \cdot A/(K_{sHA}+A) \cdot MoCO_2$;
 % decay rate
 $b_{EA}=0.05$; $b_{EH}=b_{EA}$; $b_{MH}=b_{EA}$; $b_{MA}=b_{EA}$; $b_{HA}=b_{EA}$;
 % Biomass- substrate yield
 $Y_{EA}=0.05$; $Y_{EH}=0.05$; $Y_{MH}=0.05$; $Y_{MA}=0.05$; $Y_{HA}=0.05$; %mol biomasa/mol substrat
 % Stoichiometry
 $Y_{EAH}=4$; %mol H₂/mol A
 $Y_{EHH}=1$; %mol H₂/mol H₂
 $Y_{MHCH_4}=1/4$; %mol CH₄/mol H₂
 $Y_{MACH_4}=1$; %mol meta/mol acetate
 $Y_{HAA}=1/4$; %mol acetat/mol H₂
 $Y_{EACO_2}=2$; %mol CO₂/mol acetate
 $Y_{MHCO_2}=1/4$; %mol CO₂/mol H₂
 $Y_{MACO_2}=1$; %mol CO₂/mol acetate
 $Y_{HACO_2}=1/2$; %mol CO₂/mol H₂
 % Mass transport coefficients
 $k_{LaH_2}=0.0$;
 $k_{LaCH_4}=0.0$;
 $k_{LaCO_2}=0.0$;
 % Concentration in liquid interphase
 $HG_x=HG \cdot 0.01$;
 $CH_4G_x=CH_4G \cdot 0.01$;
 $CO_2G_x=CO_2G \cdot 0.01$;
 % Differential equations
 $dydt=zeros(9,1)$;
 $dydt(1)=\mu_{EA} \cdot EA - b_{EA} \cdot EA$;
 $dydt(2)=\mu_{EH} \cdot EH - b_{EH} \cdot EH$;
 $dydt(3)=\mu_{MH} \cdot MH - b_{MH} \cdot MH$;
 $dydt(4)=\mu_{MA} \cdot MA - b_{MA} \cdot MA$;
 $dydt(5)=\mu_{HA} \cdot HA - b_{HA} \cdot HA$;
 $dydt(6)=-1/Y_{EA} \cdot \mu_{EA} \cdot EA - 1/Y_{MA} \cdot \mu_{MA} \cdot MA + 1/Y_{HA} \cdot \mu_{HA} \cdot HA$;
 $dydt(7)=Y_{EAH}/Y_{EA} \cdot \mu_{EA} \cdot EA - 1/Y_{MH} \cdot \mu_{MH} \cdot MH - 1/Y_{MA} \cdot \mu_{MA} \cdot MA - k_{LaH_2} \cdot (H - HG_x)$;
 $dydt(8)=Y_{MHCH_4}/Y_{MH} \cdot \mu_{MH} \cdot MH + Y_{MACH_4}/Y_{MA} \cdot \mu_{MA} \cdot MA - k_{LaCH_4} \cdot (CH_4 - CH_4G_x)$;

```

dydt(9)=YEACO2/YEA*muEA*EA-YMHCO2/YMH*muMH*MH+YMACO2/YMA*muMA*MA-
YHACO2/YHA*muHA*HA-kLaCO2*(CO2-CO2Gx);
dydt(10)=kLaH2*(HGx-H);
dydt(11)=kLaCH4*(CH4Gx-CH4);
dydt(12)=kLaCO2*(CO2Gx-CO2);
end

function dydt=fmec_N2continuous(t,y)
function dydt=fmec(t,y)
EA=y(1); %ARB (acetate --> H2): CH3COO- + 4 H2O --> 2 HCO3- + 9 H+ + 8e-
EH=y(2); %H2-oxidizing bacteria (H2 --> H2): H2--->2H+ + 2e- --> H2
MH=y(3); %hydrogenotrophic methanogens (H2 --> CH4): 4H2 + CO2 ---> CH4 +
2H2O
MA=y(4); %acetoclastic methanogens (acetate --> CH4): CH3COOH ---> CH4 + CO2
HA=y(5); %homoacetogenic bacteria (H2 --> acetate): HCO3- + 2H2 +0.5H+ --->
0.5CH3COO- + 2H2O
A=y(6); %acetate
H=y(7); %hydrogen in solution
CH4=y(8); %methane in solution
CO2=y(9); %CO2 in solution
HG=y(10); %H2 in gas phase
CH4G=y(11); %CH4 in gas phase
CO2G=y(12); %CO2 in gas phase
% maximum growth rate
muEAmx=0.132; %mmol/mgX-d
muEHmx=muEAmx; muMHmx=muEAmx; muMAmx=muEAmx;
muHAMx=0;

% half saturation constant
KsEA=3e-5; %mmol/cm3, mol/L
KsMH=40e-6; %mol/L 1-80 micromol/L
KsEH=KsMH; %mol/L
KsMA=4e-3; %mol/L 0.85-7 mmol/L
KsHA=KsMA;
KsCO2=0.01;
MoCO2=CO2/(KsCO2+CO2);

% Monod, specific growth rate
muEA=muEAmx*A/(KsEA+A)*MoCO2; muEH=muEHmx*H/(KsEH+H)*MoCO2;
muMH=muMHmx*H/(KsMH+H)*MoCO2; muMA=muMAmx*A/(KsMA+A)*MoCO2;
muHA=muHAMx*A/(KsHA+A)*MoCO2;

% decay rate
bEA=0.05; bEH=bEA; bMH=bEA; bMA=bEA; bHA=bEA;

% Biomass- substrate yield
YEA=0.05; YEH=0.05; YMH=0.05; YMA=0.05; YHA=0.05; %mol biomasa/mol substrat

% Stoichiometry
YEAH=4; %mol H2/mol A
YEH=1; %mol H2/mol H2
YMHCH4= 1/4; %mol CH4/molH2
YMACH4=1; %mol meta/mol acetate
YHAA=1/4; %mol acetat/mol H2
YEACO2=2; %mol CO2/mol acetate
YMHCO2=1/4; %mol CO2/mol H2
YMACO2=1; %mol CO2/mol acetate
YHACO2=1/2; %mol CO2/mol H2

```

```

% Mass transport coefficients
kLaH2=0.0;
kLaCH4=0.0;
kLaCO2=0.0;

% Concentration in liquid interphase
HGx=HG*0.01;
CH4Gx=CH4G*0.01;
CO2Gx=CO2G*0.01;

%Differential equations
dydt=zeros(9,1);
dydt(1)=muEA*EA-bEA*EA;
dydt(2)=muEH*EH-bEH*EH;
dydt(3)=muMH*MH-bMH*MH;
dydt(4)=muMA*MA-bMA*MA;
dydt(5)=muHA*HA-bHA*HA;
dydt(6)=-1/YEA*muEA*EA-1/YMA*muMA*MA+1/YHA*muHA*HA;
dydt(7)=0;
dydt(8)=0;
dydt(9)=YEACO2/YEA*muEA*EA-YMHCO2/YMH*muMH*MH+YMACO2/YMA*muMA*MA-
YHACO2/YHA*muHA*HA-kLaCO2*(CO2-CO2Gx);
dydt(10)=kLaH2*(HGx-H);
dydt(11)=kLaCH4*(CH4Gx-CH4);
dydt(12)=kLaCO2*(CO2Gx-CO2);
end
end

```

Appendix B: Glossary and abbreviations

Glossary

Anaerobic digestion: anaerobic treatment of wastewater based on microorganisms that convert organic material to methane.

Anaerobic digestion sludge: anaerobic digestion mixed liquor containing non digested organic matter and microorganisms responsible of anaerobic digestion.

Anion exchange membrane: type of membrane that is selectively permeable to anions.

Anode: electrode of an electrochemical device that accepts electrons from an electrochemical reaction.

Anode respiring bacteria: bacteria that can respire anaerobically by using the anode as the terminal electron acceptor. Other names sometimes used for these bacteria are electricigens, exoelectrogenic bacteria, or electro- chemically active bacteria.

Applied voltage: voltage provided from an external energy source for allowing H₂ generation at the cathode in a microbial electrolysis cell.

Bioelectrochemical system: an electrochemical system in which electrochemically active microorganisms catalyze the anode and/or the cathode reaction.

Bioelectrochemical wastewater treatment: wastewater treatment with a bioelectrochemical system.

Biofilm: multilayered aggregation of microorganisms on a solid support.

Biorefinery: facility that integrates biomass conversion processes and equipment to produce fuels, power, heat and value added chemicals.

Cation exchange membrane (CEM): type of membrane that is selectively permeable to cations.

Cathode: electrode of an electrochemical device that donates electrons to an electrochemical reaction.

Cathodic gas recovery (r_{CAT}): ratio of moles of hydrogen measured to moles of hydrogen that could have been produced according to current intensity measured.

Chemical oxygen demand (COD): measure used to indicate the amount of organic material in wastewater. It is expressed in mg O₂/l, which is the amount of oxygen needed to oxidize the entire organic material to carbon dioxide.

Conductive biofilm matrix: polymeric matrix produced by ARB in the biofilm that allows electron transport at a distance from the anode.

Coulombic efficiency (CE): ratio of coulombs circulated in the electrical circuit to coulombs contained in the substrate oxidized.

Cyclic voltammetry (CV): Electrochemical technique to characterize the electron transfer process where the potential of the electrode to study is varied in a ramped linear fashion and the response of the system in current intensity is monitored, $I = f(E)$. The forward and reverse scan on the electrode potential results in a cyclic response of current intensity.

Diffusion: transport of chemical species by gradient of concentration.

Electrochemically active microorganisms: microorganisms that are capable of either donating electrons to or accepting electrons from an electrode.

Electrolyte: ionized solution.

Electromotive force (emf): potential difference between the cathode and the anode, which is positive for a thermodynamically favorable reaction

Electron recycling phenomena: situation caused by syntrophic interactions between ARB, H_2 -oxidizing ARB and homoacetogenic bacteria. Hydrogen produced electrochemically at the cathode of MEC can be consumed as electron donor by H_2 -oxidizing ARB and it can be consumed to produce acetate by homoacetogenic bacteria, which can be further used as electron donor by ARB. No net hydrogen production and higher current intensity than expected result from this situation.

Energy recovery (η_w): amount of energy added to the circuit by the power source and the substrate that is recovered as hydrogen.

Exoelectrogenic bacteria: (view ARB)

Extracellular electron transfer: mechanism by which electrochemically active microorganisms donate electrons to or accept electrons from an electrode.

Fermentation: the microbial oxidation–reduction reaction using organic compounds as electron donors and acceptors in the absence of an exogenous electron acceptor.

Fuel cell: electrochemical device that oxidizes hydrogen and reduces oxygen with electricity and water as outputs of this process.

Gibbs free energy: maximum amount of useful work that can be obtained from a reaction (expressed in J/mol).

Hydraulic retention time (HRT): the average residence time of water applied to a continuous-flow system: $HRT = V/Q$, in which V is the system volume and Q is the continuous flow rate.

Hydrogen recycling phenomena: (view Electron recycling phenomena)

Homoacetogenesis: homogeneous microbial formation of acetate using an electron donor such as hydrogen.

H₂-oxidizing ARB: ARB with ability to use hydrogen as electron donor.

Methanogenesis: microbial production of methane.

Methanogenic *archaea*: microorganisms that produce methane as a metabolic byproduct in anoxic conditions. Methane can result from reduction of carbon dioxide with hydrogen (performed by hydrogenotrophic methanogens) or from acetate (performed by acetoclastic methanogens).

Microbial fuel cell (MFC): bioelectrochemical system that is capable of converting the chemical energy of dissolved organic materials directly into electrical energy.

Microbial electrolysis cell (MEC): bioelectrochemical system that is capable of generating a product (e.g. hydrogen) from dissolved organic materials and that drives the reactions with an electrical energy input.

Migration: transport of chemical species caused by an electric field

Nanowire: long and conductive appendage that ARB use for extracellular electron transfer.

Ohmic loss: voltage loss caused by the movement of ions through an electrolyte and voltage loss caused by the movement of electrons through electrodes, electrical contacts and electrical wiring of an electrical system.

Overpotential: voltage loss that results from electrode activation losses, bacterial metabolic losses and concentration losses.

Open circuit voltage/potential (OCV/OCP): voltage that can be measured after some time in the absence of current.

Polarization curve: cell potential response versus current intensity, $E_{\text{cell}} = f(I)$, performed varying the external resistance from a very high load to very small load. Infinite load corresponds to OCV.

Reference electrode: electrode with stable and well-known electrode potential. Stability is reached by buffered or saturated redox systems that maintain constant concentration of reactants.

Single chamber MXC: bioelectrochemical system lacking a membrane that physically separates oxidation and reduction reaction products. A single chamber system can also consist in a direct assembly of one electrode and membrane on the one side and the other electrode on the other, not leaving space for the corresponding electrolyte and therefore having a single chamber configuration.

Standard hydrogen electrode (SHE): The redox electrode that is the basis for thermodynamic oxidation–reduction potentials. By convention, the standard reduction potential for $2\text{H}^+ + 2\text{e}^- \rightarrow \text{H}_2$ is 0V.

Syntrophy: nutritional association among species, which live off the products of other species.

Volatile suspended solids (VSS): The filterable solids lost on ignition at 550°C. VSS gives an approximation of the biomass concentration with a value similar to dry weight.

List of acronyms and abbreviations

AC-MFC: air cathode microbial fuel cell

$A_{\text{cat}}^{\text{CEmax}}$: area of cathode maximizing CE.

ARB: anode respiring bacteria

AEM: anion exchange membrane

BES: 2-bromoethanesulfonate

CEM: cation exchange membrane

COD: chemical oxygen demand

CV: cyclic voltammetry

EET: extracellular electron transfer

GC: gas chromatography

IEA: International Energy Agency

IEM: ionic exchange membrane

MFC: microbial fuel cell

MEC: microbial electrolysis cell

MXC: MFC and MEC

OC: open circuit

OCV: open circuit voltage

OCP: open circuit potential

SHE: Standard hydrogen electrode

R_{int}: internal resistance

R_{ext}: external resistance

R_{ext,opt}: optimal external resistance

VFA: volatile fatty acids

WW: wastewater

A: ampere

E: potential

I: current intensity

P: power

S: substrate

t: time

V: volts

W: watt

Ω: ohm

η: overpotential

η_w: energy recovery

Appendix C: Curriculum Vitae

Surname, Name: Montpart Planell, Núria
Date of birth: January 6, 1985 (Barcelona, Spain)
e-mail: nmontpartplanell@gmail.com



Work experience

- Predoctoral researcher on wastewater treatment with bioelectrochemical reactors (Universitat Autònoma de Barcelona, from 2010 to 2014)
- Teacher assistant of the course Water Sanitation and Depuration Technologies (Universitat Autònoma de Barcelona, 2013)
- Teacher assistant of the course Chemical Reactors (Universitat Autònoma de Barcelona 2010, 2011)
- Undergrad research collaborator: System control in detergent granulation processes (University of California, spring 2008)

Education

- Master in Environmental Sciences and Technology, Universitat Autònoma de Barcelona (2009-2010), entitled “Redesign of a dissolved oxygen control system in an urban WWTP”
- Chemical Engineer, Universitat Autònoma de Barcelona (2003-2009). Education exchange program at University of California Santa Barbara (year 2007/08)

Participation in conferences and seminars

- 3rd International MFC Conference, Leeuwarden (The Netherlands), June 2011. Contribution with the poster entitled “Is the biofilm grown on the cathode of an air-cathode MFC that detrimental?”
- 4th International MFC Conference, Cairns (Australia), September 2013. Contribution with the oral presentation entitled “Systematic development of anodic syntrophic consortia for bioelectrochemical hydrogen production from a wider range of carbon sources”
- Eawag, Aquatic Research Institute, Dübendorf (Switzerland), March 2013. Process Engineering Department Seminars: “Biohydrogen production from wastewater with microbial electrolysis cells: steps towards scale-up”
- Universitat Autònoma de Barcelona. May 2014. Departament d’Enginyeria Química, Seminaris Científics: “Hydrogen production in bioelectrochemical systems: a new approach for wastewater treatment and valorization”

Publications

- Montpart, N.; Ribot-Llobet, E.; Garlapati, V. K.; Rago, L.; Baeza, J. A.; Guisasola, A. Methanol opportunities for electricity and hydrogen production in bioelectrochemical systems. *Int. J. Hydrogen Energy* 2014, 39, 770–777.

- Montpart, N.; Guri, S.; Vega, M. L.; Cirucci, J.; Lafuente, F. J.; Baeza, J. A.; Guisasola, A. Patent: Process for methanogenesis inhibition in single chamber microbial electrolysis cells. Ref: 12382524.2, 2012.
- Ribot-Llobet, E.; Montpart, N.; Ruiz-Franco, Y.; Rago, L.; Lafuente, J.; Baeza, J. A.; Guisasola, A. Obtaining microbial communities with exoelectrogenic activity from anaerobic sludge using a simplified procedure. *J. Chem. Technol. Biotechnol.* 2013, DOI: 10.1002/jctb.4252.

Languages

- Catalan and Spanish (mother tongues)
- English (advanced)
- German (intermediate)
- French (basic)

Computer knowledge

- Experienced user of Office products (Word, Excel, Power Point) and other specific software (Matlab, AutoCAD, GIS)

